Technische Universität München
TUM School of Engineering and Design

Structure-Preserving Model Reduction of Port-Hamiltonian Descriptor Systems

Tim Fabian Moser

Vollständiger Abdruck der von der TUM School of Engineering and Design der Technischen Universität München zur Erlangung eines

Doktors der Ingenieurwissenschaften (Dr.-Ing.)

genehmigten Dissertation.

Vorsitz:		Prof. Dr. ir. Daniel J. Rixen
Prüfer der Dissertation:	1.	Prof. Dr.-Ing. Boris Lohmann
	2.	Assistant Prof. Dr. Matthias Voigt
	3.	Prof. Dr. Bernhard Maschke

Die Dissertation wurde am 27.06.2023 bei der Technischen Universität München eingereicht und durch die TUM School of Engineering and Design am 20.10.2023 angenommen.

Abstract

Efficient multi-energy devices and networks will become increasingly important to meet the global energy demand and promote the widespread use of renewable resources. The system class of port-Hamiltonian descriptor systems (pH-DAEs) is particularly suited to model complex multi-energy systems in a flexible and modular way. Structure-preserving model order reduction (MOR) techniques are required to leverage this modeling approach in practice and to enable more efficient simulation and control.

This thesis presents novel algorithms and software for structure-preserving MOR of linear, time-invariant pH-DAEs that enable a simplified treatment of algebraic constraints commonly encountered in network modeling. We first derive a system decomposition approach for the original model's transfer function, which forms the basis for novel *interpolatory* and *optimization-based* MOR methods.

An interpolatory MOR framework for pH-DAE models in staircase form is presented, which exploits the structural properties of Rosenbrock system matrices. This Rosenbrock framework extends $\mathcal{H}_2$- and $\mathcal{H}_\infty$-inspired MOR algorithms to pH-DAE models, which exhibit a particular block structure commonly observed in practical applications. For $\mathcal{H}_2$-inspired algorithms, we propose an approach that allows the computational costs of reduction and optimization to be decoupled using surrogate models. Numerical experiments indicate that this accelerates existing approaches, especially if very large models are considered.

For optimization-based MOR, we present a flexible parameterization to create reduced-order models in pH-DAE form with minimal state-space dimension. Based on this parameterization, a new algorithm is developed which allows a direct optimization of the $\mathcal{H}_2$ error using gradient methods. By utilizing the pole-residue representation of the $\mathcal{H}_2$ norm, this approach only relies on samples of the original transfer function and its derivative.

The presented achievements are implemented in the open-source software toolbox MORpH. It supports various strategies for structure-preserving MOR and is intended to promote collaborations among researchers and the application of the port-Hamiltonian modeling paradigm in engineering practice.

Acknowledgments

First of all, I would like to express my deepest gratitude to my supervisor Prof. Dr. -Ing. Boris Lohmann for giving me the opportunity to conduct this research, for his patient and professional guidance, as well as for the freedom and encouragement he has given me to pursue my ideas. I would like to express my deepest appreciation to Prof. Dr. Volker Mehrmann and Prof. Dr. Matthias Voigt for the open-minded collaboration and the discussions that helped me frame my research and develop new ideas. I am indebted to Prof. Dr. Tatjana Stykel for her mentorship and to the examination board members Prof. Dr. Bernhard Maschke and Prof. Dr. ir. Daniel J. Rixen.

This research would not have been possible without the financial support of the German Research Foundation (Deutsche Forschungsgemeinschaft, DFG), which is gratefully acknowledged. I want to thank Dr. Paul Schwerdtner, with whom I had the pleasure of sharing many hours of hard work and inspiring discussions. I am much obliged to PD Dr.-Ing. habil. Paul Kotyczka and Tobias Thoma for all the fruitful discussions. Thanks should also go to Dr.-Ing. Maria Cruz Varona for helping me get acquainted with the software toolboxes developed at the MORLab. Moreover, I would like to thank all students who have contributed to this research as part of their theses. I am incredibly grateful to all my former colleagues for making the Chair of Automatic Control at TUM such a great place to work, but also for the friendship and all the memorable moments we shared after work.

Last but not least, I could not have undertaken this journey without my family and friends, who have always encouraged me to pursue my dreams and supported me to achieve them. I am deeply indebted to my parents, who have taught me so much about motivation, dedication, and love over all these years. Dear Lea: Thank you for all the pleasant distractions and for teaching me the art of optimism.

Munich, June 2023
Tim Moser

Contents

1 Introduction

1.1 Motivation and Scope

Climate change is one of the most significant and pressing challenges our society faces today, threatening the natural environment and the lives of billions of people. Following the Paris Agreement of 2015, the EU and its member states committed to actions aimed at cutting greenhouse gas emissions by at least 40 % by 2030 compared to 1990 levels [52]. Extending renewable energy sources is crucial to achieve this goal [74, 147] and the EU targets at least 32 % share of renewable energy in its energy consumption by 2030 [53].

To date, the different energy networks, including electricity, gas, and district heating/-cooling networks, are predominantly planned, operated and optimized independently. Due to the increasing dependencies and interactions between these networks, there is growing interest in a more holistic approach where different energy carriers (such as electricity, gas, and heat) and sectors (such as industry, transport, and residential) are combined into one, *integrated* energy system [78]. On the one hand, exploiting synergies between the currently separated networks bears several potential benefits, including increased energy efficiency, flexibility, and resilience while facilitating the integration of renewable energy sources [99, 155]. On the other hand, this paradigm shift also increases the complexity of future energy networks, making modeling and simulation inevitable [99].

We can derive several requirements for modeling these networks. First, a *multi-physics* modeling approach is required, which can capture the energy exchange between different carriers. Second, since renewable energy sources such as wind turbines or photovoltaic systems are subject to intermittencies, their efficient integration requires a modeling approach with a high temporal resolution that can couple subsystems with different time scales but also different accuracies [96]. Third, the modeling approach should be flexible and modular, such that submodels can be added or changed without jeopardizing other parts or essential properties of the network.

Integrated energy networks are an illustrative example of the multi-physics nature of many modern technical systems for which similar requirements apply. A modeling

approach that is well-suited for these systems and meets the above requirements is the *port-Hamiltonian* (pH) modeling paradigm [48, 83, 134, 135]. It arises naturally from port-based network modeling and supports the interconnection of submodels via power flows while maintaining important properties such as passivity. This enables a safe coupling of models from different physical domains and simplifies energy-based control. If networks of models are considered, additional algebraic constraints in the form of conservation and network laws commonly arise, such as mass balances in chemical processes and Kirchhoff's laws in electrical networks. Incorporating algebraic constraints in the pH paradigm yields the system class of port-Hamiltonian differential-algebraic systems (pH-DAEs) [105]. PH-DAEs often naturally emerge in modeling practice; see [14] for examples. These include, for instance, the graph-based modeling of passive electrical networks [51, 55, 72, 73] and the modeling of pressure waves in pipeline networks [49, 50].

Due to the increasing complexity of modern technical systems and demands on modeling accuracy, the number of equations required to describe the underlying physics and geometry is often very large. This includes cases where distributed parameter systems with complex geometry are spatially discretized or networks with many network components are considered. These large-scale models consume considerable computational resources for simulation, and for system analysis, optimization, or model-based controller design, they might even be infeasible. Instead of simply increasing the processing power and storage capacity (which is typically expensive), we focus on an algorithmic solution in this thesis called *model order reduction (MOR)*. Simply put, MOR aims at approximating a given large-scale model (*full-order model, FOM*) with a model of much smaller dimension (*reduced-order model, ROM*) that captures the important characteristics of the original. These characteristics include, on the one hand, the model dynamics. One is typically interested in approximating the input-output behavior, i.e., the ROM should produce similar output signals for predefined input signals relevant to the specific application. On the other hand, the ROM should preserve relevant properties of its original counterpart. The most intuitive approach to achieve this goal for pH-DAE models is *structure preservation*. Since many crucial system properties, such as stability and passivity, follow directly from the port-Hamiltonian structure, they can be preserved automatically if the pH-DAE structure is enforced for the ROM during MOR. For network modeling, this also enables a safe coupling of the ROM with other models of the network if the original model is replaced by the ROM for simulation, optimization or controller design.

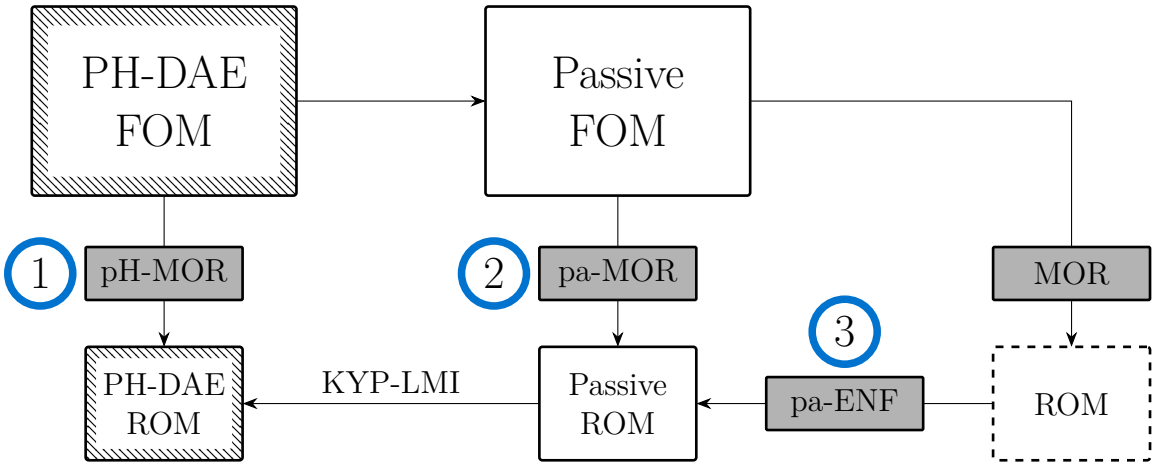

Figure 1.1: Overview of three strategies for structure-preserving MOR of linear, time-invariant pH-DAE models in state-space form. Depicted are different algorithm categories (greyed out) and three model types: pH-DAE models (hatched), passive state-space models, and general state-space models (dashed). This thesis focuses on the algorithm categories pH-MOR, pa-MOR, and pa-ENF.

This thesis focuses on the structure-preserving model order reduction of *linear, time-invariant* (LTI) pH-DAEs. Since most real-world systems are nonlinear, let us briefly give three main reasons for this choice. First, as the remainder of this chapter shows, the MOR of LTI pH-DAE models is only partially resolved and raises open research questions that need to be investigated. Second, many nonlinear physical systems exhibit a linear behavior for large ranges of operating conditions and, if the operating points are known, can be linearized in their vicinity [11]. Third, linear MOR theory has also proven helpful for parametric and nonlinear MOR as discussed e.g. in [112]. For the sake of simplicity, we generally speak of pH-DAEs in the following, bearing in mind that we always refer to the subclass of LTI pH-DAEs if not stated otherwise.

1.2 Related Work

Within the last 20 years, various algorithms have been proposed that can be utilized for the structure-preserving MOR of pH-DAEs. They mainly fall into three categories: pH-preserving MOR (pH-MOR), passivity-preserving MOR (pa-MOR), and passivity enforcement (pa-ENF). From this, three possible MOR strategies can be derived that are illustrated in Figure 1.1.

The most intuitive strategy is to directly enforce the pH-DAE form of the ROM, which is the case for algorithms in the category pH-MOR. Since every pH-DAE is inherently passive, it may also be reduced using methods in the category pa-MOR, which preserve passivity. These algorithms lead to a ROM generally not in pH-DAE form. However, under certain conditions discussed in [39], a corresponding pH representation can be computed by solving the associated *Kalman-Yakubovich-Popov* linear matrix inequality (KYP-LMI) (see, e.g., [13]). Finally, standard MOR algorithms designed for unstructured DAE models can also be applied; see [8, 23] for an overview. Applying these algorithms to pH-DAE models will generally yield ROMs that are neither passive nor in pH-DAE form and are, therefore, not in the scope of this thesis. However, if the passivity violations are only minor, the passivity of the ROM can be enforced in a post-processing step using algorithms in the category pa-ENF. This results in an additional approximation error, which is, however, expected to be small for minor passivity violations. This strategy may also require an additional transformation step via the KYP-LMI.

PH-Preserving MOR (pH-MOR) Algorithms that directly enforce the pH-DAE form of the ROM are either based on Petrov-Galerkin projections or an optimization of the reduced state-space matrices. Petrov-Galerkin methods project the original state vector onto a suitably chosen subspace. This subspace is either chosen for the *balanced truncation* of the original model, i.e., to identify and extract important states measured by controllability and observability, or to *interpolate* its transfer function, i.e., its input-output relation in the frequency domain. Structure-preserving variants of the classic balanced truncation algorithm were proposed in [118, 156, 157] based on reduced-order Dirac structures and extended in [27, 30] to enable classical a priori error bounds under certain conditions. Interpolatory MOR methods enforce interpolation conditions between the original and reduced transfer function at selected complex interpolation points (shifts). Different frameworks and algorithms for this task were studied in [50, 76, 81, 116, 117, 119, 154] and enriched with shift selection strategies in [15, 68, 69, 79]. Optimization-based techniques are directly targeted toward low errors in suitable system norms such as the $\mathcal{H}_2$ or $\mathcal{H}_\infty$ norm (see [162, Chapter 4] for details) and create ROMs by a direct optimization of matrix entries. Algorithms for the $\mathcal{H}_2$ optimization problem were formulated by a direct optimization of the reduced state-space matrices on manifolds [91, 132] or indirectly via Petrov-Galerkin projections in [84]. An $\mathcal{H}_\infty$-inspired optimization of the reduced state-space matrix entries was proposed in [142, 143] using a leveled least-squares method.

Passivity-Preserving MOR (pa-MOR) Similar to the Petrov-Galerkin methods in the category pH-MOR, passivity-preserving MOR methods also employ system balancing or interpolation. Balancing-based approaches rely on the solution of algebraic Riccati equations or a mixture of algebraic Riccati and Lyapunov equations (see, e.g., [43, 70, 75, 115, 122, 148]). With interpolatory methods, passivity of the original model can generally be retained by interpolating the original transfer function at its spectral zeros [10, 82, 144]. Another approach is to exploit the structural properties of models that arise in specific applications; see, e.g., the methods proposed in [56, 111] for RLC interconnect circuit models. Frequency-weighted approaches such as [90, 163] can be utilized if a high approximation accuracy is only required on predefined frequency intervals. Recently, a method that relies on a spectral factorization of the *Popov function*, a complex-valued matrix function, was proposed, which enables the use of both traditional balancing and interpolatory MOR methods [29].

Passivity Enforcement (pa-ENF) In order to use an unstructured ROM for our goal, it is initially required to check whether this ROM is already passive or whether passivity has to be enforced. Passivity validation techniques are either based on checking positive realness, a frequency-domain property closely linked to passivity, or whether a solution to the KYP-LMI can be found. Passivity enforcement algorithms leverage these techniques, and a comprehensive overview of the topic is provided in [64]. A common feature of most algorithms in this category is the perturbation of specific matrix entries of the ROM such that the respective passivity conditions are enforced. First, positive realness can be verified by sampling the Popov function along the imaginary axis and checking whether its eigenvalues are non-negative. Accordingly, passivity is enforced by nudging negative eigenvalues of the Popov function on the imaginary axis towards positivity (see [64, Section 10.5]). Second, it can be checked if the spectral zeros of the Popov function, which can be computed as eigenvalues of a Hamiltonian matrix, are present on the imaginary axis. If this is the case, perturbations are applied such that the spectral zeros move off the imaginary axis to render the model passive [63]. In both cases, a pH representation of the obtained passive ROM can be found using the KYP-LMI. A third possible approach is to directly search for a pH representation, either by minimal perturbations such that the KYP-LMI has a solution [64, Section 10.7] or by directly imposing a pH representation [59].

1.3 Research Objectives and Outline

The previous overview shows that the structure-preserving MOR of pH-DAE models has been an active research field, and various solutions are available. However, most of these algorithms do not apply to the entire pH-DAE system class. In fact, most of the presented work is focused on pH *ordinary* differential equation systems (pH-ODEs), i.e., models which do not include algebraic constraints. Since algebraic constraints often occur in engineering practice, particularly in network modeling (see, e.g., [14, 66, 105]), this limits their applicability to real-world problems.

Extensions to the DAE case include the positive real balanced truncation algorithm (PRBT) [122] in the category pa-MOR as well as the interpolatory MOR methods [15, 76] in the category pH-MOR. Like unstructured MOR methods based on Petrov-Galerkin projections, both approaches require a separation of algebraic and differential equations such that the original model's state-space matrices exhibit a particular block structure. For the PRBT algorithm, this is required to compute spectral projectors, which is otherwise difficult in large-scale settings [104]. The interpolatory strategies to treat the algebraic constraints in [15, 76] vary depending on the original model's Kronecker index and how the input affects the algebraic constraints. In their entirety, these strategies do not cover the whole system class of pH-DAEs, and some may not necessarily preserve the pH structure.

Even though specific block structures of the original state-space matrices naturally occur for many practical examples (see, e.g., [66, 105]), this is generally not guaranteed. Transformations to enforce these block structures may be ill-conditioned and infeasible in large-scale settings. Optimization-based MOR methods are beneficial in such cases because the ROM matrices are parameterized directly and, compared to Petrov-Galerkin methods, are not generated by operations on the FOM matrices. Interestingly, to the best of the author's knowledge, optimization-based methods have not been exploited for pH-DAE models so far.

Another issue that should be more explicitly mentioned but not underestimated is numerical software availability. Software is a key driver to promote not only scientific exchange but also the use of novel research advances in engineering practice. While several software packages exist for classic (unstructured) MOR (see, e.g., [21, 34, 107]), there is currently only few software available for the structure-preserving MOR of pH-DAEs. Available software has been chiefly published to reproduce the numerical experiments of selected research papers (see, e.g., [29, 59]).

In conclusion, the identified research gaps motivate a more holistic approach to the problem, both methodologically and in terms of implementation. In this thesis, we summarize and discuss the work in [A1–A5], which is dedicated to this challenge. The main contributions are as follows:

- The development of a system decomposition approach, which paves the way to generalize different MOR strategies to the entire system class of pH-DAEs [A5].
- An *interpolatory* MOR framework for pH-DAE models in staircase form, which exploits the structural properties of Rosenbrock system matrices [A4] combined with a method to increase computational efficiency using surrogate models [A2].
- An *optimization-based* MOR method for structure-preserving $\mathcal{H}_2$ optimization, which only relies on samples of the original transfer function and its derivative [A3, A5].
- A novel software toolbox MORpH, which is the first to implement various software solutions targeted explicitly at the storage, interconnection, and model order reduction of possibly large-scale pH-DAE models [A1].

The remainder of this thesis is organized accordingly: In Chapter 2, we recapitulate relevant results from linear systems theory and the field of model reduction that lie the foundation for our contributions in Chapter 3. The system decomposition approach is described in Section 3.1. In Sections 3.2 and 3.3, we illustrate how this approach can be exploited for interpolatory and optimization-based MOR in the $\mathcal{H}_2$ norm, respectively. Section 3.4 briefly summarizes the developed software toolbox MORpH. In Chapter 4, we discuss the obtained results with respect to different key objectives and conclude with a summary as well as a brief discussion of future research opportunities.

2 Preliminaries

In this chapter, we outline the theoretical background of our work. Section 2.1 is dedicated to the closely linked theory of passivity, positive realness, and port-Hamiltonian systems. Section 2.2 briefly summarizes relevant results from MOR. For a more comprehensive introduction to the topics in this chapter, the reader is referred to [42] for general (linear) DAE systems theory, to [48, 134] for an introduction to the port-Hamiltonian modeling paradigm, and to [8, 11, 22, 137] for model reduction fundamentals.

Notation Throughout this thesis, $\mathbb{R}$ and $\mathbb{C}$ denote the fields of real and complex numbers, respectively. We write $\mathbb{C}_-$ and $\mathbb{C}_+$ for the open left and open right complex half-planes, respectively, and $\mathbb{R}_{\geq 0}$ for the set of non-negative real numbers. We denote the ring of polynomials with coefficients in $\mathbb{R}$ by $\mathbb{R}[s]$ and the set of $n \times m$ matrices with entries in $\mathbb{R}[s]$ by $\mathbb{R}[s]^{n\times m}$. For a matrix $A \in \mathbb{C}^{n\times m}$, its transpose and conjugate transpose are denoted by A^{T} and A^{H}, respectively. The image, kernel, and rank of A are denoted by $\operatorname{im} A$, $\ker A$ and $\operatorname{rank} A$, and we use $\|A\|_2$ and $\|A\|_{\mathrm{F}}$ to denote its spectral norm and Frobenius norm, respectively. For two Hermitian matrices $A, B \in \mathbb{C}^{n\times n}$, we write $A \geq B$ if the matrix $A - B$ is positive semidefinite. The identity matrix of dimension $n \times n$ is denoted by I_n and the $n \times m$ zero matrix by $0_{n\times m}$, while we omit subindices for simplicity of notation when it is clear from the context.

2.1 Linear Systems Theory

We consider linear time-invariant (LTI) models in generalized state-space form

$$\Sigma : \begin{cases} E\dot{x}(t) = Ax(t) + Bu(t), \quad Ex(0) = Ex_0, \\ \quad y(t) = Cx(t) + Du(t), \end{cases} \tag{2.1}$$

where E, $A \in \mathbb{R}^{n\times n}$, $B \in \mathbb{R}^{n\times m}$, $C \in \mathbb{R}^{p\times n}$, and $D \in \mathbb{R}^{p\times m}$. For all $t \in \mathbb{R}_{\geq 0}$, $x(t) \in \mathbb{R}^n$ denotes the (generalized) *state vector*; $u(t) \in \mathbb{R}^m$ and $y(t) \in \mathbb{R}^p$ are the vectors of *input* and *output* signals, respectively. The state vector has an initial value $x_0 \in \mathbb{R}^n$, and n denotes the order or state-space dimension of the model. The matrix D, which directly

links inputs to outputs, is referred to as the *feedthrough* matrix. If the *descriptor* matrix E is singular, one speaks of a *differential-algebraic equation* (DAE) system and of an *ordinary differential equation* (ODE) system otherwise. Systems with $m = p = 1$ are referred to as single-input single-output (SISO) systems and as multi-input multi-output (MIMO) systems for $m, p > 1$.

Assumptions Throughout this work, we consider systems that interact with their environment through power ports. One consequence of this energy-based viewpoint is that the input and output signals are not independent but occur in collocated pairs, i.e., we assume that $p = m$. To guarantee the existence and uniqueness of solutions to (2.1), we assume that the pencil $sE - A \in \mathbb{R}[s]^{n\times n}$ is *regular*, i.e., $\det(sE - A) \neq 0$ for some $s \in \mathbb{C}$ [42]. For the system norms introduced in Section 2.2 to exist, we restrict ourselves to *asymptotically stable* systems, i.e., we assume that the set of finite eigenvalues of the matrix pencil $sE - A$ lies in the open left half-plane $\mathbb{C}_-$. Finally, we assume consistent initial conditions that are *homogeneous*, i.e., such that $Ex_0 = 0$.

After a Laplace transformation of the state-space equations in (2.1), we obtain the following equations in matrix form

$$\begin{bmatrix} 0 \\ \mathcal{L}\{y\} \end{bmatrix} = \underbrace{\begin{bmatrix} sE - A & -B \\ C & D \end{bmatrix}}_{=:\mathcal{P}(s)} \begin{bmatrix} \mathcal{L}\{x\} \\ \mathcal{L}\{u\} \end{bmatrix}, \tag{2.2}$$

where $\mathcal{L}\{f\}$ denotes the Laplace transform of a function $f(t)$, $t \in \mathbb{R}_{\geq 0}$ (see [126]). The polynomial matrix $\mathcal{P} \in \mathbb{R}[s]^{(n+m)\times(n+m)}$ is often referred to as *Rosenbrock system matrix*. In the complex frequency domain, the mapping from inputs to outputs that follows from (2.2) is given by the system's transfer function

$$H(s) := C(sE - A)^{-1}B + D. \tag{2.3}$$

We also call the state-space model Σ a *realization* of H. Note that this realization is not unique, i.e., one particular transfer function has an infinite number of different realizations. Those realizations with the smallest state-space dimension n are referred to as *minimal* realizations. The minimality of a model is tightly related to the system-theoretic concepts of controllability and observability. For DAE models, there exist different concepts which are not consistently treated in the literature; see [25] for a comprehensive overview. Consequently, there are also different definitions of minimality. We follow the characterization proposed in [25, 110, 149].

Definition 2.1. [25, 110, 149] A model Σ as in (2.1) is called a *minimal realization* of its associated transfer function H in (2.3) if and only if the following conditions are satisfied:

(i) $\operatorname{rank}\begin{bmatrix}\lambda E - A & B\end{bmatrix} = n$ for all $\lambda \in \mathbb{C}$, *(behaviorally controllable)*

(ii) $\operatorname{rank}\begin{bmatrix}E & B\end{bmatrix} = n$, *(controllable at infinity)*

(iii) $\operatorname{rank}\begin{bmatrix}\lambda E^{\mathsf{T}} - A^{\mathsf{T}} & C^{\mathsf{T}}\end{bmatrix} = n$ for all $\lambda \in \mathbb{C}$, *(behaviorally observable)*

(iv) $\operatorname{rank}\begin{bmatrix}E^{\mathsf{T}} & C^{\mathsf{T}}\end{bmatrix} = n$, *(observable at infinity)*

(v) $A \ker E \subseteq \operatorname{im} E$. *(absence of nondynamic modes)*

Transformations between realizations with the same transfer function can be expressed as operations on the Rosenbrock system matrix $\mathcal{P}$ and are characterized by the notion of *strict system equivalence*.

Lemma 2.1. [126] *Let $X \in \mathbb{R}^{m\times n}$, $Y \in \mathbb{R}^{n\times m}$ and define invertible matrices $L, M \in \mathbb{R}^{n\times n}$. Suppose that two Rosenbrock system matrices $\mathcal{P}$ and $\widetilde{\mathcal{P}}$ are related by the transformation*

$$\widetilde{\mathcal{P}}(s) = \mathcal{T}_1 \mathcal{P}(s) \mathcal{T}_2 = \begin{bmatrix} L & 0 \\ X & I_m \end{bmatrix} \mathcal{P}(s) \begin{bmatrix} M & Y \\ 0 & I_m \end{bmatrix}. \tag{2.4}$$

Then we shall say that $\mathcal{P}$ and $\widetilde{\mathcal{P}}$ are related by strict system equivalence (s.s.e.). *The two Rosenbrock system matrices give rise to the same transfer function.*

Proof. For a proof, we refer the reader to [126, Theorem 3.1]. □

The solution behavior of regular, linear DAE models Σ can be analyzed using the Weierstrass canonical form (see, e.g., [58]). Let n_f (n_∞) denote the dimension of the left and right deflating subspaces of the pencil $sE - A$ corresponding to the finite (infinite) eigenvalues. Then there exists a transformation under s.s.e. that transforms the model to Weierstrass canonical form

$$\begin{aligned} \begin{bmatrix} I_{n_f} & 0 \\ 0 & E_\infty \end{bmatrix} \begin{bmatrix} \dot{x}_f(t) \\ \dot{x}_\infty(t) \end{bmatrix} &= \begin{bmatrix} A_f & 0 \\ 0 & I_{n_\infty} \end{bmatrix} \begin{bmatrix} x_f(t) \\ x_\infty(t) \end{bmatrix} + \begin{bmatrix} B_f \\ B_\infty \end{bmatrix} u(t), \\ y(t) &= \begin{bmatrix} C_f & C_\infty \end{bmatrix} \begin{bmatrix} x_f(t) \\ x_\infty(t) \end{bmatrix} + Du(t). \end{aligned} \tag{2.5}$$

Here, the diagonal elements of matrix $A_f \in \mathbb{R}^{n_f\times n_f}$ in Jordan canonical form are the finite eigenvalues of the pencil $sE - A$ and $E_\infty \in \mathbb{R}^{n_\infty \times n_\infty}$ is also in Jordan canonical

form and nilpotent with *Kronecker index* ν, i.e., $E_\infty^{\nu-1} \neq 0$ and $E_\infty^{\nu} = 0$. Using this partitioning of the state vector, the system's transfer function may be decomposed with a Laurent expansion at infinity such that [89, 104]

$$\begin{aligned} H(s) &= C_f(sI_{n_f} - A_f)^{-1}B_f + C_\infty(sE_\infty - I_{n_\infty})^{-1}B_\infty + D \\ &= \underbrace{\sum_{k=1}^{\infty} L_{k-1}s^{-k}}_{H_{\mathrm{sp}}(s)} + \underbrace{\sum_{k=0}^{\nu-1} L_{-k-1}s^{k} + D}_{H_{\mathrm{pol}}(s)} \end{aligned} \tag{2.6}$$

with Laurent parameters

$$L_k = \begin{cases} C_f A_f^k B_f, & k = 0, 1, 2, \dots, \\ -C_\infty E_\infty^{-k-1} B_\infty, & k = -1, -2, \dots. \end{cases}$$

The transfer function is called *proper* if $\lim_{s\to\infty} H(s) < \infty$, and *improper*, otherwise. If $\lim_{s\to\infty} H(s) = 0$, it is called *strictly proper*. In the following, the strictly proper part of H is denoted by H_{sp} and H_{pol} is often referred to as the *polynomial* part of H (see, e.g., [8, 71]). As a direct consequence of (2.6), H can only be improper if $\nu \geq 2$ and is guaranteed to be proper for models with Kronecker index at most one.

2.1.1 Passivity and Positive Realness

A property that is important for the simulation and control of (multi-)physical systems and also relevant for structure-preserving MOR is the concept of passivity.

Definition 2.2. [152] A model Σ is considered *passive* if there exists a non-negative, state-dependent storage function $\mathcal{S} : \mathbb{R}^n \to \mathbb{R}_{\geq 0}$ such that for any $t_0, t_1 \in \mathbb{R}_{\geq 0}$ with $t_1 \geq t_0$ the dissipation inequality

$$\mathcal{S}(x(t_1)) - \mathcal{S}(x(t_0)) \leq \int_{t_0}^{t_1} y(\tau)^{\mathsf{T}} u(\tau) \mathrm{d}\tau \tag{2.7}$$

holds for any smooth u, x and y satisfying (2.1).

In the following, models with this property will be denoted by Σ_{pa}. It is generally challenging to directly assess passivity via the dissipation inequality (2.7) since this condition has to hold for all possible solution trajectories. Therefore, a related frequency domain property called *positive realness* is commonly used.

Definition 2.3. [7, Theorem 2.7.2] The transfer function H of a model Σ is called *positive real* if

(i) H has no poles in $\mathbb{C}_+$.

(ii) The *Popov function*

$$\Psi(s) := H(s) + H(-s)^\mathsf{T} \tag{2.8}$$

is Hermitian positive semidefinite for each $s = \mathrm{i}\omega$, $\omega \in \mathbb{R}$ which is not a pole of H.

(iii) Every pole $\mathrm{i}\omega_0 \in \mathrm{i}\mathbb{R}$ of H is at most simple. The residue $\lim_{s\to\mathrm{i}\omega_0}(s - \mathrm{i}\omega_0)H(s)$ for finite ω_0, and $\lim_{\omega\to\infty} \frac{H(\mathrm{i}\omega)}{\mathrm{i}\omega}$ for poles at infinity, is Hermitian positive semidefinite.

Every passive system has a positive real transfer function and, vice versa, if a system has a positive real transfer function and is behaviorally controllable, then it is also passive [121, 123]. Therefore, the passivity of a behaviorally controllable model Σ may be examined by evaluating the Popov function on the imaginary axis with adaptive sampling techniques (see, e.g., [40, 65]).

Besides this *external* viewpoint on passivity that considers the system's input-output relation in the frequency domain, there exists another, *internal* viewpoint that is based on the system's state-space representation. The connection between both viewpoints, also known as the *Positive Real Lemma* or *Kalman-Yakubovich-Popov (KYP) Lemma*, is obtained by differentiation of the inequality (2.7). It dates back to work in the early 1960s by Kalman [85], Yakubovich [158] and Popov [120] and was extended to the DAE case in [55, 101, 121, 123, 160].

Lemma 2.2. *Given is a model Σ with associated transfer function H. If the generalized* Kalman-Yakubovich-Popov linear matrix inequality (KYP-LMI)

$$\begin{bmatrix} -A^\mathsf{T}X - X^\mathsf{T}A & C^\mathsf{T} - X^\mathsf{T}B \\ C - B^\mathsf{T}X & D + D^\mathsf{T} \end{bmatrix} \geq 0, \quad X^\mathsf{T}E = E^\mathsf{T}X \geq 0 \tag{2.9}$$

has a solution $X \in \mathbb{R}^{n\times n}$, the system is passive and its transfer function H is positive real.

Proof. Using $\mathcal{S}(x) = \frac{1}{2}x^\mathsf{T}X^\mathsf{T}Ex$ as a candidate for the storage function, we obtain

$$\begin{aligned} 2\frac{\mathrm{d}}{\mathrm{d}t}\mathcal{S}(x(t)) &= x(t)^\mathsf{T}X^\mathsf{T}E\dot{x}(t) + \dot{x}(t)^\mathsf{T}E^\mathsf{T}Xx(t) \\ &= x(t)^\mathsf{T}X^\mathsf{T}(Ax(t) + Bu(t)) + (Ax(t) + Bu(t))^\mathsf{T}Xx(t) \\ &= 2y(t)^\mathsf{T}u(t) - \begin{bmatrix} x(t) \\ u(t) \end{bmatrix}^\mathsf{T} \begin{bmatrix} -A^\mathsf{T}X - X^\mathsf{T}A & C^\mathsf{T} - X^\mathsf{T}B \\ C - B^\mathsf{T}X & D + D^\mathsf{T} \end{bmatrix} \begin{bmatrix} x(t) \\ u(t) \end{bmatrix} \leq 2y(t)^\mathsf{T}u(t), \end{aligned}$$

and integration of this inequality yields the dissipation inequality (2.7). Positive realness of the associated transfer function H follows directly since this is implied by passivity. The reader is referred to [55] for a direct proof. □

Consequently, another option to validate passivity is the search for solutions of the KYP-LMI. Their existence is, however, only a necessary condition in the ODE case [39, 55]. For passive DAE systems, the KYP-LMI generally holds only on certain subspaces [121]. Alternatively, if the model has Kronecker index at most one, a modified KYP-LMI can be solved to check passivity. If the model contains parts with higher index, these can be extracted and treated separately [39].

2.1.2 Port-Hamiltonian Systems

The system class of linear port-Hamiltonian descriptor systems, as initially introduced in [14], embeds the passivity property with an associated storage function (the *Hamiltonian*) directly in the state-space equations.

Definition 2.4. [14, 105] A regular, linear time-invariant DAE system of the form

$$\Sigma_{\mathrm{pH}} : \begin{cases} E\dot{x}(t) = (J-R)Qx(t) + (G-P)u(t), \\ y(t) = (G+P)^{\mathsf{T}}Qx(t) + (S+N)u(t), \end{cases} \tag{2.10}$$

where E, J, R, $Q \in \mathbb{R}^{n\times n}$, G, $P \in \mathbb{R}^{n\times m}$, S, $N \in \mathbb{R}^{m\times m}$ is called a *port-Hamiltonian descriptor system* (pH-DAE) if the following properties are satisfied:

(i) The *structure matrix*

$$\Gamma := \begin{bmatrix} -Q^{\mathsf{T}}JQ & -Q^{\mathsf{T}}G \\ G^{\mathsf{T}}Q & N \end{bmatrix}$$

is skew-symmetric, i.e., $\Gamma = -\Gamma^{\mathsf{T}}$.

(ii) The *dissipation matrix*

$$W := \begin{bmatrix} Q^{\mathsf{T}}RQ & Q^{\mathsf{T}}P \\ P^{\mathsf{T}}Q & S \end{bmatrix}$$

is symmetric positive semidefinite, i.e., $W = W^{\mathsf{T}} \geq 0$.

(iii) The quadratic *Hamiltonian* $\mathcal{H} : \mathbb{R}^n \to \mathbb{R}$ defined as

$$\mathcal{H}(x) := \frac{1}{2}x^{\mathsf{T}}Q^{\mathsf{T}}Ex$$

is non-negative, i.e., $Q^{\mathsf{T}}E = E^{\mathsf{T}}Q \geq 0$.

The system has an associated transfer function

$$H(s) = (G+P)^{\mathsf{T}} Q(sE - (J-R)Q)^{-1}(G-P) + S + N.$$

For many practical examples (see, e.g., [66, 105]), we have that $Q = I_n$. Considering systems in this form is also advantageous in system analysis and perturbation theory since all coefficients appear linearly in (2.10) [105]. Moreover, if Q is not the identity matrix, it can be removed for every pH-DAE as shown in [103, 105]. For ease of notation, we will therefore consider systems with $Q = I_n$ in the remainder of this work. In this case, E is the Hessian of the Hamiltonian, and a simple additive decomposition of the Rosenbrock system matrix in symmetric and skew-symmetric parts yields

$$\mathcal{P}(s) = s \underbrace{\begin{bmatrix} E & 0 \\ 0 & 0 \end{bmatrix}}_{=:\mathcal{E}} + \underbrace{\begin{bmatrix} -J & -G \\ G^{\mathsf{T}} & N \end{bmatrix}}_{\Gamma} + \underbrace{\begin{bmatrix} R & P \\ P^{\mathsf{T}} & S \end{bmatrix}}_{W} \tag{2.11}$$

with symmetric positive semidefinite extended descriptor matrix $\mathcal{E} \in \mathbb{R}^{(n+m)\times(n+m)}$.

In finite precision arithmetic, the computation of canonical forms such as the Weierstrass form in (2.5) is challenging since this generally involves ill-conditioned transformations. A compromise in this regard are so called *staircase forms* which are typically not canonical but can still provide insight into the system's solution behavior. For (port-)Hamiltonian systems, different staircase forms have been derived in [3, 15, 105, 138], which are obtained under orthogonal transformations that preserve the internal structure of the model. While these are still sensitive to perturbations (see [32] for a discussion), for many practical examples, these staircase forms can be considered directly in the modeling process such that the final model already has staircase form or the number of required transformations is significantly reduced [66, 105]. We consider the staircase form presented in [3] for dissipative Hamiltonian descriptor systems and extended to pH-DAEs in [15].

Lemma 2.3. [3, 15] *A regular pH-DAE model* Σ_{pH} *is in* staircase form *if it has a partitioned state vector* $x(t) = \left[x_1(t)^\mathsf{T}, x_2(t)^\mathsf{T}, x_3(t)^\mathsf{T}, x_4(t)^\mathsf{T}\right]^\mathsf{T}$*, where* $x_j(t) \in \mathbb{R}^{n_j}, n_j \in \mathbb{N}_0$ *for all* $j = 1, \ldots, 4$ *and with* $n_1 = n_4$ *such that*

$$E := \begin{bmatrix} E_{11} & 0 & 0 & 0 \\ 0 & E_{22} & 0 & 0 \\ 0 & 0 & 0 & 0 \\ 0 & 0 & 0 & 0 \end{bmatrix}, \quad J := \begin{bmatrix} J_{11} & J_{12} & J_{13} & J_{14} \\ J_{21} & J_{22} & J_{23} & 0 \\ J_{31} & J_{32} & J_{33} & 0 \\ J_{41} & 0 & 0 & 0 \end{bmatrix}, \tag{2.12}$$

$$G := \begin{bmatrix} G_1 \\ G_2 \\ G_3 \\ G_4 \end{bmatrix}, P := \begin{bmatrix} P_1 \\ P_2 \\ P_3 \\ 0 \end{bmatrix}, \quad R := \begin{bmatrix} R_{11} & R_{12} & R_{13} & 0 \\ R_{21} & R_{22} & R_{23} & 0 \\ R_{31} & R_{32} & R_{33} & 0 \\ 0 & 0 & 0 & 0 \end{bmatrix}, \tag{2.13}$$

where E_{11}, E_{22} *are symmetric positive definite, and the matrices* J_{41} *and* $J_{33} - R_{33}$ *are invertible (if the blocks are nonempty). The Kronecker index* ν *of the uncontrolled system satisfies*

$$\nu = \begin{cases} 0 & \text{if and only if } n_1 = n_4 = 0 \text{ and } n_3 = 0, \\ 1 & \text{if and only if } n_1 = n_4 = 0 \text{ and } n_3 > 0, \\ 2 & \text{if and only if } n_1 = n_4 > 0. \end{cases}$$

The fact that the Kronecker index of a pH-DAE is at most two (see [102] for a proof) has many advantages. For instance, this limits the maximum possible degree of the polynomial part H_{pol} of its transfer function to one (see (2.6)). It is also advantageous for time-discretization and solving associated linear systems of equations; see [105, Section 9] for an overview.

As initially mentioned, the Hamiltonian $\mathcal{H}$ is a storage function for the dissipation inequality (2.7), and consequently, pH-DAEs are inherently passive (see, e.g., [14] for a proof). Vice versa, the connection between the classes of pH-DAEs Σ_{pH} and passive DAE systems Σ_{pa} is also established via the KYP-LMI. As shown in [39, 48], a pH realization Σ_{pH} of a passive system Σ_{pa} exists if and only if the KYP-LMI (2.9) has a solution $X \in \mathbb{R}^{n \times n}$ that satisfies

$$\ker X \subseteq \ker C \cap \ker A. \tag{2.14}$$

In particular, for passive ODE models which are behaviorally observable, the solution X is invertible (see [39]) and a pH-ODE realization can be found, for example, by left-

multiplication of the differential equations with X^T which yields a port-Hamiltonian descriptor matrix $X^\mathsf{T}E \geq 0$, $Q = I_n$ as well as

$$J = \tfrac{1}{2}(X^\mathsf{T}A - A^\mathsf{T}X), \qquad R = -\tfrac{1}{2}(X^\mathsf{T}A + A^\mathsf{T}X), \tag{2.15}$$

$$G = \tfrac{1}{2}(C^\mathsf{T} + X^\mathsf{T}B), \qquad P = \tfrac{1}{2}(C^\mathsf{T} - X^\mathsf{T}B), \tag{2.16}$$

$$N = \tfrac{1}{2}(D - D^\mathsf{T}), \qquad S = \tfrac{1}{2}(D + D^\mathsf{T}). \tag{2.17}$$

The pH structural properties in Definition 2.4 follow directly from the KYP-LMI (2.9). This approach may, however, also be used in the DAE setting: Since every passive DAE may be decomposed into a passive ODE part and an improper part that already has a pH structure, one may solve a modified KYP-LMI for the ODE part and treat the index-two part separately (see [39, A5]). We discuss this approach in more detail in Section 3.1 and conclude this section with the following statement: For minimal (and therefore behaviorally controllable and observable) models, the concepts of passivity, positive realness, and the existence of a pH-DAE realization are equivalent. This motivates the different MOR strategies depicted in Figure 1.1 since any of the three properties can be enforced for the structure-preserving MOR of pH-DAEs.

2.2 Fundamentals of Model Reduction

In the following, we recapitulate some relevant results from the field of MOR. We present the theory for general (unstructured) state-space models Σ to highlight the differences and challenges in the pH-DAE setting in Chapters 3 and 4.

The main goal of MOR is to approximate a large-scale model Σ with a ROM of order $r \ll n$

$$\widehat{\Sigma} : \begin{cases} \widehat{E}\dot{\widehat{x}}(t) = \widehat{A}\widehat{x}(t) + \widehat{B}u(t), \\ \widehat{y}(t) = \widehat{C}\widehat{x}(t) + \widehat{D}u(t), \end{cases} \tag{2.18}$$

where $\widehat{E}$, $\widehat{A} \in \mathbb{R}^{r\times r}$, $\widehat{B} \in \mathbb{R}^{r\times m}$, $\widehat{C} \in \mathbb{R}^{p\times r}$, $\widehat{D} \in \mathbb{R}^{p\times m}$, and such that the error $\|y - \widehat{y}\|$ is small in an appropriate norm for admissible inputs u. If a particular input signal u was known, one could strive to minimize the error in the output signals directly. In general, it is, however, desired that the ROM approximates the FOM well for a large class of admissible inputs. Therefore, performance measures in MOR are typically formalized in the frequency domain. If the transfer function H of an asymptotically stable model

Σ is strictly proper (proper), it is an element of the Hardy space $\mathcal{H}_2^{p\times m}$ ($\mathcal{H}_\infty^{p\times m}$). These are defined as

$$\mathcal{H}_2^{p\times m} := \left\{ H : \mathbb{C}_+ \to \mathbb{C}^{p\times m} \;\middle|\; \begin{array}{l} H \text{ is analytic and} \\ \sup_{\sigma>0} \int_{-\infty}^{\infty} \|H(\sigma+\mathrm{i}\omega)\|_{\mathrm{F}}^2 \mathrm{d}\omega < \infty \end{array} \right\}, \tag{2.19}$$

$$\mathcal{H}_\infty^{p\times m} := \left\{ H : \mathbb{C}_+ \to \mathbb{C}^{p\times m} \;\middle|\; \begin{array}{l} H \text{ is analytic and} \\ \sup_{\lambda\in\mathbb{C}_+} \|H(\lambda)\|_2 < \infty \end{array} \right\}. \tag{2.20}$$

$\mathcal{H}_2^{p\times m}$ and $\mathcal{H}_\infty^{p\times m}$ are Banach spaces and equipped with the norms

$$\|H\|_{\mathcal{H}_2} := \left(\frac{1}{2\pi}\int_{-\infty}^{\infty} \|H(\mathrm{i}\omega)\|_{\mathrm{F}}^2 \mathrm{d}\omega\right)^{1/2}, \qquad \|H\|_{\mathcal{H}_\infty} := \operatorname{ess\,sup}_{\omega\in\mathbb{R}} \|H(\mathrm{i}\omega)\|_2, \tag{2.21}$$

respectively. These norms are natural measures of the worst-case performance for many classes of input signals (see [162, Chapter 4] for an overview) and common metrics in MOR. Let $\mathcal{L}_2$ and $\mathcal{L}_\infty$ denote the respective Lebesgue spaces of functions defined for $t \in \mathbb{R}_{\geq 0}$. For the class of $\mathcal{L}_2$-bounded inputs, the following upper bounds for the output error can be derived (see [8, Section 2.1.1])

$$\begin{aligned} \|y - \widehat{y}\|_{\mathcal{L}_2} &\leq \|H - \widehat{H}\|_{\mathcal{H}_\infty} \|u\|_{\mathcal{L}_2}, \\ \|y - \widehat{y}\|_{\mathcal{L}_\infty} &\leq \|H - \widehat{H}\|_{\mathcal{H}_2} \|u\|_{\mathcal{L}_2}. \end{aligned}$$

Minimizing the error $H - \widehat{H}$ with respect to the $\mathcal{H}_2$ or the $\mathcal{H}_\infty$ norm will therefore result in low output errors for a wide range of admissible inputs. In this thesis, we focus on methods designed to yield low errors in the $\mathcal{H}_2$ norm.

2.2.1 $\mathcal{H}_2$ Computation Frameworks

There exist two frameworks in which the error $\|H - \widehat{H}\|_{\mathcal{H}_2}$ may be computed: the *Lyapunov* and *pole-residue* framework. If the ROM is computed such that $H - \widehat{H} \in \mathcal{H}_2^{p\times m}$, we have that

$$\|H - \widehat{H}\|_{\mathcal{H}_2} = \|H_{\mathrm{sp}} - \widehat{H}_{\mathrm{sp}}\|_{\mathcal{H}_2}.$$

For the sake of notational simplicity, we present the relevant results for realizations Σ with $E = I$ and $D = 0$ since the strictly proper part of every transfer function as in (2.3) has such a realization (see Section 2.1). Without loss of generality, we apply the same assumptions to $\widehat{\Sigma}$.

Lyapunov Framework The Lyapunov framework provides an *internal* view on the $\mathcal{H}_2$ error, utilizing state-space representations. For this, define an error system realization Σ_e of the form (2.1) with

$$A_e = \begin{bmatrix} A & 0 \\ 0 & \widehat{A} \end{bmatrix}, \quad B_e = \begin{bmatrix} B \\ \widehat{B} \end{bmatrix}, \quad C_e = \begin{bmatrix} C & -\widehat{C} \end{bmatrix}, \quad E_e = I_{n_e}, \quad D_e = 0, \tag{2.22}$$

where $n_e = n + r$ and which has an associated transfer function $H_e(s) = H(s) - \widehat{H}(s)$. Let $\mathcal{P}$, $\mathcal{Q} \in \mathbb{R}^{n_e \times n_e}$ denote the symmetric positive semidefinite *controllability* and *observability* Gramians, respectively, which are the solutions to the dual Lyapunov equations

$$A_e \mathcal{P} + \mathcal{P} A_e^{\mathsf{T}} + B_e B_e^{\mathsf{T}} = 0, \tag{2.23a}$$

$$A_e^{\mathsf{T}} \mathcal{Q} + \mathcal{Q} A_e + C_e^{\mathsf{T}} C_e = 0. \tag{2.23b}$$

Using Parseval's theorem (see [8]), we obtain

$$\|H - \widehat{H}\|_{\mathcal{H}_2}^2 = \|H_e\|_{\mathcal{H}_2}^2 = \operatorname{tr}(B_e^{\mathsf{T}} \mathcal{Q} B_e) = \operatorname{tr}(C_e \mathcal{P} C_e^{\mathsf{T}}). \tag{2.24}$$

If the Gramians are partitioned consistently with the matrices in (2.22) into

$$\mathcal{P} = \begin{bmatrix} \mathcal{P}_{11} & \mathcal{P}_{12} \\ \mathcal{P}_{12}^{\mathsf{T}} & \mathcal{P}_{22} \end{bmatrix}, \quad \mathcal{Q} = \begin{bmatrix} \mathcal{Q}_{11} & \mathcal{Q}_{12} \\ \mathcal{Q}_{12}^{\mathsf{T}} & \mathcal{Q}_{22} \end{bmatrix},$$

the error may be decomposed such that

$$\begin{aligned} \|H - \widehat{H}\|_{\mathcal{H}_2}^2 &= \operatorname{tr}(B^{\mathsf{T}} \mathcal{Q}_{11} B + 2 B^{\mathsf{T}} \mathcal{Q}_{12} \widehat{B} + \widehat{B}^{\mathsf{T}} \mathcal{Q}_{22} \widehat{B}) \\ &= \operatorname{tr}(C \mathcal{P}_{11} C^{\mathsf{T}} - 2 C \mathcal{P}_{12} \widehat{C}^{\mathsf{T}} + \widehat{C} \mathcal{P}_{22} \widehat{C}^{\mathsf{T}}). \end{aligned} \tag{2.25}$$

The necessary conditions for $\mathcal{H}_2$ optimality

$$\mathcal{Q}_{22} \mathcal{P}_{22} + \mathcal{Q}_{12}^{\mathsf{T}} \mathcal{P}_{12} = 0, \tag{2.26a}$$

$$\mathcal{Q}_{22} \widehat{B} + \mathcal{Q}_{12}^{\mathsf{T}} B = 0, \tag{2.26b}$$

$$\widehat{C} \mathcal{P}_{22} - C \mathcal{P}_{12} = 0, \tag{2.26c}$$

derived in [80, 153], are obtained by differentiation with respect to the reduced state-space matrices $\widehat{A}$, $\widehat{B}$, $\widehat{C}$. Note that these conditions do not depend on the submatrices $\mathcal{P}_{11}$, $\mathcal{Q}_{11}$, which is a direct consequence of the decomposition in (2.25). The summands

$B^\mathsf{T}\mathcal{Q}_{11}B$ and $C\mathcal{P}_{11}C^\mathsf{T}$ are independent of the ROM matrices and therefore vanish in the gradient.

Pole-Residue Framework The second framework gives an *external* view on the $\mathcal{H}_2$ error, which is purely based on the original and reduced system's transfer function. It exploits the fact that ${\mathcal{H}_2}^{p\times m}$ is a Hilbert space equipped with the inner product

$$\langle H_1, H_2\rangle_{\mathcal{H}_2} := \frac{1}{2\pi}\int_{-\infty}^{\infty} \operatorname{tr}\left(\overline{H_1(\mathrm{i}\omega)}H_2(\mathrm{i}\omega)^\mathsf{T}\right)\mathrm{d}\omega \tag{2.27}$$

for $H_1, H_2 \in {\mathcal{H}_2}^{p\times m}$ [8]. For the real-rational transfer functions H, $\widehat{H} \in {\mathcal{H}_2}^{p\times m}$, we may decompose the $\mathcal{H}_2$ error such that

$$\begin{aligned}\|H-\widehat{H}\|_{\mathcal{H}_2}^2 &= \langle H-\widehat{H}, H-\widehat{H}\rangle_{\mathcal{H}_2}\\ &= \langle H, H\rangle_{\mathcal{H}_2} - 2\langle H, \widehat{H}\rangle_{\mathcal{H}_2} + \langle \widehat{H}, \widehat{H}\rangle_{\mathcal{H}_2}.\end{aligned}$$

To compute the involved inner products, let us assume that the reduced transfer function $\widehat{H}$ has simple *poles* $\{\lambda_1, \ldots, \lambda_r\} \subset \mathbb{C}$. Then, $\widehat{H}$ admits the *pole-residue expansion*

$$\widehat{H}(s) = \sum_{i=1}^{r} \frac{\mathsf{l}_i\mathsf{r}_i^\mathsf{T}}{s-\lambda_i} \tag{2.28}$$

with *residues* $\mathsf{l}_i\mathsf{r}_i^\mathsf{T}$ and where $\mathsf{l}_i \in \mathbb{C}^p$, $\mathsf{r}_i \in \mathbb{C}^m$ for all $i = 1, \ldots, r$. Since $\operatorname{tr}(H(-s)\widehat{H}(s)^\mathsf{T})$ is analytic on $\mathbb{C}_-\backslash\{\lambda_1, \ldots, \lambda_r\}$, the residue theorem can be applied to compute the inner product $\langle H, \widehat{H}\rangle_{\mathcal{H}_2}$. Embedding the pole-residue expansion yields [67]

$$\langle H, \widehat{H}\rangle_{\mathcal{H}_2} = \sum_{i=1}^{r} \mathsf{l}_i^\mathsf{T} H(-\lambda_i)\mathsf{r}_i. \tag{2.29}$$

The same can be applied to the inner product $\langle \widehat{H}, \widehat{H}\rangle$ to obtain the $\mathcal{H}_2$ error expression in decomposed form [19]

$$\|H-\widehat{H}\|_{\mathcal{H}_2}^2 = \|H\|_{\mathcal{H}_2}^2 - 2\sum_{i=1}^{r}\mathsf{l}_i^\mathsf{T}H(-\lambda_i)\mathsf{r}_i + \sum_{j=1}^{r}\sum_{k=1}^{r}\frac{\mathsf{l}_j^\mathsf{T}\mathsf{l}_k\mathsf{r}_k^\mathsf{T}\mathsf{r}_j}{-\lambda_j-\lambda_k}. \tag{2.30}$$

Differentiation of this expression with respect to the reduced-order poles and residues yields the necessary conditions for $\mathcal{H}_2$ optimality in the form of tangential interpolation conditions. For SISO systems, these conditions were originally derived by Meier and Luenberger in [106] and are therefore also referred to as *Meier-Luenberger conditions*.

These results were generalized to continuous- and discrete-time MIMO systems with simple poles in [31, 44, 67].

Theorem 2.1. [31, 44, 67] *Let $H \in \mathcal{H}_2{}^{p\times m}$ denote the strictly proper transfer function of a FOM as in (2.1). Consider a ROM as in (2.18) with strictly proper transfer function $\widehat{H} \in \mathcal{H}_2{}^{p\times m}$ that admits the pole-residue expansion in (2.28). If $\widehat{H}$ is a local minimizer of $\mathcal{H}_2{}^{p\times m} \to \mathbb{R}$, $\widehat{H} \mapsto \|H - \widehat{H}\|_{\mathcal{H}_2}$, then*

$$H(-\lambda_i)\mathsf{r}_i = \widehat{H}(-\lambda_i)\mathsf{r}_i, \tag{2.31a}$$

$$\mathsf{l}_i^{\mathsf{T}} H(-\lambda_i) = \mathsf{l}_i^{\mathsf{T}} \widehat{H}(-\lambda_i), \tag{2.31b}$$

$$\mathsf{l}_i^{\mathsf{T}} H'(-\lambda_i)\mathsf{r}_i = \mathsf{l}_i^{\mathsf{T}} \widehat{H}'(-\lambda_i)\mathsf{r}_i \tag{2.31c}$$

holds for all $i = 1, \ldots, r$. Here, $H'(-\lambda_i)$ denotes the derivative of $H(s)$ with respect to s evaluated at $s = -\lambda_i$.

Throughout this work, we retain the assumption that $\widehat{H}$ allows a decomposition as in (2.28). For a generalization of the presented results to systems with higher-order poles, the interested reader is referred to [45].

The connection between the Lyapunov and pole-residue framework was established in [67] by showing the equivalence of the first-order necessary conditions presented in [80, 153] and [106], respectively, to structured orthogonality conditions. Consequently, the $\mathcal{H}_2$ optimization problem can also be solved in both frameworks. However, there are differences when it comes to numerical efficiency. Gradient-based methods using the Lyapunov framework (see, e.g., [131, 133, 145, 153, 159]) require solving a series of coupled sparse-dense Sylvester equations which can be computationally challenging, especially for large-scale models, and which restricts their applicability to small and medium-scale models. On the other hand, algorithms in the pole-residue framework only require the computation of the pole-residue expansion for the ROM and samples of the original transfer function (and its derivative) at the reduced-order poles. The pole-residue expansion can be efficiently computed using a generalized eigenvalue decomposition of the matrix pencil $s\widehat{E} - \widehat{A}$ (see, e.g., [8]), and sampling the original transfer function is also feasible in the large-scale context. Therefore, we focus on MOR methods that navigate in the pole-residue framework in this thesis and refer the interested reader to [84, 132] for $\mathcal{H}_2$-inspired, optimization-based MOR of pH-ODE models in the Lyapunov framework.

2.2.2 Projective Model Reduction

A typical way to compute ROMs is by means of *Petrov-Galerkin* projections. This approach is based on the assumption that the original state vector x evolves in an r-dimensional *trial subspace* $\mathcal{V} \subset \mathbb{R}^n$. Using a matrix $V \in \mathbb{R}^{n \times r}$ whose columns form a basis of $\mathcal{V}$, we assume that

$$x(t) \approx V\widehat{x}(t) \tag{2.32}$$

with reduced state vector $\widehat{x}(t) \in \mathbb{R}^r$ for all $t \in \mathbb{R}_{\geq 0}$. Inserting this approximation into the differential equations in (2.1) induces a residual $\varepsilon \in \mathbb{R}^n$ such that

$$EV\dot{\widehat{x}}(t) = AV\widehat{x}(t) + Bu(t) + \varepsilon(t). \tag{2.33}$$

Next, a *test subspace* $\mathcal{U} \subset \mathbb{R}^n$ with basis matrix $U \in \mathbb{R}^{n \times r}$ is defined. The reduced state vector is chosen such that the residual ε is orthogonal to $\mathcal{U}$, i.e., $U^\mathsf{T}\varepsilon(t) = 0$ for all $t \in \mathbb{R}_{\geq 0}$. This constraint is also called *Petrov-Galerkin condition*. Combining this condition with (2.33) yields the reduced dynamics

$$U^\mathsf{T}EV\dot{\widehat{x}}(t) = U^\mathsf{T}AV\widehat{x}(t) + U^\mathsf{T}Bu(t). \tag{2.34}$$

Finally, the insertion of approximation (2.32) into the output equation leads to the approximate output

$$\widehat{y}(t) = CV\widehat{x}(t) + Du(t)$$

and a reduced-order state-space realization $\widehat{\Sigma}$ as in (2.18) with

$$\widehat{E} = U^\mathsf{T}EV, \quad \widehat{A} = U^\mathsf{T}AV, \quad \widehat{B} = U^\mathsf{T}B, \quad \widehat{C} = CV, \quad \widehat{D} = D. \tag{2.35}$$

Projections with equal test and trial subspace are also referred to as *Galerkin* or *Ritz-Galerkin* projections [8]. Here, both subspaces are usually also equipped with the same basis. The reduced transfer function only depends on the subspaces $\mathcal{U}$, $\mathcal{V}$ and is invariant under a change of basis [8]. Therefore, the column vectors in U and V are often chosen orthonormal ($U^\mathsf{T}U = I_r$, $V^\mathsf{T}V = I_r$) or biorthogonal ($U^\mathsf{T}V = I_r$) to improve numerical robustness in MOR.

2.2.3 Tangential Interpolation

The challenge in projective MOR is to design the subspaces $\mathcal{U}$, $\mathcal{V}$ such that accurate approximations are obtained. One possible strategy is to choose these subspaces such

that interpolation conditions between the original and reduced transfer functions are enforced, as initially proposed by Skelton and de Villemagne [150]. For SISO systems, this approach is also referred to as *moment matching* or *rational Krylov method*, since the rational Krylov subspace methods of [128] can be employed for numerical efficiency [62]. We refer the interested reader to [8, 16] for a comprehensive overview. In this work, we only consider the more general MIMO case, where interpolation conditions are typically enforced along selected tangential directions as initially proposed in [57].

Let $\{\sigma_1, \ldots, \sigma_r\} \subset \mathbb{C}$ denote a set of r complex interpolation points with associated left and right tangential directions $\{c_1, \ldots, c_r\} \subset \mathbb{C}^p$ and $\{b_1, \ldots, b_r\} \subset \mathbb{C}^m$, respectively. Motivated by the $\mathcal{H}_2$ optimality conditions in Theorem 2.1, we strive to compute a ROM $\widehat{\Sigma}$ with associated transfer function $\widehat{H}$ such that

$$H(\sigma_i)b_i = \widehat{H}(\sigma_i)b_i, \qquad i = 1, \ldots, r, \tag{2.36a}$$

$$c_i^{\mathsf{T}} H(\sigma_i) = c_i^{\mathsf{T}} \widehat{H}(\sigma_i), \qquad i = 1, \ldots, r, \tag{2.36b}$$

$$c_i^{\mathsf{T}} H'(\sigma_i)b_i = c_i^{\mathsf{T}} \widehat{H}'(\sigma_i)b_i, \qquad i = 1, \ldots, r. \tag{2.36c}$$

which can be enforced by Petrov-Galerkin projections in the following way.

Theorem 2.2. [8, Theorem 3.3.1] *Consider a FOM Σ with transfer function H. Let a ROM $\widehat{\Sigma}$ with transfer function $\widehat{H}$ be constructed as in (2.35) with basis matrices $U, V \in \mathbb{C}^{n\times r}$. For all $i = 1, \ldots, r$, let interpolation points $\sigma_i \in \mathbb{C}$ with associated tangential directions $b_i \in \mathbb{C}^m$, $c_i \in \mathbb{C}^p$ be given such that $\sigma_i E - A$ and $\sigma_i \widehat{E} - \widehat{A}$ are nonsingular.*

(i) If

$$(\sigma_i E - A)^{-1} B b_i \in \operatorname{im} V, \qquad i = 1, \ldots, r, \tag{2.37a}$$

then (2.36a) holds,

(ii) If

$$(\sigma_i E - A)^{-\mathsf{T}} C^{\mathsf{T}} c_i \in \operatorname{im} U, \qquad i = 1, \ldots, r, \tag{2.37b}$$

then (2.36b) holds,

(iii) If

both (2.37a) and (2.37b) hold, $\qquad i = 1, \ldots, r,$

then (2.36c) holds.

The conditions in (2.36c) are also referred to as *bitangential Hermite interpolation conditions* [16]. Since all conditions in Theorem 2.2 depend on the subspaces spanned by the columns of U and V rather than the basis matrices themselves, they can again

be chosen orthonormal or biorthogonal. In particular, if the interpolation points and associated tangential directions occur in complex conjugate pairs, real basis vectors can be chosen. In this case, we will also speak of sets that are *closed under complex conjugation*.

A significant advantage of interpolatory model reduction is computational efficiency. Since most of the computational effort is spent on solving linear systems of equations (LSEs), it is particularly suited for reducing very large models. The major challenge is the choice of appropriate interpolation data such that low errors in the $\mathcal{H}_2$ or $\mathcal{H}_\infty$ norm are obtained, which is also discussed in the following chapter.

3 Summary of Achievements

In this chapter, we summarize the main contributions of the publications [A1–A5] which address the $\mathcal{H}_2$-inspired reduction of large-scale pH-DAE models. As motivated in Section 1.1, a central aspect of this task is *structure preservation*, i.e., our goal is to construct ROMs of the form

$$\widehat{\Sigma}_{\mathrm{pH}} : \begin{cases} \widehat{E}\dot{\widehat{x}}(t) = (\widehat{J} - \widehat{R})\widehat{x}(t) + (\widehat{G} - \widehat{P})u(t), \\ \widehat{y}(t) = (\widehat{G} + \widehat{P})^{\mathsf{T}}\widehat{x}(t) + (\widehat{S} + \widehat{N})u(t) \end{cases} \tag{3.1}$$

with $\widehat{E}$, $\widehat{J}$, $\widehat{R} \in \mathbb{R}^{r\times r}$, $\widehat{G}$, $\widehat{P} \in \mathbb{R}^{r\times m}$, $\widehat{S}$, $\widehat{N} \in \mathbb{R}^{m\times m}$ that fulfill the structural constraints in Definition 2.4. Given an original pH-DAE model Σ_{pH} of dimension n with transfer function H and a desired reduced order $r \ll n$ this yields the following (non-convex) optimization problem:

$$\begin{aligned} &\text{minimize} && \mathcal{J}(\widehat{H}) := \|H - \widehat{H}\|_{\mathcal{H}_2}, \\ &\text{such that} && \widehat{H} \text{ has a realization } \widehat{\Sigma}_{\mathrm{pH}}. \end{aligned} \tag{3.2}$$

We tackle this optimization problem in the computationally efficient pole-residue framework (see Section 2.2.1) and proceed as follows. In Section 3.1, we present a high-level overview of our approach: a system decomposition [A5] that separates the original transfer function into a proper and improper part with specific properties. Subsequently, two strategies are presented to create $\mathcal{H}_2$-inspired ROMs: either based on the work in [A2, A4] using Petrov-Galerkin projections (Section 3.2) or using direct optimization of parameterized reduced-order models as presented in [A3, A5] (Section 3.3). We close the chapter with a brief discussion of the software toolbox MORpH [A1] in Section 3.4. MORpH implements the algorithms discussed in this chapter and other state-of-the-art methods suitable for the structure-preserving reduction of pH-DAEs. For technical details and further information on the algorithms presented in this chapter, the reader is referred to the respective publications reprinted in Appendix A.

3.1 A System Decomposition Approach [A5]

Before different strategies for the optimization of the cost function $\mathcal{J}$ can be addressed, the ROM has to be chosen such that it is well-defined, i.e., $H - \widehat{H} \in \mathcal{H}_2^{m\times m}$. Since the decomposition in (2.6) also holds for pH-DAEs as in Definition 2.4, which have a Kronecker index of at most two, the transfer function of pH-DAEs may be decomposed such that

$$H(s) = H_{\text{sp}}(s) + H_{\text{pol}}(s) = H_{\text{sp}}(s) + D_0 + s \cdot D_1 \tag{3.3}$$

with polynomial coefficients D_0, $D_1 \in \mathbb{R}^{m\times m}$. In the following, the abbreviations $H_{\text{pol},0}(s) := D_0$ and $H_{\text{pol},1}(s) := s \cdot D_1$ are used for the constant and linear polynomial part, respectively. In Figure 3.1, this decomposition is illustrated for an exemplary pH-DAE model with Kronecker index $\nu = 2$, $n = 1502$, and $m = 1$. It is the model of a passive electrical ladder network consisting of linear resistors, capacitors, inductors, and a voltage source. Such models are typically used to simulate VLSI interconnect systems or transmission lines. The pH-DAE model in staircase form was generated using the port-Hamiltonian benchmark collection[1] to which we refer for a more detailed physical description. We will use this model throughout this chapter for illustration purposes. As shown in Figure 3.1, the magnitude of the frequency response is dominated by the constant and linear polynomial part for low and high frequencies, respectively, and by the strictly proper part in the intermediate frequency region.

If the original model is approximated with a ROM that is also in pH-DAE form, the transfer function error may be decomposed accordingly

$$H(s) - \widehat{H}(s) = (H_{\text{sp}}(s) - \widehat{H}_{\text{sp}}(s)) + (H_{\text{pol}}(s) - \widehat{H}_{\text{pol}}(s)).$$

Given our initial assumption that the finite eigenvalues of the pencils $sE - (J - R)$ and $s\widehat{E} - (\widehat{J} - \widehat{R})$ are in the open left half-plane, $H - \widehat{H} \in \mathcal{H}_2^{m\times m}$ holds if, and only if, the reduced and original polynomial parts match precisely. The strategy for MOR is the following: separate the strictly proper and polynomial parts of the original transfer function and subsequently approximate *only* the strictly proper part H_{sp} and retain the polynomial part H_{pol} that originates from the system's feedthrough and algebraic constraints. While this strategy has also been used for unstructured DAEs (see, e.g., [71]), the challenge for the system class of pH-DAEs is to implement this approach in a structure-preserving way, such that the ROM has the form in (3.1). For this, additional

[1] `https://port-hamiltonian.io`

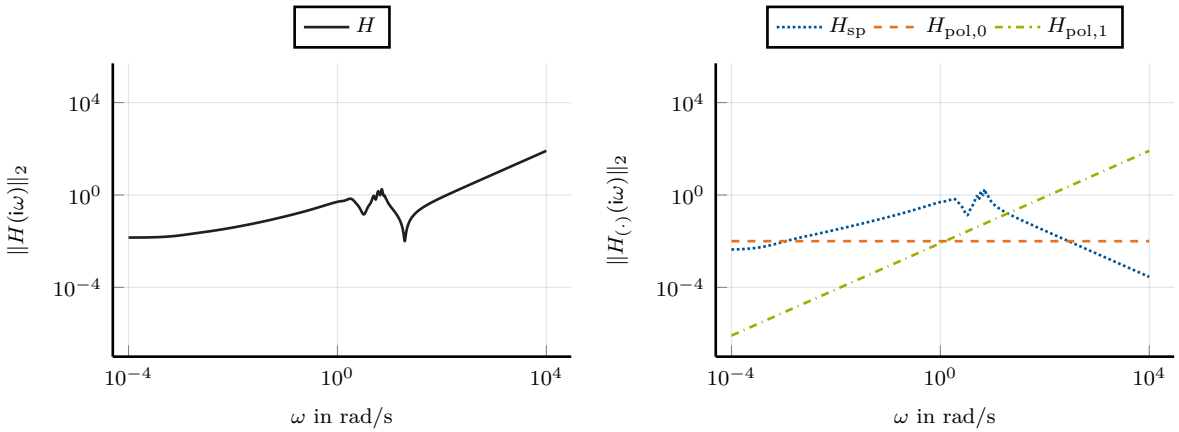

Figure 3.1: Transfer function H of an exemplary pH-DAE model with Kronecker index two (left) and its additive decomposition (right) into strictly proper part H_{sp}, constant polynomial part $H_{\mathrm{pol},0}$ and linear polynomial part $H_{\mathrm{pol},1}$.

structural properties of the decomposition in (3.3) are helpful, which were derived in [A5].

Lemma 3.1. [A5] *Given is a pH-DAE model Σ_{pH} with transfer function H that has a decomposition as in (3.3). Then,*

(i) the proper part $H_{\mathrm{p}}(s) := H_{\mathrm{sp}}(s) + D_0$ has a pH-ODE realization

$$\Sigma_{\mathrm{pH,p}} : \begin{cases} E_{\mathrm{p}}\dot{x}_{\mathrm{p}}(t) = (J_{\mathrm{p}} - R_{\mathrm{p}})x_{\mathrm{p}}(t) + (G_{\mathrm{p}} - P_{\mathrm{p}})u(t), \\ y_{\mathrm{p}}(t) = (G_{\mathrm{p}} + P_{\mathrm{p}})^{\mathsf{T}}x_{\mathrm{p}}(t) + (S_{\mathrm{p}} + N_{\mathrm{p}})u(t) \end{cases} \tag{3.4}$$

with $x_{\mathrm{p}} : \mathbb{R}_{\geq 0} \to \mathbb{R}^{n_2}$ and $E_{\mathrm{p}} > 0$, where n_2 is obtained from the staircase form in Lemma 2.3, and

(ii) D_1 is symmetric positive semidefinite.

These results enable a two-step approach for the optimization problem in (3.2). At first, the pH-ODE model $\Sigma_{\mathrm{pH,p}}$ in (3.4) is reduced in a structure-preserving way to obtain a reduced pH-ODE model

$$\widehat{\Sigma}_{\mathrm{pH,p}} : \begin{cases} \widehat{E}_{\mathrm{p}}\dot{\widehat{x}}_{\mathrm{p}}(t) = (\widehat{J}_{\mathrm{p}} - \widehat{R}_{\mathrm{p}})\widehat{x}_{\mathrm{p}}(t) + (\widehat{G}_{\mathrm{p}} - \widehat{P}_{\mathrm{p}})u(t), \\ \widehat{y}_{\mathrm{p}}(t) = (\widehat{G}_{\mathrm{p}} + \widehat{P}_{\mathrm{p}})^{\mathsf{T}}\widehat{x}_{\mathrm{p}}(t) + (\widehat{S}_{\mathrm{p}} + \widehat{N}_{\mathrm{p}})u(t) \end{cases} \tag{3.5}$$

with $\widehat{x}_{\mathrm{p}} : \mathbb{R}_{\geq 0} \to \mathbb{R}^{r_{\mathrm{p}}}$, $\widehat{E}_{\mathrm{p}} > 0$ and transfer function $\widehat{H}_{\mathrm{p}}$. Matching the constant polynomial part $H_{\mathrm{pol},0}$ of the original transfer function is achieved by enforcing

$$\widehat{S}_{\mathrm{p}} = \frac{1}{2}(D_0 + D_0^{\mathsf{T}}) \qquad \text{and} \qquad \widehat{N}_{\mathrm{p}} = \frac{1}{2}(D_0 - D_0^{\mathsf{T}}). \tag{3.6}$$

In the second step, the improper part $H_{\mathrm{pol},1}$ of the original model has to be added to $\widehat{H}_{\mathrm{p}}$. For this, we exploit the fact that D_1 is symmetric positive semidefinite and use a rank-revealing factorization $D_1 = L_1 L_1^{\mathsf{T}}$ with $L_1 \in \mathbb{R}^{m \times \ell}$ and $\ell \leq m$. As shown in [A5], a minimal realization of $H_{\mathrm{pol},1}$ in pH-DAE staircase form is given by

$$\begin{aligned} \begin{bmatrix} I_\ell & 0 \\ 0 & 0 \end{bmatrix} \dot{x}_\infty(t) &= \begin{bmatrix} 0 & I_\ell \\ -I_\ell & 0 \end{bmatrix} x_\infty(t) + \begin{bmatrix} 0 \\ L_1^{\mathsf{T}} \end{bmatrix} u(t), \\ y_\infty(t) &= \begin{bmatrix} 0 & L_1 \end{bmatrix} x_\infty(t), \end{aligned} \tag{3.7}$$

where $x_\infty(t) = \left[x_{\infty,1}(t)^{\mathsf{T}}, x_{\infty,2}(t)^{\mathsf{T}}\right]^{\mathsf{T}}$ and where $x_{\infty,1}, x_{\infty,2} : \mathbb{R}_{\geq 0} \to \mathbb{R}^\ell$. Note that a different realization was presented by Cherifi *et al.* [39], which is, however, not minimal for singular D_1.

Since both $\widehat{H}_{\mathrm{p}}$ and $H_{\mathrm{pol},1}$ have pH-DAE realizations, this is also the case for their sum. As shown in [A4], a minimal realization $\widehat{\Sigma}_{\mathrm{pH}}$ in staircase form with state-space dimension $r = r_{\mathrm{p}} + 2\ell$ is obtained using the partitioned reduced state vector $\widehat{x}(t) = \left[x_{\infty,1}(t)^{\mathsf{T}}, \widehat{x}_{\mathrm{p}}(t)^{\mathsf{T}}, x_{\infty,2}(t)^{\mathsf{T}}\right]^{\mathsf{T}}$ and matrices

$$\begin{aligned} \widehat{E} &= \begin{bmatrix} I_\ell & 0 & 0 \\ 0 & \widehat{E}_{\mathrm{p}} & 0 \\ 0 & 0 & 0 \end{bmatrix}, \quad \widehat{J} = \begin{bmatrix} 0 & 0 & I_\ell \\ 0 & \widehat{J}_{\mathrm{p}} & 0 \\ -I_\ell & 0 & 0 \end{bmatrix}, \quad \widehat{R} = \begin{bmatrix} 0 & 0 & 0 \\ 0 & \widehat{R}_{\mathrm{p}} & 0 \\ 0 & 0 & 0 \end{bmatrix}, \\ \widehat{G} &= \begin{bmatrix} 0 \\ \widehat{G}_{\mathrm{p}} \\ L_1^{\mathsf{T}} \end{bmatrix}, \quad \widehat{P} = \begin{bmatrix} 0 \\ \widehat{P}_{\mathrm{p}} \\ 0 \end{bmatrix}, \quad \widehat{S} = \widehat{S}_{\mathrm{p}}, \quad \widehat{N} = \widehat{N}_{\mathrm{p}}. \end{aligned} \tag{3.8}$$

Its transfer function $\widehat{H}$ has the same polynomial part H_{pol} as the original and consequently $H - \widehat{H} \in \mathcal{H}_2^{m \times m}$. This approach's major challenge lies in identifying the subsystem $\Sigma_{\mathrm{pH,p}}$ and the matrix D_1. While they could theoretically be obtained by computing canonical forms such as the Weierstraß form in (2.5), this is generally not possible for large-scale models (see the discussion in Section 2.1.2). We present two strategies to alleviate this problem in the following two sections.

3.2 Interpolatory Model Reduction

The presented system decomposition approach can be utilized for interpolatory model reduction. We derive a Rosenbrock framework in Section 3.2.1, which was initially published in [A4] and provides a unifying MOR framework for pH-DAEs in staircase form. The integration of shift selection strategies is demonstrated using two algorithmic examples. In Section 3.2.2, we illustrate how surrogate models can be used to further reduce the computational cost of iterative interpolatory MOR methods as proposed in [A2].

3.2.1 A Rosenbrock Framework [A4]

The Rosenbrock framework derived in [A4] is based on the observation that not only state-space transformations but also Petrov-Galerkin projections can be formulated as operations on Rosenbrock system matrices. For general state-space models, the ROM matrices as in (2.35) can be obtained directly from a reduced Rosenbrock matrix $\widehat{\mathcal{P}} \in \mathbb{R}[s]^{(r+p)\times(r+m)}$ which is computed by

$$\widehat{\mathcal{P}}(s) = U_{\mathcal{P}}^{\mathsf{T}} \mathcal{P}(s) V_{\mathcal{P}} = \begin{bmatrix} U^{\mathsf{T}} & 0 \\ 0 & I_p \end{bmatrix} \mathcal{P}(s) \begin{bmatrix} V & 0 \\ 0 & I_m \end{bmatrix} = \begin{bmatrix} s\widehat{E} - \widehat{A} & -\widehat{B} \\ \widehat{C} & \widehat{D} \end{bmatrix}. \tag{3.9}$$

The challenge for pH-DAEs is to define a similar, structure-preserving operation such that the reduced Rosenbrock system matrix $\widehat{\mathcal{P}}$ allows an additive decomposition as in (2.11) to extract a reduced pH-DAE realization. In [A4], such an operation was defined for pH-DAE models in staircase form. For the sake of notational simplicity, we use $A = J - R$, $B = G - P$, $C = (G + P)^{\mathsf{T}}$ and $D = S + N$ for the state-space matrices of the FOM Σ_{pH}. These matrices shall be partitioned as in Lemma 2.3, i.e., $A_{14} \in \mathbb{R}^{n_1 \times n_4}$ denotes the upper right block matrix of $J - R$.

Theorem 3.1. [A4] *Let $\mathcal{P}$ denote the Rosenbrock system matrix of a pH-DAE model Σ_{pH} in staircase form with transfer function H. Given a set of interpolation points $\{\sigma_1, \ldots, \sigma_{r_{\mathrm{p}}}\} \subset \mathbb{C}$ and corresponding right tangential directions $\{b_1, \ldots, b_{r_{\mathrm{p}}}\} \subset \mathbb{C}^m$ both closed under complex conjugation, define $V \in \mathbb{R}^{n \times r_{\mathrm{p}}}$ such that (2.37a) holds with*

a decomposition $V = [V_1^\mathsf{T}, V_2^\mathsf{T}, V_3^\mathsf{T}, V_4^\mathsf{T}]^\mathsf{T}$ *with* $V_j \in \mathbb{R}^{n_j \times r_\mathrm{p}}$ *for all* $j = 1, \ldots, 4$ *as in Lemma 2.3. Define the matrices*

$$U_\mathcal{P} := \begin{bmatrix} 0 & A_{14}^{-\mathsf{T}} C_4^\mathsf{T} \\ V_2 & 0 \\ -A_{33}^{-\mathsf{T}} A_{23}^\mathsf{T} V_2 & A_{33}^{-\mathsf{T}} (C_3^\mathsf{T} - A_{13}^\mathsf{T} A_{14}^{-\mathsf{T}} C_4^\mathsf{T}) \\ 0 & 0 \\ 0 & I_m \end{bmatrix}, \quad V_\mathcal{P} := \begin{bmatrix} 0 & A_{14}^{-\mathsf{T}} B_4 \\ V_2 & 0 \\ 0 & 0 \\ 0 & 0 \\ 0 & I_m \end{bmatrix}. \tag{3.10}$$

Then, the transfer function $\widehat{H}$ *associated with the reduced Rosenbrock system matrix*

$$\widehat{\mathcal{P}}(s) = U_\mathcal{P}^\mathsf{T} \mathcal{P}(s) V_\mathcal{P}$$

satisfies the tangential interpolation conditions (2.36a), matches the polynomial part of H *and has a pH-DAE realization.*

The beauty of using structure-preserving Rosenbrock operations for MOR is that, similar to the unstructured case in (3.9), a pH-DAE realization of the ROM can directly be obtained from $\widehat{\mathcal{P}}$. In fact, a decomposition into symmetric and skew-symmetric parts yields a form similar to (2.11):

$$\widehat{\mathcal{P}}(s) = s \underbrace{\begin{bmatrix} \widehat{E}_\mathrm{p} & 0 \\ 0 & D_1 \end{bmatrix}}_{\widehat{\mathcal{E}}} + \underbrace{\begin{bmatrix} -\widehat{J}_\mathrm{p} & -\widehat{G}_\mathrm{p} \\ \widehat{G}_\mathrm{p}^\mathsf{T} & \widehat{N}_\mathrm{p} \end{bmatrix}}_{\widehat{\Gamma}} + \underbrace{\begin{bmatrix} \widehat{R}_\mathrm{p} & \widehat{P}_\mathrm{p} \\ \widehat{P}_\mathrm{p}^\mathsf{T} & \widehat{S}_\mathrm{p} \end{bmatrix}}_{\widehat{W}}, \tag{3.11}$$

where $\widehat{E}_\mathrm{p} > 0$ [A4, Lemma 3.1]. This immediately reveals a pH realization $\widehat{\Sigma}_{\mathrm{pH,p}}$ for the proper part of $\widehat{H}$ as in (3.5) as well as the improper part of the original transfer function with matrix D_1. Since the improper part remains unchanged during the reduction, a minimal pH-DAE realization of the transfer function $\widehat{H}$ can be computed as in (3.8).

Note that Theorem 3.1 holds irrespective of the original model's Kronecker index. For any $j \in \{1, \ldots, 4\}$ with $n_j = 0$ in Lemma 2.3, the j-th block row in $U_\mathcal{P}$ and $V_\mathcal{P}$ is left empty. This enables a unifying approach that can be used for all pH-DAEs in staircase form. Similar to the MOR methods proposed for proper, semi-explicit pH-DAEs in [15, 50, 76], the interpolation conditions are enforced with only the block matrix V_2 of V. For numerical stability, V is typically chosen such that $V_2^\mathsf{T} V_2 = I_{r_\mathrm{p}}$ and the reader is referred to the discussion in [50] for details.

As mentioned in Section 2.2, the major challenge of interpolatory MOR approaches is the choice of suitable interpolation data. The use of Rosenbrock system matrices for

MOR can indeed be interpreted as a novel interpolation *framework* in the sense that it enables the integration of different shift selection strategies. In the following, we briefly illustrate this fact utilizing the two algorithms IRKA-PH [68] and TRKSM [46, 47] and the interested reader is referred to [A4] for technical details.

IRKA-PH The fact that the necessary $\mathcal{H}_2$ optimality conditions in Theorem 2.1 are formulated as tangential interpolation conditions motivates interpolatory MOR techniques for $\mathcal{H}_2$ reduction. Since the optimal interpolation data, i.e., the negative reduced-order poles and residue vectors, are not known in advance, the idea behind the *Iterative Rational Krylov Algorithm* (IRKA) [67] is to compute these iteratively employing a fixed-point iteration. For pH-DAE models, we additionally demand that the ROM is also in pH-DAE form. Therefore, fewer degrees of freedom are available for interpolation, and it is generally only possible to fulfill a subset of (2.31), e.g., the conditions in (2.31a). Enforcing these conditions iteratively leads to the IRKA-PH algorithm originally proposed for pH-ODE models in [68].

As shown in [A4], integrating this concept into the Rosenbrock framework for tangential interpolation is straightforward. Starting with some initial interpolation data, a ROM is computed in each iteration using Theorem 3.1. Assuming that the eigenvalues of the pencil $s\widehat{E}_\mathrm{p} - (\widehat{J}_\mathrm{p} - \widehat{R}_\mathrm{p})$ are simple, the strictly proper part $\widehat{H}_\mathrm{sp}$ of $\widehat{H}$ admits a pole-residue decomposition as in (2.28). The shifts and right tangential directions are then set to the negative reduced-order poles and right residue vectors, respectively. Upon convergence, the improper part is integrated to obtain a ROM as in (3.8), which satisfies the subset (2.31a) of $\mathcal{H}_2$ optimality conditions in (2.31). We summarize this approach in Algorithm 3.1.

Even though it is generally only possible to satisfy a subset of $\mathcal{H}_2$ optimality conditions with Algorithm 3.1, further degrees of freedom can still be exploited. This is because the transfer function obtained from the Galerkin projection in Theorem 3.1 changes between the interpolation points if a different realization of the FOM transfer function is chosen. As initially shown for ODE systems in [29], favorable realizations for the MOR of systems with positive real transfer functions can be found by means of the KYP lemma. In [A4], these results were extended to pH-DAEs. Here, the matrix V_2 in $U_\mathcal{P}$ is pre-multiplied by solutions of a modified KYP-LMI for the subsystem $\Sigma_{\mathrm{pH,p}}$ of the FOM. This does not affect the results in Theorem 3.1 but potentially leads to better approximations in the $\mathcal{H}_2$ norm as illustrated by numerical examples in [A4].

Algorithm 3.1: IRKA-PH for pH-DAEs [A4]

Input : Original model Σ_{pH} in staircase form with Rosenbrock matrix $\mathcal{P}$; initial interpolation data $\{\sigma_1, \ldots, \sigma_{r_\mathrm{p}}\} \subset \mathbb{C}$ and $\{b_1, \ldots, b_{r_\mathrm{p}}\} \subset \mathbb{C}^m$ (both closed under complex conjugation).

Output: Reduced-order model $\widehat{\Sigma}_{\mathrm{pH}}$.

while *not converged* **do**
- Compute $V = [V_1^\mathsf{T}, V_2^\mathsf{T}, V_3^\mathsf{T}, V_4^\mathsf{T}]^\mathsf{T} \in \mathbb{R}^{n \times r_\mathrm{p}}$ s.t. (2.37a) holds and $V_2^\mathsf{T} V_2 = I_{r_\mathrm{p}}$.
- Compute $\widehat{\mathcal{P}}(s) = U_\mathcal{P}^\mathsf{T} \mathcal{P}(s) V_\mathcal{P}$ with $U_\mathcal{P}$, $V_\mathcal{P} \in \mathbb{R}^{(n+m)\times(r_\mathrm{p}+m)}$ as in (3.10).
- Decompose the strictly proper part $\widehat{H}_{\mathrm{sp}}$ of $\widehat{H}$ s.t. $\widehat{H}_{\mathrm{sp}}(s) = \sum_{i=1}^{r_\mathrm{p}} \frac{\mathsf{l}_i \mathsf{r}_i^\mathsf{T}}{s-\lambda_i}$.
- $\sigma_i \leftarrow -\lambda_i$ and $b_i \leftarrow \mathsf{r}_i$ for all $i = 1, \ldots, r_\mathrm{p}$

end

Decompose $\widehat{\mathcal{P}}$ as in (3.11) and $D_1 = L_1 L_1^\mathsf{T}$ with $L_1 \in \mathbb{R}^{m \times \ell}$.

Compute the reduced pH-DAE $\widehat{\Sigma}_{\mathrm{pH}}$ in staircase form as in (3.8).

TRKSM In Algorithm 3.1, a new ROM must be computed in every iteration; consequently, its computational effort is tightly connected to convergence speed. *Adaptive* reduction algorithms also compute new interpolation data in each iteration but, in contrast, build up the trial subspace $\mathcal{V}$ incrementally. This entails computational advantages compared to algorithms such as IRKA-PH since shifts from previous iterations are retained, and large-scale LSEs only have to be solved for the new shifts. Moreover, since the reduced order r increases iteratively until convergence, it is not necessary to select this parameter in advance, leading to a higher degree of automation. The difficulty in designing adaptive MOR methods is the following: In each iteration, from a set of candidates, identify those shifts that create basis vectors that add rank to the reduction matrix V, i.e., which extend the trial subspace $\mathcal{V}$, without actually having to compute these basis vectors [151]. Various methods have been proposed for unstructured state-space models to solve this problem; see, e.g., [9, 47, 54, 62, 88, 112, 151, 161] and the references therein. Since most of these methods employ Galerkin projections to create the ROM, they can directly be incorporated into the Rosenbrock framework. In [A4], this was exemplarily shown for the *tangential rational Krylov subspace method* (TRKSM) proposed in [46, 47] for unstructured state-space models. It uses a residual term to identify regions in the complex plane where the accuracy of the ROM is still poor. First numerical examples in [A4] indicate that these approaches have the potential to yield comparable $\mathcal{H}_2$ errors as IRKA-PH combined with a significantly lower computational cost in large-scale settings. Another option to reduce the computational cost is by using surrogate models.

Algorithm 3.2: Confined IRKA-PH (CIRKA-PH) for pH-DAEs [A4]

Input : Original model Σ_{pH} in staircase form; initial interpolation data $\{\sigma_1, \ldots, \sigma_{r_\mathrm{p}}\} \subset \mathbb{C}$ and $\{b_1, \ldots, b_{r_\mathrm{p}}\} \subset \mathbb{C}^m$ (both closed under complex conjugation).

Output: Reduced-order model $\widehat{\Sigma}_{\mathrm{pH}}$, surrogate model $\Sigma^{\mu}_{\mathrm{pH}}$.

1 Initialize $\Sigma^{\mu}_{\mathrm{pH}}$.
2 **while** *not converged* **do**
3 $\quad \Sigma^{\mu}_{\mathrm{pH}} \leftarrow \mathrm{update}(\Sigma_{\mathrm{pH}}, \Sigma^{\mu}_{\mathrm{pH}}, \{\sigma_1, \ldots, \sigma_{r_\mathrm{p}}\}, \{b_1, \ldots, b_{r_\mathrm{p}}\})$
4 $\quad [\widehat{\Sigma}^{\mu}_{\mathrm{pH}}, \{\lambda_1, \ldots, \lambda_{r_\mathrm{p}}\}, \{\mathsf{r}_1, \ldots, \mathsf{r}_{r_\mathrm{p}}\}] \leftarrow \text{IRKA-PH}(\Sigma^{\mu}_{\mathrm{pH}}, \{\sigma_1, \ldots, \sigma_{r_\mathrm{p}}\}, \{b_1, \ldots, b_{r_\mathrm{p}}\})$
5 $\quad \sigma_i \leftarrow \lambda_i$ and $b_i \leftarrow \mathsf{r}_i$ for all $i = 1, \ldots, r_\mathrm{p}$
6 **end**
7 $\widehat{\Sigma}_{\mathrm{pH}} \leftarrow \widehat{\Sigma}^{\mu}_{\mathrm{pH}}$

3.2.2 Surrogate-Based Reduction [A2]

In [36, 37, 112], a modification of IRKA for general state-space models called *confined* IRKA (CIRKA) was proposed that allows decoupling the cost of optimization and reduction using a medium-sized surrogate model (also called *model function*). The use of surrogate models is motivated by the fact that both interpolatory methods and the optimization problem in (3.2) are *local* by nature (see [112]). On the one hand, interpolatory methods approximate the original transfer function locally around selected interpolation points. On the other hand, due to the non-convexity of (3.2), solvers such as IRKA-PH typically strive to find local minima in the proximity of the initial ROM. If the FOM of dimension n is replaced locally by a surrogate model of dimension n^μ such that $n^\mu \ll n$, the optimization of the ROM with respect to the surrogate model can be conducted at a significantly lower cost.

A structure-preserving variant called *CIRKA-PH* suitable for pH-ODE systems, was proposed in [A2]. Here, we briefly present the generalization to pH-DAE systems in staircase form using the Rosenbrock framework. Structure preservation is enforced by also choosing the surrogate model as a pH-DAE model $\Sigma^{\mu}_{\mathrm{pH}}$ with associated transfer function H^μ. A high-level overview of the method is provided in Algorithm 3.2. Initially, a surrogate model $\Sigma^{\mu}_{\mathrm{pH}}$ is chosen such that $n^\mu > r$ and we refer to [36] for different initialization strategies. CIRKA-PH then runs an outer loop which executes Algorithm 3.1 iteratively on the $\Sigma^{\mu}_{\mathrm{pH}}$. Its backbone is the update of the surrogate model in Line 3: Since the ROM is optimized with respect to $\Sigma^{\mu}_{\mathrm{pH}}$, it is generally not guaranteed that it is also optimal with respect to the FOM. Therefore, in each iteration, $\Sigma^{\mu}_{\mathrm{pH}}$ is updated such that it *additionally* interpolates the FOM Σ_{pH} at the optimal interpolation data found by IRKA-PH in the previous iteration. The reasoning behind this

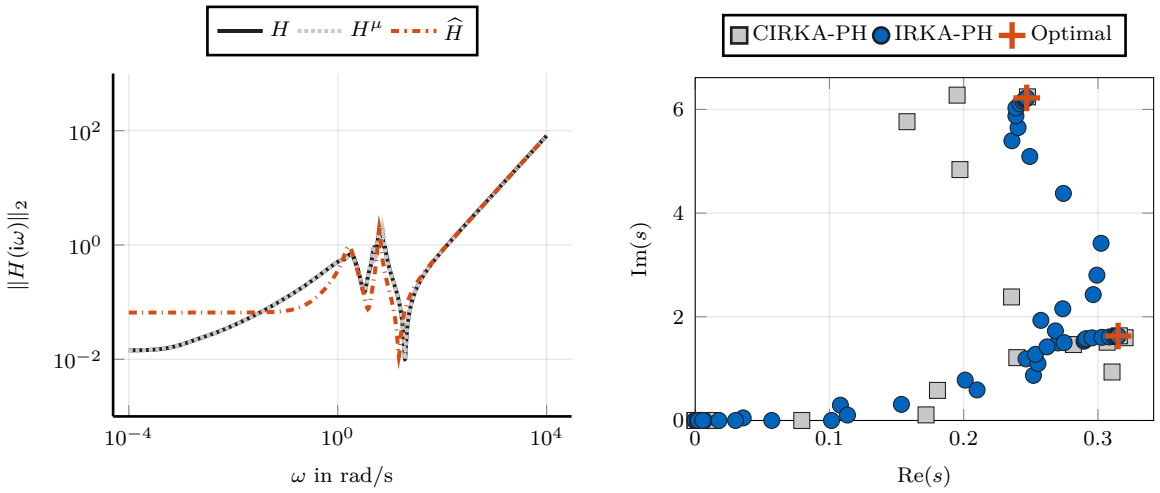

(a) (b)

Figure 3.2: MOR of the model depicted in Figure 3.1 to $r = 6$ using IRKA-PH and CIRKA-PH. (a) Frequency responses of the FOM Σ_{pH}, the surrogate model $\Sigma_{\mathrm{pH}}^{\mu}$, and the obtained ROM $\widehat{\Sigma}_{\mathrm{pH}}$. (b) Entirety of shifts in the first quadrant used by IRKA-PH and CIRKA-PH to interpolate the FOM Σ_{pH}.

update is the following: Before convergence, i.e., when the optimal interpolation data found by IRKA-PH still change substantially, interpolation points in new regions are added, and therefore, $\Sigma_{\mathrm{pH}}^{\mu}$ becomes an increasingly better approximation of Σ_{pH}. Upon convergence, when the optimal interpolation data is identical between two subsequent iterations (up to a certain tolerance), we have that

$$\widehat{H}(-\lambda_i)\mathsf{r}_i = H^{\mu}(-\lambda_i)\mathsf{r}_i = H(-\lambda_i)\mathsf{r}_i, \quad i = 1, \ldots, r_{\mathrm{p}},$$

and the ROM fulfills (2.31a).

Note that the working principle of adaptive MOR methods such as TRKSM is very similar. Let us consider an illustrative example to compare the computational costs of Algorithm 3.1 to Algorithm 3.2. We apply both algorithms to the pH-DAE model whose frequency response is shown in Figure 3.1 and compute ROMs with $r = 6$ ($r_{\mathrm{p}} = 4$). For initial shifts at zero, both algorithms converge to the same local optimum, and the frequency responses of the ROM $\widehat{\Sigma}_{\mathrm{pH}}$ obtained by both algorithms as well as the surrogate model $\Sigma_{\mathrm{pH}}^{\mu}$ of CIRKA-PH are plotted in Figure 3.2a. The surrogate model has dimension $n^{\mu} = 36$ and captures the input-output behavior of the FOM well over the entire frequency range. For large n and $r < n^{\mu} \ll n$, the significant computational cost of both algorithms is solving the large-scale LSEs that are required to compute the matrix V in Theorem 3.1. In IRKA-PH, this has to be done for r_{p} shifts in each

iteration. In Figure 3.2b, all shifts in the first quadrant of the complex plane are plotted. Since all complex shifts occur in complex conjugate pairs, it is sufficient to solve one LSE for each pair and therefore the number of blue circles in Figure 3.2b corresponds to the number of large-scale LSEs IRKA-PH solves. For CIRKA-PH, large-scale LSEs are only solved in the update of the surrogate model (Line 3). The gray squares in Figure 3.2b show the locations of shifts in the first quadrant used for this update. This illustrates that the number of large-scale LSEs solved is significantly smaller than for IRKA-PH. Also, it can be observed that all shifts used to create the surrogate model lie in the vicinity of the optimal shifts (depicted as red crosses), which confirms our intuition of a *local* approximation of the FOM.

3.3 Optimization-Based Model Reduction [A3, A5]

The Rosenbrock framework embodies an *internal* viewpoint on model reduction, which relies on the time-domain representation of the FOM, i.e., the equations in (2.10). With the Galerkin projections used in Theorem 3.1, the ROM matrices are created by operations on the original state-space matrices. Consequently, the algorithms presented in the previous chapter rely on the realization, i.e., the *inner* structure, of the FOM.

At the same time, the cost function of the optimization problem (3.2) we are trying to solve relies only on the transfer function of the FOM. The transfer function provides an *external* viewpoint that considers the input-output characteristics of the system. This raises the question of whether tackling the $\mathcal{H}_2$ optimization problem from this external viewpoint is also possible. This section summarizes an optimization approach developed in [A3] for pH-ODE models and extended to the DAE case in [A5]. It directly parameterizes the ROM and can be implemented to rely only on samples of the FOM's transfer function and its derivative.

3.3.1 Parameterization of Reduced-Order Models

Our approach is based on a flexible, direct parameterization of the ROM matrix entries with a parameter vector $\theta \in \mathbb{R}^{n_\theta}$ that utilizes the system decomposition presented in Section 3.1. In the first step, the subsystem $\widehat{\Sigma}_{\mathrm{pH,p}}$ with dimension r_p in the form of (3.5) is parameterized. It has an associated structure matrix $\widehat{\Gamma}_\mathrm{p} \in \mathbb{R}^{q\times q}$ and dissipation matrix $\widehat{W}_\mathrm{p} \in \mathbb{R}^{q\times q}$ with $q = r_\mathrm{p} + m$ (see Definition 2.4). These matrices govern the system's energy routing and dissipation and are subject to the pH structural constraints $\widehat{\Gamma}_\mathrm{p} = -\widehat{\Gamma}_\mathrm{p}^\mathsf{T}$ and $\widehat{W}_\mathrm{p} = \widehat{W}_\mathrm{p}^\mathsf{T} \geq 0$, respectively. From an energy-based viewpoint, it is

therefore natural to parameterize these matrices separately, i.e., we first define two parameter vectors θ_Γ and θ_W from which the actual state-space matrices are derived.

Let us first consider the energy routing of the system. Using $\theta_\Gamma = [\theta_1, \ldots, \theta_{q(q-1)/2}]^\mathsf{T} \in \mathbb{R}^{q(q-1)/2}$, we parameterize $\widehat{\Gamma}_\mathrm{p}$ as the sum of a strictly-upper triangular matrix and its negative transpose as originally proposed in [142]

$$\widehat{\Gamma}_\mathrm{p}(\theta_\Gamma) := \begin{bmatrix} 0 & \theta_1 & \theta_2 & \cdots & \theta_{q-1} \\ 0 & 0 & \theta_q & \cdots & \theta_{2q-3} \\ 0 & 0 & 0 & \ddots & \vdots \\ 0 & 0 & 0 & 0 & \theta_{q(q-1)/2} \\ 0 & 0 & 0 & 0 & 0 \end{bmatrix} - \begin{bmatrix} 0 & \theta_1 & \theta_2 & \cdots & \theta_{q-1} \\ 0 & 0 & \theta_q & \cdots & \theta_{2q-3} \\ 0 & 0 & 0 & \ddots & \vdots \\ 0 & 0 & 0 & 0 & \theta_{q(q-1)/2} \\ 0 & 0 & 0 & 0 & 0 \end{bmatrix}^\mathsf{T}. \tag{3.12}$$

The state-space matrices $\widehat{J}_\mathrm{p}, \widehat{G}_\mathrm{p}$ and $\widehat{N}_\mathrm{p}$ can be extracted from $\widehat{\Gamma}_\mathrm{p}$ via

$$\widehat{J}_\mathrm{p}(\theta_\Gamma) = -\begin{bmatrix} I_{r_\mathrm{p}} & 0 \end{bmatrix} \widehat{\Gamma}_\mathrm{p}(\theta_\Gamma) \begin{bmatrix} I_{r_\mathrm{p}} & 0 \end{bmatrix}^\mathsf{T}, \tag{3.13}$$

$$\widehat{G}_\mathrm{p}(\theta_\Gamma) = -\begin{bmatrix} I_{r_\mathrm{p}} & 0 \end{bmatrix} \widehat{\Gamma}_\mathrm{p}(\theta_\Gamma) \begin{bmatrix} 0 & I_m \end{bmatrix}^\mathsf{T}, \tag{3.14}$$

$$\widehat{N}_\mathrm{p}(\theta_\Gamma) = \begin{bmatrix} 0 & I_m \end{bmatrix} \widehat{\Gamma}_\mathrm{p}(\theta_\Gamma) \begin{bmatrix} 0 & I_m \end{bmatrix}^\mathsf{T}. \tag{3.15}$$

For the dissipation matrix $\widehat{W}_\mathrm{p}$ and the associated state-space matrices $\widehat{R}_\mathrm{p}, \widehat{P}_\mathrm{p}$ and $\widehat{S}_\mathrm{p}$, we may apply a similar strategy employing a Cholesky factorization with $\theta_W \in \mathbb{R}^{q(q+1)/2}$, see [A5] for details. Consequently, the subsystem $\widehat{\Sigma}_\mathrm{pH,p}$ is parameterized by q^2 degrees of freedom, which can, however, not all be exploited for model reduction. To keep the $\mathcal{H}_2$ error bounded, the matrix $\widehat{S}_\mathrm{p}$ ($\widehat{N}_\mathrm{p}$) has to match the (skew-)symmetric part of the constant polynomial part D_0 of the original transfer function (see Section 3.1). This is achieved by fixing the last $m(m-1)/2$ parameters in θ_Γ and the last $m(m+1)/2$ parameters in θ_W, respectively, such that (3.6) holds. The final parameter vector $\theta \in \mathbb{R}^{n_\theta}$ contains the remaining $n_\theta = r_\mathrm{p}(r_\mathrm{p} + 2m)$ degrees of freedom and parameterizes a ROM of the form

$$\widehat{\Sigma}_\mathrm{pH,p}(\theta) : \begin{cases} \dot{\widehat{x}}_\mathrm{p}(t) = (\widehat{J}_\mathrm{p}(\theta) - \widehat{R}_\mathrm{p}(\theta))\widehat{x}_\mathrm{p}(t) + (\widehat{G}_\mathrm{p}(\theta) - \widehat{P}_\mathrm{p}(\theta))u(t), \\ \widehat{y}_\mathrm{p}(t) = (\widehat{G}_\mathrm{p}(\theta) + \widehat{P}_\mathrm{p}(\theta))^\mathsf{T}\widehat{x}_\mathrm{p}(t) + (\widehat{S}_\mathrm{p} + \widehat{N}_\mathrm{p})u(t), \end{cases} \tag{3.16}$$

which can be utilized for optimizing the $\mathcal{H}_2$ error. If the original transfer function H has an improper part $H_{\mathrm{pol},1} \neq 0$, it can be attached to $\widehat{H}_\mathrm{p}$ as described in Section 3.1, yielding a ROM of the form (3.8). Note that using an explicit state-space representation ($\widehat{E}_\mathrm{p} = I_{r_\mathrm{p}}$) for the subsystem $\widehat{\Sigma}_\mathrm{pH,p}$ is not restrictive since every pH-ODE model of dimension r_p can be transformed to this form.

Remark 3.1. There are alternative ways to embed the geometry of the pH structural constraints into the optimization problem. For pH-ODE models, a formulation on Rie-

mannian matrix manifolds was presented in the pole-residue and Lyapunov frameworks in [A3] and [132], respectively. This requires the use of Riemannian solvers such as the Riemannian trust-region method [2] that has also been used for stability-preserving MOR (see, e.g., [131, 133]).

3.3.2 Structure-Preserving $\mathcal{H}_2$ Optimization

With the proposed parameterization of the ROM, the $\mathcal{H}_2$ error is bounded and can be expressed in the pole-residue framework as shown in Section 2.2.1. Let $\mathcal{S} \subset \mathbb{R}^{n_\theta}$ denote the set of parameter vectors θ for which the transfer function $\widehat{H}(\cdot, \theta)$ has simple finite poles. For every $\theta \in \mathcal{S}$, the strictly proper part of $\widehat{H}(\cdot, \theta)$ admits a pole-residue expansion of the form

$$\widehat{H}_{\mathrm{sp}}(s, \theta) = \sum_{i=1}^{r_{\mathrm{p}}} \frac{\mathsf{l}_i(\theta)\mathsf{r}_i(\theta)^{\mathsf{T}}}{s - \lambda_i(\theta)}. \tag{3.17}$$

We define the vector-valued function $\phi : \mathcal{S} \to \mathbb{C}^{n_\phi}$ with $n_\phi = r_{\mathrm{p}}(2m + 1)$ such that

$$\phi(\theta) := [\mathsf{l}_1(\theta)^{\mathsf{T}}, \ldots, \mathsf{l}_{r_{\mathrm{p}}}(\theta)^{\mathsf{T}}, \mathsf{r}_1(\theta)^{\mathsf{T}}, \ldots, \mathsf{r}_{r_{\mathrm{p}}}(\theta)^{\mathsf{T}}, \lambda_1(\theta), \ldots, \lambda_{r_{\mathrm{p}}}(\theta)]^{\mathsf{T}}.$$

To optimize the $\mathcal{H}_2$ error, we apply the error expression in (2.30) and neglect the term $\|H_{\mathrm{sp}}\|_{\mathcal{H}_2}^2$ which is very expensive to compute for large-scale models but independent of the parameter vector θ. With

$$\mathcal{G}(\phi; H) := -2 \sum_{i=1}^{r_{\mathrm{p}}} \mathsf{l}_i^{\mathsf{T}} H_{\mathrm{sp}}(-\lambda_i)\mathsf{r}_i + \sum_{j=1}^{r_{\mathrm{p}}} \sum_{k=1}^{r_{\mathrm{p}}} \frac{\mathsf{l}_j^{\mathsf{T}}\mathsf{l}_k\mathsf{r}_k^{\mathsf{T}}\mathsf{r}_j}{-\lambda_j - \lambda_k}, \tag{3.18}$$

the optimization problem in (3.2) can be formulated as

$$\min_{\theta \in \mathcal{S}} \mathcal{F}(\theta; H) := (\mathcal{G} \circ \phi)(\theta) \tag{3.19}$$

with objective functional $\mathcal{F} : \mathcal{S} \to \mathbb{R}$. Evaluations of $\mathcal{F}$ only require *samples* of the strictly proper part H_{sp} of the original transfer function. If the FOM has staircase form, a realization of H_{sp} can be obtained by simple transformations as shown in [A4, A5]. However, this realization is generally dense and, therefore, computationally intensive to store and evaluate. Fortunately, it is not even necessary to compute such a realization. Since $\mathcal{F}$ only relies on samples of H_{sp}, we may use an indirect sampling approach, where for all $s \in \mathbb{C}$

$$H_{\mathrm{sp}}(s) = H(s) - H_{\mathrm{pol}}(s). \tag{3.20}$$

The polynomial coefficients D_0, D_1 of H_{pol} can be computed offline before the actual optimization. This can be done, for instance, by using sampling-based approaches such as [12, 140], which, again, rely only on samples of H. Our approach (*Pole-Residue OPTimization*, PROPT) is summarized in Algorithm 3.3. In the following, we briefly discuss the numerical solution of the optimization problem (3.19) in Line 3 and possible strategies to choose the initial parameter vector θ_0, which is crucial given that (3.19) is non-convex.

Optimization Since for any $\bar{\theta} \in \mathcal{S}$, $\mathcal{F}$ is differentiable in a neighborhood of $\bar{\theta}$, it can be optimized locally with gradient-based optimization algorithms as illustrated for the trust-region algorithm in [A3, A5]. The derivative at $\bar{\theta}$ is given by

$$\mathrm{D}\mathcal{F}(\bar{\theta}) = \left(\nabla\mathcal{F}(\bar{\theta})\right)^{\mathsf{T}} = \mathrm{D}\mathcal{G}(\phi(\bar{\theta})) \cdot \mathrm{D}\phi(\bar{\theta}) \tag{3.21}$$

with Jacobians $\mathrm{D}\mathcal{G}(\phi(\bar{\theta})) \in \mathbb{C}^{1\times n_\phi}$ and $\mathrm{D}\phi(\bar{\theta}) \in \mathbb{C}^{n_\phi \times n_\theta}$. The Jacobian $\mathrm{D}\mathcal{G}(\phi(\bar{\theta}))$ was derived in [19] and requires additional r_{p} evaluations of the first derivative of H_{sp} which can again be computed *indirectly* using (3.20). For the Jacobian $\mathrm{D}\mathcal{G}(\phi(\bar{\theta}))$, consider the spectral decomposition

$$(\widehat{J}_{\text{p}}(\theta) - \widehat{R}_{\text{p}}(\theta))Z(\theta) = Z(\theta)\Lambda(\theta), \tag{3.22}$$

where $\Lambda \in \mathbb{C}^{r_{\text{p}}\times r_{\text{p}}}$ is a diagonal matrix with the poles as entries, and the corresponding right eigenvectors are the columns in $Z \in \mathbb{C}^{r_{\text{p}}\times r_{\text{p}}}$. The residual vectors are given by

$$\begin{aligned}
\mathsf{l}_i(\theta) &= (\widehat{G}_{\text{p}}(\theta) + \widehat{P}_{\text{p}}(\theta))^{\mathsf{T}} Z(\theta) e_i, \\
\mathsf{r}_i(\theta) &= (\widehat{G}_{\text{p}}(\theta) - \widehat{P}_{\text{p}}(\theta))^{\mathsf{T}} Z(\theta)^{-\mathsf{T}} e_i,
\end{aligned}$$

where e_i denotes the i-th standard basis vector of $\mathbb{R}^{r_{\text{p}}}$. Therefore, the computation of $\mathrm{D}\phi(\bar{\theta})$ requires differentiation of the eigenvalues and eigenvectors in (3.22) with respect to the parameter vector θ. A large body of research exists on this topic and the interested reader is referred to the literature reviews provided in [94, 109]. Non-iterative methods generally fall into two categories [109]: *adjoint* methods such as [1, 97], which use both right and left eigenvectors, and *direct* methods such as [109, 127] which only require right eigenvectors. As shown in [109], the numerical efficiency of the methods depends on the problem size, i.e., the dimension of the reduced-order model. Since n_θ is quadratic in r_{p}, it is also crucial that the derivatives can be computed in a block-wise fashion using Kronecker products. In [A3], the differentiation of the eigenvectors

Algorithm 3.3: PROPT for pH-DAEs [A5]

Input : Original transfer function H; initial parameter vector $\theta_0 \in \mathcal{S}$.
Output: Reduced-order model $\widehat{\Sigma}_{\mathrm{pH}}$.

1 Compute $D_0, D_1 \in \mathbb{R}^{m\times m}$ of H_{pol}.
2 Solve

$$\theta_{\mathrm{fin}} = \operatorname*{arg\,min}_{\theta\in\mathcal{S}} \mathcal{F}(\theta; H)$$

using (3.20).
3 Construct $\Sigma_{\mathrm{pH,p}}(\theta_{\mathrm{fin}})$ as in (3.16) s.t. $\widehat{S}_{\mathrm{p}} + \widehat{N}_{\mathrm{p}} = D_0$.
4 Construct $\widehat{\Sigma}_{\mathrm{pH}}$ using $D_1 = L_1 L_1^{\mathsf{T}}$, $L_1 \in \mathbb{R}^{m\times \ell}$ as in (3.8).

and eigenvalues with respect to θ was presented using the adjoint method [97], which performed well across numerous experiments. The software toolbox MORpH discussed in the following chapter additionally implements block formulations of the direct methods [109, 127].

In conclusion, apart from the computation and differentiation of the small-sized spectral decomposition in (3.22), PROPT only relies on evaluations of H and its derivative, which are computationally feasible also for very large models. This is demonstrated in [A3, A5] for different numerical examples.

3.3.3 Initialization Strategies

Due to the non-convexity of (3.19), the best local optimization algorithms can aim for is convergence to a stationary point with $\nabla\mathcal{F}(\theta_{\mathrm{fin}}) = 0$. The convergence speed to and quality of this stationary point strongly depends on the initial parameter vector θ_0 (see, e.g., the discussion in [35, 67]). Besides a random choice of θ_0, it is also possible to use ROMs created by other (computationally cheap) structure-preserving reduction methods such as IRKA-PH, as suggested in [132]. However, since IRKA-PH generally fulfills only a subset of the necessary $\mathcal{H}_2$ optimality conditions, its generated models are typically far from being locally $\mathcal{H}_2$-optimal.

It is also possible to use *unstructured* ROMs of the form (2.1) for initialization. In general, such a ROM has no pH-DAE realization since its transfer function is not positive real. For an asymptotically stable ROM, the (real) minimum eigenvalue of the associated Popov function along the imaginary axis $\lambda_{\min}(\Psi(\mathrm{i}\omega))$ is a continuous function of $\omega \in \mathbb{R}$ [64]. The maximum violation of positive realness $\delta_{\max} = \sup_{\omega\in\mathbb{R}} -\lambda_{\min}(\Psi(\mathrm{i}\omega))$ can be regarded as a measure for the "distance" of the unstructured ROM to passiv-

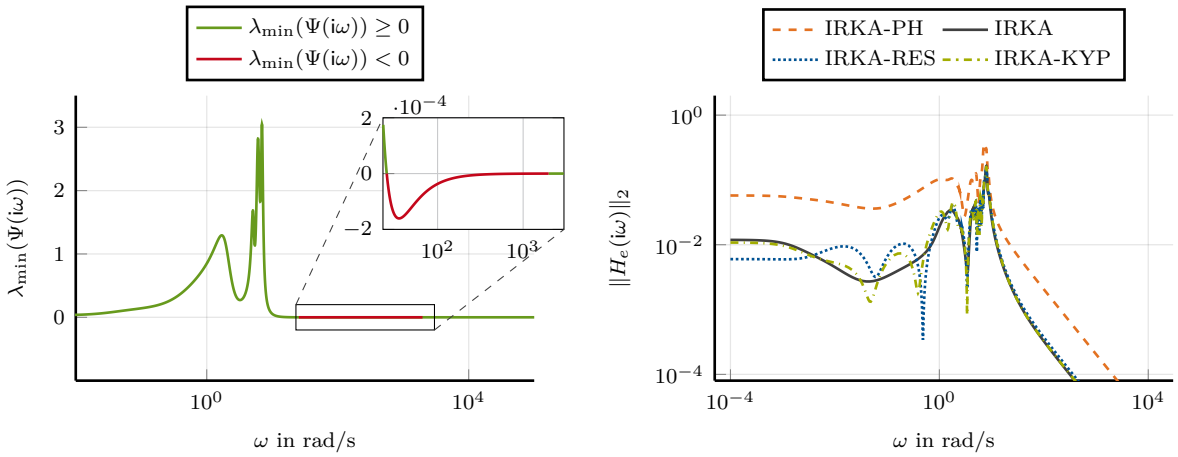

(a) (b)

Figure 3.3: $\mathcal{H}_2$ initialization for the strictly proper part in Figure 3.1. (a) Popov function of the ROM produced by IRKA ($r = 10$). (b) Frequency errors for different models ($r = 10$) created by IRKA, IRKA-PH, IRKA plus subsequent residual optimization (IRKA-RES), and IRKA plus KYP perturbation (IRKA-KYP).

ity. An estimation of $\delta_{\max}$ may be obtained quite efficiently using adaptive sampling techniques such as [65].

If the ROM is an $\mathcal{H}_2$-optimal approximation and therefore approximates the original pH-DAE well over the entire imaginary axis, violations of positive realness are expected to be minor. For illustration, let us consider the approximation of the strictly proper part of the transfer function in Figure 3.1 (which also has a pH-DAE realization) with ROMs of dimension $r = 10$. Figure 3.3a depicts the minimum eigenvalue of the Popov function for the ROM produced by IRKA. As expected, the ROM has only minor violations of positive realness with $\delta_{\max} \approx 1.6 \cdot 10^{-4}$ but yields a better $\mathcal{H}_2$ approximation than its structure-preserving variant IRKA-PH.

One way to enforce passivity for unstructured ROMs are methods that perturb the output matrix of the unstructured ROM (see [64, Chapter 10] for an overview). In [26], a different approach was proposed that first lifts the minimum eigenvalue of the Popov function above zero by introducing an additional feedthrough term and subsequently computes an initial pH-DAE ROM using the solution of the resulting (perturbed) KYP inequality. In Figure 3.3b, this algorithm is referred to as IRKA-KYP and yields frequency errors comparable to IRKA.

In the pole-residue framework, provided that the unstructured ROM is asymptotically stable, one possibility is to retain the poles of this model and to only optimize the residues. This idea was proposed in [A5] for systems with a strictly proper transfer

function and extended to systems with feedthrough terms in [26]. Due to the reduced number of optimization parameters and the fact that the poles remain unchanged, this optimization typically converges quickly and is, therefore, also suitable for initialization. In Figure 3.3b, this algorithm is called IRKA-RES.

Note that if the original transfer function contains improper parts, the unstructured ROM created by any $\mathcal{H}_2$-inspired algorithm matches this improper part exactly. Since the state-space dimension of the unstructured ROM is assumed to be small, a system decomposition approach for unstructured state-space models (see, e.g., [24, 71]) can be performed to extract the improper part and treat it separately as described in Section 3.1.

3.4 Numerical Software [A1]

Efficient software solutions are inevitable in MOR to deal with truly large-scale models that occur in real-world applications. On the one hand, to increase memory efficiency, the exploitation of sparsity patterns is necessary, which typically arise in matrices originating from the spatial discretization of PDEs [129]. On the other hand, to increase computational efficiency, solvers of large-scale LSEs and large-scale linear matrix equations such as Lyapunov or algebraic Riccati equations are required for interpolatory and balancing-based MOR methods, respectively. In [A1], we presented a novel software toolbox MORpH which is, to the best of our knowledge, the first software toolbox for the sparse representation, interconnection, and structure-preserving model reduction of port-Hamiltonian descriptor systems. The Cambridge Academic Content Dictionary [33] defines the verb *morph* as "to change gradually in appearance or form". In MORpH, the overarching concept of this process is *structure preservation*: All transformations, interconnections, and reductions are performed with the ultimate goal of preserving the pH structure.

3.4.1 An Object-Oriented Approach

The pH modeling paradigm is most potent for network modeling, where subsystems are modeled independently and subsequently coupled to a network of models, possibly across different physical domains and levels of accuracy. This motivates an object-oriented programming (OOP) approach. In MORpH, large-scale pH-DAEs are represented as instances (objects) of the *phs* class which embodies the pH structure via attributes and defines methods that determine the behavior of its instances.

The attributes that define a *phs* object are the state-space matrices of its pH-DAE representation (2.10), which are saved in MATLAB's sparse matrix format to save memory for large-scale models. Additional logical attributes such as `isMIMO` or `hasStaircase` provide access to model properties relevant for MOR. Upon creation of a *phs* object, the pH structural constraints in Definition 2.4 are verified using the function `inputValidation`.

Once a *phs* object is created, it can be interacted with using methods of the *phs* class that enable the analysis, transformation, and interconnection of pH-DAE models. First, methods for analysis overload functions of MATLAB's Control System Toolbox, such as `bode` to visualize the model's bode plot or `step` to simulate its step response. Second, methods for transformation enable transformations of the pH-DAE realization under strict system equivalence (see Lemma 2.1). For instance, the method `toStaircase` transforms a pH-DAE model into staircase form. Third, methods for interconnection allow the coupling of two *phs* objects in a power-preserving way using different Dirac structure representations. This includes, for example, the negative feedback interconnection `feedback`, which can be applied to design energy-based controllers.

In MORpH, reduced-order models are considered special representatives of pH-DAE models. We employ the OOP concept of inheritance for their definition: We define a child class *phsRed* which inherits certain attributes and methods from its parent class *phs* but implements some additional features. For example, since ROMs are generally dense, their state-space matrices are stored in the full matrix format in *phsRed*.

3.4.2 Strategies for Model Reduction

As discussed in Section 1.2, different strategies can be pursued to reduce pH-DAE models in a structure-preserving way. Figure 3.4 provides an overview of how the strategies depicted in Figure 1.1 are implemented in MORpH. It shows the MATLAB class definitions and functions (or function categories) implemented by MORpH.

For MOR methods in the category pH-MOR, the pH structural properties of the FOM Σ_{pH} are directly preserved, i.e., a pH-DAE realization $\widehat{\Sigma}_{\text{pH}}$ of the ROM is directly obtained. In the category pa-MOR, we summarize algorithms that are passivity-preserving, i.e., they reduce a passive FOM Σ_{pa} in general state-space form (2.1) to a passive ROM $\widehat{\Sigma}_{\text{pa}}$ in state-space form. In MORpH, passive FOMs are stored using the *sss* class defined in the sss toolbox presented in [34] and *phs* objects can be converted to *sss* objects via `phs2sss`. Since the obtained ROMs stored as *ss* objects are minimal and passive, they admit a pH-DAE realization which can be found by solving the KYP-

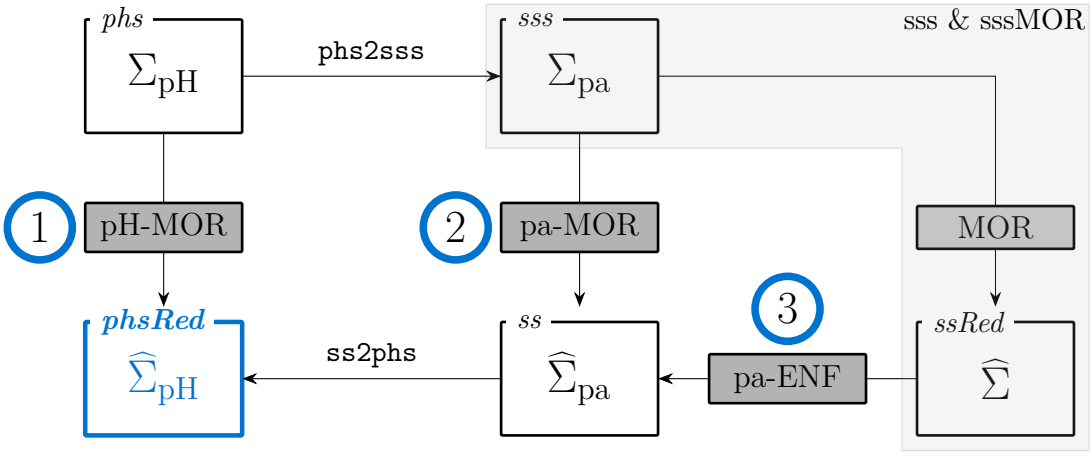

Figure 3.4: Overview of the classes and function categories in the software toolboxes MORpH and sss/sssMOR. Reprinted from [A1].

LMI in (2.9) for the passive ROM. This conversion step is implemented in the function `ss2phs` and yields the desired pH-DAE realization, stored as a *phsRed* object. Generally, classic MOR algorithms such as balanced truncation or IRKA can be exploited for the structure-preserving MOR of pH-DAEs if combined with an additional passivity enforcement (pa-ENF) step. To apply classic MOR algorithms, MORpH provides interfaces to the sssMOR toolbox presented in [34]. These algorithms yield LTI models $\widehat{\Sigma}$ represented as instances of the *ssRed* class, the counterpart of *phsRed* in MORpH. The implemented methods in the pa-ENF category perturb the output matrix of the obtained ROM with respect to some error metric until the model is passive. Subsequently, a pH-DAE realization for the obtained passive ROM can again be computed using the function `ss2phs`.

All methods in MORpH have been validated using various benchmarks generated with the port-Hamiltonian benchmark collection[2]. A comparative study with selected algorithms from all categories can be found in [A1], and the associated code to reproduce the results is publicly available [108]. MORpH is open-source and available on GitHub[3]. It contains several demo scripts which provide an introduction to how to use the toolbox and guidelines on how to contribute to the project.

[2] `https://port-hamiltonian.io`
[3] `https://github.com/MORLab/MORpH`

3.4.3 Third-Party Software

The MORpH toolbox partially relies on third-party software, which is mainly used for optimization and the numerical solution of large-scale problems and is gratefully acknowledged. The optimization solvers of the software packages MANOPT [28] and GRANSO [41] are used for optimization-based MOR methods. If the KYP-LMI in (2.9) is formulated as a constrained optimization problem, it can be solved efficiently with CVX [60, 61] or YALMIP [95]. To be capable of dealing with truly large-scale models, MORpH uses several numerical software tools that are dedicated to exploiting sparsity and typically employ iterative solvers for large-scale problems. These include the M-M.E.S.S. toolbox [130] for the solution of large-scale algebraic Riccati and Lyapunov equations, SADPA [125] and SAMDP [124] for computing dominant spectral zeros, and the functions `linorm_subsp` [5, 141] as well as `hinorm` [20] to compute the $\mathcal{H}_\infty$ norm of large-scale models.

4 Discussion and Future Work

In the last two decades, many advances have been made in structure-preserving MOR, passivity-preserving MOR, and passivity enforcement. As illustrated in Figure 1.1, the developed algorithms in these fields can be leveraged for the structure-preserving MOR of pH-DAEs in different ways. In Section 4.1, we discuss the properties of selected algorithms and the contributions presented in this thesis with respect to distinct key objectives. We conclude with a summary and further research opportunities in Section 4.2.

4.1 Discussion

We identify the following key objectives for algorithms that are relevant in the context of this thesis:

(1) *Applicability*: The method applies to the entire system class of linear, time-invariant pH-DAEs with the assumptions made in Section 2.1.

(2) *Structure preservation*: The method preserves the pH-DAE form of the FOM.

(3) *Minimality*: The method allows for treating algebraic constraints such that ROMs with minimal state-space realizations are obtained.

(4) *Accuracy*: The ROM produced by the method accurately captures the original input-output behavior over a wide range of admissible inputs.

(5) *Computational efficiency*: The method directly works with the original (typically sparse) state-space matrices and does not rely on computationally expensive or numerically unstable operations.

(6) *Availability*: An open-source implementation of the method is publicly available.

While objectives (2),(4), and (5) are often mentioned in the literature (see, e.g., [11, 67]), objectives (1) and (3) are especially relevant for systems with algebraic equations which typically require a separate treatment. Objective (6) is relevant mainly from a

practical point of view: The availability of software enables the application of a method to real-world problems, which is essential for its evaluation. In the following, we discuss the presented contributions and relevant state-of-the-art methods concerning these objectives. To raise awareness of existing tradeoffs between objectives, we combine the topics of structure preservation and minimality as well as accuracy and computational efficiency.

Applicability In the context of model reduction, the pH-DAE system class can be decomposed into six relevant subclasses depending on the Kronecker index ν and whether the transfer function contains improper parts or not. These are listed in Table 4.1 with the corresponding properties.

Table 4.1: Six different categories of pH-DAEs that are relevant for MOR. The categories result from combinations of the model's Kronecker index ν and the degree of the polynomial part of its transfer function. Adapted from [A4].

Category	ν	n_2	n_3	n_4/n_1	D_1
Index-zero (pH-ODE)	0	$\neq 0$	0	0	0
Index-one	1	$\neq 0$	$\neq 0$	0	0
Proper index-two	2	$\neq 0$	0	$\neq 0$	0
Improper index-two	2	$\neq 0$	0	$\neq 0$	$\neq 0$
Proper index-one, index-two	2	$\neq 0$	$\neq 0$	$\neq 0$	0
Improper index-one, index-two	2	$\neq 0$	$\neq 0$	$\neq 0$	$\neq 0$

Existing interpolatory MOR methods typically require the FOM state-space matrices to have particular block structures, such as the staircase form in Lemma 2.3. This holds for methods proposed for general, unstructured state-space models (see [8] for an overview) but also for structure-preserving methods proposed for pH-DAEs (see [15, 76]). While this seems like a substantial restriction at first glance, it is important to note that in many practical cases, models in (or close to) staircase form naturally emerge; see also the discussion in Section 2.1.2. Extensions of the structure-preserving IRKA-PH algorithm proposed for the pH-ODE subclass in [68] to other pH-DAE subclasses were discussed in [15, 76]. Except for the proper index-two case, which shares similarities to the pH-ODE case from a MOR point of view, the proposed methods require the FOM to be in staircase form. Moreover, to the author's knowledge, the treatment of mixed index-one and index-two constraints ($n_3 \neq 0$, $n_4 \neq 0$) has yet to be addressed.

The passivity-preserving approach proposed in [122] is more general in this sense since it works for models with arbitrary Kronecker index. However, it relies on the

projection of Lur'e and discrete-time Lyapunov equations. To solve these equations efficiently in the large-scale case, iterative low-rank methods such as the Smith or alternating direction implicit (ADI) method [146] are applied, which require knowledge of specific spectral projectors. The explicit computation of these projectors is generally challenging and requires the matrices E and A to have special block structures [104].

The contributions in this thesis advance the state of the art in different ways concerning applicability. First, the system decomposition approach presented in [A5] enables a generalization of existing state-of-the-art methods initially designed for pH-ODE systems to the entire system class of pH-DAEs for applications where the proper subsystem $\Sigma_{\mathrm{pH,p}}$ can be extracted from the original model. This is, for example, the case for models that exhibit the staircase form in Lemma 2.3. In the large-scale case, the direct application of the MOR methods to $\Sigma_{\mathrm{pH,p}}$ requires that the corresponding state-space matrices are still sparse. If the model has an index-one part ($n_3 \neq 0$), the state-space matrices of $\Sigma_{\mathrm{pH,p}}$ may become dense, which limits this approach to medium-sized models (see the discussion in [A4, Section 3.2]).

Second, the proposed Rosenbrock framework provides a more general approach than existing interpolatory MOR methods. While it also requires the FOM to be in staircase form, the framework treats all system categories in Table 4.1 in a unifying way and also covers models with mixed index-one and index-two constraints.

Third, if the original state-space matrices do not exhibit any particular structure and transformations are not feasible, the proposed optimization-based algorithm PROPT can be exploited. Due to its formulation in the pole-residue framework, it only relies on the transfer function of the FOM and is, therefore, less reliant on its specific state-space realization. This is also an advantage of this approach compared to other Riemannian $\mathcal{H}_2$ optimization methods formulated in the Lyapunov framework [84, 132], which do not have this property and have not been formulated for systems with algebraic constraints so far.

Structure Preservation and Minimality For ODE systems, one can typically assume that the ROM is minimal for all MOR methods since, otherwise, its state-space dimension could be further reduced without changing the transfer function. In the presence of algebraic constraints, the preservation of the pH structure and a ROM realization of minimal state-space dimension seem to be conflicting goals in state-of-the-art methods.

In interpolatory MOR, the treatment of algebraic constraints has been approached in two ways: either by preserving the algebraic constraint structure or by matching

its impact on the transfer function with appropriate feedthrough terms. The former approach requires that the algebraic equations of the model can be separated from differential equations and was proposed for the index-one case in [15, 76]. While this simplified treatment helps to enforce the pH structure, it does not necessarily result in minimal ROMs since redundant algebraic equations are not reduced (see also [15, Remark 2]). Suppose the product $\nu \cdot m$ is smaller than the dimension n_∞ (see Section 2.1). In that case, the order of the ROM can be reduced significantly by truncating states that correspond to zero improper Hankel singular values [104]. While such a reduction can be performed by balancing the ROM using projected, discrete-time Lyapunov equations [104], it does not generally preserve the pH structure.

If not the algebraic constraints themselves are preserved, but only their impact on the transfer function, the polynomial part H_{pol} of the original transfer function must be attached to the ROM by changing the feedthrough matrix. This approach, initially proposed for unstructured DAE systems in [71], was adapted to index-one and improper index-two pH-DAEs in [15]. While this second approach generally yields ROMs of minimal dimension, preservation of the pH-DAE structure is not guaranteed.

The algorithms presented in this thesis provide a solution to this tradeoff. First, since they belong to the algorithm group pH-MOR (see Figure 1.1), the pH structure of the ROM is directly enforced. This may also be an advantage from a numerical point of view. The recovery of the pH-DAE form, which is required if indirect reduction algorithms of the categories pa-MOR or pa-ENF are applied, may lead to minor passivity violations that originate from ill-conditioned solutions of the KYP-LMI. Second, by attaching the minimal realization (3.7) of H_{pol} to the proper part of the ROM, the proposed system decomposition approach also guarantees minimal realizations. Note that a similar way of incorporating improper parts of the transfer function was proposed by Cherifi et al. [39, Section 5] which, however, does not yield a minimal realization if the polynomial coefficient D_1 is singular.

Accuracy and Computational Efficiency Before comparing the different MOR strategies with respect to approximation accuracy and computational efficiency, let us raise awareness of some general challenges. On the one hand, the experiments typically conducted in publications of the field only provide insights for specific numerical examples and do not allow general conclusions on approximation accuracy. This underpins the need for a port-Hamiltonian benchmark collection, similar to the Oberwolfach benchmark collection for linear first- and second-order systems [87], enabling better communication of research results and comparability across algorithms. On the other

hand, the assessment of computational efficiency depends not only on theoretical but also on technical aspects, for instance, how well computationally demanding tasks are solved using concurrent programming techniques. In the following discussion, we discuss some of the insights that the numerical experiments conducted in the attached publications of this thesis provided and focus on the *theoretical* aspects of computational efficiency.

Let us first focus on *interpolation-based* MOR methods. Similar to other structure-preserving methods, the proposed Rosenbrock framework only allows enforcing half of the $\mathcal{H}_2$ optimality conditions. The other half is essentially "sacrificed" to preserve the pH structural constraints. This is why the structure-preserving IRKA-PH algorithm typically yields ROMs with larger $\mathcal{H}_2$ errors than the unstructured IRKA algorithm for many numerical examples. Incorporating minimal solutions of the KYP-LMI as originally shown for ODE systems in [29] can improve the accuracy of IRKA-PH significantly. In [A4], we showed a simple way to extend this result to the DAE case. However, this extension is limited to cases where the proper subsystem of the FOM can be extracted and is still sparse, which is not necessarily the case for models with an index-one part. An advantage of interpolatory MOR is its computational efficiency for very large-scale models since only solutions of linear systems are required. Compared to balancing-based approaches, no large-scale linear matrix equations such as Lyapunov, algebraic Riccati, or Lur'e equations have to be solved except for the case where minimal solutions of the KYP-LMI are used to improve approximation quality. A way to increase the efficiency of IRKA-PH even further is by utilizing surrogate models, as in the proposed algorithm CIRKA-PH. The numerical experiments conducted in [A2] suggest that the underlying decoupling of reduction and optimization costs is especially beneficial if very large models are considered for which the cost of reduction is dominant.

The conducted numerical experiments in [A1–A5] also allow us to draw some conclusions regarding *optimization-based* MOR methods. At first, it has to be decided whether the $\mathcal{H}_2$ or $\mathcal{H}_\infty$ norm is targeted. This depends on whether a small maximum or mean error is desired in the output signal and, therefore, on the specific application. Suppose the FOM has many characteristic peaks in its frequency response and is challenging to approximate. In that case, optimization-based algorithms typically perform well in the particular error norm they are designed for while being less accurate in the other. Since the $\mathcal{H}_2$ optimization problem we focused on in this thesis is non-convex, convergence to the global optimum is not guaranteed, and the quality of the local optimum obtained upon convergence strongly depends on the initial model. The conducted experiments

suggest that using unstructured ROMs combined with a residual optimization step as proposed in [A5] may be beneficial in some cases to avoid the algorithm getting stuck in flat local optima.

Regarding computational complexity, the optimization-based method PROPT is sensitive to an increase of the state-space dimension r_p of the proper subsystem. With the proposed parameterization, the length of θ grows quadratically with r_p, limiting this approach to ROMs with approximately $r_\mathrm{p} < 30$. On the one hand, the proposed pole-residue framework bears computational advantages compared to recently proposed optimization-based methods formulated in the Lyapunov framework (see [84, 132]) since no solutions of large-scale Lyapunov equations are required to evaluate the cost function and its gradient. This is especially beneficial when models with very large state-space dimensions are considered. On the other hand, an eigenvalue problem of dimension r_p has to be differentiated. From a computational point of view, this makes the gradient computation more sensitive to an increase of the reduced order compared to methods formulated in the Lyapunov framework. Note that the presented parameterization in (3.16) is redundant since one particular transfer function $\widehat{H}_\mathrm{p}$ has infinitely many realizations $\widehat{\Sigma}_{\mathrm{pH,p}}$. However, adding dimensionality to optimization problems can also be beneficial to change the optimization landscape favorably, as typically applied in the training of neural networks. Due to the flexible parameterization chosen for the ROM, it is also possible to reduce the number of optimization parameters. For instance, $\widehat{R}_\mathrm{p}$ could also be parameterized as a diagonal or tridiagonal matrix. However, how to use this flexibility is an open research question. Similar to the problem of choosing a reduced order r, it is challenging to select a suitable parameterization for a specific application in advance.

Another way to reduce the computational burden of optimization-based algorithms is the choice of a more accurate initialization. In the conducted experiments in [A5], using unstructured ROMs for initialization combined with a residual optimization as described in Section 3.3.3 led to a significant speed-up in optimization. However, in this case, the method relies on unstructured MOR methods, which revokes the advantage of being more independent of the original system's realization. Since passivity enforcement methods typically retain the unstructured ROM's dynamics and feedthrough matrix, these are also suitable for $\mathcal{H}_2$ initialization. However, they typically come with a higher computational cost than the KYP initialization method proposed in Section 3.3.3 since the perturbations of the unstructured ROM are optimized.

Availability When computationally demanding tasks are considered, the actual implementation of an algorithm clearly sets the boundaries of its applicability. For a brief illustration, let us consider the gradient computation in the optimization-based algorithm PROPT. As mentioned in Section 3.3.2, this requires the differentiation of an eigenvalue problem with respect to the matrix entries of the parameterized ROM. While many different algorithms can be used for this task in theory, not all are suitable for our application. Since the number of optimization parameters grows quadratically with r_p, it is crucial that the derivatives are not computed in a loopwise but blockwise fashion. For some algorithms, we can exploit the structure of the matrices to compute several derivatives at once using Kronecker products. In our experiments, this led to a more than 100 times faster gradient computation for larger reduced orders, which significantly shifts the boundaries of the method, given that the gradient has to be computed in each iteration.

In numerical linear algebra research, the role of software can therefore not be overstated. Since it is often not possible to completely grasp all implementation aspects of an algorithm simply by studying the associated research paper, it is crucial that software is shared within but also outside the research community to promote interdisciplinary use. With MORpH, we published an open-source software toolbox specifically designed to tackle different availability aspects. First, it provides an overview of the three possible MOR strategies described in Section 1.2 by implementing various algorithms for which mostly no open-source software has been available before. Second, the system decomposition approach described in Section 3.1 extends the availability of many algorithms initially designed for ODE systems to medium-sized DAEs. Third, the toolbox is enriched with demo scripts containing different examples and detailed documentation that are supposed to enable users with different backgrounds to get acquainted with the topic. Last but not least, it is open to contributions from the research community, which are highly encouraged.

4.2 Conclusion and Outlook

In this thesis, we summarized and discussed novel model reduction algorithms and software for the system class of linear, time-invariant port-Hamiltonian descriptor systems originally published in [A1–A5]. We proposed a system decomposition approach that enables a simple treatment of polynomial parts in the original transfer function that may originate from algebraic constraints. This approach is used to derive two new

MOR methods using tangential interpolation and direct system parameter optimization, respectively.

At first, we considered practical examples where the FOM has staircase form, i.e., its state-space matrices exhibit a particular block structure. For these models, we exploited the structural properties of the Rosenbrock system matrix to develop a unifying approach using tangential interpolation that simplifies the treatment of algebraic constraints. We showed that different shift selection strategies can be integrated into this framework while guaranteeing minimal ROMs in pH-DAE form.

If the FOM is not in staircase form, the transformation to such a form might require in-depth knowledge of the problem at hand or expensive computations in the large-scale case. For these cases, we developed a new optimization-based MOR algorithm that directly optimizes the matrix entries of the ROM with respect to the $\mathcal{H}_2$ error. Using a formulation in the computationally efficient pole-residue framework makes our approach less dependent on the original system's state-space realization. It only relies on evaluations of the associated transfer function and its derivative. Compared to state-of-the-art methods, the direct $\mathcal{H}_2$ optimization also applies to large-scale pH models governed by algebraic constraints.

These contributions ultimately led to the open-source software toolbox MORpH, the first to address the structure-preserving representation, analysis, interconnection, and model reduction of large-scale pH-DAEs. With interfaces to the sss and sssMOR toolboxes for unstructured MOR and implementations of various state-of-the-art algorithms for passivity-preserving MOR and passivity enforcement, MORpH supports the three different strategies for model reduction outlined in Section 1.2.

The discussion in Section 4.1 motivates future work that builds upon the presented contributions. First, the view of model reduction through the lens of Rosenbrock matrices may provide further benefits than the ones presented in this work. On the one hand, it may be beneficial to identify further degrees of freedom for the reduction via Petrov-Galerkin projections. On the other hand, further analysis of its structure is required to assess whether the (potentially restrictive) assumption of the FOM being in staircase form can be relaxed for specific pH-DAE subclasses. Moreover, we proposed a simple way to integrate solutions of the KYP-LMI, which bears the potential to improve the approximation quality of interpolatory MOR algorithms significantly [29]. Our approach relies on the computation of the proper original subsystem, which may be infeasible in the large-scale context. Therefore, it has to be investigated whether this can also be achieved by solving a KYP-LMI for the original (sparse) state-space matrices using approximate low-rank solvers such as [100]. Regarding the optimization-based

approach PROPT, there is still potential to improve the computational costs associated with the method. Less redundant parameterizations of the ROM should be investigated since PROPT may suffer from slow convergence for a large number of parameters. Repeated cost function and gradient evaluations may be computationally demanding for very large-scale models, even though they only rely on samples of the original transfer function at the mirrored eigenvalues of the ROM. One possibility to reduce the cost of this sampling would be to use inexact solutions of the involved linear systems as discussed, e.g., in [18] for interpolatory MOR. Alternatively, the FOM could also be replaced locally with a (significantly smaller) surrogate model, as in CIRKA-PH, at a point in the optimization where the eigenvalues of the ROM do not change significantly anymore. Even though optimality with respect to the FOM would generally be lost, the surrogate model can be used to fine-tune the residual vectors at a substantially lower cost.

The new degrees of freedom, especially for the proposed optimization-based approach, can also be used to drop some of the assumptions made throughout this thesis. First, as typical for most standard MOR algorithms, we assumed asymptotic stability of the FOM. However, the pencil $sE-(J-R)$ may also contain finite eigenvalues on the imaginary axis, which occur, for instance, in the port-Hamiltonian modeling of poroelastic networks [6]. For linear, stable ODE systems, the subsystem with purely imaginary eigenvalues has a generalized Hamiltonian structure [113], which can be reduced separately in a structure-preserving way using symplectic MOR methods (see, e.g., [98, 114]). An extension to the DAE setting with the system decomposition approach proposed in this thesis could be one possible way of tackling this problem. Second, we assumed homogeneous initial conditions for the FOM. For inhomogeneous initial conditions, the output y of the FOM is a superposition of two signals: one that originates from the input u and one that originates from the non-zero initial state vector x_0 [17]. If the initial state vector is not known a priori or different initial values are relevant for the application at hand, the initial-state-to-output map must also be approximated. Different methods have been proposed for linear, time-invariant ODE systems; see, e.g., [17, 77, 92, 139] and the references therein. In the pH-DAE setting, we additionally require that the ROM is again in pH-DAE form and that the initial state vector of the ROM is *consistent*, i.e., such that the associated initial value problem has a solution. For optimization-based methods, extending the ROM parameterization may be beneficial to enforce these additional constraints. Third, we laid our focus on linear, time-invariant pH systems in this thesis which is also the case for most state-of-the-art methods. The treatment of other system classes such as linear time-variant, paramet-

ric, discrete-time, or non-linear pH systems has only received little attention so far (see, e.g., [4, 38, 86, 93, 136]) and bears many exciting research possibilities.

Lastly, since the port-Hamiltonian modeling paradigm is still a relatively new research field, it has yet to be applied more extensively in modeling practice. Technical applications where pH-DAE models naturally emerge, such as modeling electrical circuits with modified nodal analysis, are promising starting points for collaborations among researchers and engineers. In the long term, we envision a port-Hamiltonian research platform for this purpose and the software toolbox MORpH as well as the port-Hamiltonian benchmark collection can be considered as first incentives towards this goal.

5 References

Own Publications

[A1] T. Moser, J. Durmann, M. Bonauer, and B. Lohmann. MORpH: Model reduction of linear port-Hamiltonian systems in MATLAB. *at - Automatisierungstechnik,* 71.6 (2023), 476–489 (cf. pp. 7, 25, 41, 43, 49, 51, 71).

[A2] T. Moser, J. Durmann, and B. Lohmann. Surrogate-based $\mathcal{H}_2$ model reduction of port-Hamiltonian systems. In: *2021 European Control Conference (ECC).* Rotterdam, The Netherlands, 2021, 2058–2065 (cf. pp. 7, 25, 29, 33, 49, 51, 86).

[A3] T. Moser and B. Lohmann. A new Riemannian framework for efficient $\mathcal{H}_2$-optimal model reduction of port-Hamiltonian systems. In: *Proceedings of 59th IEEE Conference on Decisison and Control (CDC).* Jeju Island, Republic of Korea, 2020, 5043–5049 (cf. pp. 7, 25, 35, 37–39, 49, 51, 95, 130).

[A4] T. Moser and B. Lohmann. A Rosenbrock framework for tangential interpolation of port-Hamiltonian descriptor systems. *Mathematical and Computer Modelling of Dynamical Systems,* 29.1 (2023), 210–235 (cf. pp. 7, 25, 28–33, 37, 46, 47, 49, 51, 103).

[A5] P. Schwerdtner, T. Moser, V. Mehrmann, and M. Voigt. Optimization-based model order reduction of port-Hamiltonian descriptor systems. *Systems & Control Letters,* 182 (2023), 105655 (cf. pp. 7, 17, 25–28, 35–40, 47, 49–51, 130).

Other Publications

[1] N. van der Aa, H. ter Morsche, and R. Mattheij. Computation of eigenvalue and eigenvector derivatives for a general complex-valued eigensystem. *The Electronic Journal of Linear Algebra,* 16 (2007), 300–314 (cf. p. 38).

[2] P.-A. Absil, C. Baker, and K. Gallivan. Trust-region methods on Riemannian manifolds. *Foundations of Computational Mathematics,* 7.3 (2006), 303–330 (cf. p. 37).

[3] F. Achleitner, A. Arnold, and V. Mehrmann. Hypocoercivity and controllability in linear semi-dissipative Hamiltonian ordinary differential equations and differential-algebraic equations. *ZAMM Zeitschrift für Angewandte Mathematik und Mechanik,* (2021) (cf. pp. 15, 16).

[4] B. M. Afkham and J. S. Hesthaven. Structure-preserving model-reduction of dissipative Hamiltonian systems. *Journal of Scientific Computing,* 81.1 (2018), 3–21 (cf. p. 54).

[5] N. Aliyev, P. Benner, E. Mengi, P. Schwerdtner, and M. Voigt. Large-scale computation of $\mathcal{L}_\infty$-norms by a greedy subspace method. *SIAM Journal on Matrix Analysis and Applications,* 38.4 (2017), 1496–1516 (cf. p. 44).

[6] R. Altmann, V. Mehrmann, and B. Unger. Port-Hamiltonian formulations of poroelastic network models. *Mathematical and Computer Modelling of Dynamical Systems,* 27.1 (2021), 429–452 (cf. p. 53).

[7] B. D. O. Anderson and S. Vongpanitlerd. *Network Analysis and Synthesis – A Modern Systems Theory Approach.* Englewood Cliffs, NJ, USA: Prentice-Hall, 1973 (cf. p. 12).

[8] A. C. Antoulas, C. A. Beattie, and S. Güğercin. *Interpolatory Methods for Model Reduction.* Philadelphia, PA, USA: Society for Industrial and Applied Mathematics, 2020 (cf. pp. 4, 9, 12, 18–23, 46).

[9] A. C. Antoulas, P. Benner, and L. Feng. Model reduction by iterative error system approximation. *Mathematical and Computer Modelling of Dynamical Systems,* 24.2 (2018), 103–118 (cf. p. 32).

[10] A. Antoulas. A new result on passivity preserving model reduction. *Systems & Control Letters,* 54.4 (2005), 361–374 (cf. p. 5).

[11] A. C. Antoulas. *Approximation of Large-Scale Dynamical Systems.* Philadelphia, PA, USA: Society for Industrial and Applied Mathematics, 2005 (cf. pp. 3, 9, 45).

[12] A. C. Antoulas, I. V. Gosea, and M. Heinkenschloss. Data-Driven Model Reduction for a Class of Semi-Explicit DAEs Using the Loewner Framework. In: *Progress in Differential-Algebraic Equations II.* Ed. by T. Reis, S. Grundel, and S. Schöps. Differential-Algebraic Equations Forum. Cham, Switzerland: Springer, 2020, 185–210 (cf. p. 38).

[13] C. Beattie, V. Mehrmann, and P. Van Dooren. Robust port-Hamiltonian representations of passive systems. *Automatica,* 100 (2019), 182–186 (cf. p. 4).

[14] C. Beattie, V. Mehrmann, H. Xu, and H. Zwart. Linear port-Hamiltonian descriptor systems. *Mathematics of Control, Signals, and Systems,* 30.17 (2018) (cf. pp. 2, 6, 14, 16).

[15] C. A. Beattie, S. Gugercin, and V. Mehrmann. Structure-preserving Interpolatory Model Reduction for Port-Hamiltonian Differential-Algebraic Systems. In: *Realization and Model Reduction of Dynamical Systems: A Festschrift in Honor of the 70th Birthday of Thanos Antoulas.* Ed. by C. Beattie, P. Benner, M. Embree, S. Gugercin, and S. Lefteriu. Cham, Switzerland: Springer International Publishing, 2022, 235–254 (cf. pp. 4, 6, 15, 16, 30, 46, 48).

[16] C. Beattie and S. Gugercin. Model Reduction by Rational Interpolation. In: *Model Reduction and Approximation.* Philadelphia, PA, USA: Society for Industrial and Applied Mathematics, 2017, 297–334 (cf. p. 23).

[17] C. Beattie, S. Gugercin, and V. Mehrmann. Model reduction for systems with inhomogeneous initial conditions. *Systems & Control Letters,* 99 (2017), 99–106 (cf. p. 53).

[18] C. Beattie, S. Gugercin, and S. Wyatt. Inexact solves in interpolatory model reduction. *Linear Algebra and its Applications,* 436.8 (2012), 2916–2943 (cf. p. 53).

[19] C. A. Beattie and S. Gugercin. A trust region method for optimal $\mathcal{H}_2$ model reduction. In: *Proceedings of the 48h IEEE Conference on Decision and Control (CDC) held jointly with 2009 28th Chinese Control Conference*. Shanghai, China, 2009 (cf. pp. 20, 38).

[20] P. Benner and M. Voigt. A structured pseudospectral method for $\mathcal{H}_\infty$-norm computation of large-scale descriptor systems. *Mathematics of Control, Signals, and Systems,* 26 (2013), 303–338 (cf. p. 44).

[21] P. Benner and S. W. R. Werner. MORLAB—The Model Order Reduction LABoratory. In: *Model Reduction of Complex Dynamical Systems*. Ed. by P. Benner, T. Breiten, H. Faßbender, M. Hinze, T. Stykel, and R. Zimmermann. Cham, Switzerland: Springer International Publishing, 2021, 393–415 (cf. p. 6).

[22] P. Benner, D. C. Sorensen, and V. Mehrmann, eds. *Dimension Reduction of Large-Scale Systems*. Berlin/Heidelberg, Germany: Springer, 2005 (cf. p. 9).

[23] P. Benner and T. Stykel. Model Order Reduction for Differential-Algebraic Equations: A Survey. In: *Surveys in Differential-Algebraic Equations IV*. Ed. by A. Ilchmann and T. Reis. Differential-Algebraic Equations Forum. Berlin/Heidelberg, Germany: Springer, 2017, 107–160 (cf. p. 4).

[24] P. Benner and S. W. R. Werner. Hankel-norm approximation of large-scale descriptor systems. *Advances in Computational Mathematics,* 46.40 (2020) (cf. p. 41).

[25] T. Berger and T. Reis. Controllability of Linear Differential-Algebraic Systems—A Survey. In: *Surveys in Differential-Algebraic Equations I*. Ed. by A. Ilchmann and T. Reis. Differential-Algebraic Equations Forum. Berlin/Heidelberg, Germany: Springer, 2013, 1–61 (cf. pp. 10, 11).

[26] M. Bonauer. Model reduction of port-Hamiltonian systems via passivity enforcement. MA thesis. Technical University of Munich, 2022 (cf. pp. 40, 41).

[27] P. Borja, J. M. A. Scherpen, and K. Fujimoto. Extended balancing of continuous LTI systems: A structure-preserving approach. *IEEE Transactions on Automatic Control,* 68.1 (2023), 257–271 (cf. p. 4).

[28] N. Boumal, B. Mishra, P.-A. Absil, and R. Sepulchre. Manopt, a Matlab toolbox for optimization on manifolds. *Journal of Machine Learning Research,* 15.42 (2014), 1455–1459 (cf. p. 44).

[29] T. Breiten and B. Unger. Passivity preserving model reduction via spectral factorization. *Automatica,* 142 (2022), 110368 (cf. pp. 5, 6, 31, 49, 52).

[30] T. Breiten, R. Morandin, and P. Schulze. Error bounds for port-Hamiltonian model and controller reduction based on system balancing. *Computers & Mathematics with Applications,* 116 (2022), 100–115 (cf. p. 4).

[31] A. Bunse-Gerstner, D. Kubalińska, G. Vossen, and D. Wilczek. $\mathcal{H}_2$-norm optimal model reduction for large scale discrete dynamical MIMO systems. *Journal of Computational and Applied Mathematics,* 233.5 (2010), 1202–1216 (cf. p. 21).

[32] R. Byers, V. Mehrmann, and H. Xu. A structured staircase algorithm for skew-symmetric/symmetric pencils. eng. *ETNA. Electronic Transactions on Numerical Analysis [electronic only],* 26 (2007), 1–33 (cf. p. 15).

[33] Cambridge University Press. *Cambridge Academic Content Dictionary.* New York City, NY, USA: Cambridge University Press, 2008 (cf. p. 41).

[34] A. Castagnotto, M. C. Varona, L. Jeschek, and B. Lohmann. sss & sssMOR: Analysis and reduction of large-scale dynamic systems in MATLAB. *at - Automatisierungstechnik,* 65.2 (2017), 134–150 (cf. pp. 6, 42, 43).

[35] A. Castagnotto, S. Hu, and B. Lohmann. An approach for globalized $\mathcal{H}_2$-optimal model reduction. *IFAC-PapersOnLine,* 51.2 (2018), 196–201 (cf. p. 39).

[36] A. Castagnotto and B. Lohmann. A new framework for $\mathcal{H}_2$-optimal model reduction. *Mathematical and Computer Modelling of Dynamical Systems,* 24.3 (2018), 236–257 (cf. pp. 33, 86).

[37] A. Castagnotto, H. K. F. Panzer, and B. Lohmann. Fast $\mathcal{H}_2$-optimal model order reduction exploiting the local nature of Krylov-subspace methods. In: *2016 European Control Conference (ECC).* Aalborg, Denmark, 2016, 1958–1969 (cf. pp. 33, 86).

[38] S. Chaturantabut, C. Beattie, and S. Gugercin. Structure-preserving model reduction for nonlinear port-Hamiltonian systems. *SIAM Journal on Scientific Computing,* 38.5 (2016), B837–B865 (cf. p. 54).

[39] K. Cherifi, H. Gernandt, and D. Hinsen. *The difference between port-Hamiltonian, passive and positive real descriptor systems.* arXiv Preprint arXiv:2204.04990. 2022 (cf. pp. 4, 14, 16, 17, 28, 48).

[40] A. Chinea, S. Grivet-Talocia, S. B. Olivadese, and L. Gobbato. High-performance passive macromodeling algorithms for parallel computing platforms. *IEEE Transactions on Components, Packaging and Manufacturing Technology,* 3.7 (2013), 1188–1203 (cf. p. 13).

[41] F. E. Curtis, T. Mitchell, and M. L. Overton. A BFGS-SQP method for nonsmooth, nonconvex, constrained optimization and its evaluation using relative minimization profiles. *Optimization Methods and Software,* 32.1 (2017), 148–181 (cf. p. 44).

[42] L. Dai. *Singular Control Systems.* Vol. 118. Lecture Notes in Control and Information Sciences. Berlin/Heidelberg, Germany: Springer, 1989 (cf. pp. 9, 10).

[43] U. Desai and D. Pal. A transformation approach to stochastic model reduction. *IEEE Transactions on Automatic Control,* 29.12 (1984), 1097–1100 (cf. p. 5).

[44] P. van Dooren, K. Gallivan, and P.-A. Absil. $\mathcal{H}_2$-optimal model reduction of MIMO systems. *Applied Mathematics Letters,* 21.12 (2008), 1267–1273 (cf. p. 21).

[45] P. van Dooren, K. A. Gallivan, and P.-A. Absil. $\mathcal{H}_2$-optimal model reduction with higher-order poles. *SIAM Journal on Matrix Analysis and Applications,* 31.5 (2010), 2738–2753 (cf. p. 21).

[46] V. Druskin and V. Simoncini. Adaptive rational Krylov subspaces for large-scale dynamical systems. *Systems & Control Letters,* 60.8 (2011), 546–560 (cf. pp. 31, 32).

[47] V. Druskin, V. Simoncini, and M. Zaslavsky. Adaptive tangential interpolation in rational Krylov subspaces for MIMO dynamical systems. *SIAM Journal on Matrix Analysis and Applications,* 35.2 (2014), 476–498 (cf. pp. 31, 32).

[48] V. Duindam, A. Macchelli, S. Stramigioli, and H. Bruyninckx. *Modeling and Control of Complex Physical Systems: The Port-Hamiltonian Approach.* Berlin/-Heidelberg, Germany: Springer, 2009 (cf. pp. 2, 9, 16).

[49] H. Egger and T. Kugler. Damped wave systems on networks: exponential stability and uniform approximations. *Numerische Mathematik,* 138.4 (2017), 839–867 (cf. p. 2).

[50] H. Egger, T. Kugler, B. Liljegren-Sailer, N. Marheineke, and V. Mehrmann. On structure-preserving model reduction for damped wave propagation in transport networks. *SIAM Journal on Scientific Computing,* 40.1 (2018), A331–A365 (cf. pp. 2, 4, 30).

[51] D. Estévez-Schwarz and C. Tischendorf. Structural analysis for electrical circuits and consequences for MNA. *International Journal of Circuit Theory and Applications,* 28.2 (2000), 131–162 (cf. p. 2).

[52] European Commission. *A policy framework for climate and energy in the period from 2020 to 2030.* Retrieved April 1, 2023, from `https://eur-lex.europa.eu/legal-content/EN/TXT/?uri=COM:2014:15:FIN` (cf. p. 1).

[53] European Parliament and Council. *Directive (EU) 2018/2001 of the European Parliament and of the Council of 11 December 2018 on the promotion of the use of energy from renewable sources.* Retrieved April 1, 2023, from `http://data.europa.eu/eli/dir/2018/2001/oj` (cf. p. 1).

[54] M. Frangos and I. M. Jaimoukha. Adaptive rational interpolation: Arnoldi and Lanczos-like equations. *European Journal of Control,* 14.4 (2008), 342–354 (cf. p. 32).

[55] R. W. Freund and F. Jarre. An extension of the positive real lemma to descriptor systems. *Optimization Methods and Software,* 19.1 (2004), 69–87 (cf. pp. 2, 13, 14).

[56] R. Freund. SPRIM: structure-preserving reduced-order interconnect macromodeling. In: *2004 IEEE/ACM International Conference on Computer Aided Design (ICCAD).* San Jose, CA, USA (cf. p. 5).

[57] K. Gallivan, A. Vandendorpe, and P. V. Dooren. Model reduction of MIMO systems via tangential interpolation. *SIAM Journal on Matrix Analysis and Applications,* 26.2 (2004), 328–349 (cf. p. 23).

[58] F. R. Gantmacher. *The Theory of Matrices.* Vol. 2. New York City, NY, USA: Chelsea Publishing Co., 1959 (cf. p. 11).

[59] N. Gillis and P. Sharma. Finding the nearest positive-real system. *SIAM Journal on Numerical Analysis,* 56.2 (2018), 1022–1047 (cf. pp. 5, 6).

[60] M. Grant and S. Boyd. Graph Implementations for Nonsmooth Convex Programs. In: *Recent Advances in Learning and Control.* Ed. by V. Blondel, S. Boyd, and H. Kimura. Lecture Notes in Control and Information Sciences, vol. 371. London, UK: Springer, 2008, 95–110 (cf. p. 44).

[61] M. Grant and S. Boyd. *CVX: Matlab software for disciplined convex programming, version 2.1.* `http://cvxr.com/cvx`. 2014 (cf. p. 44).

[62] E. J. Grimme. Krylov projection methods for model reduction. PhD thesis. University of Illinois at Urbana-Champaign, 1997 (cf. pp. 23, 32).

[63] S. Grivet-Talocia. Passivity enforcement via perturbation of Hamiltonian matrices. *IEEE Transactions on Circuits and Systems I: Regular Papers,* 51.9 (2004), 1755–1769 (cf. p. 5).

[64] S. Grivet-Talocia and B. Gustavsen. *Passive Macromodeling: Theory and Applications.* Ed. by K. Chang. Wiley Series in Mircowave and Optical Engineering. Hoboken, NJ, USA: John Wiley & Sons, 2016 (cf. pp. 5, 39, 40).

[65] S. Grivet-Talocia. An adaptive sampling technique for passivity characterization and enforcement of large interconnect macromodels. *IEEE Transactions on Advanced Packaging,* 30.2 (2007), 226–237 (cf. pp. 13, 40).

[66] C. Güdücü, J. Liesen, V. Mehrmann, and D. B. Szyld. On non-Hermitian positive (semi)definite linear algebraic systems arising from dissipative Hamiltonian DAEs. *SIAM Journal on Scientific Computing,* 44.4 (2022), A2871–A2894 (cf. pp. 6, 15).

[67] S. Gugercin, A. C. Antoulas, and C. Beattie. $\mathcal{H}_2$ model reduction for large-scale linear dynamical systems. *SIAM Journal on Matrix Analysis and Applications,* 30.2 (2008), 609–638 (cf. pp. 20, 21, 31, 39, 45).

[68] S. Gugercin, R. V. Polyuga, C. Beattie, and A. van der Schaft. Structure-preserving tangential interpolation for model reduction of port-Hamiltonian systems. *Automatica,* 48.9 (2012), 1963–1974 (cf. pp. 4, 31, 46).

[69] S. Gugercin, R. Polyuga, C. Beattie, and A. van der Schaft. Interpolation-based $\mathcal{H}_2$ model reduction for port-Hamiltonian systems. In: *Proceedings of the 48h IEEE Conference on Decision and Control (CDC) held jointly with 2009 28th Chinese Control Conference.* Shanghai, China, 2009, 5362–5369 (cf. p. 4).

[70] S. Gugercin and A. C. Antoulas. A survey of model reduction by balanced truncation and some new results. *International Journal of Control,* 77.8 (2004), 748–766 (cf. p. 5).

[71] S. Gugercin, T. Stykel, and S. Wyatt. Model reduction of descriptor systems by interpolatory projection methods. *SIAM Journal on Scientific Computing,* 35.5 (2013), B1010–B1033 (cf. pp. 12, 26, 41, 48).

[72] M. Günther and U. Feldmann. CAD-based electric-circuit modeling in industry. Part I: Mathematical structure and index of network equations. *Surveys on Mathematics for Industry,* 8 (1999), 97–129 (cf. p. 2).

[73] M. Günther and U. Feldmann. CAD-based electric-circuit modeling in industry. Part II: Impact of circuit configurations and parameters. *Surveys on Mathematics for Industry,* 8 (1999), 131–157 (cf. p. 2).

[74] H. Hafeznia, A. Aslani, S. Anwar, and M. Yousefjamali. Analysis of the effectiveness of national renewable energy policies: A case of photovoltaic policies. *Renewable and Sustainable Energy Reviews,* 79 (2017), 669–680 (cf. p. 1).

[75] P. Harshavardhana, E. Jonckheere, and L. Silverman. Stochastic balancing and approximation – Stability and minimality. In: *The 22nd IEEE Conference on Decision and Control*. San Antonio, TX, USA, 1983 (cf. p. 5).

[76] S.-A. Hauschild, N. Marheineke, and V. Mehrmann. Model reduction techniques for linear constant coefficient port-Hamiltonian differential-algebraic systems. *Control & Cybernetics,* 48.1 (2019), 125–152 (cf. pp. 4, 6, 30, 46, 48).

[77] M. Heinkenschloss, T. Reis, and A. Antoulas. Balanced truncation model reduction for systems with inhomogeneous initial conditions. *Automatica,* 47.3 (2011), 559–564 (cf. p. 53).

[78] S. H. R. Hosseini, A. Allahham, S. L. Walker, and P. Taylor. Optimal planning and operation of multi-vector energy networks: A systematic review. *Renewable and Sustainable Energy Reviews,* 133 (2020), 110216 (cf. p. 1).

[79] Y. Huang, Y.-L. Jiang, and K.-L. Xu. Structure-preserving model reduction of port-Hamiltonian systems based on projection. *Asian Journal of Control,* 23.4 (2020), 1782–1791 (cf. p. 4).

[80] D. Hyland and D. Bernstein. The optimal projection equations for model reduction and the relationships among the methods of Wilson, Skelton, and Moore. *IEEE Transactions on Automatic Control,* 30.12 (1985), 1201–1211 (cf. pp. 19, 21).

[81] T. C. Ionescu and A. Astolfi. Families of moment matching based, structure preserving approximations for linear port-Hamiltonian systems. *Automatica,* 49.8 (2013), 2424–2434 (cf. p. 4).

[82] R. Ionutiu, J. Rommes, and A. C. Antoulas. Passivity-preserving model reduction using dominant spectral-zero interpolation. *IEEE Transactions on Computer-Aided Design of Integrated Circuits and Systems,* 27.12 (2008), 2250–2263 (cf. p. 5).

[83] B. Jacob and H. J. Zwart. *Linear Port-Hamiltonian Systems on Infinite-dimensional Spaces*. Operator Theory: Advances and Applications. Birkhäuser Basel, 2012 (cf. p. 2).

[84] Y.-L. Jiang and K.-L. Xu. Model order reduction of port-Hamiltonian systems by Riemannian modified Fletcher–Reeves scheme. *IEEE Transactions on Circuits and Systems II: Express Briefs,* 66.11 (2019), 1825–1829 (cf. pp. 4, 21, 47, 50).

[85] R. E. Kalman. Lyapunov functions for the problem of Lur'e in automatic control. *Proceedings of the National Academy of Sciences,* 49.2 (1963), 201–205 (cf. p. 13).

[86] Y. Kawano and J. M. Scherpen. Structure preserving truncation of nonlinear port Hamiltonian systems. *IEEE Transactions on Automatic Control,* 63.12 (2018), 4286–4293 (cf. p. 54).

[87] J. G. Korvink and E. B. Rudnyi. Oberwolfach Benchmark Collection. In: *Dimension Reduction of Large-Scale Systems.* Ed. by P. Benner, D. C. Sorensen, and V. Mehrmann. Lecture Notes in Computational Science and Engineering. Berlin/Heidelberg, Germany: Springer, 2005, 311–315 (cf. p. 48).

[88] A. Köhler, S. Reitz, and P. Schneider. Sensitivity analysis and adaptive multi-point multi-moment model order reduction in MEMS design. *Analog Integrated Circuits and Signal Processing,* 71.1 (2012), 49–58 (cf. p. 32).

[89] F. Lewis. Adjoint matrix, Bezout theorem, Cayley-Hamilton theorem, and Fadeev's method for the matrix pencil $(sE - A)$. In: *The 22nd IEEE Conference on Decision and Control.* San Antonio, TX, USA, 1983 (cf. p. 12).

[90] X. Li, S. Yin, and H. Gao. Passivity-preserving model reduction with finite frequency $\mathcal{H}_\infty$ approximation performance. *Automatica,* 50.9 (2014), 2294–2303 (cf. p. 5).

[91] Z.-X. Li, Y.-L. Jiang, and K.-L. Xu. Riemannian optimization model order reduction method for general linear port-Hamiltonian systems. *IMA Journal of Mathematical Control and Information,* 39.2 (2022), 590–608 (cf. p. 4).

[92] B. Liljegren-Sailer. *Effective error estimation for model reduction with inhomogeneous initial conditions.* arXiv Preprint arXiv:2201.06631. 2022 (cf. p. 53).

[93] B. Liljegren-Sailer. On port-Hamiltonian modeling and structure-preserving model reduction. PhD Thesis. Universität Trier, 2020 (cf. p. 54).

[94] A. J. Liounis and J. A. Christian. Techniques for generating analytic covariance expressions for eigenvalues and eigenvectors. *IEEE Transactions on Signal Processing,* 64.7 (2016), 1808–1821 (cf. p. 38).

[95] J. Löfberg. YALMIP : A toolbox for modeling and optimization in MATLAB. In: *2004 IEEE International Conference on Robotics and Automation (IEEE Cat. No.04CH37508).* New Orleans, LA, USA, 2004 (cf. p. 44).

[96] H. Lund, P. A. Østergaard, D. Connolly, and B. V. Mathiesen. Smart energy and smart energy systems. *Energy,* 137 (2017), 556–565 (cf. p. 1).

[97] J. R. Magnus. On differentiating eigenvalues and eigenvectors. *Econometric Theory,* 1.2 (1985), 179–191 (cf. pp. 38, 39).

[98] M. Mamunuzzaman and H. Zwart. *Structure preserving model order reduction of port-Hamiltonian systems.* arXiv Preprint arXiv:2203.07751. 2022 (cf. p. 53).

[99] P. Mancarella. MES (multi-energy systems): An overview of concepts and evaluation models. *Energy,* 65 (2014), 1–17 (cf. p. 1).

[100] A. Massoudi, M. R. Opmeer, and T. Reis. The ADI method for bounded real and positive real Lur'e equations. *Numerische Mathematik,* 135.2 (2016), 431–458 (cf. p. 52).

[101] I. Masubuchi. Dissipativity inequalities for continuous-time descriptor systems with applications to synthesis of control gains. *Systems & Control Letters,* 55.2 (2006), 158–164 (cf. p. 13).

[102] C. Mehl, V. Mehrmann, and M. Wojtylak. Linear algebra properties of dissipative Hamiltonian descriptor systems. *SIAM Journal on Matrix Analysis and Applications,* 39.3 (2018), 1489–1519 (cf. p. 16).

[103] C. Mehl, V. Mehrmann, and M. Wojtylak. Distance problems for dissipative Hamiltonian systems and related matrix polynomials. *Linear Algebra and its Applications,* 623 (2021), 335–366 (cf. p. 15).

[104] V. Mehrmann and T. Stykel. Balanced Truncation Model Reduction for Large-Scale Systems in Descriptor Form. In: *Dimension Reduction of Large-Scale Systems.* Ed. by P. Benner, D. C. Sorensen, and V. Mehrmann. Lecture Notes in Computational Science and Engineering. Berlin/Heidelberg, Germany: Springer, 2005, 83–115 (cf. pp. 6, 12, 47, 48).

[105] V. Mehrmann and B. Unger. Control of port-Hamiltonian differential-algebraic systems and applications. *Acta Numerica,* 32 (2023), 395–515 (cf. pp. 2, 6, 14–16).

[106] L. Meier and D. Luenberger. Approximation of linear constant systems. *IEEE Transactions on Automatic Control,* 12.5 (1967), 585–588 (cf. pp. 20, 21).

[107] R. Milk, S. Rave, and F. Schindler. pyMOR – Generic algorithms and interfaces for model order reduction. *SIAM Journal on Scientific Computing,* 38.5 (2016), S194–S216 (cf. p. 6).

[108] T. Moser. *Benchmark systems and code for article: MORpH: Model reduction of linear port-Hamiltonian systems in MATLAB.* `https://doi.org/10.5281/zenodo.7081776`. 2022 (cf. p. 43).

[109] D. V. Murthy and R. T. Haftka. Derivatives of eigenvalues and eigenvectors of a general complex matrix. *International Journal for Numerical Methods in Engineering,* 26.2 (1988), 293–311 (cf. pp. 38, 39).

[110] C. Oara and A. Varga. Computation of general inner-outer and spectral factorizations. *IEEE Transactions on Automatic Control,* 45.12 (2000), 2307–2325 (cf. pp. 10, 11).

[111] A. Odabasioglu, M. Celik, and L. Pileggi. PRIMA: passive reduced-order interconnect macromodeling algorithm. *IEEE Transactions on Computer-Aided Design of Integrated Circuits and Systems,* 17.8 (1998), 645–654 (cf. p. 5).

[112] H. K. F. Panzer. Model order reduction by Krylov subspace methods with global error bounds and automatic choice of parameters. Dissertation. Munich: Technical University of Munich, 2014 (cf. pp. 3, 32, 33, 86).

[113] L. Peng and K. Carlberg. *Structure-preserving model reduction for marginally stable LTI systems.* arXiv Preprint arXiv:1704.04009. 2017 (cf. p. 53).

[114] L. Peng and K. Mohseni. Symplectic model reduction of Hamiltonian systems. *SIAM Journal on Scientific Computing,* 38.1 (2016), A1–A27 (cf. p. 53).

[115] J. Phillips, L. Daniel, and L. Miguel Silveira. Guaranteed passive balancing transformations for model order reduction. In: *Proceedings 2002 Design Automation Conference (IEEE Cat. No.02CH37324).* New Orleans, LA, USA, 2002, 52–57 (cf. p. 5).

[116] R. V. Polyuga and A. van der Schaft. Structure preserving model reduction of port-Hamiltonian systems by moment matching at infinity. *Automatica,* 46.4 (2010), 665–672 (cf. p. 4).

[117] R. V. Polyuga and A. van der Schaft. Structure preserving moment matching for port-Hamiltonian systems: Arnoldi and Lanczos. *IEEE Transactions on Automatic Control,* 56.6 (2011), 1458–1462 (cf. p. 4).

[118] R. V. Polyuga and A. van der Schaft. Effort- and flow-constraint reduction methods for structure preserving model reduction of port-Hamiltonian systems. *Systems & Control Letters,* 61.3 (2012), 412–421 (cf. p. 4).

[119] R. V. Polyuga and A. van der Schaft. Moment matching for linear port-Hamiltonian systems. In: *2009 European Control Conference (ECC).* Aalborg, Denmark, 2009, 4715–4720 (cf. p. 4).

[120] V. M. Popov. On absolute stability of non-linear automatic control systems. *Avtomatika i Telemekhanika,* 22 (8 1961), 961–979 (cf. p. 13).

[121] T. Reis, O. Rendel, and M. Voigt. The Kalman-Yakubovich-Popov inequality for differential-algebraic systems. *Linear Algebra and its Applications,* 485 (2015), 153–193 (cf. pp. 13, 14).

[122] T. Reis and T. Stykel. Positive real and bounded real balancing for model reduction of descriptor systems. *International Journal of Control,* 83.1 (2009), 74–88 (cf. pp. 5, 6, 46).

[123] T. Reis and M. Voigt. The Kalman-Yakubovich-Popov inequality for differential-algebraic systems: Existence of nonpositive solutions. *Systems & Control Letters,* 86 (2015), 1–8 (cf. p. 13).

[124] J. Rommes and N. Martins. Efficient computation of multivariable transfer function dominant poles using subspace acceleration. *IEEE Transactions on Power Systems,* 21.4 (2006), 1471–1483 (cf. p. 44).

[125] J. Rommes and N. Martins. Efficient computation of transfer function dominant poles using subspace acceleration. *IEEE Transactions on Power Systems,* 21.3 (2006), 1218–1226 (cf. p. 44).

[126] H. H. Rosenbrock. *State-Space and Multivariable Theory.* London: Nelson-Wiley, 1970 (cf. pp. 10, 11).

[127] C. S. Rudisill. Derivatives of eigenvalues and eigenvectors for a general matrix. *American Institute of Aeronautics and Astronautics (AIAA) Journal,* 12.5 (1974), 721–722 (cf. pp. 38, 39).

[128] A. Ruhe. Rational Krylov algorithms for nonsymmetric eigenvalue problems. In: *Recent Advances in Iterative Methods.* Ed. by G. Golub, M. Luskin, and A. Greenbaum. New York City, NY, USA: Springer, 1994, 149–164 (cf. p. 23).

[129] Y. Saad. *Iterative Methods for Sparse Linear Systems.* Philadelphia, PA, USA: Society for Industrial and Applied Mathematics, 2003 (cf. p. 41).

[130] J. Saak, M. Köhler, and P. Benner. *M-M.E.S.S.-2.1 – The matrix equations sparse solvers library.* `https://doi.org/10.5281/zenodo.3606345`. 2022 (cf. p. 44).

[131] H. Sato and K. Sato. Riemannian trust-region methods for $\mathcal{H}_2$ optimal model reduction. In: *2015 54th IEEE Conference on Decision and Control (CDC).* Osaka, Japan, 2015 (cf. pp. 21, 37).

[132] K. Sato. Riemannian optimal model reduction of linear port-Hamiltonian systems. *Automatica,* 93 (2018), 428–434 (cf. pp. 4, 21, 37, 39, 47, 50).

[133] K. Sato and H. Sato. Structure-preserving $\mathcal{H}_2$ optimal model reduction based on the Riemannian trust-region method. *IEEE Transactions on Automatic Control,* 63.2 (2018), 505–512 (cf. pp. 21, 37).

[134] A. van der Schaft and D. Jeltsema. Port-Hamiltonian Systems Theory: An Introductory Overview. In: *Foundations and Trends in Systems and Control.* Vol. 1. 2-3. Hanover, MA, USA: now Publishers Inc., 2014, 173–378 (cf. pp. 2, 9).

[135] A. J. van der Schaft. Port-Hamiltonian Differential-Algebraic Systems. In: *Surveys in Differential-Algebraic Equations I.* Ed. by A. Ilchmann and T. Reis. Differential-Algebraic Equations Forum. Berlin/Heidelberg, Germany: Springer, 2013, 173–226 (cf. p. 2).

[136] T. M. Scheuermann, P. Kotyczka, and B. Lohmann. On parametric structure preserving model order reduction of linear port-Hamiltonian systems. *at - Automatisierungstechnik,* 67.7 (2019), 521–525 (cf. p. 54).

[137] W. H. A. Schilders, H. A. van der Vorst, and J. Rommes, eds. *Model Order Reduction: Theory, Research Aspects and Applications.* Berlin/Heidelberg, Germany: Springer, 2008 (cf. p. 9).

[138] L. Scholz. Condensed forms for linear port-Hamiltonian descriptor systems. *The Electronic Journal of Linear Algebra,* 35 (2019), 65–89 (cf. p. 15).

[139] C. Schröder and M. Voigt. Balanced truncation model reduction with a priori error bounds for LTI systems with nonzero initial value. *Journal of Computational and Applied Mathematics,* 420 (2023), 114708 (cf. p. 53).

[140] P. Schwerdtner, E. Mengi, and M. Voigt. Certifying global optimality for the $\mathcal{L}_\infty$-norm computation of large-scale descriptor systems. *IFAC-PapersOnLine,* 53.2 (2020), 4279–4284 (cf. p. 38).

[141] P. Schwerdtner and M. Voigt. Computation of the $\mathcal{L}_\infty$-norm using rational interpolation. *IFAC-PapersOnLine,* 51.25 (2018), 84–89 (cf. p. 44).

[142] P. Schwerdtner and M. Voigt. *SOBMOR: Structured optimization-based model order reduction.* arXiv Preprint arXiv:2011.07567. 2022 (cf. pp. 4, 36, 130).

[143] P. Schwerdtner and M. Voigt. Adaptive sampling for structure preserving model order reduction of port-Hamiltonian systems. *IFAC-PapersOnline,* 54.19 (2021), 143–148 (cf. p. 4).

[144] D. Sorensen. Passivity preserving model reduction via interpolation of spectral zeros. *Systems & Control Letters,* 54.4 (2005), 347–360 (cf. p. 5).

[145] J. Spanos, M. Milman, and D. Mingori. A new algorithm for $\mathcal{L}_2$ optimal model reduction. *Automatica,* 28.5 (1992), 897–909 (cf. p. 21).

[146] T. Stykel. Low-rank iterative methods for projected generalized Lyapunov equations. *ETNA. Electronic Transactions on Numerical Analysis,* 30 (2008), 187–202 (cf. p. 47).

[147] S.-B. Tsai, Y. Xue, J. Zhang, Q. Chen, Y. Liu, J. Zhou, and W. Dong. Models for forecasting growth trends in renewable energy. *Renewable and Sustainable Energy Reviews,* 77 (2017), 1169–1178 (cf. p. 1).

[148] K. Unneland, P. van Dooren, and O. Egeland. A novel scheme for positive real balanced truncation. In: *2007 American Control Conference.* New York City, NY, USA, 2007, 947–952 (cf. p. 5).

[149] G. Verghese, B. Levy, and T. Kailath. A generalized state-space for singular systems. *IEEE Transactions on Automatic Control,* 26.4 (1981), 811–831 (cf. pp. 10, 11).

[150] C. Villemagne and R. Skelton. Model reductions using a projection formulation. In: *26th IEEE Conference on Decision and Control.* Los Angeles, CA, USA, 1987 (cf. p. 23).

[151] J. F. Villena and L. M. Silveira. Multi-dimensional automatic sampling schemes for multi-point modeling methodologies. *IEEE Transactions on Computer-Aided Design of Integrated Circuits and Systems,* 30.8 (2011), 1141–1151 (cf. p. 32).

[152] J. C. Willems. Dissipative dynamical systems – Part I: General theory. *Archive for Rational Mechanics and Analysis,* 45.5 (1972), 321–351 (cf. p. 12).

[153] D. Wilson. Optimum solution of model-reduction problem. *Proceedings of the Institution of Electrical Engineers,* 117.6 (1970), 1161–1165 (cf. pp. 19, 21).

[154] T. Wolf, B. Lohmann, R. Eid, and P. Kotyczka. Passivity and structure preserving order reduction of linear port-Hamiltonian systems using Krylov subspaces. *European Journal of Control,* 16.4 (2010), 401–406 (cf. p. 4).

[155] J. Wu, J. Yan, H. Jia, N. Hatziargyriou, N. Djilali, and H. Sun. Integrated energy systems. *Applied Energy,* 167 (2016), 155–157 (cf. p. 1).

[156] Y. Wu, B. Hamroun, Y. L. Gorrec, and B. Maschke. Structure preserving reduction of port-Hamiltonian system using a modified LQG method. In: *Proceedings of the 33rd Chinese Control Conference*. Nanjing, China, 2014 (cf. p. 4).

[157] Y. Wu, B. Hamroun, Y. L. Gorrec, and B. Maschke. Reduced order LQG control design for port Hamiltonian systems. *Automatica,* 95 (2018), 86–92 (cf. p. 4).

[158] V. A. Yakubovich. The solution of some matrix inequalities encountered in automatic control theory. *Doklady Akademii Nauk SSSR,* 143.6 (1962), 1304–1307 (cf. p. 13).

[159] W.-Y. Yan and J. Lam. An approximate approach to $\mathcal{H}_2$ optimal model reduction. *IEEE Transactions on Automatic Control,* 44.7 (1999), 1341–1358 (cf. p. 21).

[160] L. Zhang, J. Lam, and S. Xu. On positive realness of descriptor systems. *IEEE Transactions on Circuits and Systems I: Fundamental Theory and Applications,* 49.3 (2002), 401–407 (cf. p. 13).

[161] W. Zhao, G. K. H. Pang, and N. Wong. Automatic adaptive multi-point moment matching for descriptor system model order reduction. In: *2013 International Symposium onVLSI Design, Automation, and Test (VLSI-DAT)*. Hsinchu, Taiwan, 2013 (cf. p. 32).

[162] K. Zhou, J. C. Doyle, and K. Glover. *Robust and Optimal Control*. Englewood Cliffs, NJ, USA: Prentice-Hall, 1995 (cf. pp. 4, 18).

[163] U. Zulfiqar, W. Tariq, L. Li, and M. Liaquat. A passivity-preserving frequency-weighted model order reduction technique. *IEEE Transactions on Circuits and Systems II: Express Briefs,* 64.11 (2017), 1327–1331 (cf. p. 5).

Appendix A
Publications

A.1 MORpH: Model Reduction of Linear Port-Hamiltonian Systems in MATLAB

Summary: In this article, we present MORpH: a free, open-source MATLAB toolbox for the efficient storage, analysis, interconnection and structure-preserving MOR of pH-DAE models. The toolbox is structured in two main parts, and the article is organized accordingly. The first part presents the definition of the *phs* class to represent sparse, large-scale pH-DAE models in MATLAB. In MORpH, pH-DAE models are represented by *phs* objects and may be modified and interconnected, while the preservation of the pH structural constraints is either directly enforced or validated if performed by the user. The second part of MORpH is a collection of state-of-the-art MOR algorithms to reduce large-scale pH-DAE models in a structure-preserving way. These algorithms fall into three major categories: pH-preserving MOR, passivity-preserving MOR, and passivity enforcement. After introducing the theoretical background, the working principle of each algorithm is briefly described. We explain how MORpH supports users with different experience levels and how algorithms initially designed for pH-ODE models can be extended to models with algebraic constraints using a system decomposition approach. Numerical examples using two models from the port-Hamiltonian benchmark collection illustrate the applicability and performance of selected algorithms. The article concludes with remarks on how to get familiar with and contribute to the MORpH toolbox.

CRediT author statement:

Tim Moser:	Conceptualization, Data Curation, Investigation, Methodology, Software, Visualization, Writing - Original Draft
Julius Durmann:	Software, Writing - Original Draft
Maximilian Bonauer:	Software, Writing - Original Draft
Boris Lohmann:	Conceptualization, Funding Acquisition, Supervision, Writing - Review & Editing

Reference: T. Moser, J. Durmann, M. Bonauer, and B. Lohmann. MORpH: Model reduction of linear port-Hamiltonian systems in MATLAB. *at - Automatisierungstechnik,* 71.6 (2023), 476–489. https://doi.org/10.1515/auto-2022-0119

Tools

Tim Moser*, Julius Durmann, Maximilian Bonauer and Boris Lohmann

MORpH: Model reduction of linear port-Hamiltonian systems in MATLAB

MORpH: Modellreduktion linearer port-Hamiltonscher Systeme in MATLAB

https://doi.org/10.1515/auto-2022-0119
Received September 15, 2022; accepted December 1, 2022

Abstract: We present a novel software toolbox MORpH for the efficient storage, analysis, interconnection and structure-preserving model order reduction (MOR) of linear port-Hamiltonian differential-algebraic equation systems (pH-DAEs). The model class of pH-DAEs enables energy-based modeling and a flexible coupling of models across different physical domains. This makes them particularly suited for the simulation and control of complex technical systems. To promote the use of recent theoretical findings in engineering practice, efficient software solutions are required. In this work, we illustrate how possibly large-scale pH-DAEs can be efficiently stored and interconnected in MATLAB in an object-oriented way. We discuss three structure-preserving MOR strategies that are supported by MORpH and demonstrate the application and performance of selected MOR algorithms by means of two benchmark examples.

Keywords: descriptor systems; passivity; port-Hamiltonian systems; structure-preserving model reduction.

Zusammenfassung: In diesem Beitrag wird eine neue Software-Toolbox MORpH vorgestellt, die eine effiziente Speicherung, Analyse, Vernetzung sowie strukturerhaltende Modellordnungsreduktion (MOR) von linearen port-Hamiltonschen differential-algebraischen Modellen (pH-DAEs) ermöglicht. Die Modellklasse der pH-DAEs erlaubt eine energiebasierte Modellierung und eine flexible Kopplung von Modellen über verschiedene physikalische Domänen hinweg. Hierdurch ist sie besonders für die Simulation und Regelung komplexer technischer Systeme geeignet. Um die Anwendung neuer theoretischer Erkenntnisse in der Ingenieurspraxis zu fördern, sind effiziente Softwarelösungen erforderlich. In diesem Beitrag zeigen wir, wie potenziell große pH-DAEs effizient und objektorientiert in MATLAB gespeichert und vernetzt werden können. Wir diskutieren drei strukturerhaltende MOR-Strategien, die von MORpH unterstützt werden, und demonstrieren die Anwendung ausgewählter MOR-Algorithmen anhand zweier Benchmarks.

Schlagwörter: port-Hamiltonsche Systeme; Differential-Algebraische Systeme; Passivität; Strukturerhaltende Modellreduktion.

1 Introduction

Due to the ever-increasing complexity of today's technical systems, modeling and simulation have become an integral part of their development. A key factor in the modeling process is *flexibility*: It is essential that parts of the model can be easily modified, enriched with new data or extended without having to change other parts of the model or jeopardizing important system-theoretic properties. The port-Hamiltonian (pH) modeling paradigm is particularly suited in this regard since it enables a hierarchical modeling approach where parts of the system can be modeled separately and subsequently interconnected to a network of models in a structured way, possibly across different physical domains.

If one additionally deals with large-scale models, potentially originating from the spatial discretization of distributed-parameter systems, MOR is an effective tool to reduce simulation times and speed up the development process. In order to leverage the advantages of the pH paradigm also for the reduced-order model (ROM), it is important that these algorithms are *structure-preserving*, meaning that the

***Corresponding author: Tim Moser**, TUM School of Engineering and Design, Department of Engineering Physics and Computation, Technical University of Munich, Boltzmannstr. 15, 85748 Garching, Germany,
E-mail: tim.moser@tum.de
Julius Durmann, **Maximilian Bonauer and Boris Lohmann**, TUM School of Engineering and Design, Department of Engineering Physics and Computation, Technical University of Munich, Boltzmannstr. 15, 85748 Garching, Germany

ROM fulfills the same pH structural properties as its original counterpart. Preservation of the pH structure can be established in different ways. Traditional approaches try to directly enforce the pH structure on the ROM (see, e.g., [1–5] and the references therein). Due to the tight connection between pH systems and passive systems as well as positive real systems [6], it is also possible to apply MOR methods that preserve passivity or positive realness to the original model and subsequently try to find a pH representation for the ROM (see, e.g., [7–9]). Moreover, there is a large body of research on how to establish passivity for models that are close to being passive by using passivity enforcement techniques (see [10] for an overview). In the context of MOR, these can also be exploited if the original pH model is first reduced using standard MOR techniques and subsequently perturbed to obtain either a passive model or directly a pH representation.

Despite the fact that all of these areas have been very active fields of research in the last two decades, there is still very little software available. Compared to the MOR of general (unstructured) systems for which different software packages exist (see, e.g., [11–13]), the available software for pH systems is usually provided to accompany and reproduce the numerical experiments of specific research papers (see, e.g., [7, 14]). However, software and benchmarks can be considered key drivers not only to develop and evaluate novel numerical methods but also to make them accessible to engineering practice.

In this work, we therefore propose a novel software toolbox which is, to the best of our knowledge, the first to implement a diverse set of algorithms specifically targeted at the storage, analysis and MOR of linear pH systems. The software is open-source and provides interfaces for users with different experience levels as well as to other software packages. It is easy to extend and therefore open to contributions from the (pH-)MOR community which are highly encouraged.

The MORpH toolbox is structured in two main parts: the *phs* class definition to represent linear (possibly large-scale) pH models in MATLAB as well as MOR algorithms to reduce these models in a structure-preserving way. We organize this paper accordingly: In Section 2 we describe how the *phs* class and its corresponding functions can be used to efficiently store, analyze and interconnect sparse pH models of possibly large state-space dimension. In Section 3 we provide an overview of how the three mentioned structure-preserving MOR approaches are supported in our toolbox. We illustrate the applicability and performance of selected MOR algorithms using two benchmark examples in Section 4 and conclude with some remarks on how to get started with and contribute to the MORpH toolbox in Sections 5 and 6.

2 Sparse port-Hamiltonian systems

2.1 Preliminaries

We consider linear time-invariant (LTI) systems of the form

$$\Sigma: \begin{cases} E\dot{x}(t) = Ax(t) + Bu(t), \quad Ex(0) = 0, \\ y(t) = Cx(t) + Du(t), \end{cases} \tag{1}$$

with state vector $x(t) \in \mathbb{R}^n$, inputs $u(t) \in \mathbb{R}^m$, outputs $y(t) \in \mathbb{R}^m$ for all $t \in [0, \infty)$ and constant matrices $E, A \in \mathbb{R}^{n\times n}$, $B \in \mathbb{R}^{n\times m}$, $C \in \mathbb{R}^{m\times n}$ and $D \in \mathbb{R}^{m\times m}$. We call systems where the descriptor matrix E is the identity matrix *explicit* and *implicit* otherwise. Systems with singular descriptor matrix E are referred to as differential-algebraic equation (DAE) systems and ordinary differential equation (ODE) otherwise. In the following, we will assume that the system is *regular*, i.e., the matrix pencil $sE - A$ is invertible for some $s \in \mathbb{C}$. Then, the input-output behavior of the system in the frequency domain is described by its transfer function

$$H(s) = C(sE - A)^{-1}B + D. \tag{2}$$

In this work, we focus on pH-DAEs, a subclass of the system class in (1) with additional structural properties that allow a physical interpretation and consequently, an energy-based viewpoint.

Definition 1. [15, 16] A linear time-invariant descriptor system

$$\Sigma_{\mathrm{pH}}: \begin{cases} E\dot{x}(t) = (J - R)Qx(t) + (G - P)u(t), \\ y(t) = (G + P)^{\mathsf{T}}Qx(t) + (S + N)u(t), \end{cases} \tag{3}$$

where $E, Q, J, R \in \mathbb{R}^{n\times n}$, $G, P \in \mathbb{R}^{n\times m}$, $S, N \in \mathbb{R}^{m\times m}$, is called a *pH-DAE*, if the following conditions are satisfied:

(i) The structure matrix

$$\Gamma := \begin{bmatrix} Q^{\mathsf{T}}JQ & Q^{\mathsf{T}}G \\ -G^{\mathsf{T}}Q & N \end{bmatrix}$$

is skew-symmetric, i.e., $\Gamma = -\Gamma^{\mathsf{T}}$.

(ii) The dissipation matrix

$$W := \begin{bmatrix} Q^{\mathsf{T}}RQ & Q^{\mathsf{T}}P \\ P^{\mathsf{T}}Q & S \end{bmatrix}$$

is positive semidefinite, i.e., $W = W^{\mathsf{T}} \geq 0$.

(iii) The Hamiltonian is quadratic; it reads

$$\mathcal{H}(x) = \frac{1}{2} x^\mathsf{T} Q^\mathsf{T} E x,$$

with $Q^\mathsf{T}E = E^\mathsf{T}Q \geq 0$.

Systems with invertible descriptor matrix E are referred to as port-Hamiltonian ordinary differential equation systems (pH-ODEs) in the following. As shown in [15, 17], the modeling of physical systems often naturally leads to pH-DAE realizations which are in (or close to) *staircase form* derived in [18, 19]. This form reveals further properties of the pH-DAE system, such as its differentiation index. Conversely, every pH-DAE as in Definition 1 can be transformed to staircase form via orthogonal transformations that preserve the pH structure. The staircase form is also beneficial in the context of MOR since it enables a decomposition of the transfer function which is discussed in more detail in Section 3.3.3.

2.2 The *phs* class

In MATLAB, small to medium-scale LTI models Σ can be represented as instances of the *ss* class and sparse large-scale models with the class *sparss* which are both part of the Control System Toolbox. However, storing pH-DAEs Σ_{pH} in this way would generally result in a loss of the pH structure. In MORpH, we therefore introduce two new system classes *phs* and *phsRed* to represent (sparse) large-scale and (full) small to medium-scale pH-DAEs, respectively. Figure 1 provides an overview of the most important properties and functions. The class *phsRed* is derived from *phs* with additional properties to represent ROMs. We describe this class in more detail in Section 3.3.1. In the following, we focus on properties and functions of the *phs* class and show how its instances can be interconnected in a structure-preserving way.

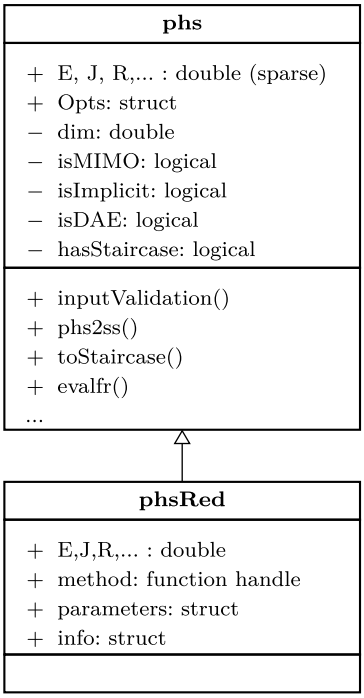

Figure 1: UML class diagram of the classes *phs* to represent sparse pH-DAEs (see Section 2.2) and *phsRed* to represent reduced-order pH-DAEs (see Section 3.3.1).

2.2.1 Properties

Each instance of the *phs* class stores the system matrices E, J, R, Q, G, P, S, and N in the sparse matrix format per default to reduce storage demands. Additionally, each instance has a set of private variables which describe important properties of the system, such as `dim`, the dimension n of the system. Further logical properties which may be relevant for simulation and MOR include, for instance, the parameter `isMIMO` to check whether the system has multiple inputs and `hasStaircase`, which is true when the system has staircase form. These properties cannot be altered directly because they depend on the system matrices. Their purpose is to provide quick access to information which would otherwise require the check of certain conditions every time it is requested.

2.2.2 Object construction

A *phs* object can be created by passing the respective system matrices. Supported input patterns include

```
sys = phs (J, R, Q, G)
sys = phs (J, R, Q, G, E, P, S, N)
sys = phs (..., Opts)
```

At creation of a *phs* object, the system matrices are validated by the function `inputValidation`. Compared to the classes *ss* and *sparss* where the matrices are checked for correct dimensions, this additionally requires validation of the symmetry and definiteness properties presented in Definition 1. For instance, we need the smallest real eigenvalue of W to determine whether it is positive semidefinite. For this, we choose MATLAB's built-in functions `eig` for small models and `eigs` for large-scale models. In floating-point arithmetic, this value can only be computed within a certain error range and therefore, a tolerance is used for the validity decision.

If any of the constraints is violated, object creation will fail and the function will throw an error indicating the corresponding constraint violation. Users may change the tolerance value manually or deactivate system validation completely, which may be beneficial for very large systems to save computation time. These configurations may be applied by passing the struct `Opts` to the constructor. The respective fields are named `inputValidation` and `inputTolerance`.

2.2.3 Functions

The *phs* class implements functions which facilitate interaction with its instances. These functions enable the user to analyze the underlying pH system, to access instance properties, and to transform an instance. The following is a non-exhaustive list of examples:

1. System analysis:
   - Computation of important system properties, e.g., with functions `eig, eigs, norm`, `freqresp`.
   - Visualization of system properties, e.g., with functions `bode, step, impulse`, `pzmap`.
   - Most functions in this category use or behave in a similar fashion to their counterparts from the Control System Toolbox for better usability.
2. Property access:
   - Setter methods allow the modification of the system matrices, e.g.:
     ```
     sys.S = 0
     ```
   - This automatically triggers an update of the deduced logical properties of the *phs* object (see Figure 1). For example, upon changing the descriptor matrix `sys.E` of a system from $E = I_n$ to $E \neq I_n$, the logical property `isImplicit` is automatically updated from `false` to `true`.
   - The pH structural constraints are not validated automatically but can (and should) be checked by a manual call of the validation routine:
     ```
     isPH = phs.inputValidation(sys)
     ```
3. System transformation:
   - *phs* objects can be converted to *ss* objects from the Control System Toolbox and *sss* objects from the sss/sssMOR Toolbox [12] by the functions `phs2ss` and `phs2sss`, respectively.
   - *phs* objects may be transformed to other representations. For example, ODE systems may be transformed to explicit form ($E = I_n$) via `makeExplicit` and DAE systems to staircase form via `toStaircase`.
   - All transformations in this category retain the system's transfer function H.

2.2.4 Power-preserving interconnection

An important property of pH models is that if they are interconnected in a power-preserving way, the interconnected model is again pH. This enables a network modeling approach, where different subsystems are modeled independently and subsequently coupled, possibly across different physical domains. Power preservation of the interconnection is ensured by means of Dirac structures. Consider the interconnection of two pH systems Σ^1_{pH} and Σ^2_{pH} as in (3) with power-conjugated input-output pairs (u_1, y_1) and (u_2, y_2), respectively, using a Dirac structure $\mathcal{D}_I$ (see Figure 2(a)). The external port of the resulting interconnected system is given by (u, y).

Let us define the vectors of flows $f_I := \left[y_1^\mathsf{T}, y_2^\mathsf{T}, y^\mathsf{T}\right]^\mathsf{T} \in \mathcal{F}$ and efforts $e_I := \left[u_1^\mathsf{T}, u_2^\mathsf{T}, u^\mathsf{T}\right]^\mathsf{T} \in \mathcal{E}$ with $\mathcal{E} = \mathcal{F}^*$. In linear coordinates, the matrix kernel representation of the Dirac structure $\mathcal{D}_I \subset \mathcal{F} \times \mathcal{E}$ is stated as

$$\mathcal{D}_I := \{(f_I, e_I) \in \mathcal{F} \times \mathcal{E} \mid F_I f_I + E_I e_I = 0\},$$

with $E_I, F_I \in \mathbb{R}^{n_I \times n_I}$ that satisfy the conditions

(i) $E_I F_I^\mathsf{T} + F_I E_I^\mathsf{T} = 0$,
(ii) $\operatorname{rank}[E_I, F_I] = n_I$,

where $n_I = \dim \mathcal{F}$ (see [20, Chapter 2.4]). The Hamiltonian of the interconnected system is the sum of the Hamiltonians of its subsystems.

The MORpH toolbox supports the intuitive construction of pH networks by its object-oriented nature and different Dirac structure representations. These include *gyrator* and *transformer* interconnections as well as the negative feedback interconnection which is beneficial for energy-based control of pH systems and depicted in Figure 2(b). Its Dirac structure $\mathcal{D}_I$ is represented by

$$E_I = \begin{bmatrix} -I & 0 & I \\ 0 & -I & 0 \\ 0 & 0 & 0 \end{bmatrix}, \qquad F_I = \begin{bmatrix} 0 & -I & 0 \\ I & 0 & 0 \\ I & 0 & I \end{bmatrix}. \tag{4}$$

with the same splitting as in f_I, e_I and we obtain the interconnected system via

```
sysI = feedback(sys1, sys2)
```

Remark 1. The MORpH toolbox also supports interconnections of pH-DAEs that are not structure preserving. Arithmetic operations on *phs* objects are also possible. For instance, the error system between two pH systems, which is important for MOR, can simply be computed via:

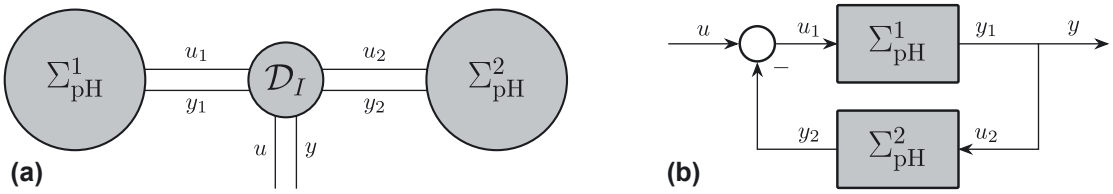

Figure 2: Power-preserving interconnections of pH-DAEs supported by MORpH. (a) Schematic of the power-preserving interconnection of two pH systems Σ^1_{pH}, Σ^2_{pH} using a Dirac structure $\mathcal{D}_I$. The external, power-conjugated input-output pair of the interconnected system is given by (u, y). (b) Negative feedback interconnection as an example with a Dirac structure representation as in (4).

```
sysErr = sys1 - sys2
```

In this case, the interconnected model `sysErr` is represented as a sparse *sss* object of the sss/sssMOR toolbox [12].

3 Model reduction of pH-DAEs

Before we start with the description and implementation details of the different MOR methods implemented in MORpH, let us first recapitulate some properties of pH-DAEs that are relevant for MOR purposes.

3.1 Preliminaries

The goal of structure-preserving MOR of pH-DAEs is to find a ROM:

$$\widehat{\Sigma}_{\mathrm{pH}}: \begin{cases} \widehat{E}\dot{\widehat{x}}(t) = (\widehat{J} - \widehat{R})\widehat{Q}\widehat{x}(t) + (\widehat{G} - \widehat{P})u(t), \\ \widehat{y}(t) = (\widehat{G} + \widehat{P})^{\mathsf{T}}\widehat{Q}\widehat{x}(t) + (\widehat{S} + \widehat{N})u(t), \end{cases} \tag{5}$$

where $\widehat{E}, \widehat{Q}, \widehat{J}, \widehat{R} \in \mathbb{R}^{r\times r}$, $\widehat{G}, \widehat{P} \in \mathbb{R}^{r\times m}$, $\widehat{S}, \widehat{N} \in \mathbb{R}^{m\times m}$ with the same structural constraints (i)–(iii) as in Definition 1 and such that $r \ll n$ as well as $y \approx \widehat{y}$ for certain inputs u. The ROM has an associated transfer function $\widehat{H}$ and its approximation quality is typically assessed by the $\mathcal{H}_2$ and $\mathcal{H}_\infty$ norm of the error function $H - \widehat{H}$ (see Remark 1).

The main difference to classic MOR methods for general LTI systems is that we demand a preservation of the pH structural constraints in the reduction process. For this task, two closely related properties can be exploited: passivity and positive realness.

3.1.1 Passivity and positive realness

A physical property which is of crucial importance for the interconnection and time-domain simulation of LTI systems is the concept of *passivity*.

Definition 2. [21] An LTI system Σ is considered passive if there exists a state-dependent, non-negative storage function $\mathcal{S}(x)\colon \mathbb{R}^n \to \mathbb{R}_{\geq 0}$ such that for any $\tau \in \mathbb{R}$ with $\tau > 0$ the dissipation inequality

$$\mathcal{S}(x(\tau)) - \mathcal{S}(x(0)) \leq \int_0^\tau y(t)^T u(t)\,\mathrm{d}t, \tag{6}$$

holds for any smooth u, y and solution trajectory x satisfying (1).

We will denote LTI systems with this property by Σ_{pa}. Since it is difficult to assess passivity via the dissipation inequality, a related property of the system's transfer function H is frequently used.

Definition 3. [22, Theorem 2.7.2] A transfer function H is called positive real if

(i) *H has no poles for all $s \in \mathbb{C}, \mathrm{Re}(s) > 0$.*

(ii) The *Popov function*

$$\Psi(s) := H(s) + H(-s)^{\mathsf{T}} \tag{7}$$

is positive semidefinite for each $s = \mathrm{i}\omega$ with $\omega \in \mathbb{R}$ which is not a pole of H.

(iii) Every pole $\mathrm{i}\omega_0 \in \mathrm{i}\mathbb{R}$ of H is at most simple. The residue matrix $\lim_{s\to\mathrm{i}\omega_0}(s - \mathrm{i}\omega_0)H(s)$ for finite ω_0, and $\lim_{\omega\to\infty}\frac{H(\mathrm{i}\omega)}{\mathrm{i}\omega}$ for poles at infinity, is Hermitian positive semidefinite.

All pH systems Σ_{pH} are inherently passive and all passive LTI systems Σ_{pa} do in turn have a positive real transfer function. Conversely, a system Σ with positive real transfer function is passive if it is *behaviorally controllable*, i.e., $\mathrm{rank}[(sE - A), B] = n$ for all $s \in \mathbb{C}$. The question that remains is which passive systems Σ_{pa} admit a pH representation Σ_{pH}.

3.1.2 The Kalman–Yakubovich–Popov inequality

As shown in [6, 20], a pH representation Σ_{pH} of a passive system Σ_{pa} exists if and only if the *Kalman–Yakubovich–Popov*

(KYP) inequality

$$\begin{bmatrix} -A^\mathsf{T}X - X^\mathsf{T}A & C^\mathsf{T} - X^\mathsf{T}B \\ C - B^\mathsf{T}X & D + D^\mathsf{T} \end{bmatrix} \geq 0, \quad X^\mathsf{T}E = E^\mathsf{T}X \geq 0, \tag{8}$$

has a solution $X \in \mathbb{R}^{n\times n}$, such that

$$\ker X \subseteq \ker C \cap \ker A. \tag{9}$$

In particular, for passive ODE systems which are *behaviorally observable*, i.e., $\operatorname{rank}[(sE - A)^\mathsf{T}, C^\mathsf{T}] = n$ for all $s \in \mathbb{C}$, the solution X is invertible and a pH-ODE representation can be found, for example, by setting $Q = X$ and

$$\begin{aligned} J &= \frac{1}{2}(AX^{-1} - X^{-T}A^T), & R &= -\frac{1}{2}(AX^{-1} + X^{-T}A^T), \\ G &= \frac{1}{2}(X^{-T}C^T + B), & P &= \frac{1}{2}(X^{-T}C^T - B), \\ N &= \frac{1}{2}(D - D^T), & S &= \frac{1}{2}(D + D^T). \end{aligned}$$

This result is also beneficial in the DAE setting: Since every passive DAE may be decomposed into a passive ODE part and an improper part that already has pH structure (see [5, 6] and Section 3.3.3), it is sufficient to solve a *modified* KYP inequality for the ODE part.

What are the consequences of these results for model reduction? We may generally assume that a ROM $\widehat{\Sigma}$ is minimal (and therefore behaviorally controllable and observable) since otherwise, its state-space dimension r could be further reduced without changing its transfer function $\widehat{H}$ until a minimal representation is obtained. Consequently, for ROMs, the concepts of passivity, positive realness and the existence of a pH representation are equivalent and instead of searching directly for reduced ROMs $\widehat{\Sigma}_{\text{pH}}$ in pH form one can also search for passive (or positive real) ROMs $\widehat{\Sigma}_{\text{pa}}$.

3.2 Overview of MOR methods

These theoretical findings unveil three different strategies for the structure-preserving MOR of pH-DAEs which are depicted in Figure 3:

1. PH-preserving MOR (pH-MOR).
2. Passivity-preserving MOR (pa-MOR) + KYP Transformation (`ss2phs`).
3. Standard MOR (sss-MOR) + Passivity Enforcement (pa-ENF) + KYP Transformation (`ss2phs`).

The MORpH toolbox supports each of these pathways with a set of algorithms that are listed in Table 1 for each category pH-MOR, pa-MOR and pa-ENF with their corresponding references. In the following, we will only outline the basic functionality of each algorithm to provide an overview and we refer the reader to the given references in Table 1 and to the respective functions and demo scripts in the MORpH toolbox for further information.

3.2.1 PH-preserving MOR (pH-MOR)

There are two major approaches to directly search for a ROM in pH form: using Petrov–Galerkin projections or an optimization of the reduced system matrices.

Petrov–Galerkin methods are based on an approximation $x(t) \approx V\hat{x}(t)$ of the original state vector, where the columns of $V \in \mathbb{R}^{n\times r}$ form a basis for a suitably chosen subspace of dimension r. Similar to traditional MOR methods, this subspace is either chosen to *balance* the original system or to *interpolate* its transfer function.

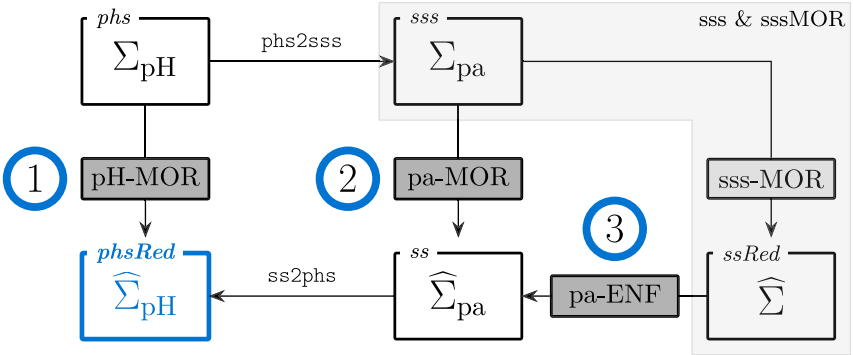

Figure 3: Overview of different MOR strategies for pH-DAEs supported by MORpH. The goal is to find a ROM $\widehat{\Sigma}_{\text{pH}}$ which is stored as a *phsRed* object and highlighted in blue. The boxes pH-MOR, pa-MOR and pa-ENF represent different algorithm categories and the function `ss2phs` computes a pH representation for a passive system by solving the KYP inequality in (8). The interface to the MATLAB toolboxes sss and sssMOR is grayed out.

Table 1: Model reduction and passivity enforcement methods supported by MORpH. Depending on their configuration, some algorithms may rely on third-party software which is to be downloaded separately and described in more detail in the Appendix.

Category	Method	Function	Principle	References
pH-MOR	Effort-constraint method	`ecm`	Balancing	[23]
	PH-balancing	`balPH`	Balancing	[1]
	Arnoldi-PH	`arnoldiPH`	Interpolation	[24]
	IRKA-PH	`irkaPH`	$\mathcal{H}_2$-inspired interpolation	[3, 19]
	CIRKA-PH	`cirkaPH`	$\mathcal{H}_2$-inspired interpolation	[25]
	TRKSM-PH	`trksmPH`	Adaptive interpolation	[26, 27, 33]
	PROPT	`prOpt`	$\mathcal{H}_2$-inspired optimization	[5, 29, 34]
	LYAPOPT	`lyapOpt`	$\mathcal{H}_2$-inspired optimization	[28]
	SOBMOR	`sobmor`	$\mathcal{H}_\infty$-inspired optimization	[5, 30, 34]
	IHA-PH	`ihaPH`	Interpolation + feedthrough opt.	[33, 35, 36]
pa-MOR	Spectral factor MOR	`sfmor`	Spectral factorization	[7]
	Positive real balancing	`prbt`	Balancing	[31, 32]
	Mixed Gramian balancing	`prbt`	Balancing	[9]
	Dominant spectral zero method	`dszm`	Interpolation	[8]
pa-ENF	Local passivity enforcement	`locPasEnf`	Sampling + eigenvalue perturbation	[10]
	Hamiltonian passivity enforcement	`hamPasEnf`	Eigenvalue perturbation	[10, 37]
	Positive real passivity enforcement	`prlPasEnf`	Optimization	[10]

Structure-preserving variants of the classic balanced truncation algorithm implemented in MORpH are the effort-constraint method `ecm` [23] and a recently proposed variant `balPH` [1] that enables a classical *a priori* error bound under certain conditions. Interpolatory MOR methods enforce tangential interpolation conditions between the original and reduced transfer function at selected complex interpolation points or *shifts*. In `arnoldiPH` [24], these shifts can be chosen manually. In `irkaPH` [3] and its adaptation `cirkaPH` [25] they are chosen automatically in an $\mathcal{H}_2$-inspired way using fixed-point iterations and in `trksmPH` [26, 27] the ROM is built adaptively, meaning that in each iteration one or several new shifts are chosen in regions where the approximation quality of the ROM is still poor.

Optimization-based techniques are targeted toward low errors in either the $\mathcal{H}_2$ or $\mathcal{H}_\infty$ norm. The $\mathcal{H}_2$ optimization problem can be formulated based on Lyapunov equations (`lyapOpt`) [28] or based on the pole-residue expansion of the ROM (`prOpt`) [29]. An $\mathcal{H}_\infty$-inspired optimization of system parameters is implemented in `sobmor` [30].

An example of how different algorithms of the MORpH toolbox can be combined is the method implemented in `ihaPH` which combines the interpolatory approach `irkaPH` (or `cirkaPH`) with an $\mathcal{H}_\infty$-inspired optimization of the reduced feedthrough matrices $\widehat{S}$, $\widehat{N}$. All methods in this category directly yield reduced pH-DAEs $\widehat{\Sigma}_{\mathrm{pH}}$ represented by *phsRed* objects which are described in more detail in Section 3.3.1.

3.2.2 Passivity-preserving MOR (pa-MOR) and KYP transformation

Since every pH-DAE as in Definition 1 is inherently passive (and therefore positive real), it may also be reduced by MOR methods which preserve passivity (or positive realness).

The different approaches for passivity-preserving MOR (pa-MOR) implemented in the MORpH toolbox are again based on either system balancing or tangential interpolation. Balancing-based approaches rely on the solution of algebraic Riccati equations or a mixture of Riccati and Lyapunov equations (`prbt`) [31, 32, 9]. With interpolatory methods, passivity of the original model can be retained by interpolating the original system at its spectral zeros (`dszm`) [8]. The algorithm `sfmor` [7] relies on a spectral factorization of the Popov function in (7). If, instead of the original model, the corresponding spectral factor is considered, both traditional balancing and interpolatory techniques for general LTI systems can be applied to find a reduced spectral factor and subsequently compute the corresponding passive ROM.

Then, under the assumption that the obtained ROM $\widehat{\Sigma}_{\mathrm{pa}}$ is minimal, a pH representation $\widehat{\Sigma}_{\mathrm{pH}}$ can be computed

by the function ss2phs which solves the KYP inequality in (8).

3.2.3 Standard MOR (sss-MOR) and passivity enforcement (pa-ENF)

The application of standard (unstructured) MOR techniques to pH systems will generally lead to ROMs $\widehat{\Sigma}$ which are neither passive nor in pH form. However, if the ROM accurately approximates the input-output characteristics of the passive full-order model (FOM) Σ_{pa}, one can hope that the passivity violations are only minor. In this case, passivity of the ROM can be enforced in a post-processing step by slight perturbations of its system matrix entries (pa-ENF). This step evidently introduces an additional approximation error which is, however, expected to be small if the passivity violations are minor.

After reduction, for which any of the unstructured MOR algorithms of the sssMOR toolbox [12] can be used, this strategy initially requires a passivity check of the obtained unstructured ROM $\widehat{\Sigma}$ to determine whether a perturbation is necessary. Passivity validation techniques rely on checking positive realness, i.e., the conditions in Definition 3, or whether a solution to the KYP inequality in (8) can be found.

Existing passivity enforcement techniques are closely linked to these passivity validation techniques. Positive realness is usually verified by sampling the Popov function Ψ along the imaginary axis. Accordingly, passivity is enforced by identifying local passivity violations on the imaginary axis and nudging the negative eigenvalues of Ψ towards positivity (`locPasEnf`) [10]. An alternative way to assess positive realness is checking if spectral zeros of Ψ are present on the imaginary axis. The spectral zeros can then be calculated as eigenvalues of a Hamiltonian matrix associated with the inverted system representation of Ψ. If this matrix has purely imaginary eigenvalues, these are perturbed in `hamPasEnf` such that they move off the imaginary axis to render the system passive [37]. In both methods, the obtained passive ROM is transformed to pH form via the function ss2phs. The third approach implemented in `prlPasEnf` searches for the minimum perturbation such that the KYP inequality in (8) has an invertible solution [10] and therefore, a pH representation is directly obtained.

3.3 Implementation

3.3.1 The *phsRed* class

Since reduced pH-DAEs $\widehat{\Sigma}_{\text{pH}}$ have the same structural properties as their original counterparts Σ_{pH}, it is reasonable to represent them in a similar way. In MORpH, systems $\widehat{\Sigma}_{\text{pH}}$ are represented as objects of the *phsRed* class (see Figure 1). This class *inherits* all attributes and methods from its superclass *phs* and consequently one can, for instance, run functions such as the input validation also on ROMs. This is important since even structure-preserving algorithms may destroy the pH structure due to numerical errors. It also means that ROMs can be interconnected with other pH systems as described in Section 2.2.4. As shown in Figure 1, there are, however, some differences. Compared to *phs*, the system matrices are not represented sparse since the ROM matrices are comparatively small and generally dense. In this case, a sparse representation may even increase storage demands. Also, since every *phsRed* object has an associated MOR method, one can store information on this method with three public attributes:

1. `method`: Function handle of the generating MOR method.
2. `parameters`: Struct with parameters used for the MOR method.
3. `info`: Struct with information on the MOR method, such as the number of iterations in optimization-based methods.

This quite general definition of MOR information enables the necessary flexibility to account for a variety of MOR methods and also allows a straightforward nesting of information if different methods are applied consecutively.

3.3.2 MOR functions

In MORpH, the signatures of the functions in Table 1 follow a similar pattern as in other MOR packages (see, e.g., [12, 13]):

```
[sysOut, ...] = fct(sysIn, ..., Opts)
```

Every function `fct` expects at least a system `sysIn` as an input. The output system `sysOut` is either a reduced system (for pH-MOR and pa-MOR functions), transformed system (for `phs2sss` and `ss2phs`), or perturbed version (for pa-ENF functions) of the input system `sysIn`. The involved system classes can be extracted from Figure 3 for each category. For example, the algorithms of the category pH-MOR expect *phs* objects as inputs and produce *phsRed* objects as outputs. In addition to the system output `sysOut`, some functions return variables which give more details on the results.

Some methods may require or accept additional, function-specific input arguments. For example, the projection-based method `arnoldiPH` expects a set of points

at which the transfer function is interpolated. Moreover, all algorithms allow detailed configuration by the structure array (struct) of execution parameters `Opts`. The structure fields vary from function to function and are explained in the header of each function.

Prior to execution, most of the toolbox functions perform a step we call *input parsing*. Not only is this step responsible for interpreting different input schemes (function overloading), it also checks the given arguments for validity and coherence and sets default values for non-provided arguments. This allows us to reduce runtime errors and to inform the user early on if provided arguments are not applicable.

To parse the option struct `Opts`, we provide and employ the implementation `phsMOR_parseOpts` which validates options based on a set of default parameters. It checks input types, compares values to constraints, sets default values where required, and is compatible with nested options.

To illustrate the configuration process, let us consider the following call of the IRKA-PH algorithm:

```
sysRed = irkaPH(sys, s0, Opts)
```

The (optional) input variable s0 is a vector of initial interpolation points. The input parsing step ensures that the length of this vector does not exceed the order of the original system. A potential value for the (optional) parameter `Opts` is a struct with fields

```
  maxIter: positive integer
      tol: non-negative double
 stopCrit: string
arnoldiPH: struct
      ...
```

Here, the entries `maxIter`, `tol`, and `stopCrit` define termination conditions for the iterative algorithm. `stopCrit` refers to a set of convergence criteria. The option struct with name `arnoldiPH` is passed on to the subroutine with the same name. Among others, we provide default values for `maxIter` and `tol` and a set of valid strings for `stopCrit`. These are used for checking user inputs with `phsMOR_parseOpts`. Execution parameters which are not provided will be filled with default values.

3.3.3 A system decomposition approach

Not all of the algorithms listed in Table 1 are suitable for the entire system class of pH-DAEs. In particular, many methods are proposed for pH-ODEs only, i.e., they require the descriptor matrix E to be invertible. With the MORpH toolbox, these methods can still be applied to pH-DAEs using a function wrapper which is based on a system decomposition approach that exploits the pH structural constraints.

As shown in [5], the transfer function of every pH-DAE Σ_{pH} may be decomposed into the sum

$$H(s) = H_{\mathrm{p}}(s) + \mathcal{D}_1 \cdot s, \tag{10}$$

such that

(i) H_{p} denotes the transfer function of a pH-ODE system,
(ii) $\mathcal{D}_1 \in \mathbb{R}^{m\times m}$ is symmetric positive semidefinite.

Note that the ROM $\widehat{\Sigma}_{\mathrm{pH}}$ has to match the *improper* polynomial part $\mathcal{D}_1 \cdot s$ of the FOM Σ_{pH} exactly in order to keep the $\mathcal{H}_2$ and $\mathcal{H}_\infty$ errors bounded. Using a rank-revealing factorization $\mathcal{D}_1 = LL^{\mathsf{T}}$ with $L \in \mathbb{R}^{m\times q}$, this polynomial part may be represented by the following pH-DAE

$$\begin{aligned} \begin{bmatrix} I_q & 0 \\ 0 & 0 \end{bmatrix} \dot{x}_{\mathrm{pol}}(t) &= \begin{bmatrix} 0 & I_q \\ -I_q & 0 \end{bmatrix} x_{\mathrm{pol}}(t) + \begin{bmatrix} 0 \\ L^{\mathsf{T}} \end{bmatrix} u(t), \\ y_{\mathrm{pol}}(t) &= \begin{bmatrix} 0 & L \end{bmatrix} x_{\mathrm{pol}}(t), \end{aligned} \tag{11}$$

with x_{pol} partitioned as $x_{\mathrm{pol}}(t) = \left[x_1(t)^{\mathsf{T}}, x_2(t)^{\mathsf{T}}\right]^{\mathsf{T}}$, where $x_1(t), x_2(t) \in \mathbb{R}^q$ for each $t \in [0, \infty)$.

A corresponding pH-ODE representation for the remaining transfer function H_{p} can be found, for instance, using staircase transformations as in [18] (see [5] for details). This pH-ODE may then be reduced by any MOR method suitable for pH-ODEs, yielding a ROM with transfer function $\widehat{H}_{\mathrm{p}}$. The final ROM $\widehat{\Sigma}_{\mathrm{pH}}$ in pH-DAE form with transfer function

$$\widehat{H}(s) = \widehat{H}_{\mathrm{p}}(s) + \mathcal{D}_1 \cdot s, \tag{12}$$

is obtained by interconnecting both the reduced pH-ODE part and the system in (11) in a structure-preserving way (see Section 2.2.4).

In MORpH, this system decomposition approach is implemented by the function `pHMOR_DAE_Wrapper`. For instance, the IRKA-PH algorithm may be applied to pH-DAEs, simply via

```
redSys = pHMOR_DAE_Wrapper(@irkaPH, ...
                                sys, s0, Opts)
```

We highlight that generally, and especially if the original model does not have staircase form, the pH-ODE system with transfer function H_{p} is dense, which may significantly increase the computational costs of the reduction. Moreover, the computation of staircase forms relies on a

series of rank conditions which may be sensitive under perturbations (see, e.g., [17, 38]). Therefore, especially for large-scale systems, more efficient approaches are required which exploit the sparsity of the original system matrices and do not rely on (possibly expensive and ill-conditioned) transformations. This is an open research problem which was recently addressed in, e.g., [5, 16, 19, 33, 34].

4 Numerical examples

To demonstrate the functionality of the MORpH toolbox, we apply a selection of the methods in Table 1 to two pH-DAE benchmark models. All computations were conducted using MATLAB R2021b (version 9.11.0.1873467) on an Intel® Core™i7-8700 CPU (3.20 GHz, 6-Core) with 32 GB RAM. The code to compute the results presented in this section is publicly available at [39]. All MOR algorithms were executed with their default parameters, which may be obtained from the input parsing section in each function.

4.1 Benchmark models

The first benchmark (`msd_ode`) is the pH-ODE model of a large-scale mass-spring-damper chain with 10,000 states and two inputs and outputs. To demonstrate the system decomposition approach presented in Section 3.3.3, we additionally consider an electrical circuit modeled by a medium-sized pH-DAE in staircase form with differentiation index two (`rcl_dae2`). The properties of both models, represented as *phs* objects, are summarized in Table 2 and the corresponding frequency responses are given in Figure 4. It shows that the transfer function of `rcl_dae2` contains a linear improper part $\mathcal{D}_1 \cdot s$ (originating from the algebraic constraints) which can be treated with the system decomposition approach from Section 3.3.3. Both models are taken from the port-Hamiltonian benchmark collection[1] to which we refer for a more detailed physical description. The system matrices are publicly available at [39].

Table 2: *phs* properties of the considered benchmark models.

Model	dim	isMIMO	isDAE	hasStaircase
msd_ode	10,000	1	0	0
rcl_dae2	1502	0	1	1

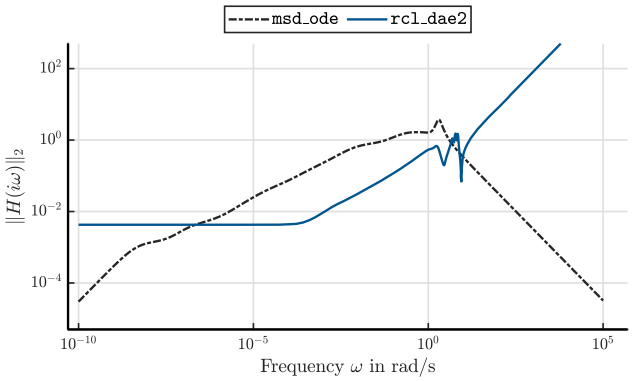

Figure 4: Frequency responses of the mass-spring-damper chain `msd_ode` and the electric circuit `rcl_dae2`.

4.2 Results

We first consider model `msd_ode` and create ROMs with dimension $r = 10$. Figure 5 shows the frequency error plots for a selection of MOR algorithms with different functionality. Figure 5(a) contains the results for different pH-MOR algorithms. It can be observed that $\mathcal{H}_2$-inspired algorithms produce higher errors for low frequencies while $\mathcal{H}_\infty$-inspired methods generally produce lower maximum gains but higher errors in high-frequency regions. The results for selected algorithms from the pa-MOR and pa-ENF groups are plotted in Figure 5(b). The passivity enforcement methods `prlPasEnf` and `locPasEnf` were applied to a (non-passive) ROM $\widehat{\Sigma}$ created with the (unstructured) IRKA algorithm, which was also used to reduce the spectral factor in `sfmor`. Consequently, all three methods produce errors which are very similar to the ones obtained with IRKA (which are not plotted here). The large-scale algebraic Riccati equations in `sfmor` and `prbt` are solved with the iterative low-rank method in [40] that is implemented in the M-M.E.S.S. toolbox [41]. In the case of `prbt`, the method fails to compute an accurate solution to one of the two Riccati equations with the default settings, which leads to larger errors compared to the other algorithms. This is a potential drawback of all algorithms that rely on the solution of large-scale matrix equations.

For the medium-sized pH-DAE model `rcl_dae2` we choose the same settings and compute reduced order models with different dimensions for each algorithm. In Figure 6, we plot the $\mathcal{H}_2$ and $\mathcal{H}_\infty$ errors over the dimension r of the *proper* part of the ROM. Note that the final dimension of the ROMs is always increased by two due to the attachment of the improper part. Figure 6 shows that the errors decrease for all methods if the reduced order r is increased, which is expected. The fact that the errors decrease quite slowly is an indication that the `rcl_dae2` model is quite

1 https://port-hamiltonian.io.

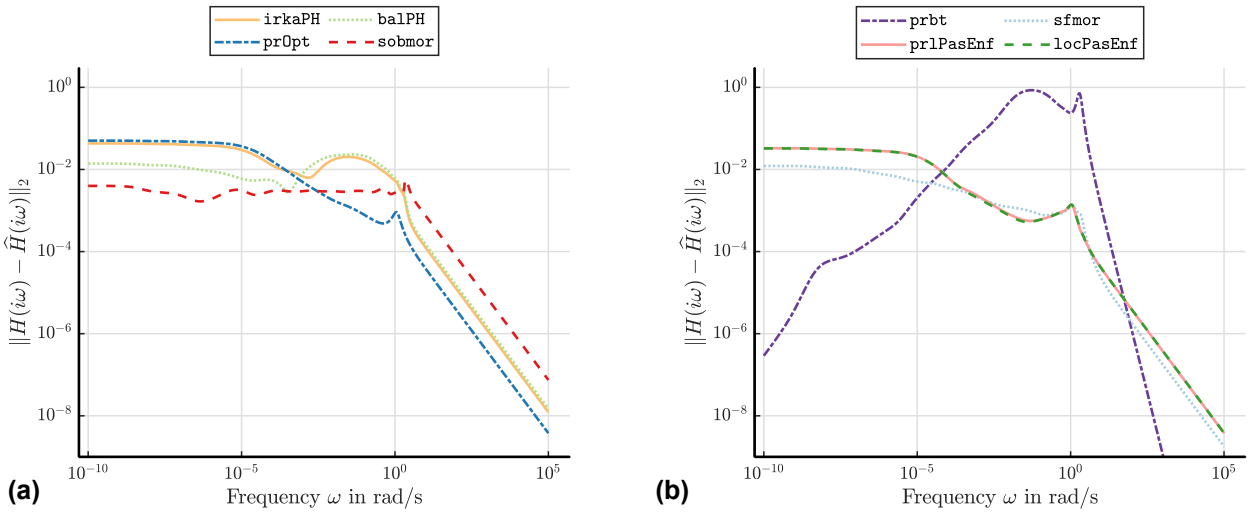

Figure 5: Reduction of the large-scale mass-spring-damper model `msd_ode`. Frequency errors for a selection of (a) PH-MOR algorithms (b) Pa-MOR and pa-ENF algorithms.

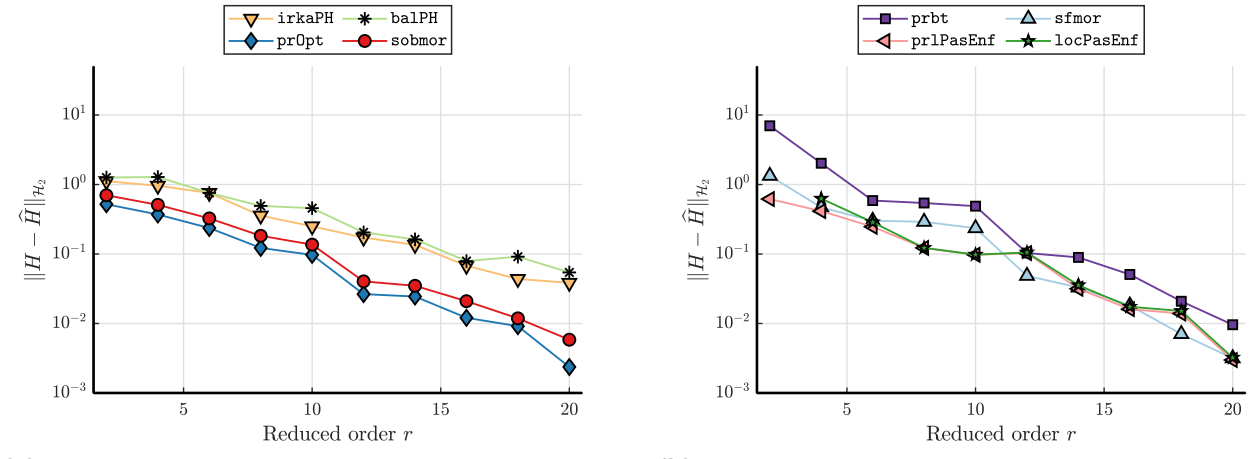

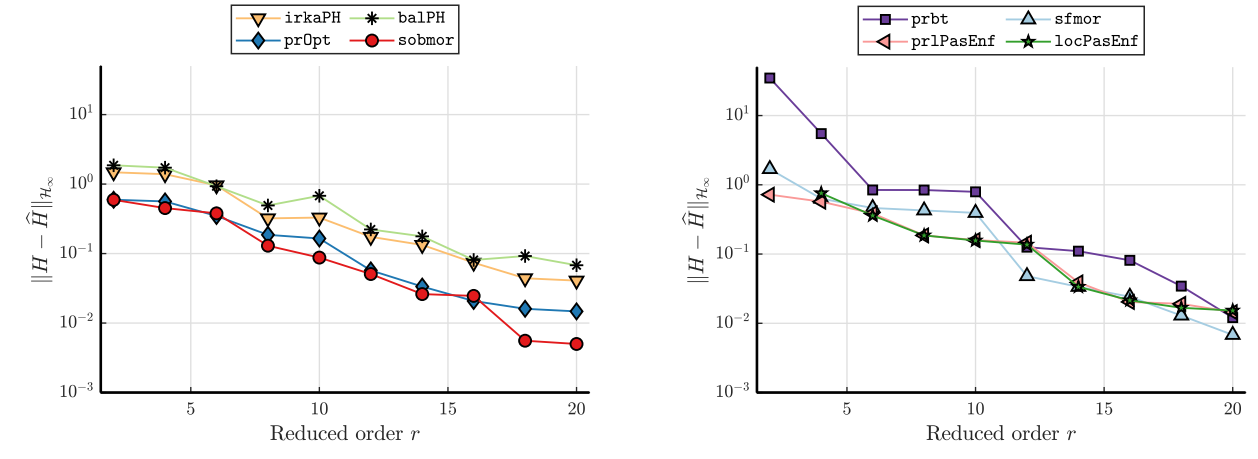

Figure 6: Reduction of the pH-DAE system rcl_dae2. Shown are the $\mathcal{H}_2$ and $\mathcal{H}_\infty$ errors for different reduced orders r and selected algorithms from the MOR categories pH-MOR (left) and pa-MOR/pa-ENF (right).

difficult to approximate. One consequence is that methods that are specifically tailored towards minimizing one of the two error norms generally perform better in this norm but worse in the other. Another consequence is that unstructured MOR methods typically do not yield passive ROMs and are therefore not suited for a structure-preserving reduction. In this case, the unstructured IRKA algorithm only delivers a ROM which is passive (and therefore has a pH representation) for $r = 8$. However, the unstructured ROMs produced by IRKA do not significantly violate the passivity constraints which is why the passivity enforcement techniques `prlPasEnf` and `locPasEnf` do not produce significant errors in their perturbation and perform well in both norms. A possible disadvantage of the (indirect) reduction methods in pa-MOR and pa-ENF can be observed for $r = 2$. Here, the algorithm `locPasEnf` produces a ROM $\widehat{\Sigma}_{\text{pa}}$ which is very close to the passivity constraint and no solution of the KYP inequality, and therefore no pH representation $\widehat{\Sigma}_{\text{pH}}$, can be found.

5 Getting started

The MORpH toolbox is available on GitHub[2] and can be cloned with Git or downloaded as a ZIP archive. After downloading the source code, the script `setup_morph` helps setting up the MATLAB environment for the toolbox. It adds the toolbox to the MATLAB path, checks the path for third-party software and assists with its installation if desired.

Once the toolbox is installed, the demo files may give a first impression on how to use the toolbox. They are located in directory `\demos` and are implemented in the Live Code File Format (.mlx). This allows to enhance code snippets on how to use an algorithm with explanations of theoretical aspects. Additional to these introductory files, we also provide detailed documentation to every class and function. This information can either be directly accessed from the file header or it can be prompted to the console with MATLAB's `help` or `doc` commands.

Contributions to our toolbox are welcome. In case you would like to enhance existing code or add new algorithms, you can do so by creating a fork of our repository and starting a pull request. To ensure a coherent appearance of the toolbox, coding guidelines and the header template can be found in the `\src` directory.

2 https://github.com/MORLab/MORpH.

6 Conclusions

We have presented MORpH – a free, open-source MATLAB toolbox to store, analyze and reduce large-scale pH-DAEs. The MORpH toolbox has similar functionalities as toolboxes for general LTI systems but additionally considers pH structural constraints. This includes the validation of constraints upon creation of a pH model and the preservation of constraints during model reduction. For the latter, we presented three different paths that can be taken, all of which are supported by different algorithms in our toolbox. Using a system decomposition approach, we showed that methods which are originally designed for ODE systems can also be applied to DAE systems with MORpH. Since this approach may involve several transformations and is therefore limited to medium-sized systems, future research is devoted to the development of methods that are capable of working with the original (sparse) system matrices. We envision a port-Hamiltonian research platform which promotes the collaboration among researchers from different disciplines and consider this toolbox, accompanied by the port-Hamiltonian benchmark collection, as a first incentive towards this goal.

Acknowledgement: The authors would like to thank Zeyad Hassan, Honglin Kang, and Nora Reinbold for their help with the implementation of MORpH.
Author contributions: All the authors have accepted responsibility for the entire content of this submitted manuscript and approved submission.
Research funding: This research has been funded by the Deutsche Forschungsgemeinschaft (DFG, German Research Foundation) – Project number 418612884.
Conflict of interest statement: The authors declare no conflicts of interest regarding this article.

Appendix

Third-party software

The MORpH toolbox partially relies on the following (open-source) third-party software which has to be downloaded separately and which we gratefully acknowledge:

- The optimization software MANOPT [42] and GRANSO [43] for optimization-based MOR methods such as `lyapOpt`.
- The M-M.E.S.S. toolbox [41] for the solution of large-scale algebraic Riccati and Lyapunov equations as in `prbt`.

- SADPA [44] and SAMDP [45] for computing dominant spectral zeros in `dszm`.
- The optimization software CVX [46, 47] and YALMIP [48] for solving the KYP inequality (8) in `ss2phs`.
- The functions `linorm_subsp` [49, 50] and `hinorm` [51] to compute the $\mathcal{H}_\infty$ norm of large-scale models in `ihaPH`.

Similar to the call of subroutines in a MORpH function, the use of third-party software may be enforced and configured via the `Opts` struct (see Section 3.3.2). In `lyapOpt`, for example, the maximum number of optimization iterations by the third-party software MANOPT can be set to 500 via

```
Opts.manopt.maxiter = 500
```

Depending on the configuration, the input parser of each function then searches for required third-party software and, if not yet installed, assists with installation instructions.

References

[1] T. Breiten, R. Morandin, and P. Schulze, "Error bounds for port-Hamiltonian model and controller reduction based on system balancing," arXiv Preprint arXiv:2012.15266, 2020.

[2] S. Chaturantabut, C. Beattie, and S. Gugercin, "Structure-preserving model reduction for nonlinear port-Hamiltonian systems," *SIAM J. Sci. Comput.*, vol. 38, no. 5, pp. B837—B865, 2016.

[3] S. Gugercin, R. V. Polyuga, C. Beattie, and A. van der Schaft, "Structure-preserving tangential interpolation for model reduction of port-Hamiltonian systems," *Automatica*, vol. 48, no. 9, pp. 1963—1974, 2012.

[4] B. Liljegren-Sailer and N. Marheineke, "On port-Hamiltonian approximation of a nonlinear flow problem on networks," *SIAM J. Sci. Comput.*, vol. 44, no. 3, pp. B834—B859, 2022.

[5] T. Moser, P. Schwerdtner, V. Mehrmann, and M. Voigt, "Structure-preserving model order reduction for index two port-Hamiltonian descriptor systems," arXiv Preprint arXiv:2206.03942, 2022.

[6] K. Cherifi, H. Gernandt, and D. Hinsen, "The difference between port-Hamiltonian, passive and positive real descriptor systems," arXiv Preprint arXiv:2204.04990, 2022.

[7] T. Breiten and B. Unger, "Passivity preserving model reduction via spectral factorization," *Automatica*, vol. 142, p. 110368, 2022.

[8] R. Ionutiu, J. Rommes, and A. C. Antoulas, "Passivity-preserving model reduction using dominant spectral-zero interpolation," *IEEE Trans. Comput. Aided Des. Integrated Circ. Syst.*, vol. 27, no. 12, pp. 2250—2263, 2008.

[9] K. Unneland, P. Van Dooren, and O. Egeland, "A novel scheme for positive real balanced truncation," in *2007 American Control Conference*, 2007, pp. 947—952.

[10] S. Grivet-Talocia and B. Gustavsen, *Passive Macromodeling: Theory and Applications*, Hoboken, NJ, John Wiley & Sons, Inc., 2016.

[11] R. Milk, S. Rave, and F. Schindler, "pyMOR — generic algorithms and interfaces for model order reduction," *SIAM J. Sci. Comput.*, vol. 38, no. 5, pp. S194—S216, 2016.

[12] A. Castagnotto, M. Cruz Varona, L. Jeschek, and B. Lohmann, "sss & sssMOR: analysis and reduction of large-scale dynamic systems in MATLAB," *Automatisierungstechnik*, vol. 65, no. 2, pp. 134—150, 2017.

[13] P. Benner and S. W. R. Werner, "MORLAB—the model order reduction LABoratory," in *Model Reduction of Complex Dynamical Systems*, P. Benner, T. Breiten, H. Faßbender, M. Hinze, T. Stykel, and R. Zimmermann, Eds., Cham, Springer International Publishing, 2021, pp. 393—415.

[14] N. Gillis and P. Sharma, "Finding the nearest positive-real system," *SIAM J. Numer. Anal.*, vol. 56, no. 2, pp. 1022—1047, 2018.

[15] C. Beattie, V. Mehrmann, H. Xu, and H. Zwart, "Linear port-Hamiltonian descriptor systems," *Math. Control Signals Syst.*, vol. 30, no. 17, pp. 1—27, 2018.

[16] S. A. Hauschild, N. Marheineke, and V. Mehrmann, "Model reduction techniques for linear constant coefficient port-Hamiltonian differential-algebraic systems," *Control Cybern.*, vol. 48, no. 1, pp. 125—152, 2019.

[17] C. Güdücü, J. Liesen, V. Mehrmann, and D. B. Szyld, "On non-Hermitian positive (semi)definite linear algebraic systems arising from dissipative Hamiltonian DAEs," arXiv Preprint arXiv:2111.05616, 2021.

[18] F. Achleitner, A. Arnold, and V. Mehrmann, "Hypocoercivity and controllability in linear semi-dissipative Hamiltonian ordinary differential equations and differential-algebraic equations," *ZAMM Z. fur Angew. Math. Mech.*, 2021. https://doi.org/10.1002/zamm.202100171.

[19] C. A. Beattie, S. Gugercin, and V. Mehrmann, "Structure-preserving interpolatory model reduction for port-Hamiltonian differential-algebraic systems," in *Realization and Model Reduction of Dynamical Systems: A Festschrift in Honor of the 70th Birthday of Thanos Antoulas*, C. Beattie, P. Benner, M. Embree, S. Gugercin, and S. Lefteriu, Eds., Cham, Springer, 2022.

[20] V. Duindam, A. Macchelli, S. Stramigioli, and H. Bruyninckx, *Modeling and Control of Complex Physical Systems*, Berlin, Heidelberg, Springer-Verlag, 2009.

[21] J. C. Willems, "Dissipative dynamical systems Part II: linear systems with quadratic supply rates," *Arch. Ration. Mech. Anal.*, vol. 45, no. 5, pp. 352—393, 1972.

[22] B. D. O. Anderson and S. Vongpanitlerd, *Network Analysis and Synthesis — A Modern Systems Theory Approach*, Englewood Cliffs, NJ, Prentice-Hall, 1973.

[23] R. V. Polyuga and A. van der Schaft, "Effort- and flow-constraint reduction methods for structure preserving model reduction of port-Hamiltonian systems," *Syst. Control Lett.*, vol. 61, no. 3, pp. 412—421, 2012.

[24] R. V. Polyuga and A. van der Schaft, "Structure preserving moment matching for port-Hamiltonian systems: Arnoldi and Lanczos," *IEEE Trans. Automat. Control*, vol. 56, no. 6, pp. 1458—1462, 2011.

[25] T. Moser, J. Durmann, and B. Lohmann, "Surrogate-based $\mathcal{H}_2$ model reduction of port-Hamiltonian systems," in *2021 Eur. Control Conf. (ECC)*, 2021, pp. 2058—2065.

[26] V. Druskin and V. Simoncini, "Adaptive rational Krylov subspaces for large-scale dynamical systems," *Syst. Control Lett.*, vol. 60, no. 8, pp. 546—560, 2011.

[27] V. Druskin, V. Simoncini, and M. Zaslavsky, "Adaptive tangential interpolation in rational Krylov subspaces for MIMO dynamical

systems," *SIAM J. Matrix Anal. Appl.*, vol. 35, no. 2, pp. 476—498, 2014.
[28] K. Sato, "Riemannian optimal model reduction of linear port-Hamiltonian systems," *Automatica J. IFAC*, vol. 93, pp. 428—434, 2018.
[29] T. Moser and B. Lohmann, "A new Riemannian framework for efficient $\mathcal{H}_2$-optimal model reduction of port-Hamiltonian systems," in *Proceedings of 59th IEEE Conference on Decisison and Control (CDC)*, Jeju Island, Republic of Korea, 2020, pp. 5043—5049.
[30] P. Schwerdtner and M. Voigt, "Structure preserving model order reduction by parameter optimization," arXiv Preprint arXiv:2011.07567, 2020.
[31] U. Desai and D. Pal, "A transformation approach to stochastic model reduction," *IEEE Trans. Automat. Control*, vol. 29, no. 12, pp. 1097—1100, 1984.
[32] J. Phillips, L. Daniel, and L. M. Silveira, "Guaranteed passive balancing transformations for model order reduction," in *Proceedings 2002 Design Automation Conference (IEEE Cat. No.02CH37324)*, 2002, pp. 52—57.
[33] T. Moser and B. Lohmann, "A Rosenbrock framework for tangential interpolation of port-Hamiltonian descriptor systems," arXiv Preprint arXiv:2210.16071, 2022.
[34] P. Schwerdtner, T. Moser, V. Mehrmann, and M. Voigt, "Structure-preserving model order reduction for index one port-Hamiltonian descriptor systems," arXiv Preprint arXiv:2206.01608, 2022.
[35] G. Flagg, C. A. Beattie, and S. Gugercin, "Interpolatory $\mathcal{H}_\infty$ model reduction," *Syst. Control Lett.*, vol. 627, pp. 567—574, 2013.
[36] A. Castagnotto, C. Beattie, and S. Gugercin, "Interpolatory methods for $\mathcal{H}_\infty$ model reduction of multi-input/multi-output systems," in *Modeling, Simulation and Applications*, Cham, Springer International Publishing, 2017, pp. 349—365.
[37] S. Grivet-Talocia, "Passivity enforcement via perturbation of Hamiltonian matrices," *IEEE Trans. Circuits Syst. I: Regul. Pap*, vol. 51, no. 9, pp. 1755—1769, 2004.
[38] V. Mehrmann and B. Unger, "Control of port-Hamiltonian differential-algebraic systems and applications," arXiv Preprint arXiv:2201.06590, 2022.
[39] T. Moser, "Benchmark systems and code for article: MORpH: model reduction of linear port-Hamiltonian systems in MATLAB," 2022. https://doi.org/10.5281/zenodo.7081776.
[40] P. Benner, Z. Bujanovic, P. Kürschner, and J. Saak, "RADI: a low-rank ADI-type algorithm for large scale algebraic Riccati equations," *Numer. Math.*, vol. 138, no. 2, pp. 301—330, 2017.
[41] J. Saak, M. Köhler, and P. Benner, *M-M.E.S.S.-2.1 — The Matrix Equations Sparse Solvers Library*, 2022. Available at: https://www.mpi-magdeburg.mpg.de/projects/mess.
[42] N. Boumal, B. Mishra, P. A. Absil, and R. Sepulchre, "Manopt, a matlab toolbox for optimization on manifolds," *J. Mach. Learn. Res.*, vol. 15, no. 42, pp. 1455—1459, 2014.
[43] F. E. Curtis, T. Mitchell, and M. L. Overton, "A BFGS-SQP method for nonsmooth, nonconvex, constrained optimization and its evaluation using relative minimization profiles," *Optim. Methods Software*, vol. 32, no. 1, pp. 148—181, 2017.
[44] J. Rommes and N. Martins, "Efficient computation of transfer function dominant poles using subspace acceleration," *IEEE Trans. Power Syst.*, vol. 21, no. 3, pp. 1218—1226, 2006.
[45] J. Rommes and N. Martins, "Efficient computation of multivariable transfer function dominant poles using subspace acceleration," *IEEE Trans. Power Syst.*, vol. 21, no. 4, pp. 1471—1483, 2006.
[46] M. Grant and S. Boyd, "CVX: matlab software for disciplined convex programming, version 2.1," 2014. Available at: http://cvxr.com/cvx.
[47] M. Grant and S. Boyd, "Graph implementations for nonsmooth convex programs," in *Recent Advances in Learning and Control. Lecture Notes in Control and Information Sciences*, V. Blondel, S. Boyd, and H. Kimura, Eds., London, Springer, 2008, pp. 95—110.
[48] J. Löfberg, "YALMIP: a toolbox for modeling and optimization in MATLAB," in *Proceedings of the CACSD Conference*, Taipei, Taiwan, 2004.
[49] N. Aliyev, P. Benner, E. Mengi, P. Schwerdtner, and M. Voigt, et al., "Large-scale computation of $\mathcal{L}_\infty$-norms by a greedy subspace method," *SIAM J. Matrix Anal. Appl.*, vol. 38.4, pp. 1496—1516, 2017.
[50] P. Schwerdtner and M. Voigt, "Computation of the $\mathcal{L}_\infty$-norm using rational interpolation," in *IFACPapersOnLine 51.25 (2018). 9th IFAC Symposium on Robust Control Design ROCOND*, 2018, pp. 84—89.
[51] P. Benner and M. Voigt, "A structured pseudospectral method for $\mathcal{L}_\infty$-norm computation of large-scale descriptor systems," *Math. Control. Signals, Syst.*, vol. 26, no. 2, pp. 303—338, 2013.

Bionotes

Tim Moser, Technical University of Munich, TUM School of Engineering and Design, Department of Engineering Physics and Computation, Boltzmannstr. 15, 85748 Garching, Germany.

Julius Durmann, Technical University of Munich, TUM School of Engineering and Design, Department of Engineering Physics and Computation, Boltzmannstr. 15, 85748 Garching, Germany.

Maximilian Bonauer, Technical University of Munich, TUM School of Engineering and Design, Department of Engineering Physics and Computation, Boltzmannstr. 15, 85748 Garching, Germany.

Boris Lohmann, Technical University of Munich, TUM School of Engineering and Design, Department of Engineering Physics and Computation, Boltzmannstr. 15, 85748 Garching, Germany.

A.2 Surrogate-Based $\mathcal{H}_2$ Model Reduction of Port-Hamiltonian Systems

Summary: Interpolation-based MOR methods are especially suitable for very large pH-DAE models due to their low computational cost and memory requirements. However, $\mathcal{H}_2$-inspired methods such as IRKA-PH typically search for optimal interpolation data iteratively, which may lead to increased computational costs in cases of slow convergence. In this article, we propose a novel structure-preserving, $\mathcal{H}_2$-inspired algorithm called CIRKA-PH, which extends the work in [36, 37, 112] to linear, time-invariant pH-ODE models. CIRKA-PH decouples the cost of reduction and optimization by running the local $\mathcal{H}_2$ optimization not on the FOM but on a lower-dimensional *surrogate model*. This surrogate model interpolates the FOM locally, and the associated interpolation data is enriched in each iteration with interpolation data found by IRKA-PH in the previous iteration. Before convergence, i.e., when the interpolation data found by IRKA-PH still change substantially, the surrogate model becomes an increasingly better approximation of the FOM. Upon convergence, the obtained ROM satisfies a subset of $\mathcal{H}_2$ optimality conditions with respect to the surrogate model and the FOM. If the final size of the surrogate model is significantly smaller than the FOM, this approach yields computational advantages, which we first analyze theoretically and then validate by numerical experiments.

CRediT author statement:

Tim Moser:	Conceptualization, Data Curation, Investigation, Methodology, Software, Visualization, Writing - Original Draft
Julius Durmann:	Investigation, Software, Writing - Original Draft
Boris Lohmann:	Conceptualization, Funding Acquisition, Supervision, Writing - Review & Editing

Surrogate-Based $\mathcal{H}_2$ Model Reduction of Port-Hamiltonian Systems

Tim Moser, Julius Durmann and Boris Lohmann

Abstract— **Interpolatory methods for structure-preserving model reduction of port-Hamiltonian systems are especially suitable for very large-scale models, owing to their low computational cost and memory requirements. $\mathcal{H}_2$-based techniques iteratively search for models which fulfill a subset of first-order $\mathcal{H}_2$-optimality conditions. In each iteration, a new reduced-order model is computed, which might weaken the computational advantages in cases of slow convergence. We propose a new structure-preserving framework for port-Hamiltonian systems based on surrogate modeling. By exploiting the local nature of the $\mathcal{H}_2$-optimization problem, the cost of optimization is decoupled from the cost of reduction. Consequently, $\mathcal{H}_2$-based interpolatory methods can be accelerated significantly and especially for very large-scale port-Hamiltonian systems, which is illustrated by a numerical example.**

I. INTRODUCTION

With today's technical systems constantly increasing in complexity, numerical modeling and analysis have become an integral part of their development and maintenance. Most of these systems are *multi-physics systems*, meaning they are governed by phenomena from different physical domains and the energy exchange between these domains. The port-based network modeling approach provides an energy-based way of modeling these systems. The energy serves as the lingua franca between the different physical domains, which exchange energy via power flows. This modeling approach naturally leads to port-Hamiltonian system (PHS) representations [1]. The energy-based modeling approach and desirable system properties, such as inherent passivity, also motivate an energy-based controller design. If controllers are formulated as virtual port-Hamiltonian systems, they can be interconnected with the plant and used to shape the energetic behavior of the coupled system (see [1]–[3] and references therein).

Depending on the physical system at hand and the desired accuracy, models in high state-space dimension may arise in the modeling stage, for instance during the spatial discretization of distributed parameter systems (see e.g. [4]). These models are computationally demanding at best and may be even infeasible for simulation or real-time control. Model reduction addresses this issue by generating reduced-order models, which approximate the original model with respect to predefined goals. In order to reduce port-Hamiltonian systems, we identify three major goals. First, we strive for a reduced-order model, which approximates the relevant dynamics of the original well with respect to a certain system norm. We will focus on algorithms that try to minimize the error between the reduced-order model and its original in the $\mathcal{H}_2$-norm. Second, it is desirable to preserve the port-Hamiltonian structure in the reduction process in order to exploit its advantageous characteristics e.g. for interconnection with other subsystems or subsequent controller design. Our third goal relates to numerical efficiency, meaning that the computation of the reduced-order model should be both numerically stable and computationally tractable even for very large-scale models.

Existing methods for structure-preserving $\mathcal{H}_2$-inspired model reduction of port-Hamiltonian systems can be divided into two subgroups: interpolatory methods [5], [6] and Riemannian methods [7], [8]. Algorithms in both classes are iterative, meaning they compute a series of reduced-order port-Hamiltonian models. With regard to the predefined goals, these methods are both structure-preserving and achieve small $\mathcal{H}_2$-errors upon convergence (see e.g. [8]). However, the fact that a new reduced-order model is computed in each iteration might lead to high computational efforts in cases of slow convergence where the number of iterations is large. Consequently, their computational efficiency is tightly connected to the convergence speed.

In this contribution, we propose a new framework for interpolatory model reduction of port-Hamiltonian systems that is based on the work in [9]–[11] on general linear time-invariant (LTI) systems. The port-Hamiltonian form of the reduced-order model is guaranteed by a structure-preserving Petrov-Galerkin projection as proposed in [6]. The cost of optimization and reduction is decoupled via a two-step approach, where information of previous iterations is utilized to create a medium-sized surrogate model of the original system on which the actual optimization is conducted. With the application of appropriate update rules for this surrogate model, the reduced-order model fulfills a subset of the well-known $\mathcal{H}_2$-optimality conditions upon convergence similar to existing interpolatory approaches.

The remainder of the paper is structured as follows: We first briefly summarize the fundamentals of $\mathcal{H}_2$-optimal interpolatory model reduction for general linear time-invariant systems (Section II). The $\mathcal{H}_2$-optimization problem is formulated for port-Hamiltonian systems in Section III and a discussion of existing interpolatory solutions in Section IV motivates the use of surrogate models for computational purposes. In Section V, we present our new surrogate-based framework, apply it to an existing interpolatory method and discuss its theoretical computational advantages. Section VI validates these theoretical considerations by a numerical experiment.

Funded by the Deutsche Forschungsgemeinschaft (DFG, German Research Foundation) – Project number 418612884.

T. Moser, J. Durmann and B. Lohmann are with the Chair of Automatic Control, Technical University of Munich, 85748 Garching/Munich, Germany {tim.moser, julius.durmann, lohmann}@tum.de

II. PRELIMINARIES

Consider a linear time-invariant system in state-space representation

$$\begin{aligned} \mathbf{E}\dot{\mathbf{x}}(t) &= \mathbf{A}\mathbf{x}(t) + \mathbf{B}\mathbf{u}(t) \\ \mathbf{y}(t) &= \mathbf{C}\mathbf{x}(t) + \mathbf{D}\mathbf{u}(t) \end{aligned} \quad \text{with} \quad \mathbf{x}(0) = \mathbf{0}, \tag{1}$$

with regular descriptor matrix $\mathbf{E} \in \mathbb{R}^{n\times n}$, state vector $\mathbf{x}(t) \in \mathbb{R}^n$, input $\mathbf{u}(t) \in \mathbb{R}^m$ and output $\mathbf{y}(t) \in \mathbb{R}^p$. Under the assumption that $\mathbf{x}(t=0) = \mathbf{0}$, its transfer function is given by $\mathbf{G}(s) = \mathbf{C}(s\mathbf{E} - \mathbf{A})^{-1}\mathbf{B} + \mathbf{D} \in \mathbb{C}^{p\times m}$.

In the context of model reduction, we generally strive for a reduced-order model

$$\begin{aligned} \hat{\mathbf{E}}\dot{\hat{\mathbf{x}}}(t) &= \hat{\mathbf{A}}\hat{\mathbf{x}}(t) + \hat{\mathbf{B}}\mathbf{u}(t) \\ \hat{\mathbf{y}}(t) &= \hat{\mathbf{C}}\hat{\mathbf{x}}(t) + \hat{\mathbf{D}}\mathbf{u}(t) \end{aligned} \quad \text{with} \quad \hat{\mathbf{x}}(0) = \mathbf{0}, \tag{2}$$

with reduced state vector $\hat{\mathbf{x}}(t) \in \mathbb{R}^r$ and $r \ll n$, such that $\hat{\mathbf{y}}(t) \in \mathbb{R}^p$ approximates the original output $\mathbf{y}(t)$ well with respect to a certain norm.

A. Model Reduction by Tangential Interpolation

One way to generate reduced-order models is by means of Petrov-Galerkin projections where bases $\mathbf{V}, \mathbf{W} \in \mathbb{R}^{n\times r}$ of r-dimensional subspaces are defined such that

$$\begin{aligned} \hat{\mathbf{E}} &= \mathbf{W}^T\mathbf{E}\mathbf{V}, & \hat{\mathbf{B}} &= \mathbf{W}^T\mathbf{B}, \\ \hat{\mathbf{A}} &= \mathbf{W}^T\mathbf{A}\mathbf{V}, & \hat{\mathbf{C}} &= \mathbf{C}\mathbf{V}, \end{aligned} \qquad \hat{\mathbf{D}} = \mathbf{D}.$$

As the feedthrough matrix is not affected by this projection, we assume $\mathbf{D} = \hat{\mathbf{D}} = \mathbf{0}$ without loss of generality. In interpolatory model reduction (see [12, Ch. 3] for details), the matrices $\mathbf{V}$ and $\mathbf{W}$ are chosen such that the reduced-order transfer function $\hat{\mathbf{G}}(s)$ tangentially interpolates the original transfer function $\mathbf{G}(s)$ at certain interpolation points or shifts $\sigma_i \in \mathbb{C}$. We assume that these interpolation points are distinct and that $(\mathbf{A} - \sigma_i\mathbf{E})$ is invertible for all $i = 1, \ldots, r$. The interpolation conditions

$$\mathbf{G}(\sigma_i)\,\mathbf{r}_i = \hat{\mathbf{G}}(\sigma_i)\,\mathbf{r}_i \qquad \text{for } i = 1, \ldots, r \tag{3}$$

can then be enforced by

$$(\sigma_i\mathbf{E} - \mathbf{A})^{-1}\mathbf{B}\,\mathbf{r}_i \in \mathcal{R}(\mathbf{V}) \quad \text{for } i = 1, \ldots, r, \tag{4}$$

where $\mathbf{r}_i$ is the right tangential direction at σ_i and $\mathcal{R}(\mathbf{V})$ denotes the range of matrix $\mathbf{V}$. If $\mathbf{V}$ is chosen as the *primitive* basis

$$\mathbf{V} = [(\sigma_1\mathbf{E} - \mathbf{A})^{-1}\mathbf{B}\mathbf{r}_1, \ldots, (\sigma_r\mathbf{E} - \mathbf{A})^{-1}\mathbf{B}\mathbf{r}_r],$$

then $\mathbf{V}$ solves the following Sylvester equation

$$\mathbf{E}\mathbf{V}\mathbf{S}_V - \mathbf{A}\mathbf{V} = \mathbf{B}\mathbf{R}_V, \tag{5}$$

where $\mathbf{S}_V = \operatorname{diag}(\sigma_1, \ldots, \sigma_r)$ and $\mathbf{R}_V = [\mathbf{r}_1, \ldots, \mathbf{r}_r]$. On the assumption that $(\mathbf{A} - \sigma_i\mathbf{E})$ is invertible for all $i = 1, \ldots, r$, the regular matrix pencils $(\mathbf{A} - \lambda\mathbf{E})$ and $(\mathbf{S}_V - \lambda\mathbf{I}_r)$ have disjoint spectra and thus, matrix $\mathbf{V}$ is a unique solution to (5) [13].

Remark 1: Note that the interpolation conditions are guaranteed by $\mathcal{R}(\mathbf{V})$ and independent of the choice of basis $\mathbf{V}$. Thus, replacing $\mathbf{V}$ by $\bar{\mathbf{V}} = \mathbf{V}\mathbf{T}_V$ with invertible $\mathbf{T}_V \in \mathbb{C}^{r\times r}$ retains the interpolation properties in (3) and $\bar{\mathbf{V}}$ solves a corresponding Sylvester equation with $\bar{\mathbf{S}}_V = \mathbf{T}_V^{-1}\mathbf{S}_V\mathbf{T}_V$ and $\bar{\mathbf{R}}_V = \mathbf{R}_V\mathbf{T}_V$. This fact can be exploited for numerical purposes or to keep the bases real in order to generate reduced-order matrices that are also real, which is usually desired in the port-Hamiltonian setting.

Dual results hold for $\mathbf{W}$, which can be utilized to enforce left tangential interpolation conditions by solving a dual Sylvester equation [14]. However, for port-Hamiltonian systems, $\mathbf{W}$ is chosen differently to ensure structure preservation as shown in Section IV. For the sake of brevity, we denote the Petrov-Galerkin projection of a port-Hamiltonian system $\boldsymbol{\Sigma}$ with $\mathbf{W}$ and $\mathbf{V}$ by $\mathbf{W}^T\boldsymbol{\Sigma}\mathbf{V}$.

B. $\mathcal{H}_2$-Optimal Model Reduction

The goal of $\mathcal{H}_2$-optimal model reduction is to find a reduced-order model with dimension r and transfer function $\hat{\mathbf{G}}(s)$ that is a solution to the following non-convex optimization problem

$$\|\mathbf{G} - \hat{\mathbf{G}}\|_{\mathcal{H}_2} = \min_{\dim(\tilde{\mathbf{G}})=r} \|\mathbf{G} - \tilde{\mathbf{G}}\|_{\mathcal{H}_2}, \tag{6}$$

where

$$\|\mathbf{G}\|_{\mathcal{H}_2} = \left(\frac{1}{2\pi}\int_{-\infty}^{\infty} \|\mathbf{G}(i\omega)\|_{\mathrm{F}}^2\, d\omega\right)^{\frac{1}{2}}.$$

The following error bound in the $\mathcal{L}_\infty$-norm exists for the time domain error between the outputs $\mathbf{y}(t)$ and $\hat{\mathbf{y}}(t)$ [15]

$$\|\mathbf{y} - \hat{\mathbf{y}}\|_{\mathcal{L}_\infty} \le \|\mathbf{G} - \hat{\mathbf{G}}\|_{\mathcal{H}_2}\|\mathbf{u}\|_{\mathcal{L}_2}.$$

Thus, $\mathcal{H}_2$-optimal model reduction aims for small maximum output errors in the time domain over all $\mathcal{L}_2$-bounded inputs.

The $\mathcal{H}_2$-error $\|\mathbf{G} - \hat{\mathbf{G}}\|_{\mathcal{H}_2}$ can be computed in two different frameworks: the Lyapunov framework and the pole-residue framework. In the Lyapunov framework, the evaluation of the $\mathcal{H}_2$-error requires the solution of coupled Lyapunov equations whereas in the pole-residue framework, the $\mathcal{H}_2$-error is expressed with the pole-residue expansions of $\mathbf{G}(s)$ and $\hat{\mathbf{G}}(s)$. Consequently, Lyapunov-based methods such as [16], [17] and interpolatory methods such as [18], [19] exist for solving (6). In the pole-residue framework, the first-order necessary optimality conditions can be formulated as tangential interpolation conditions between $\mathbf{G}(s)$ and $\hat{\mathbf{G}}(s)$.

Theorem 1: [12, Th. 5.1.1] Let $\mathbf{G}(s)$ denote the transfer function of the full-order model (1). Consider a reduced-order model (2) with transfer function in pole-residue expansion $\hat{\mathbf{G}}(s) = \sum_{i=1}^{r} \frac{\hat{\mathbf{c}}_i\hat{\mathbf{b}}_i^T}{s-\hat{\lambda}_i}$ with $\hat{\mathbf{b}}_i \in \mathbb{C}^m, \hat{\mathbf{c}}_i \in \mathbb{C}^p$ and simple but possibly complex poles $\hat{\lambda}_i \in \mathbb{C}$. If $\hat{\mathbf{G}}(s)$ is a local minimizer of (6), then the following tangential interpolation conditions hold for all $i = 1, \ldots, r$:

$$\mathbf{G}(-\hat{\lambda}_i)\hat{\mathbf{b}}_i = \hat{\mathbf{G}}(-\hat{\lambda}_i)\hat{\mathbf{b}}_i, \tag{7a}$$

$$\hat{\mathbf{c}}_i^T\mathbf{G}(-\hat{\lambda}_i) = \hat{\mathbf{c}}_i^T\hat{\mathbf{G}}(-\hat{\lambda}_i), \tag{7b}$$

$$\hat{\mathbf{c}}_i^T\mathbf{G}'(-\hat{\lambda}_i)\hat{\mathbf{b}}_i = \hat{\mathbf{c}}_i^T\hat{\mathbf{G}}'(-\hat{\lambda}_i)\hat{\mathbf{b}}_i. \tag{7c}$$

III. PROBLEM STATEMENT

Consider linear port-Hamiltonian systems in input-state-output representation without algebraic constraints

$$\boldsymbol{\Sigma} \begin{cases} \dot{\mathbf{x}} = (\mathbf{J}-\mathbf{R})\mathbf{Q}\mathbf{x} + (\mathbf{B}-\mathbf{P})\mathbf{u}, \\ \mathbf{y} = (\mathbf{B}+\mathbf{P})^T\mathbf{Q}\mathbf{x} + (\mathbf{M}+\mathbf{S})\mathbf{u}, \end{cases} \tag{8}$$

with $\mathbf{x}(t) \in \mathbb{R}^n$, $\mathbf{J}, \mathbf{R}, \mathbf{Q} \in \mathbb{R}^{n\times n}$, $\mathbf{B}, \mathbf{P} \in \mathbb{R}^{n\times m}$ and $\mathbf{M}, \mathbf{S} \in \mathbb{R}^{m\times m}$.

The quadratic Hamiltonian $H(\mathbf{x}) = \frac{1}{2}\mathbf{x}^T\mathbf{Q}\mathbf{x}$ with energy matrix $\mathbf{Q} = \mathbf{Q}^T$ represents the internal energy of the system. The system matrices satisfy the following (skew-)symmetry and non-negativity conditions

$$\mathbf{J} = -\mathbf{J}^T,\ \mathbf{M} = -\mathbf{M}^T,\ \mathbf{Z} = \mathbf{Z}^T = \begin{bmatrix} \mathbf{R} & \mathbf{P} \\ \mathbf{P}^T & \mathbf{S} \end{bmatrix} \geq 0.$$

If these matrix properties hold and $\mathbf{Q}$ is symmetric positive-definite, which we assume in the context of this paper, then the Hamiltonian $H(\mathbf{x})$ is a storage function and system $\boldsymbol{\Sigma}$ is passive:

$$\begin{aligned} \frac{d}{dt}H(\mathbf{x}) &= \mathbf{u}^T\mathbf{y} - \begin{bmatrix} \mathbf{Q}\mathbf{x} \\ \mathbf{u} \end{bmatrix}^T \begin{bmatrix} \mathbf{R} & \mathbf{P} \\ \mathbf{P}^T & \mathbf{S} \end{bmatrix} \begin{bmatrix} \mathbf{Q}\mathbf{x} \\ \mathbf{u} \end{bmatrix} \\ &\leq \mathbf{u}^T\mathbf{y}. \end{aligned}$$

For $\mathbf{x}(t=0) = \mathbf{0}$, the input-output behavior of the system is characterized by the following transfer function:

$$\mathbf{G}(s) = (\mathbf{B}+\mathbf{P})^T\mathbf{Q}\left(s\mathbf{I}_n - (\mathbf{J}-\mathbf{R})\mathbf{Q}\right)^{-1}(\mathbf{B}-\mathbf{P}) + (\mathbf{M}+\mathbf{S}).$$

Our goal is to approximate system (8) with a reduced model in port-Hamiltonian form

$$\hat{\boldsymbol{\Sigma}} \begin{cases} \dot{\hat{\mathbf{x}}} = (\hat{\mathbf{J}}-\hat{\mathbf{R}})\hat{\mathbf{Q}}\hat{\mathbf{x}} + (\hat{\mathbf{B}}-\hat{\mathbf{P}})\mathbf{u}, \\ \hat{\mathbf{y}} = (\hat{\mathbf{B}}+\hat{\mathbf{P}})^T\hat{\mathbf{Q}}\hat{\mathbf{x}} + (\hat{\mathbf{M}}+\hat{\mathbf{S}})\mathbf{u}, \end{cases} \tag{9}$$

with reduced state vector $\hat{\mathbf{x}}(t) \in \mathbb{R}^r$ and $\hat{\mathbf{J}}, \hat{\mathbf{R}}, \hat{\mathbf{Q}} \in \mathbb{R}^{r\times r}$, $\hat{\mathbf{B}}, \hat{\mathbf{P}} \in \mathbb{R}^{r\times m}$, $\hat{\mathbf{M}}, \hat{\mathbf{S}} \in \mathbb{R}^{m\times m}$ such that $r \ll n$.

Hence, the structure-preserving $\mathcal{H}_2$-optimal model reduction of port-Hamiltonian systems (8) can be formulated in its most general form by the following non-convex optimization problem

$$\|\mathbf{G} - \hat{\mathbf{G}}\|_{\mathcal{H}_2} = \min_{(\tilde{\mathbf{J}},\tilde{\mathbf{M}},\tilde{\mathbf{Q}},\tilde{\mathbf{Z}},\tilde{\mathbf{B}})\in\mathcal{M}} \|\mathbf{G} - \tilde{\mathbf{G}}\|_{\mathcal{H}_2}, \tag{10}$$

where $\hat{\mathbf{G}}(s)$ denotes the transfer function of $\hat{\boldsymbol{\Sigma}}$. The reduced-order port-Hamiltonian systems of dimension r live on the matrix product manifold (see e.g. [8])

$$\mathcal{M} = \mathrm{Skew}_r \times \mathrm{Skew}_m \times \mathrm{Sym}_r^{\mathrm{P}} \times \mathrm{Sym}_{r+m}^{\mathrm{PS}} \times \mathbb{R}^{r\times m},$$

where Skew_r, $\mathrm{Sym}_r^{\mathrm{P}}$ and $\mathrm{Sym}_r^{\mathrm{PS}}$ denote the manifolds of skew-symmetric, symmetric positive-definite and symmetric positive semi-definite matrices in $\mathbb{R}^{r\times r}$, respectively. As initially mentioned, solving (10) has been approached in two different ways. Riemannian methods [7], [8] *directly* solve (10) with Riemannian optimization techniques on the manifold $\mathcal{M}$. In the following, we focus on interpolatory methods (see e.g. [5], [6]) which *indirectly* solve (10) using model reduction by tangential interpolation as described in Section II-A.

IV. INTERPOLATORY $\mathcal{H}_2$-BASED MODEL REDUCTION OF PHS

Interpolation conditions and structure preservation can be enforced in the following way.

Theorem 2: [6] Apply the Petrov-Galerkin projection with $\bar{\mathbf{V}}$ and $\mathbf{W} = \mathbf{Q}\bar{\mathbf{V}}(\bar{\mathbf{V}}^T\mathbf{Q}\bar{\mathbf{V}})^{-1}$ to $\boldsymbol{\Sigma}$, where $\bar{\mathbf{V}}$ is a real, orthonormal basis of the subspace spanned by

$$\begin{aligned} \mathbf{V} = [&(\sigma_1\mathbf{I}_n - (\mathbf{J}-\mathbf{R})\mathbf{Q})^{-1}(\mathbf{B}-\mathbf{P})\mathbf{r}_1, \dots \\ &\dots, (\sigma_r\mathbf{I}_n - (\mathbf{J}-\mathbf{R})\mathbf{Q})^{-1}(\mathbf{B}-\mathbf{P})\mathbf{r}_r], \end{aligned} \tag{11}$$

with distinct interpolation points σ_i. Then the reduced-order model $\hat{\boldsymbol{\Sigma}} = \mathbf{W}^T\boldsymbol{\Sigma}\bar{\mathbf{V}}$ is in port-Hamiltonian form and fulfills

$$\mathbf{G}(\sigma_i)\,\mathbf{r}_i = \hat{\mathbf{G}}(\sigma_i)\,\mathbf{r}_i \qquad \text{for } i = 1, \dots, r. \tag{12}$$

Proof: Considering the fact that $\mathbf{W}$ and $\bar{\mathbf{V}}$ are bitangential, the projection $\mathbf{W}^T\boldsymbol{\Sigma}\bar{\mathbf{V}}$ leads to the following reduced-order matrices:

$$\begin{aligned} &\hat{\mathbf{J}} = \mathbf{W}^T\mathbf{J}\mathbf{W}, \quad \hat{\mathbf{B}} = \mathbf{W}^T\mathbf{B}, \quad \hat{\mathbf{M}} = \mathbf{M}, \quad \hat{\mathbf{S}} = \mathbf{S}, \\ &\hat{\mathbf{R}} = \mathbf{W}^T\mathbf{R}\mathbf{W}, \quad \hat{\mathbf{P}} = \mathbf{W}^T\mathbf{P}, \quad \hat{\mathbf{Q}} = \bar{\mathbf{V}}^T\mathbf{Q}\bar{\mathbf{V}}. \end{aligned}$$

Given the fact that $\mathbf{W}$ has full column rank, owing to the structure of $\bar{\mathbf{V}}$ and positive-definiteness of $\mathbf{Q}$, the skew-symmetry of $\hat{\mathbf{J}}$ and $\hat{\mathbf{M}}$ as well as the positive-definiteness of $\hat{\mathbf{Q}}$ is guaranteed. It holds that

$$\hat{\mathbf{Z}} = \begin{bmatrix} \mathbf{W} & \mathbf{0} \\ \mathbf{0} & \mathbf{I}_m \end{bmatrix}^T \begin{bmatrix} \mathbf{R} & \mathbf{P} \\ \mathbf{P}^T & \mathbf{S} \end{bmatrix} \begin{bmatrix} \mathbf{W} & \mathbf{0} \\ \mathbf{0} & \mathbf{I}_m \end{bmatrix} \geq 0.$$

Thus, $\hat{\boldsymbol{\Sigma}}$ is port-Hamiltonian and passive with storage function $\hat{H}(\hat{\mathbf{x}}) = \frac{1}{2}\hat{\mathbf{x}}^T\hat{\mathbf{Q}}\hat{\mathbf{x}}$. The tangential interpolation property in (12) follows from (4), the fact that $\mathcal{R}(\mathbf{V}) = \mathcal{R}(\bar{\mathbf{V}})$ and Remark 1. ∎

Corollary 1: The matrix $\mathbf{V}$ of Theorem 2 also solves the Sylvester equation

$$\mathbf{V}\mathbf{S}_V - (\mathbf{J}-\mathbf{R})\mathbf{Q}\mathbf{V} = (\mathbf{B}-\mathbf{P})\mathbf{R}_V,$$

where $\mathbf{S}_V = \mathrm{diag}(\sigma_1, \dots, \sigma_r)$ and $\mathbf{R}_V = [\mathbf{r}_1, \dots, \mathbf{r}_r]$.

Note that other options for structure-preserving tangential interpolation of PHS have been proposed ([20], [5]). For common interpolation data, they all yield an equivalent reduced transfer function $\hat{\mathbf{G}}(s)$ and only the coordinates of the resulting reduced models vary. If the original model $\boldsymbol{\Sigma}$ is in scaled energy coordinates, i.e. $\mathbf{Q} = \mathbf{I}_n$, all methods even share the same reduced-order realization $\hat{\boldsymbol{\Sigma}}$.

Moreover, interpolatory methods for port-Hamiltonian systems share the property that while $\mathbf{V}$ can be chosen to fulfill the interpolation conditions in (4), $\mathbf{W}$ is fully determined by the energy matrix $\mathbf{Q}$ as well as $\mathbf{V}$ and cannot be chosen freely, for example to enforce left tangential interpolation conditions as in Hermite interpolation methods for general LTI systems. Hence, only $r \cdot m$ degrees of freedom are available to meet the $r\cdot(2m)$ first-order necessary conditions for $\mathcal{H}_2$-optimality in Theorem 1 (see [21]). This inevitably leads to the fact that interpolatory methods generally cannot achieve $\mathcal{H}_2$-optimality and structure preservation at the same time, while exceptions are discussed in [7], [22]. This also becomes evident if we relate those techniques to the optimization problem (10). Within the projection framework,

Algorithm 1 IRKA-PH [6]

Input: Original model $\boldsymbol{\Sigma}$ of dimension n, set of initial expansion points $\{\sigma_i\}_{i=1}^r$ and tangent directions $\{\mathbf{r}_i\}_{i=1}^r$
Output: Reduced model $\hat{\boldsymbol{\Sigma}}$ of dimension r

while not converged **do**
  Construct $\mathbf{V}$ as in (11)
  Compute real basis $\bar{\mathbf{V}} \in \mathbb{R}^{n\times r}$ with $\mathcal{R}(\mathbf{V}) = \mathcal{R}(\bar{\mathbf{V}})$
  $\mathbf{W} = \mathbf{Q}\bar{\mathbf{V}}(\bar{\mathbf{V}}^T\mathbf{Q}\bar{\mathbf{V}})^{-1}$
  $\hat{\boldsymbol{\Sigma}} \leftarrow \mathbf{W}^T\boldsymbol{\Sigma}\bar{\mathbf{V}}$
  Compute $\hat{\mathbf{b}}_i, \hat{\mathbf{c}}_i \in \mathbb{C}^m, \hat{\lambda}_i \in \mathbb{C}$ s.t. $\hat{\mathbf{G}}(s) = \sum_{i=1}^{r} \frac{\hat{\mathbf{c}}_i\hat{\mathbf{b}}_i^T}{s-\hat{\lambda}_i}$
  $\sigma_i \leftarrow -\hat{\lambda}_i$ and $\mathbf{r}_i \leftarrow \hat{\mathbf{b}}_i \quad$ for $i = 1, \ldots, r$
end while

the matrices of $\mathcal{M}$ cannot be optimized independently which imposes an additional restriction to the search on the manifold $\mathcal{M}$. This has been shown in [7] using a simple example.

However, the optimality conditions can be partially met. A modified version of the Iterative Rational Krylov Algorithm (IRKA) based on Theorem 2 was developed in [6], which preserves the port-Hamiltonian structure and also satisfies equation (7a) upon convergence. This algorithm named IRKA-PH is illustrated in Algorithm 1. For large dimensions n of the original model $\boldsymbol{\Sigma}$, the numerical cost of IRKA-PH is dominated by the construction of matrix $\mathbf{V}$ as in (11), which effectively requires r solves of large-scale linear systems of equations (LSE) in each iteration [11]. The total computational cost of IRKA-PH can thus be approximated by

$$\mathcal{C}_n(\text{IRKA-PH}) \approx \underbrace{k^I}_{\text{optimization}} \cdot \underbrace{r\,\mathcal{C}_n(\text{LSE})}_{\text{reduction}}, \tag{13}$$

where $\mathcal{C}_n(\text{LSE})$ denotes the cost of solving an LSE of dimension n and k^I is the number of iterations required in Algorithm 1 until (7a) is satisfied. It is important to note that this cost strongly depends on the algorithm used to solve the LSE. For instance, if an LU decomposition is used, the LU factors can be used for pairs of complex-conjugated shifts for which the factor r in (13) then reduces to $r/2$. In the following, we generalize our theoretical considerations using the worst-case scenario (13).

V. THE MODEL FUNCTION FRAMEWORK

In IRKA-PH, the cost of computing one full *reduction* with interpolatory methods is directly coupled with the constant k^I that represents the performance of the *optimization* algorithm. The computational efficiency of this method thus highly depends on the convergence speed which is in turn affected by the initial interpolation data.

We propose a new framework for port-Hamiltonian systems that enables us to decouple the costs of reduction and optimization for interpolatory methods using surrogate models or *model functions*. The creation of these model functions is based on the work in [9]–[11] and adapted to the port-Hamiltonian system class in order to ensure structure preservation. Fig. 1 illustrates the notation used for

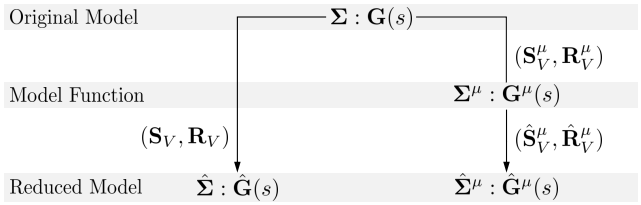

Fig. 1: Notation of involved models and interpolation data for conventional interpolatory methods (left) and in the model function framework (right)

direct reductions and indirect reductions via model functions. All quantities related to model functions are denoted by a superscript μ. Note that we loosely speak of $\mathcal{H}_2$-optimality and of an $\mathcal{H}_2$-optimal model $\hat{\boldsymbol{\Sigma}}$ in the following, if $\hat{\boldsymbol{\Sigma}}$ fulfills (7a) with respect to $\boldsymbol{\Sigma}$, bearing in mind that it is generally not possible to satisfy all necessary optimality conditions (7) with interpolatory methods.

A. Definition of Model Functions

The use of surrogate models is motivated by the local nature of both interpolatory methods and the problem of $\mathcal{H}_2$-optimal model reduction. On the one hand, interpolatory methods locally approximate the original transfer function around chosen interpolation points. On the other hand, owing to the non-convexity of problem (10) as mentioned above, the best we can yield for with iterative methods is finding a local minimum in the proximity of the initial iterate. These properties motivate the idea of approximating the original model $\boldsymbol{\Sigma}$ locally by a model function $\boldsymbol{\Sigma}^\mu$ with transfer function $\mathbf{G}^\mu(s)$ of much smaller dimension n^μ.

Definition 1: Consider a full-order port-Hamiltonian model $\boldsymbol{\Sigma}$ as in (8). Let $\mathbf{V}^\mu, \mathbf{W}^\mu \in \mathbb{C}^{n\times n^\mu}$ be projection matrices that satisfy the following equations

$$\mathbf{V}^\mu\mathbf{S}_V^\mu - (\mathbf{J}-\mathbf{R})\mathbf{Q}\mathbf{V}^\mu = (\mathbf{B}-\mathbf{P})\mathbf{R}_V^\mu, \tag{14a}$$

$$\mathbf{W}^\mu = \mathbf{Q}\mathbf{V}^\mu((\mathbf{V}^\mu)^T\mathbf{Q}\mathbf{V}^\mu)^{-1}, \tag{14b}$$

where $\mathbf{S}_V^\mu = \operatorname{diag}(\sigma_1^\mu, \ldots, \sigma_{n^\mu}^\mu)$, $\mathbf{R}_V^\mu = [\mathbf{r}_1^\mu, \ldots, \mathbf{r}_{n^\mu}^\mu]$ with distinct interpolation points $\sigma_j^\mu \in \mathbb{C}$ and tangential directions $\mathbf{r}_j^\mu \in \mathbb{C}^m$. The model function $\boldsymbol{\Sigma}^\mu$ with transfer function $\mathbf{G}^\mu(s)$ is then defined by the projection $\boldsymbol{\Sigma}^\mu = (\mathbf{W}^\mu)^T\boldsymbol{\Sigma}\mathbf{V}^\mu$.

Assume that we find a reduced-order model $\hat{\boldsymbol{\Sigma}}^\mu$ of dimension r with transfer function $\hat{\mathbf{G}}^\mu(s)$ by approximating $\boldsymbol{\Sigma}^\mu$ in an $\mathcal{H}_2$-optimal way

$$\|\mathbf{G}^\mu - \hat{\mathbf{G}}^\mu\|_{\mathcal{H}_2} = \min_{(\tilde{\mathbf{J}},\tilde{\mathbf{M}},\tilde{\mathbf{Q}},\tilde{\mathbf{Z}},\tilde{\mathbf{B}})\in\mathcal{M}} \|\mathbf{G}^\mu - \tilde{\mathbf{G}}\|_{\mathcal{H}_2}. \tag{15}$$

If $r < n^\mu \ll n$ holds, we expect that this approximate problem can be solved at a much lower computational cost than the original problem (10) of approximating $\boldsymbol{\Sigma}$.

B. $\mathcal{H}_2$-Optimality

However, in general, a solution $\hat{\boldsymbol{\Sigma}}^\mu$ to the approximate problem (15) is not a solution to the original problem (10). Hence, we generally cannot deduce the $\mathcal{H}_2$-optimality of $\hat{\boldsymbol{\Sigma}}^\mu$ with respect to the original system $\boldsymbol{\Sigma}$ from its $\mathcal{H}_2$-optimality

with respect to the model function $\boldsymbol{\Sigma}^\mu$. We establish this connection by choosing the intermediate model function $\boldsymbol{\Sigma}^\mu$ appropriately.

Theorem 3: Consider a full-order port-Hamiltonian model $\boldsymbol{\Sigma}$ as in (8) and let $\mathbf{G}(s)$ denote its transfer function. Let the model function $\boldsymbol{\Sigma}^\mu$ with its corresponding transfer function $\mathbf{G}^\mu(s)$ be defined as in Definition 1. Additionally, let $\hat{\mathbf{V}}^\mu, \hat{\mathbf{W}}^\mu \in \mathbb{C}^{n^\mu \times r}$ be projection matrices that satisfy the following equations

$$\hat{\mathbf{V}}^\mu \hat{\mathbf{S}}_V^\mu - (\mathbf{J}^\mu - \mathbf{R}^\mu)\mathbf{Q}^\mu \hat{\mathbf{V}}^\mu = (\mathbf{B}^\mu - \mathbf{P}^\mu)\hat{\mathbf{R}}_V^\mu, \tag{16a}$$

$$\hat{\mathbf{W}}^\mu = \mathbf{Q}^\mu \hat{\mathbf{V}}^\mu ((\hat{\mathbf{V}}^\mu)^T \mathbf{Q}^\mu \hat{\mathbf{V}}^\mu)^{-1}, \tag{16b}$$

where $\hat{\mathbf{S}}_V^\mu = \operatorname{diag}(\hat{\sigma}_1^\mu, \ldots, \hat{\sigma}_r^\mu)$, $\hat{\mathbf{R}}_V^\mu = [\hat{\mathbf{r}}_1^\mu, \ldots, \hat{\mathbf{r}}_r^\mu]$ with distinct interpolation points $\hat{\sigma}_i^\mu \in \mathbb{C}$ and tangential directions $\hat{\mathbf{r}}_i^\mu \in \mathbb{C}^m$. The reduced-order model $\hat{\boldsymbol{\Sigma}}^\mu$ with transfer function $\hat{\mathbf{G}}^\mu(s)$ results from the projection $\hat{\boldsymbol{\Sigma}}^\mu = (\hat{\mathbf{W}}^\mu)^T \boldsymbol{\Sigma}^\mu \hat{\mathbf{V}}^\mu$ (see Fig. 1). Assume that the interpolation data $(\hat{\mathbf{S}}_V^\mu, \hat{\mathbf{R}}_V^\mu)$ are optimal with respect to $\boldsymbol{\Sigma}^\mu$, i.e. for all $i = 1, \ldots, r$ we have $\hat{\sigma}_i^\mu = -\hat{\lambda}_i$ and $\hat{\mathbf{r}}_i^\mu = \hat{\mathbf{b}}_i$ where $\hat{\mathbf{G}}^\mu(s) = \sum_{i=1}^{r} \frac{\hat{\mathbf{c}}_i \hat{\mathbf{b}}_i^T}{s - \hat{\lambda}_i}$ is the pole-residue expansion of the reduced model $\hat{\boldsymbol{\Sigma}}^\mu$.

If, for every $i \in \{1, \ldots, r\}$ there exists a $j \in \{1, \ldots, n^\mu\}$ such that

$$\hat{\sigma}_i^\mu = \sigma_j^\mu, \quad \hat{\mathbf{r}}_i^\mu = \mathbf{r}_j^\mu, \tag{17}$$

then $\hat{\boldsymbol{\Sigma}}^\mu$ also satisfies the first-order $\mathcal{H}_2$-optimality condition

$$\mathbf{G}(-\hat{\lambda}_i)\hat{\mathbf{b}}_i = \hat{\mathbf{G}}^\mu(-\hat{\lambda}_i)\hat{\mathbf{b}}_i \quad \text{for } i = 1, \ldots, r, \tag{18}$$

with respect to the original model $\boldsymbol{\Sigma}$.

Proof: From the results of Theorem 2, Corollary 1 and conditions $\hat{\sigma}_i^\mu = -\hat{\lambda}_i$ and $\hat{\mathbf{r}}_i^\mu = \hat{\mathbf{b}}_i$ we obtain

$$\mathbf{G}^\mu(-\hat{\lambda}_i)\hat{\mathbf{b}}_i = \hat{\mathbf{G}}^\mu(-\hat{\lambda}_i)\hat{\mathbf{b}}_i \quad \text{for } i = 1, \ldots, r, \tag{19}$$

if equation (16) holds. Combining the subset condition (17) and Definition 1 leads to

$$\mathbf{G}(-\hat{\lambda}_i)\hat{\mathbf{b}}_i = \mathbf{G}^\mu(-\hat{\lambda}_i)\hat{\mathbf{b}}_i \quad \text{for } i = 1, \ldots, r, \tag{20}$$

Equation (18) then follows from the combination of (19) and (20). ∎

Consequently, if the interpolation data to generate $\boldsymbol{\Sigma}^\mu$ include the optimal shifts and tangential directions found by solving the approximate problem, $\hat{\boldsymbol{\Sigma}}^\mu$ is also optimal with respect to $\boldsymbol{\Sigma}$. Note that this also holds if, for instance, orthogonal and real projection matrices are used instead of $\mathbf{V}^\mu, \hat{\mathbf{V}}^\mu$ as long as they span the same subspaces, respectively (see Remark 1).

If the *primitive* bases $\mathbf{V}^\mu, \hat{\mathbf{V}}^\mu, \mathbf{V}$ are used, we can even show equality between the state-space realization $\hat{\boldsymbol{\Sigma}}^\mu$ and the realization of the model $\hat{\boldsymbol{\Sigma}}$ that we would obtain from a direct approximation of $\boldsymbol{\Sigma}$ with the same optimal interpolation data, i.e. $(\mathbf{S}_V, \mathbf{R}_V) = (\hat{\mathbf{S}}_V^\mu, \hat{\mathbf{R}}_V^\mu)$.

Corollary 2: Consider a full-order port-Hamiltonian model $\boldsymbol{\Sigma}$ as in (8) and let $\mathbf{V}, \mathbf{W} \in \mathbb{C}^{n \times r}$ be projection matrices that satisfy the following equations

$$\mathbf{V}\hat{\mathbf{S}}_V^\mu - (\mathbf{J} - \mathbf{R})\mathbf{Q}\mathbf{V} = (\mathbf{B} - \mathbf{P})\hat{\mathbf{R}}_V^\mu, \tag{21a}$$

$$\mathbf{W} = \mathbf{Q}\mathbf{V}(\mathbf{V}^T\mathbf{Q}\mathbf{V})^{-1}. \tag{21b}$$

If all assumptions of Theorem 3 hold, then the model $\hat{\boldsymbol{\Sigma}} = \mathbf{W}^T\boldsymbol{\Sigma}\mathbf{V}$ has the same state-space realization as $\hat{\boldsymbol{\Sigma}}^\mu$.

Proof: We prove that $\hat{\boldsymbol{\Sigma}}$ and $\hat{\boldsymbol{\Sigma}}^\mu$ are equal by showing that they have the same projection matrices, i.e.

$$\mathbf{V} = \mathbf{V}^\mu \hat{\mathbf{V}}^\mu, \tag{22a}$$

$$\mathbf{W} = \mathbf{W}^\mu \hat{\mathbf{W}}^\mu. \tag{22b}$$

From $\boldsymbol{\Sigma}^\mu = (\mathbf{W}^\mu)^T \boldsymbol{\Sigma} \mathbf{V}^\mu$ and (16a) we obtain that

$$(\mathbf{W}^\mu)^T \left(\mathbf{V}^\mu \hat{\mathbf{V}}^\mu \hat{\mathbf{S}}_V^\mu - (\mathbf{J} - \mathbf{R})\mathbf{Q}\mathbf{V}^\mu \hat{\mathbf{V}}^\mu - (\mathbf{B} - \mathbf{P})\hat{\mathbf{R}}_V^\mu \right)$$

is equal to zero. We assume existence and uniqueness of the solution $\hat{\mathbf{V}}^\mu$ to Sylvester equation (16a). For each column of (16a) we have

$$(\mathbf{W}^\mu)^T \left((\hat{\sigma}_i^\mu \mathbf{I}_n - (\mathbf{J} - \mathbf{R})\mathbf{Q})\, \mathbf{V}^\mu \hat{\mathbf{V}}_i^\mu - (\mathbf{B} - \mathbf{P})\hat{\mathbf{r}}_i^\mu \right) = \mathbf{0}. \tag{23}$$

We now determine column $\hat{\mathbf{V}}_i^\mu$ as a standard basis vector that selects the j-th column of $\mathbf{V}^\mu$. For this column, according to (14a), the following holds

$$\left(\sigma_j^\mu \mathbf{I}_n - (\mathbf{J} - \mathbf{R})\mathbf{Q}\right) \mathbf{V}_j^\mu - (\mathbf{B} - \mathbf{P})\mathbf{r}_j^\mu = \mathbf{0}.$$

Owing to the subset condition (17), we can then solve (23) by selecting those columns $\mathbf{V}_j^\mu$ for which $\sigma_j^\mu = \hat{\sigma}_i^\mu$ and $\mathbf{r}_j^\mu = \hat{\mathbf{r}}_i^\mu$ holds. Repeating this procedure for all $i = 1, \ldots, r$ leads to a matrix $\hat{\mathbf{V}}^\mu$ of standard basis vectors such that

$$\hat{\mathbf{S}}_V^\mu = (\hat{\mathbf{V}}^\mu)^T \mathbf{S}_V^\mu \hat{\mathbf{V}}^\mu,$$

which uniquely solves (16a). Comparing (23) with the columns of (21a) reveals that the product $\mathbf{V}^\mu\hat{\mathbf{V}}^\mu$ is then also a solution to (21a). From the uniqueness of $\mathbf{V}$, we deduce the necessity of $\mathbf{V} = \mathbf{V}^\mu\hat{\mathbf{V}}^\mu$. The proof is completed by the fact that

$$\begin{aligned}
\mathbf{W} &= \mathbf{Q}\mathbf{V}(\mathbf{V}^T\mathbf{Q}\mathbf{V})^{-1} \\
&= \mathbf{Q}(\mathbf{V}^\mu\hat{\mathbf{V}}^\mu)((\mathbf{V}^\mu\hat{\mathbf{V}}^\mu)^T\mathbf{Q}(\mathbf{V}^\mu\hat{\mathbf{V}}^\mu))^{-1} \\
&= \mathbf{Q}\mathbf{V}^\mu((\mathbf{V}^\mu)^T\mathbf{Q}\mathbf{V}^\mu)^{-1}\mathbf{Q}^\mu\hat{\mathbf{V}}^\mu((\hat{\mathbf{V}}^\mu)^T\mathbf{Q}^\mu\hat{\mathbf{V}}^\mu)^{-1} \\
&= \mathbf{W}^\mu\hat{\mathbf{W}}^\mu,
\end{aligned}$$

combining $\mathbf{V} = \mathbf{V}^\mu\hat{\mathbf{V}}^\mu$ and (14b), (16b), (21b). ∎

Remark 2: For the proof of Corollary 2, we assumed the uniqueness of the solutions $\mathbf{V}^\mu, \hat{\mathbf{V}}^\mu, \mathbf{V}$ to the Sylvester equations (14a), (16a), (21a), respectively. For instance, in the case of $\mathbf{V}$, this holds if, and only if, the regular matrix pencils $((\mathbf{J} - \mathbf{R})\mathbf{Q} - \lambda\mathbf{I}_n)$ and $(\hat{\mathbf{S}}_V^\mu - \lambda\mathbf{I}_r)$ have disjoint spectra [13]. As the eigenvalues of pencil $(\hat{\mathbf{S}}_V^\mu - \lambda\mathbf{I}_r)$ are the optimal frequencies $\{-\hat{\lambda}_i\}_{i=1}^r$ and $\boldsymbol{\Sigma}$ and $\hat{\boldsymbol{\Sigma}}$ are both stable by design, this will generally hold in practice. A similar argumentation holds for $\mathbf{V}^\mu$ and $\hat{\mathbf{V}}^\mu$.

Remark 3: By choosing the model function $\boldsymbol{\Sigma}^\mu$ as a port-Hamiltonian system, we can guarantee its stability. Note that this is not the case if the model function framework is applied to general LTI systems as in [11].

Remark 4: The model function framework can be extended to linear time-invariant port-Hamiltonian differential-algebraic systems (PH-DAEs). The transfer function of a

PH-DAE can be separated in a strictly proper part and a polynomial part. The order of the polynomial part depends on the index of the system, which is at most two for PH-DAEs [23]. In order to apply the model function framework to these systems, the model function has to match the polynomial part of the original transfer function exactly in order to keep the error bounded. This is a subject of future research.

Ensuring the subset condition (17) stated in Theorem 3 poses a challenge for practical implementations as we do not know the optimal tangential interpolation data $(\hat{\mathbf{S}}_V^\mu, \hat{\mathbf{R}}_V^\mu)$ in advance. We can enforce this condition in an iterative fashion. In each iteration, we first solve the approximate problem (15). In the following iteration, we then update the model function $\boldsymbol{\Sigma}^\mu$ such that it interpolates $\boldsymbol{\Sigma}$ at the optimal interpolation data found in the previous iteration. Upon convergence, i.e. when the optimal interpolation data between two iterations are identical, the subset condition (17) is satisfied. This strategy is also plausible before convergence, i.e. when the optimal interpolation data changes significantly between two iterations. In this case, $\boldsymbol{\Sigma}^\mu$ is enhanced in new regions of the frequency domain and thus becomes a better approximation of $\boldsymbol{\Sigma}$.

Note that the use of model functions provides a general framework in the sense that any structure-preserving, $\mathcal{H}_2$-based interpolatory optimization algorithm could be used to find the optimal interpolation data that solve the approximate problem. As an illustrative example, we apply the model function framework to IRKA-PH (see Algorithm 1).

C. Confined IRKA-PH

Owing to the local validity of using $\boldsymbol{\Sigma}^\mu$ instead of $\boldsymbol{\Sigma}$ for the optimization, which is *confined* to the vicinity of the interpolation frequencies in $\mathbf{S}_V^\mu$, we call the combination of both approaches in Algorithm 2 confined IRKA-PH (CIRKA-PH). Despite the fact that orthonormal, real bases are used for $\mathbf{V}^\mu, \hat{\mathbf{V}}^\mu$ for numerical reasons, we represent the set of shifts $\{\hat{\sigma}_i^\mu\}_{i=1}^r$ with $\hat{\mathbf{S}}_V^\mu$ and tangential directions $\{\hat{\mathbf{r}}_i^\mu\}_{i=1}^r$ with $\hat{\mathbf{R}}_V^\mu$ for the sake of brevity. The same holds for $(\mathbf{S}_V^\mu, \mathbf{R}_V^\mu)$.

Let n_k^μ and n^μ denote the dimension of the model function in the k-th iteration and after the final iteration, respectively. In principle, there are various strategies to initialize and update the model function $\boldsymbol{\Sigma}^\mu$ which are, however, all subject to the condition that $n_k^\mu > r$ and the subset condition (17) for $\mathcal{H}_2$-optimality. Condition $n_k^\mu > r$ is especially relevant at the initialization of $\boldsymbol{\Sigma}^\mu$ in the first iteration, where more interpolation data than $(\hat{\mathbf{S}}_V^0, \hat{\mathbf{R}}_V^0)$ must be used to create the model function. For possible strategies we refer to [11]. After the initial iteration, we also have several options to enforce the subset condition (17) by updating the model function. For instance, the most trivial strategy is to add the whole set of new interpolation data $(\hat{\mathbf{S}}_V, \hat{\mathbf{R}}_V)$ to $(\mathbf{S}_V^\mu, \mathbf{R}_V^\mu)$. However, this increases the order n_k^μ of the model function by r in each iteration. To keep n^μ low, it might be beneficial to only add those pairs of shifts and tangential directions that are not yet comprised in $(\mathbf{S}_V^\mu, \mathbf{R}_V^\mu)$ and that extend the validity of $\boldsymbol{\Sigma}^\mu$ to new frequency regions. We use the latter approach for the numerical examples provided in Section VI.

Algorithm 2 Confined IRKA-PH (CIRKA-PH)

Input: Original model $\boldsymbol{\Sigma}$, set of initial interpolation data $(\hat{\mathbf{S}}_V^0, \hat{\mathbf{R}}_V^0)$
Output: Reduced model $\hat{\boldsymbol{\Sigma}}$, model function $\boldsymbol{\Sigma}^\mu$

```
Initialize Σ^μ to empty
Ŝ_V ← Ŝ_V^0, R̂_V ← R̂_V^0
while not converged do
    [Σ^μ, S_V^μ, R_V^μ] ← updateModelFct(Σ, Σ^μ, Ŝ_V, R̂_V)
    [Σ̂^μ, Ŝ_V^μ, R̂_V^μ] ← IRKA-PH (Σ^μ, Ŝ_V, R̂_V)
    Ŝ_V ← Ŝ_V^μ, R̂_V ← R̂_V^μ
end while
Σ̂ ← Σ̂^μ
```

Let k^μ denote the total number of iterations of CIRKA-PH. In the k-th iteration, the dimension of the model function is increased to $n_k^\mu = n_{k-1}^\mu + n_k^{\mu,+}$ where $n_k^{\mu,+}$ is the number of new shifts used to update $\boldsymbol{\Sigma}^\mu$. The computational cost of CIRKA-PH can be approximated by

$$\mathcal{C}_n(\text{CIRKA-PH}) \approx \underbrace{\sum_{k=1}^{k^\mu} n_k^{\mu,+} \cdot \mathcal{C}_n(\text{LSE})}_{\boldsymbol{\Sigma}^\mu \text{ update}} + \underbrace{\sum_{k=1}^{k^\mu} r \cdot k_k^I \cdot \mathcal{C}_{n_k^\mu}(\text{LSE})}_{\text{optimization}}. \tag{25}$$

Here, we again neglect the computation of the small eigenvalue problem of dimension r and the orthogonalization of $\mathbf{V}^\mu$ and $\hat{\mathbf{V}}^\mu$. If we compare this expression with the computational cost (13) of IRKA-PH, we observe that the close coupling of *reduction* (i.e. retrieving information from the full-order model $\boldsymbol{\Sigma}$) and *optimization* (i.e. finding optimal interpolation data) is loosened by introducing the model function. In fact, for $r < n^\mu \ll n$, the update of the model function accounts for the major computational cost and is independent of the k_k^I steps needed to find optimal interpolation data in the k-th iteration. Hence, for very large-scale models $\boldsymbol{\Sigma}$, we expect $\mathcal{C}_{n_k^\mu}(\text{LSE}) \ll \mathcal{C}_n(\text{LSE})$ for all $k = 1, \ldots, k^\mu$ and thus we expect CIRKA-PH to be effective as long as

$$\sum_{k=1}^{k^\mu} n_k^{\mu,+} < r \cdot k^I.$$

VI. NUMERICAL EXAMPLES

We validate our theoretical considerations for the introduced CIRKA-PH algorithm by applying it to a multi-input/multi-output (MIMO) port-Hamiltonian system and comparing the resulting reduced-order models with those obtained by the IRKA-PH algorithm.

We consider the mass-spring-damper (MSD) system as described in [6], i.e. a MIMO port-Hamiltonian system with

TABLE I: Reduction of the MSD model with $n = 500$ and reduced order r

	CIRKA-PH					IRKA-PH		
r	t/s	n_{LU}	k^μ	$\sum k^I$	n^μ	t/s	n_{LU}	k^I
10	0.3	28	6	190	58	0.1	278	54
30	0.8	58	5	121	124	0.3	1048	62
50	2.0	85	5	83	198	0.5	1214	44

$\frac{n}{2}$ coupled MSD elements with the following masses, spring constants and damping coefficients:

$$m_i = 4\,\text{kg},\ k_i = 4\,\frac{\text{N}}{\text{m}},\ c_i = 1\,\frac{\text{Ns}}{\text{m}}, \qquad i = 1, ..., \frac{n}{2}.$$

We take a closer look at the original model orders $n = 500$ and $n = 10{,}000$.

Both systems are approximated with reduced-order models of dimension $r \in \{10, 30, 50\}$ obtained by IRKA-PH and CIRKA-PH. All tests have been carried out by initializing shifts with zeros and tangent directions by vectors with only ones as entries. The following convergence criterion was used

$$\frac{1}{r}\sum_{i=1}^{r}\left|\frac{\hat\sigma^\mu_{i,k} - \hat\sigma^\mu_{i,k-1}}{\hat\sigma^\mu_{i,k-1}}\right| < 10^{-6},$$

where $\hat\sigma^\mu_{i,k}$ denotes the i-th optimal shift found at iteration k. For IRKA-PH, we chose a maximum number of 200 iterations. For CIRKA-PH, we allowed 20 outer iterations and 50 inner IRKA-PH iterations per outer iteration at most.

Tables I and II show the computational demands of reducing both sample systems. In particular, the execution time t in seconds, the number of n-dimensional LU decompositions n_{LU} required for solving the large-scale LSEs of dimension n, the number of outer iterations k^μ of CIRKA-PH, and the (total) number of IRKA iterations $\sum_{k=1}^{k^\mu} k^I_k$ are displayed. Additionally, we provide the dimension of the final model function n^μ.

In both cases, CIRKA-PH carries out more IRKA-PH iterations and significantly less large-scale LU decompositions. For $n = 500$, the size of the model function n^μ is relatively close to the original model size n. Consequently, the approximation of $\boldsymbol{\Sigma}$ by $\boldsymbol{\Sigma}^\mu$ does not lead to computational advantages. However, note that for medium-sized systems, Riemannian reduction methods as in [7], [8] proved to be advantageous compared to interpolatory methods, as truly $\mathcal{H}_2$-optimal models can be found at manageable computational costs.

For $n = 10{,}000$, we observe that the model function framework provides a better trade-off between increasing iterations in total and lowering costs per iteration. Significantly smaller model functions for which $n^\mu \ll n$ accelerate convergence considerably. This supports our theoretical considerations in Section V. In accordance with [11], we therefore expect this framework to offer even more significant advantages over IRKA-PH for very large original orders $n > 10^5$.

All reduced-order models presented in this section satisfy the first $\mathcal{H}_2$-optimality condition (7a). Table III shows the approximation quality of the reduced-order models by means of the relative $\mathcal{H}_2$-error norms. In addition, Fig. 2 illustrates the frequency response of the original system $\mathbf{G}(s)$ for $n = 500$ and of the reduced-order models with $r = 10$ and $r = 30$ obtained by CIRKA-PH. Both the $\mathcal{H}_2$-errors and the frequency responses in Fig. 2 indicate that the input-output behavior of the original systems can be captured quite accurately with relatively small reduced orders.

TABLE II: Reduction of the MSD model with $n = 10{,}000$ and reduced order r

	CIRKA-PH					IRKA-PH		
r	t/s	n_{LU}	k^μ	$\sum k^I$	n^μ	t/s	n_{LU}	k^I
10	1.1	40	8	217	68	3.8	326	60
30	5.4	110	7	231	183	42.2	2091	119
50	35.8	207	10	436	340	171.7	6051	200

TABLE III: Shift deviation $\Delta\hat{\boldsymbol{\sigma}}$ and relative $\mathcal{H}_2$-error norms $e = \|\mathbf{G} - \hat{\mathbf{G}}\|_{\mathcal{H}_2}/\|\mathbf{G}\|_{\mathcal{H}_2}$

n	r	$e_{CIRKA-PH}$	$e_{IRKA-PH}$	$\Delta\hat{\boldsymbol{\sigma}}$
500	10	0.2422	0.2422	5.19×10^{-6}
	30	0.0105	0.0105	1.87×10^{-7}
	50	0.0004	0.0004	1.69×10^{-6}
10,000	10	0.2422	0.2422	3.01×10^{-6}
	30	0.0102	0.0102	5.63×10^{-8}
	50	0.0007	0.0007	6.98×10^{-5}

In all considered cases, the $\mathcal{H}_2$-errors of CIRKA-PH are almost identical to those of IRKA-PH. The difference in the vector of shifts in the 1-norm

$$\Delta\hat{\boldsymbol{\sigma}} = \sum_{i=1}^{r} |\hat\sigma^\mu_i - \hat\sigma_i|$$

reveals that this is no coincidence but a result of almost identical sets of interpolation points upon convergence. Note, however, that this is not guaranteed since both algorithms could converge to different solutions in other scenarios [11].

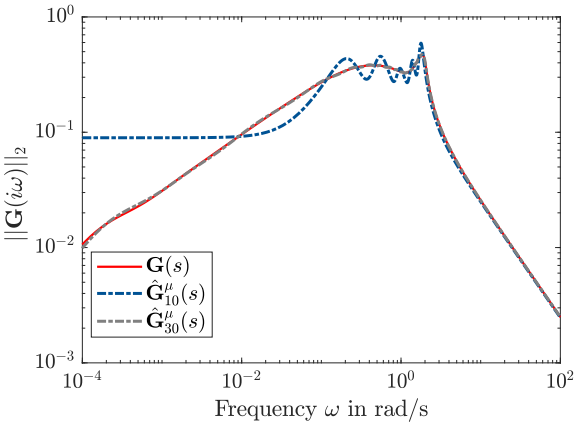

Fig. 2: Frequency response of the MSD model with $n = 500$ and two reduced-order models with $r \in \{10, 30\}$ obtained by CIRKA-PH

VII. CONCLUDING REMARKS

We have presented a new framework for interpolatory $\mathcal{H}_2$-inspired model reduction of linear port-Hamiltonian systems. The framework exploits the local nature of the $\mathcal{H}_2$-optimization problem and tangential interpolation by the use of surrogate models. By updating these surrogate models iteratively, a subset of first-order $\mathcal{H}_2$-optimality conditions is satisfied upon convergence and the port-Hamiltonian structure is retained. Numerical examples indicate that the decoupling of the cost of reduction and optimization has the potential to accelerate existing approaches significantly and especially in large-scale settings for which interpolatory methods are particularly powerful.

ACKNOWLEDGMENTS

We would like to thank Paul Kotyczka, Julio Pérez and Alexander Wischnewski for the thorough review of the manuscript.

REFERENCES

[1] V. Duindam, A. Macchelli, S. Stramigioli, and H. Bruyninckx, *Modeling and Control of Complex Physical Systems*. Springer Berlin Heidelberg, 2009.

[2] R. Ortega, A. J. Van Der Schaft, I. Mareels, and B. Maschke, "Putting energy back in control," *IEEE Control Systems Magazine*, vol. 21, no. 2, pp. 18–33, 2001.

[3] A. van der Schaft and D. Jeltsema, "Port-Hamiltonian systems theory: An introductory overview," *Foundations and Trends in Systems and Control*, vol. 1, no. 2-3, pp. 173–378, 2014.

[4] P. Kotyczka, *Numerical Methods for Distributed Parameter Port-Hamiltonian Systems*. TUM.University Press, 2019, Habilitation.

[5] S. Gugercin, R. Polyuga, C. Beattie, and A. van der Schaft, "Interpolation-based $\mathcal{H}_2$ model reduction for port-Hamiltonian systems," in *Proceedings of the 48h IEEE Conference on Decision and Control (CDC) held jointly with 2009 28th Chinese Control Conference*, 2009, pp. 5362–5369.

[6] S. Gugercin, R. V. Polyuga, C. Beattie, and A. van der Schaft, "Structure-preserving tangential interpolation for model reduction of port-Hamiltonian systems," *Automatica*, vol. 48, no. 9, pp. 1963–1974, 2012.

[7] K. Sato, "Riemannian optimal model reduction of linear port-Hamiltonian systems," *Automatica*, vol. 93, pp. 428–434, 2018.

[8] T. Moser and B. Lohmann, "A new Riemannian framework for efficient $\mathcal{H}_2$-optimal model reduction of port-Hamiltonian systems," in *2020 59th IEEE Conference on Decision and Control (CDC)*, 2020, pp. 5043–5049.

[9] H. K. F. Panzer, "Model order reduction by Krylov subspace methods with global error bounds and automatic choice of parameters," Dissertation, Technical University of Munich, Munich, 2014.

[10] A. Castagnotto, H. K. F. Panzer, and B. Lohmann, "Fast $\mathcal{H}_2$-optimal model order reduction exploiting the local nature of Krylov-subspace methods," in *2016 European Control Conference (ECC)*, 2016, pp. 1958–1969.

[11] A. Castagnotto and B. Lohmann, "A new framework for $\mathcal{H}_2$-optimal model reduction," *Mathematical and Computer Modelling of Dynamical Systems*, vol. 24, no. 3, pp. 236–257, 2018.

[12] A. C. Antoulas, C. A. Beattie, and S. Güğercin, *Interpolatory Methods for Model Reduction*. Society for Industrial and Applied Mathematics, 2020.

[13] K. E. Chu, "The solution of the matrix equations AXB-CXD=E and (YA-DZ,YC-BZ)=(E,F)," *Linear Algebra and its Applications*, vol. 93, pp. 93–105, 1987.

[14] K. Gallivan, A. Vandendorpe, and P. V. Dooren, "Sylvester equations and projection-based model reduction," *Journal of Computational and Applied Mathematics*, vol. 162, no. 1, pp. 213–229, 2004.

[15] C. Beattie and S. Gugercin, "Model reduction by rational interpolation," in *Model Reduction and Approximation*, Society for Industrial and Applied Mathematics, 2017, pp. 297–334.

[16] D. Wilson, "Optimum solution of model-reduction problem," *Proceedings of the Institution of Electrical Engineers*, vol. 117, no. 6, pp. 1161–1165, 1970.

[17] W.-Y. Yan and J. Lam, "An approximate approach to $\mathcal{H}_2$ optimal model reduction," *IEEE Transactions on Automatic Control*, vol. 44, no. 7, pp. 1341–1358, 1999.

[18] L. Meier and D. Luenberger, "Approximation of linear constant systems," *IEEE Transactions on Automatic Control*, vol. 12, no. 5, pp. 585–588, 1967.

[19] C. A. Beattie and S. Gugercin, "Krylov-based minimization for optimal $\mathcal{H}_2$ model reduction," in *2007 46th IEEE Conference on Decision and Control (CDC)*, IEEE, 2007.

[20] T. Wolf, B. Lohmann, R. Eid, and P. Kotyczka, "Passivity and structure preserving order reduction of linear port-Hamiltonian systems using Krylov subspaces," *European Journal of Control*, vol. 16, no. 4, pp. 401–406, 2010.

[21] P. V. Dooren, K. Gallivan, and P.-A. Absil, "$\mathcal{H}_2$-optimal model reduction of MIMO systems," *Applied Mathematics Letters*, vol. 21, no. 12, pp. 1267–1273, 2008.

[22] R. V. Polyuga and A. van der Schaft, "Structure preserving moment matching for port-Hamiltonian systems: Arnoldi and Lanczos," *IEEE Transactions on Automatic Control*, vol. 56, no. 6, pp. 1458–1462, 2011.

[23] C. Mehl, V. Mehrmann, and M. Wojtylak, "Linear algebra properties of dissipative Hamiltonian descriptor systems," *SIAM Journal on Matrix Analysis and Applications*, vol. 39, no. 3, pp. 1489–1519, 2018.

A.3 A New Riemannian Framework for Efficient $\mathcal{H}_2$-Optimal Model Reduction of Port-Hamiltonian Systems

Summary: This article presents a new optimization framework for $\mathcal{H}_2$-optimal model reduction of large-scale pH-ODE models. In contrast to traditional MOR methods, which typically indirectly create a reduced state-space realization via Petrov-Galerkin projections, our method is based on a direct optimization of the reduced state-space matrices. Similar to other optimization-based MOR methods, we incorporate the pH structural constraints by formulating the problem on a Riemannian product manifold. We show that by using the pole-residue formulation of the $\mathcal{H}_2$ error, the cost function and its Riemannian gradient can be computed efficiently and rely only on samples of the original transfer function and its derivative. Consequently, our approach does not require transformations of the original state-space realization or iterative solutions of large-scale Lyapunov equations. To solve the non-convex optimization problem, we employ a Riemannian trust-region method which guarantees the preservation of the pH structure and local $\mathcal{H}_2$ optimality upon convergence. We conclude with numerical experiments in which we demonstrate the applicability of our method to large-scale models.

CRediT author statement:

Tim Moser:	Conceptualization, Data Curation, Investigation, Methodology, Software, Visualization, Writing - Original Draft
Boris Lohmann:	Conceptualization, Funding Acquisition, Supervision, Writing - Review & Editing

A New Riemannian Framework for Efficient $\mathcal{H}_2$-Optimal Model Reduction of Port-Hamiltonian Systems

Tim Moser and Boris Lohmann

***Abstract*— We present a new framework for $\mathcal{H}_2$-optimal model reduction of linear port-Hamiltonian systems. The approach retains structural properties of the original system, such as passivity, and is based on the efficient pole-residue formulation of the $\mathcal{H}_2$-error norm. This makes Riemannian optimization computationally feasible for large-scale dynamical systems as well, which is supported by a numerical example.**

I. INTRODUCTION

The port-Hamiltonian systems paradigm provides an energy-based framework for the modeling and control of complex finite- and infinite-dimensional physical systems. The geometric description via (Stokes-)Dirac structures allows us to easily interconnect systems of different physical domains, which makes this approach especially suitable for multi-physics systems [1]. By exploiting its inherent system characteristics such as passivity, the modeling in port-Hamiltonian form facilitates the subsequent controller design. If controllers are also formulated as port-Hamiltonian systems, they can be designed to shape the energetic behavior of the coupled system consisting of plant and controller. This approach, for instance, paved the way for a paradigm shift in robotics towards safe interaction and human-robot collaboration (see e.g. [2]). However, depending on the physical system at hand and the desired accuracy of its model, systems in high state-space dimension may arise in the modeling stage (see e.g. [3] for structure-preserving discretization) which are computationally infeasible for simulation or real-time control. Model reduction addresses this issue by generating reduced-order models which approximate the original model with respect to predefined goals. For port-Hamiltonian systems, one goal is to preserve the port-Hamiltonian structure in the reduction process in order to exploit the strengths mentioned above.

Structure-preserving model reduction of linear port-Hamiltonian systems has been addressed in several ways. Methods based on reduced-order Dirac structures were presented in [4]. Interpolatory reduction methods for single-input/single-output (SISO) port-Hamiltonian systems were introduced in [5] and expanded to multi-input/multi-output (MIMO) systems in [6]. In the context of this paper, we would like to focus on different approaches striving for $\mathcal{H}_2$-optimality in the sense that the $\mathcal{H}_2$-error between the original and reduced model is as small as possible.

Funded by the Deutsche Forschungsgemeinschaft (DFG, German Research Foundation) – Project number 418612884.

T. Moser and B. Lohmann are with the Chair of Automatic Control, Technical University of Munich, 85748 Garching/Munich, Germany {tim.moser,lohmann}@tum.de

There are two main frameworks in which this non-convex optimization problem can be formulated. In the Lyapunov-based framework, the first-order conditions for (local) $\mathcal{H}_2$-optimality result in coupled Lyapunov equations [7], [8]. The second framework may be derived from pole-residue expansions of the reduced model and leads to interpolation conditions for the reduced-order model, also known as the Meier-Luenberger conditions [9] for SISO systems. A connection between both frameworks was established in [10] by showing equivalence of the corresponding first-order conditions to structured orthogonality conditions based on Hilbert spaces.

In the Lyapunov framework, various methods have been developed for general linear time-invariant (LTI) SISO systems to solve this optimization problem. Gradient-based algorithms, such as [7], [11], [12] and [13], require iterative solves of coupled sparse-dense Lyapunov equations. For large-scale dynamical systems, this is computationally expensive despite significant improvements in the field of solving these equations numerically during the last two decades (see [14] for a comprehensive overview). Finding $\mathcal{H}_2$-optimal approximations of port-Hamiltonian systems is even more challenging since additional structural system properties must be retained during the reduction. Recently, a gradient-based method [15] has been developed in the Lyapunov framework. The author shows that by formulating the optimization problem on Riemannian matrix manifolds, it is possible to achieve both structure preservation and $\mathcal{H}_2$-optimality. However, the method may require an initial large-scale Cholesky decomposition and, similar to its Euclidean counterparts, iterative solving of coupled Lyapunov equations which makes it less suitable for large-scale systems.

On the other hand, in the pole-residue framework, the computation of the first-order conditions solely requires evaluations of the original and reduced-order model at the mirror images of reduced-order poles, which makes this approach more applicable in large-scale settings. Beattie and Gugercin developed gradient-based methods for general LTI systems both in a projective [16] and non-projective manner [17]. Formulating the problem in the pole-residue framework as a fixed point iteration led to the even more efficient and thus widely applied iterative rational Krylov algorithm (IRKA) [10]. However, IRKA does not guarantee a decrease in the $\mathcal{H}_2$-error in every iteration. It generates a series of reduced models which, so far, has only been proven to converge for symmetric state-space systems [18], whereas port-Hamiltonian systems are, in general, non-symmetric. In [6], a modified version of IRKA (IRKA-PH)

was proposed in order to preserve the port-Hamiltonian form during the reduction. Since IRKA-PH is based on Petrov-Galerkin projections, some degrees of freedom (exactly half of them in the SISO case) must be given up in order to preserve the port-Hamiltonian structure. This inevitably leads to the fact that it is generally not possible to satisfy all $\mathcal{H}_2$-optimality conditions in this projective framework [6]. Hence, to the best of the authors' knowledge, there is no $\mathcal{H}_2$-optimal method to reduce port-Hamiltonian systems in the pole-residue framework.

We address this issue and propose a novel Riemannian framework for the $\mathcal{H}_2$-optimal reduction of port-Hamiltonian systems. We incorporate geometric constraints using the Riemannian problem formulation of [15] and exploit the computationally efficient pole-residue formulation of the $\mathcal{H}_2$-error proposed in [9]. By this means, preservation of the port-Hamiltonian structure and $\mathcal{H}_2$-optimality upon convergence are guaranteed and the approach does not rely on iterative solves of large-scale Lyapunov equations. Consequently, this framework is also accessible for the reduction of large-scale systems.

II. PROBLEM FORMULATION

We consider linear single-input/single-output port-Hamiltonian systems without algebraic constraints of the following form

$$\begin{aligned} \dot{\mathbf{x}} &= (\mathbf{J}-\mathbf{R})\mathbf{Q}\mathbf{x} + \mathbf{b}u \\ y &= \mathbf{b}^T\mathbf{Q}\mathbf{x} \end{aligned} \tag{1}$$

with $\mathbf{J},\mathbf{R},\mathbf{Q} \in \mathbb{R}^{n\times n}$ and $\mathbf{b},\mathbf{x} \in \mathbb{R}^n$. The internal energy of the system is represented by the quadratic Hamiltonian $H(\mathbf{x}) = \frac{1}{2}\mathbf{x}^T\mathbf{Q}\mathbf{x}$ with energy matrix $\mathbf{Q} = \mathbf{Q}^T$. For $\mathbf{Q} > 0$ and dissipation matrix $\mathbf{R} = \mathbf{R}^T \geq 0$, the system is passive, i.e. $\dot{H}(t) \leq u(t)y(t)$ for all t. The internal energy flow among energy storage elements and the flow across its system boundary is described by the skew-symmetric interconnection matrix $\mathbf{J} = -\mathbf{J}^T$ and the port matrix $\mathbf{b}$, respectively.

In the context of this paper, we are striving for a reduced port-Hamiltonian system

$$\begin{aligned} \dot{\hat{\mathbf{x}}} &= (\hat{\mathbf{J}}-\hat{\mathbf{R}})\hat{\mathbf{x}} + \hat{\mathbf{b}}u \\ y &= \hat{\mathbf{b}}^T\hat{\mathbf{x}} \end{aligned} \tag{2}$$

with $\hat{\mathbf{J}},\hat{\mathbf{R}} \in \mathbb{R}^{r\times r}$, $\hat{\mathbf{b}},\hat{\mathbf{x}} \in \mathbb{R}^r$ and with $\hat{\mathbf{J}} = -\hat{\mathbf{J}}^T$, $\hat{\mathbf{R}} = \hat{\mathbf{R}}^T > 0$, and $r \ll n$. Note that the assumption that $\hat{\mathbf{Q}} = \mathbf{I}_r$ is not restrictive. We may transform every reduced-order model with $\tilde{\mathbf{Q}} \neq \mathbf{I}_r$ ($\tilde{\mathbf{Q}} = \tilde{\mathbf{Q}}^T > 0$) to the form of (2) by $\hat{\mathbf{x}} = \mathbf{L}^T\tilde{\mathbf{x}}$ without changing the transfer function, where $\mathbf{L}$ is obtained via a Cholesky factorization $\tilde{\mathbf{Q}} = \mathbf{L}\mathbf{L}^T$. However, by using (2), we can reduce the number of optimization parameters by the $\frac{r(r+1)}{2}$ independent entries of $\tilde{\mathbf{Q}}$.

Our goal is to approximate the transfer function $G(s) = \mathbf{b}^T\mathbf{Q}(s\mathbf{I}_n - (\mathbf{J}-\mathbf{R})\mathbf{Q})^{-1}\mathbf{b}$ of the (stable) original system (1) with respect to the $\mathcal{H}_2$-norm

$$\|G\|_{\mathcal{H}_2} = \left(\frac{1}{2\pi}\int_{-\infty}^{\infty}|G(i\omega)|^2 d\omega\right)^{\frac{1}{2}}$$

in an optimal way and, at the same time, preserve its port-Hamiltonian structure. Hence, the following optimization problem can be formulated [15]:

$$\min_{(\hat{\mathbf{J}},\hat{\mathbf{R}},\hat{\mathbf{b}})\in\mathcal{M}} \mathcal{F} := \|G-\hat{G}\|_{\mathcal{H}_2}^2 \tag{3}$$

where $\mathcal{M}$ is the product manifold $\mathrm{Skew}_r \times \mathrm{Sym}_r^+ \times \mathbb{R}^r$ and $\hat{G}(s) = \hat{\mathbf{b}}^T(s\mathbf{I}_r - (\hat{\mathbf{J}}-\hat{\mathbf{R}}))^{-1}\hat{\mathbf{b}}$. Here, Skew_r and Sym_r^+ denote the manifolds of skew-symmetric and symmetric positive-definite matrices in $\mathbb{R}^{r\times r}$, respectively. By formulating the optimization problem on the product manifold $\mathcal{M}$, it is guaranteed that the (stable) reduced-order model (2) is port-Hamiltonian for any given order $r \ll n$.

In the following, we first derive the gradient of $\mathcal{F}$ with respect to the optimization parameters $\hat{\mathbf{J}}$, $\hat{\mathbf{R}}$ and $\hat{\mathbf{b}}$ in the Euclidean space $\mathbb{R}^{r\times r}\times\mathbb{R}^{r\times r}\times\mathbb{R}^r$ using the efficient pole-residue formulation of $\mathcal{F}$. We then transfer the optimization problem to the manifold $\mathcal{M}$ and demonstrate the performance of this new framework using a trust-region method.

III. COST FUNCTION AND EUCLIDEAN GRADIENT OF $\mathcal{H}_2$-ERROR

We consider the pole-residue definition of the $\mathcal{H}_2$-error initially proposed in [19].

Lemma 1. Assuming distinct poles λ_i and $\hat{\lambda}_j$ for the original system (1) and the reduced system (2), respectively, the partial fraction decomposition of the original transfer function is given by $G(s) = \sum_{i=1}^n \frac{\phi_i}{s-\lambda_i}$ and for the reduced system by $\hat{G}(s) = \sum_{j=1}^r \frac{\hat{\phi}_j}{s-\hat{\lambda}_j}$ with residues ϕ_i and $\hat{\phi}_j$. Then, the cost function $\mathcal{F}$ can be expressed as

$$\begin{aligned} \mathcal{F} = &\sum_{i=1}^n \phi_i(G(-\lambda_i) - \hat{G}(-\lambda_i)) \\ &+ \sum_{j=1}^r \hat{\phi}_j(\hat{G}(-\hat{\lambda}_j) - G(-\hat{\lambda}_j)). \end{aligned} \tag{4}$$

Using the fact that $\langle G,\hat{G}\rangle_{\mathcal{H}_2} = \sum_{j=1}^r \hat{\phi}_j G(-\hat{\lambda}_j)$ [17, Theorem 2.1] we get

$$\mathcal{F} = \|G\|_{\mathcal{H}_2}^2 - 2\sum_{j=1}^r \hat{\phi}_j G(-\hat{\lambda}_j) + \sum_{k,l=1}^r \frac{\hat{\phi}_k\hat{\phi}_l}{-\hat{\lambda}_k-\hat{\lambda}_l}, \tag{5}$$

where the first addend does not depend on the choice of the reduced-order model. Hence, we will minimize $\mathcal{F} - \|G\|_{\mathcal{H}_2}^2$ and refer to it as $\mathcal{F}$ in the following. This formulation is powerful from a computational point of view because it does not rely on the solution of a large-scale Lyapunov equation.

Next, we derive the gradient of the cost functional $\mathcal{F}$ in the Euclidean space.

Lemma 2. [16, Theorem 2.1] The partial derivatives of $\mathcal{F}$ with respect to the reduced-order residues $\hat{\phi}_j$ and poles $\hat{\lambda}_j$ are

$$\frac{\partial\mathcal{F}}{\partial\hat{\phi}_j} = 2(\hat{G}(-\hat{\lambda}_j) - G(-\hat{\lambda}_j)), \quad j = 1\dots r, \tag{6a}$$

$$\frac{\partial\mathcal{F}}{\partial\hat{\lambda}_j} = 2\hat{\phi}_j(G'(-\hat{\lambda}_j) - \hat{G}'(-\hat{\lambda}_j)), \quad j = 1\dots r. \tag{6b}$$

Remark 1. In this framework, the necessary conditions for $\mathcal{H}_2$-optimality, known as the Meier-Luenberger [9] conditions, become immediately evident. Each $\mathcal{H}_2$-optimal reduced-order model with distinct poles interpolates both $G(s)$ and its first derivative $G'(s)$ at all mirrored reduced-order poles $-\hat{\lambda}_j$.

Remark 2. With interpolatory model reduction techniques such as IRKA-PH [6], it is generally not possible to satisfy both necessary conditions (6a) and (6b) and preserve the port-Hamiltonian structure at the same time. IRKA-PH iteratively creates bases $\mathbf{V} \in \mathbb{R}^{n\times r}$ of Krylov subspaces which are parameterized by r interpolation points. Consequently, the $2r$ conditions in (6a) and (6b) can only be met for particular port-Hamiltonian systems, e.g. if $\mathbf{J} = \mathbf{0}$ [20], [15]. From a physical point of view, this limitation also becomes evident: for $\mathbf{Q} = \mathbf{I}_n$ the reduced-order interconnection and dissipation matrix gained by IRKA-PH are $\hat{\mathbf{J}} = \mathbf{V}^T\mathbf{J}\mathbf{V}$ and $\hat{\mathbf{R}} = \mathbf{V}^T\mathbf{R}\mathbf{V}$, respectively. Thus, the two different physical phenomena of dissipation and energy exchange are approximated by the same projection. As stated in (3), we resolve this limitation by optimizing $\hat{\mathbf{J}}$, $\hat{\mathbf{R}}$ and $\hat{\mathbf{b}}$ independently.

Next, we investigate the partial derivatives of the vector-valued functions $\hat{\boldsymbol{\lambda}} = [\hat{\lambda}_1, \dots, \hat{\lambda}_r]^T$ and $\hat{\boldsymbol{\phi}} = [\hat{\phi}_1, \dots, \hat{\phi}_r]^T$ with respect to the Euclidean optimization parameters $(\hat{\mathbf{J}}, \hat{\mathbf{R}}, \hat{\mathbf{b}}) \in \mathbb{R}^{r\times r} \times \mathbb{R}^{r\times r} \times \mathbb{R}^r$. Let $\mathbf{q}$ denote the parameter vector

$$\mathbf{q} = \operatorname{vec}\left(\left[\hat{\mathbf{J}}, \hat{\mathbf{R}}, \hat{\mathbf{b}}\right]\right) \in \mathbb{R}^{r(2r+1)}, \tag{7}$$

where vec() is the vectorization operator.

A. Euclidean Jacobian $D\hat{\boldsymbol{\lambda}}(\mathbf{q})$

The system matrix $\hat{\mathbf{J}} - \hat{\mathbf{R}}$ and its eigenvalue $\hat{\lambda}_j$ are implicitly related by $(\hat{\mathbf{J}} - \hat{\mathbf{R}})\mathbf{z}_j = \hat{\lambda}_j \mathbf{z}_j$, where $\mathbf{z}_j$ denotes the corresponding right eigenvector.

Theorem 1. The partial derivative of $\hat{\lambda}_j$ with respect to the (k,l)-th matrix entry of $\hat{\mathbf{J}}$ is given by

$$\frac{\partial \hat{\lambda}_j}{\partial \hat{J}_{k,l}} = \frac{\mathbf{w}_j^* \mathbf{E}_{k,l} \mathbf{z}_j}{\mathbf{w}_j^* \mathbf{z}_j}, \tag{8}$$

where $\mathbf{w}_j^*$ fulfills the eigenvalue relation $(\hat{\mathbf{J}} - \hat{\mathbf{R}})^* \mathbf{w}_j = \overline{\hat{\lambda}}_j \mathbf{w}_j$ and $\mathbf{E}_{k,l} \in \mathbb{R}^{r\times r}$ is the single-entry matrix with entry 1 at position (k,l) and zeros otherwise.

Proof. We assume distinct eigenvalues in the context of this paper. Hence, it can be shown that a neighborhood $\mathcal{N}(\hat{\mathbf{J}} - \hat{\mathbf{R}}) \subset \mathbb{C}^{r\times r}$ exists, on which unique C^∞-functions $\lambda(\hat{\mathbf{J}} - \hat{\mathbf{R}})$ and $\mathbf{z}(\hat{\mathbf{J}} - \hat{\mathbf{R}})$ are defined, for which $\lambda(\hat{\mathbf{J}} - \hat{\mathbf{R}}) = \hat{\lambda}_j$ and $\mathbf{z}(\hat{\mathbf{J}} - \hat{\mathbf{R}}) = \mathbf{z}_j$ [21, Chapter 9]. Equation (8) then follows by differentiating the eigenvalue relation and using the fact that $\frac{\partial(\hat{\mathbf{J}} - \hat{\mathbf{R}})}{\partial \hat{J}_{k,l}} = \mathbf{E}_{k,l}$. □

As a result of Theorem 1, the Jacobian of the eigenvalues with respect to $\hat{\mathbf{R}}$ is given by

$$\mathrm{D}_{\mathrm{vec}(\hat{\mathbf{R}})} \hat{\boldsymbol{\lambda}}(\mathbf{q}) = -\mathrm{D}_{\mathrm{vec}(\hat{\mathbf{J}})} \hat{\boldsymbol{\lambda}}(\mathbf{q}) \in \mathbb{C}^{r\times r^2}.$$

Since the eigenvalues do not depend on the input matrix $\hat{\mathbf{b}}$, the following holds

$$\mathrm{D}_{\hat{\mathbf{b}}} \hat{\boldsymbol{\lambda}}(\mathbf{q}) = \mathbf{0}_{r\times r}.$$

The Euclidean Jacobian $\mathrm{D}\hat{\boldsymbol{\lambda}}(\mathbf{q})$ is then given by

$$\mathrm{D}\hat{\boldsymbol{\lambda}}(\mathbf{q}) = [\mathrm{D}_{\mathrm{vec}(\hat{\mathbf{J}})} \hat{\boldsymbol{\lambda}}(\mathbf{q}), \mathrm{D}_{\mathrm{vec}(\hat{\mathbf{R}})} \hat{\boldsymbol{\lambda}}(\mathbf{q}), \mathrm{D}_{\hat{\mathbf{b}}} \hat{\boldsymbol{\lambda}}(\mathbf{q})] \in \mathbb{C}^{r\times r(2r+1)}.$$

Note that $\mathrm{D}\hat{\boldsymbol{\lambda}}(\mathbf{q})$ solely depends on the reduced matrices of system (2) and only requires solving two small eigenvalue problems of dimension r.

B. Euclidean Jacobian $D\hat{\boldsymbol{\phi}}(\mathbf{q})$

Next, we examine the sensitivity of the residue vector function $\hat{\boldsymbol{\phi}}$ with respect to the optimization parameters $\mathbf{q}$. The eigendecomposition of matrix $\hat{\mathbf{J}} - \hat{\mathbf{R}}$ is given by

$$(\hat{\mathbf{J}} - \hat{\mathbf{R}})\mathbf{Z} = \mathbf{Z}\boldsymbol{\Lambda},$$

where $\mathbf{Z}$ is the matrix composed of all (right) eigenvectors $\mathbf{z}_j$ and $\boldsymbol{\Lambda} = \operatorname{diag}(\hat{\lambda}_j)$. If we transfer system (2) to modal form such that $\mathbf{Z}^{-1}(\hat{\mathbf{J}} - \hat{\mathbf{R}})\mathbf{Z} = \boldsymbol{\Lambda}$, the residue $\hat{\phi}_j$ to the corresponding eigenvalue $\hat{\lambda}_j$ is given by:

$$\hat{\phi}_j = \hat{\mathbf{b}}^T \mathbf{Z} \mathbf{E}_{j,j} \mathbf{Z}^{-1} \hat{\mathbf{b}}. \tag{9}$$

The (j,k)-th entry of the Jacobian $\mathrm{D}\hat{\boldsymbol{\phi}}(\hat{\mathbf{b}})$ is then given by

$$\begin{aligned} \frac{\partial \hat{\phi}_j}{\partial \hat{b}_k} &= \mathbf{e}_j^T \mathbf{Z}^{-1} \left[\frac{\partial \hat{\mathbf{b}}}{\partial \hat{b}_k} \hat{\mathbf{b}}^T + \hat{\mathbf{b}} \left(\frac{\partial \hat{\mathbf{b}}}{\partial \hat{b}_k} \right)^T \right] \mathbf{Z}\mathbf{e}_j \\ &= \mathbf{e}_j^T \mathbf{Z}^{-1} \left[\mathbf{e}_k \hat{\mathbf{b}}^T + \hat{\mathbf{b}} \mathbf{e}_k^T \right] \mathbf{Z}\mathbf{e}_j \end{aligned} \tag{10}$$

for all $j,k = 1, ..., r$ and where $\mathbf{e}_j$ denotes the j-th standard basis vector of $\mathbb{R}^r$.

Theorem 2. The partial derivative of $\hat{\phi}_j$ with respect to the (k,l)-th entry of the interconnection matrix $\hat{\mathbf{J}}$ is given by

$$\begin{aligned} \frac{\partial \hat{\phi}_j}{\partial \hat{J}_{k,l}} =& \mathbf{e}_j^T \mathbf{Z}^{-1} \hat{\mathbf{b}} \hat{\mathbf{b}}^T \frac{\partial \mathbf{Z}}{\partial \hat{J}_{k,l}} \mathbf{e}_j \\ &- \mathbf{e}_j^T \mathbf{Z}^{-1} \frac{\partial \mathbf{Z}}{\partial \hat{J}_{k,l}} \mathbf{Z}^{-1} \hat{\mathbf{b}} \hat{\mathbf{b}}^T \mathbf{Z} \mathbf{e}_j. \end{aligned} \tag{11}$$

The Moore-Penrose pseudo inverse of a matrix is denoted by $()^+$. Then $\frac{\partial \mathbf{Z}}{\partial \hat{J}_{k,l}}$ is composed of the following column vectors

$$\frac{\partial \mathbf{z}_j}{\partial \hat{J}_{k,l}} = \left[\hat{\lambda}_j \mathbf{I}_r - (\hat{\mathbf{J}} - \hat{\mathbf{R}}) \right]^+ \left(\mathbf{I}_r - \frac{\mathbf{z}_j \mathbf{w}_j^*}{\mathbf{w}_j^* \mathbf{z}_j} \right) \mathbf{E}_{k,l} \mathbf{z}_j \tag{12}$$

for all $j,k,l = 1, ..., r$.

Proof. We deduce the existence of the functions λ and $\mathbf{z}$ on a neighborhood $\mathcal{N}(\hat{\mathbf{J}} - \hat{\mathbf{R}}) \subset \mathbb{C}^{r\times r}$ from Theorem 1 and obtain (11) by differentiating (9). Equation (12) results from differentiating both sides of $(\hat{\mathbf{J}} - \hat{\mathbf{R}})\mathbf{z}_j = \hat{\lambda}_j \mathbf{z}_j$ and substituting $\frac{\partial \hat{\lambda}_j}{\partial \hat{J}_{k,l}}$ by (8). We use the Moore-Penrose pseudo inverse for the singular matrix pencil $\left[\hat{\lambda}_j \mathbf{I}_r - (\hat{\mathbf{J}} - \hat{\mathbf{R}}) \right]$. The fact that $\frac{\partial(\hat{\mathbf{J}} - \hat{\mathbf{R}})}{\partial \hat{J}_{k,l}} = \mathbf{E}_{k,l}$ and

$$\frac{\partial \mathbf{Z}^{-1}}{\partial \hat{J}_{k,l}} = -\mathbf{Z}^{-1} \frac{\partial \mathbf{Z}}{\partial \hat{J}_{k,l}} \mathbf{Z}^{-1}$$

complete the proof. □

Similar to above, the Jacobian $\mathrm{D}_{\mathrm{vec}(\hat{\mathbf{R}})}\hat{\boldsymbol{\phi}}(\mathbf{q})$ is given by

$$\mathrm{D}_{\mathrm{vec}(\hat{\mathbf{R}})}\hat{\boldsymbol{\phi}}(\mathbf{q}) = -\mathrm{D}_{\mathrm{vec}(\hat{\mathbf{J}})}\hat{\boldsymbol{\phi}}(\mathbf{q}) \in \mathbb{C}^{r\times r^2}. \tag{13}$$

Combining the results of (10), (11) and (13), we construct the Jacobian

$$\mathrm{D}\hat{\boldsymbol{\phi}}(\mathbf{q}) = [\mathrm{D}_{\mathrm{vec}(\hat{\mathbf{J}})}\hat{\boldsymbol{\phi}}(\mathbf{q}), \mathrm{D}_{\mathrm{vec}(\hat{\mathbf{R}})}\hat{\boldsymbol{\phi}}(\mathbf{q}), \mathrm{D}_{\hat{\mathbf{b}}}\hat{\boldsymbol{\phi}}(\mathbf{q})] \in \mathbb{C}^{r\times r(2r+1)}$$

Note that $\mathrm{D}\hat{\boldsymbol{\phi}}(\mathbf{q})$ only relies on computations in small order r. If we assume that the eigendecomposition of matrix $\hat{\mathbf{J}}-\hat{\mathbf{R}}$ has already been computed for $\mathrm{D}\hat{\boldsymbol{\lambda}}(\mathbf{q})$, the computational cost of $\mathrm{D}\hat{\boldsymbol{\phi}}(\mathbf{q})$ is dominated by the r solves of (12) which can be computed easily for small orders.

We obtain the Euclidean gradient $\nabla_{\mathbf{q}}\mathcal{F}$ in its vectorized form by

$$\nabla\mathcal{F}_{\mathbf{q}}^T = \left[\mathrm{D}_{\hat{\boldsymbol{\phi}}}\mathcal{F}, \mathrm{D}_{\hat{\boldsymbol{\lambda}}}\mathcal{F}\right] \begin{bmatrix} \mathrm{D}\hat{\boldsymbol{\phi}}(\mathbf{q}) \\ \mathrm{D}\hat{\boldsymbol{\lambda}}(\mathbf{q}) \end{bmatrix} \in \mathbb{R}^{r(2r+1)}, \tag{14}$$

where $\mathrm{D}_{\hat{\boldsymbol{\phi}}}\mathcal{F} = \left[\frac{\partial\mathcal{F}}{\partial\hat{\phi}_1}, ..., \frac{\partial\mathcal{F}}{\partial\hat{\phi}_r}\right]$ and $\mathrm{D}_{\hat{\boldsymbol{\lambda}}}\mathcal{F} = \left[\frac{\partial\mathcal{F}}{\partial\hat{\lambda}_1}, ..., \frac{\partial\mathcal{F}}{\partial\hat{\lambda}_r}\right]$ follow from (6a) and (6b), respectively. The major computational cost of $\nabla\mathcal{F}_{\mathbf{q}}$ is the evaluation of $G(-\hat{\lambda}_j))$ in (6a). Note that for the computation of (6b), the factorizations during the computation of (6a) can be re-used and thus, only additional triangular solves are needed.

IV. RIEMANNIAN OPTIMIZATION

So far, we have only considered the input-output behavior of system (2) but ignored the specific structure of the interconnection and dissipation matrices. More specifically, we have assumed that $\hat{\mathbf{J}}, \hat{\mathbf{R}} \in \mathbb{R}^{r\times r}$. However, in order to preserve the port-Hamiltonian structure, we also have to guarantee that $\hat{\mathbf{J}} \in \mathrm{Skew}_r$ and $\hat{\mathbf{R}} \in \mathrm{Sym}_r^+$. We incorporate these geometric constraints in the following by transferring the optimization problem to the product manifold $\mathcal{M}$ and by this means obtain an unconstrained optimization problem on a constrained search space. Iterative optimization algorithms are based on local approximations of the cost functional by its first (and second) order derivatives and select the next iterate by determining an update direction and step size. The transfer of conventional optimization algorithms in Euclidean space to a Riemannian manifold is established by the use of a retraction and a Riemannian metric. A retraction $R_x : T_x\mathcal{M} \to \mathcal{M}$ at $x \in \mathcal{M}$ is a continuously differentiable mapping between the manifold $\mathcal{M}$ and its tangent space $T_x\mathcal{M}$ at x (see [22, Definition 4.1.1]). The tangent space $T_x\mathcal{M}$ is a local approximation of the manifold $\mathcal{M}$ at x and is an Euclidean space if it is equipped with a smoothly varying inner product $\langle\cdot,\cdot\rangle_x$ called the Riemannian metric. The main concept of Riemannian optimization is to shift the cost functional $\mathcal{F}$ to the Euclidean space $T_x\mathcal{M}$, where it can be approximated and minimized with conventional methods. Subsequently, we project the new iterate back onto the manifold using the retraction.

Given the fact that Skew_r and $\mathbb{R}^r$ are Euclidean spaces, they can be equipped with the Frobenius inner product. For the manifold Sym_r^+ we use the Riemannian metric $\langle\boldsymbol{\eta}_1, \boldsymbol{\eta}_2\rangle_{\hat{\mathbf{R}}} = \mathrm{tr}(\hat{\mathbf{R}}^{-1}\boldsymbol{\eta}_1\hat{\mathbf{R}}^{-1}\boldsymbol{\eta}_2)$ [23] which leads to the following Riemannian metric for the manifold $\mathcal{M}$:

$$\begin{aligned}&\langle(\boldsymbol{\xi}_1,\boldsymbol{\eta}_1,\boldsymbol{\zeta}_1),(\boldsymbol{\xi}_2,\boldsymbol{\eta}_2,\boldsymbol{\zeta}_2)\rangle_{(\hat{\mathbf{J}},\hat{\mathbf{R}},\hat{\mathbf{b}})}\\ &\quad:= \mathrm{tr}(\boldsymbol{\xi}_1^T\boldsymbol{\xi}_2) + \mathrm{tr}(\hat{\mathbf{R}}^{-1}\boldsymbol{\eta}_1\hat{\mathbf{R}}^{-1}\boldsymbol{\eta}_2) + \mathrm{tr}(\boldsymbol{\zeta}_1^T\boldsymbol{\zeta}_2),\end{aligned} \tag{15}$$

where tr() denotes the trace of a matrix. Note that the inverse of $\hat{\mathbf{R}}$ exists for all $\hat{\mathbf{R}} \in \mathrm{Sym}_r^+$. In Euclidean spaces the most trivial retraction, which is also an exponential map, is simply given by straight lines and thus, for instance, in the case of Skew_r we have $\mathrm{Exp}_{\hat{\mathbf{J}}}(\boldsymbol{\xi}) = \hat{\mathbf{J}} + \boldsymbol{\xi}$. When Sym_r^+ is endowed with the Riemannian metric as in (15), the exponential map can be derived from the geodesic in [24, Chapter 6]:

$$\mathrm{Exp}_{\hat{\mathbf{R}}}(\boldsymbol{\eta}) = \hat{\mathbf{R}}^{\frac{1}{2}}\exp(\hat{\mathbf{R}}^{-\frac{1}{2}}\boldsymbol{\eta}\hat{\mathbf{R}}^{-\frac{1}{2}})\hat{\mathbf{R}}^{\frac{1}{2}}.$$

In order to avoid the computational complexity and numerical difficulties associated with the matrix exponential exp(), we approximate the exponential map by a second-order model as proposed in [25]

$$R_{\hat{\mathbf{R}}}(\boldsymbol{\eta}) = \hat{\mathbf{R}} + \boldsymbol{\eta} + \frac{1}{2}\boldsymbol{\eta}\hat{\mathbf{R}}^{-1}\boldsymbol{\eta}.$$

It can be shown that $R_{\hat{\mathbf{R}}}(\boldsymbol{\eta}) \in \mathrm{Sym}_r^+$ for all $\hat{\mathbf{R}} \in \mathrm{Sym}_r^+$ and $\boldsymbol{\eta} \in T_{\hat{\mathbf{R}}}\mathrm{Sym}_r^+$. We thus define the following retraction for $\mathcal{M}$

$$\begin{aligned}&\mathrm{R}_{(\hat{\mathbf{J}},\hat{\mathbf{R}},\hat{\mathbf{b}})}(\boldsymbol{\xi},\boldsymbol{\eta},\boldsymbol{\zeta})\\ &\quad:= (\hat{\mathbf{J}}+\boldsymbol{\xi}, \hat{\mathbf{R}}+\boldsymbol{\eta}+\frac{1}{2}\boldsymbol{\eta}\hat{\mathbf{R}}^{-1}\boldsymbol{\eta}, \hat{\mathbf{b}}+\boldsymbol{\zeta}).\end{aligned} \tag{16}$$

For the sake of brevity, we abbreviate the subscript $(\hat{\mathbf{J}}, \hat{\mathbf{R}}, \hat{\mathbf{b}})$ with $\boldsymbol{\chi}$ in the following. With the use of (15), the second order approximation of $\mathcal{F}$ on $T_{\boldsymbol{\chi}}\mathcal{M}$ is given by

$$\begin{aligned}m_{\boldsymbol{\chi}}(\boldsymbol{\xi},\boldsymbol{\eta},\boldsymbol{\zeta}) &= \mathcal{F}(\hat{\mathbf{J}},\hat{\mathbf{R}},\hat{\mathbf{b}})\\ &\quad+ \langle\mathrm{grad}\mathcal{F}(\hat{\mathbf{J}},\hat{\mathbf{R}},\hat{\mathbf{b}}),(\boldsymbol{\xi},\boldsymbol{\eta},\boldsymbol{\zeta})\rangle_{\boldsymbol{\chi}}\\ &\quad+ \frac{1}{2}\langle\mathrm{Hess}\mathcal{F}(\hat{\mathbf{J}},\hat{\mathbf{R}},\hat{\mathbf{b}})[\boldsymbol{\xi},\boldsymbol{\eta},\boldsymbol{\zeta}],(\boldsymbol{\xi},\boldsymbol{\eta},\boldsymbol{\zeta})\rangle_{\boldsymbol{\chi}},\end{aligned}$$

where $\mathrm{grad}\mathcal{F}(\hat{\mathbf{J}},\hat{\mathbf{R}},\hat{\mathbf{b}})$ denotes the Riemannian gradient and $\mathrm{Hess}\mathcal{F}(\hat{\mathbf{J}},\hat{\mathbf{R}},\hat{\mathbf{b}})$ the Riemannian Hessian.

In the proposed pole-residue framework, the Euclidean gradient has been formulated in vectorized form and we thus simply gain the derivatives in matrix form by reshaping (14). We obtain the Riemannian gradient of $\frac{\partial\mathcal{F}}{\partial\hat{\mathbf{J}}}$ by an orthogonal projection onto Skew_r using the projector $\mathrm{sk}(\mathbf{X}) = \frac{1}{2}(\mathbf{X}-\mathbf{X}^T)$. For Sym_r^+, we refer to the derivation in [26, Chapter III.C] and we denote the symmetric part of a matrix by $\mathrm{sym}(\mathbf{X}) = \frac{1}{2}(\mathbf{X}+\mathbf{X}^T)$. Using the matrix form of (14), we obtain the Riemannian gradient of $\mathcal{F}$

$$\mathrm{grad}\mathcal{F}(\hat{\mathbf{J}},\hat{\mathbf{R}},\hat{\mathbf{b}}) = \left[\mathrm{sk}\left(\frac{\partial\mathcal{F}}{\partial\hat{\mathbf{J}}}\right), \hat{\mathbf{R}}\mathrm{sym}\left(\frac{\partial\mathcal{F}}{\partial\hat{\mathbf{R}}}\right)\hat{\mathbf{R}}, \frac{\partial\mathcal{F}}{\partial\hat{\mathbf{b}}}\right].$$

This novel formulation of the Riemannian gradient of $\mathcal{F}$ for port-Hamiltonian systems may be used for various solvers such as trust-region or conjugate-gradient methods. See e.g. [27] for structure-preserving model reduction of port-Hamiltonian systems with a modified Fletcher-Reeves scheme. In the following, we describe and evaluate its

Algorithm 1 $\mathcal{H}_2$-Optimal RTR Method for PHS

Input: Initial iterate $(\hat{\mathbf{J}}_0, \hat{\mathbf{R}}_0, \hat{\mathbf{b}}_0) \in \mathcal{M}$
parameters $r \in [2, n), \bar{\Delta} > 0, \Delta_0 \in (0, \bar{\Delta}), \rho' \in [0, \frac{1}{4})$
Output: $\mathcal{H}_2$-optimal model $(\hat{\mathbf{J}}, \hat{\mathbf{R}}, \hat{\mathbf{b}})$

for $k = 0, 1, 2, \ldots$ **do**
  Solve trust-region subproblem as in [28]
    $\min_{(\boldsymbol{\xi},\boldsymbol{\eta},\boldsymbol{\zeta}) \in T_{\boldsymbol{\chi}_k}\mathcal{M}} m_{\boldsymbol{\chi}_k}(\boldsymbol{\xi}, \boldsymbol{\eta}, \boldsymbol{\zeta})$
    subject to $\|(\boldsymbol{\xi}, \boldsymbol{\eta}, \boldsymbol{\zeta})\|_{\boldsymbol{\chi}_k} \leq \Delta_k$
  Evaluate ρ_k as in (17);
  if $\rho_k < \frac{1}{4}$ **then**
    $\Delta_{k+1} = \frac{1}{4}\Delta_k$;
  else if $\rho_k > \frac{3}{4}$ **and** $\|(\boldsymbol{\xi}_k, \boldsymbol{\eta}_k, \boldsymbol{\zeta}_k)\|_{\boldsymbol{\chi}_k} = \Delta_k$ **then**
    $\Delta_{k+1} = \min(2\Delta_k, \bar{\Delta})$;
  else
    $\Delta_{k+1} = \Delta_k$;
  end if
  if $\rho_k > \rho'$ **then**
    $(\hat{\mathbf{J}}_{k+1}, \hat{\mathbf{R}}_{k+1}, \hat{\mathbf{b}}_{k+1}) = \mathrm{R}_{\boldsymbol{\chi}_k}(\boldsymbol{\xi}_k, \boldsymbol{\eta}_k, \boldsymbol{\zeta}_k)$
  else
    $(\hat{\mathbf{J}}_{k+1}, \hat{\mathbf{R}}_{k+1}, \hat{\mathbf{b}}_{k+1}) = (\hat{\mathbf{J}}_k, \hat{\mathbf{R}}_k, \hat{\mathbf{b}}_k)$
  end if
end for

performance in the trust-region framework which proved to be suitable for model reduction both in Euclidean space (see [17]) and on manifolds (see [13], [15]). However, it should be noted that the presented framework is not dependent on the optimization algorithm itself. For a comprehensive review on Riemannian optimization on matrix manifolds and implementation details, we refer to [22].

Riemannian trust-region (RTR) methods differ from trust-region methods in Euclidean space in the sense that the second-order approximation at a point $\boldsymbol{\chi}_k$ is performed in the tangent space $T_{\boldsymbol{\chi}_k}\mathcal{M}$ and mapped back onto the manifold via the retraction $R_{\boldsymbol{\chi}_k}$. The quality of the model in the k-th iteration is thus assessed with

$$\rho_k = \frac{\mathcal{F}(\hat{\mathbf{J}}_k, \hat{\mathbf{R}}_k, \hat{\mathbf{b}}_k) - \mathcal{F}(\mathrm{R}_{\boldsymbol{\chi}_k}(\boldsymbol{\xi}_k, \boldsymbol{\eta}_k, \boldsymbol{\zeta}_k))}{m_{\boldsymbol{\chi}_k}(\mathbf{0}, \mathbf{0}, \mathbf{0}) - m_{\boldsymbol{\chi}_k}(\boldsymbol{\xi}_k, \boldsymbol{\eta}_k, \boldsymbol{\zeta}_k)}. \tag{17}$$

Based on ρ_k, the new iterate $\mathrm{R}_{\boldsymbol{\chi}_k}(\boldsymbol{\xi}_k, \boldsymbol{\eta}_k, \boldsymbol{\zeta}_k)$ is accepted and the trust-region radius is updated.

In the pole-residue framework, the computation of the Riemannian Hessian is quite cumbersome. Fortunately, in order to minimize the local model $m_{\boldsymbol{\chi}_k}$, the Hessian is not necessarily required. In fact, global convergence can be guaranteed under weak assumptions if $\mathrm{Hess}\mathcal{F}(\hat{\mathbf{J}}, \hat{\mathbf{R}}, \hat{\mathbf{b}})[\boldsymbol{\xi}, \boldsymbol{\eta}, \boldsymbol{\zeta}]$ is replaced by a uniformly bounded, symmetric linear operator H_k [22]. In [28], a nonlinear finite-difference approximation H_k^{FD} of the Riemannian Hessian was proposed that is relatively cheap to compute as it only requires another gradient evaluation. The author showed that global convergence can be retained using H_k^{FD} as an approximation of the Hessian if the truncated conjugate-gradient method to minimize $m_{\boldsymbol{\chi}_k}$ is slightly modified. Using this approximation, we obtain Algorithm 1.

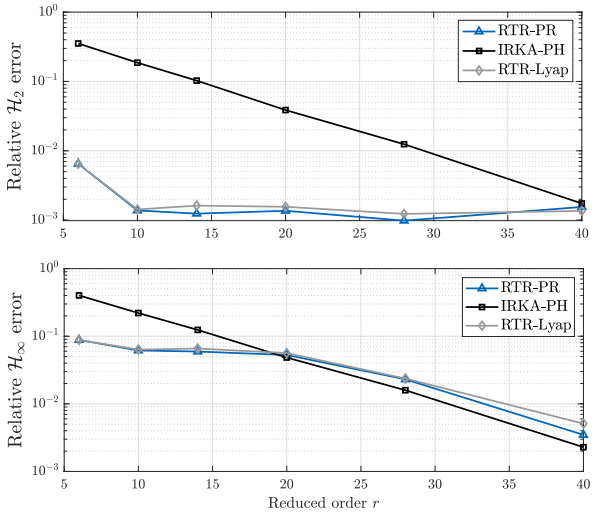

Fig. 1: Relative $\mathcal{H}_2$- and $\mathcal{H}_\infty$-error norms for different reduced orders ($n = 500$)

V. NUMERICAL EXPERIMENTS

In this section, we illustrate the performance of the proposed approach for a medium- and large-scale port-Hamiltonian system. As a full-order model we use the coupling of $\frac{n}{2}$ mass-spring-damper elements. Each subsystem consists of a spring k_i, damper c_i, mass m_i and is described by two state variables, the displacement and momentum of the mass m_i. Thus, the system has n state variables in total. System input u is the external force applied to the first mass and output y is the velocity of the first mass, so $\mathbf{b} = \mathbf{e}_2$ and $\mathbf{b}^T\mathbf{Q} = \frac{1}{m_1}\mathbf{e}_2^T$. The interconnection matrix $\mathbf{J} = \mathrm{diag}(\mathbf{J}_i)$, dissipation matrix $\mathbf{R} = \mathrm{diag}(\mathbf{R}_i)$, and energy matrix $\mathbf{Q}$ all have block diagonal structure with

$$\mathbf{J}_i = \begin{bmatrix} 0 & 1 \\ -1 & 0 \end{bmatrix}, \quad \mathbf{R}_i = \begin{bmatrix} 0 & 0 \\ 0 & c_i \end{bmatrix}, \quad i = 1, \ldots, \frac{n}{2}.$$

The $(2i-1:2i+1), (2i-1:2i+1)$-th elements of $\mathbf{Q}$ are given by the block

$$\mathbf{Q}_i = \begin{bmatrix} k_{i-1} + k_i & 0 & -k_i \\ 0 & \frac{1}{m_i} & 0 \\ -k_i & 0 & k_i + k_{i+1} \end{bmatrix}, \quad i = 1, \ldots, \frac{n}{2} - 1,$$

where $k_0 = 0$ and also $Q_{n,n} = 1/m_{n/2}$ holds. We use the same parameters as in [6] and [15] in order to compare our results to the approaches presented in those papers. Additionally, we transform the system with state-space transformation $\mathbf{x} = \mathbf{L}^T\tilde{\mathbf{x}}$ in order to obtain $\mathbf{Q} = \mathbf{I}_n$ as this is required for the Algorithm proposed in [15].

There are several options to compute an initial iterate $(\hat{\mathbf{J}}_0, \hat{\mathbf{R}}_0, \hat{\mathbf{b}}_0)$ for Algorithm 1. One might for example create a reduced model of (1) with a Krylov subspace method choosing $\mathbf{V} \in \mathbb{R}^{n \times r}$ as an input Krylov subspace and $\mathbf{W} = \mathbf{Q}\mathbf{V}(\mathbf{V}^T\mathbf{Q}\mathbf{V})^{-1}$ (see [6]). The projection matrix $\mathbf{V}$

TABLE I: Gradient norms $\|\mathrm{grad}\mathcal{F}(\hat{\mathbf{J}}, \hat{\mathbf{R}}, \hat{\mathbf{b}})\|$

r	6	20	40
IRKA-PH	5.9×10^{-3}	1.9×10^{-4}	6.0×10^{-7}
RTR-PR	1.7×10^{-8}	2.5×10^{-6}	2.8×10^{-6}
RTR-Lyap	4.2×10^{-7}	1.2×10^{-6}	4.1×10^{-6}

can be generated for instance by placing the interpolation points logarithmically over a certain frequency range. In the following, we use IRKA-PH to initialize our algorithm with a stopping criterion of 10^{-3} in the norm of the relative change of interpolation points. It is anticipated that the choice of the initial iterate has a significant impact on convergence speed and a thorough analysis is part of future work. For the implementation, we used the MATLAB toolbox Manopt [29] for optimization on matrix manifolds.

A. *Mass-Spring-Damper Model with* $n = 500$

First, we consider a mass-spring-damper model with 250 subsystems and 500 state variables respectively. We compare the Riemannian trust-region method in our new pole-residue framework (RTR-PR) with the IRKA-PH algorithm of [6] and the Riemannian trust-region method in the Lyapunov framework (RTR-Lyap) proposed in [15].

Fig. 1 shows the relative $\mathcal{H}_2$- and $\mathcal{H}_\infty$-error norms for each of these three algorithms and different reduced orders. With respect to the $\mathcal{H}_2$-norm, our algorithm has a similar performance as the Lyapunov-based approach RTR-Lyap. This illustrates that the computation of the Euclidean gradient in the pole-residue framework leads to comparable results if the optimization parameters and the Riemannian metric and retraction are chosen equally. Compared to IRKA-PH, the theoretical considerations of Remark 2 are especially supported for small reduced orders r. Here, the Riemannian optimization methods perform significantly better than IRKA-PH because, for non-symmetric systems, Galerkin-based methods only fulfill half of the first-order conditions for local $\mathcal{H}_2$-optimality. This is substantiated by the selected gradient norms given in Table I. In this example, IRKA-PH only manages to find local $\mathcal{H}_2$-optima for large reduced orders. In the $\mathcal{H}_\infty$-norm, the Riemannian methods perform significantly better for small reduced orders as well and decrease similar to IRKA-PH for $r > 20$.

The strengths of the proposed algorithm for small reduced orders also hold from a computational viewpoint. The major additional cost compared to IRKA-PH are the computation of the pseudo inverse in (12) and the triangular solves of (6b) for each reduced-order pole $\hat{\lambda}_j$. So in the case of large reduced orders r, the additional computational cost per iteration compared to IRKA-PH has a significant impact and IRKA-PH may be the choice to go with. However, this clearly also depends on the convergence speed of the selected optimization algorithm. Fig. 2 illustrates the evolution of the relative $\mathcal{H}_2$-error and norm of the Riemannian gradient both for IRKA-PH and Algorithm 1 ($r = 6$). To sum up, in the case of small reduced orders, our approach can significantly improve the performance of IRKA-PH in the $\mathcal{H}_2$-norm with relatively low computational cost.

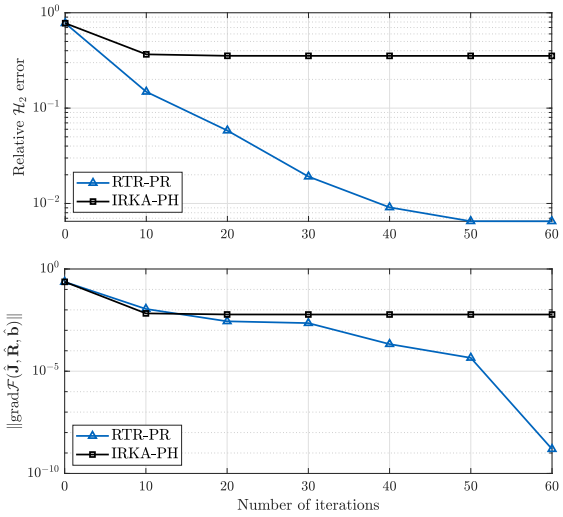

Fig. 2: Evolution of the relative $\mathcal{H}_2$-error and gradient norm ($r = 6, n = 500$)

B. *Mass-Spring-Damper Model with* $n = 10000$

To illustrate that the proposed framework is also suitable for the efficient reduction of large-scale systems, we consider a mass-spring-damper model of order $n = 10000$. For a reduced order of $r = 20$, the amplitude plot of the error system $G_e(j\omega) = G(j\omega) - \hat{G}(j\omega)$ is depicted in Fig. 3. Compared to IRKA-PH, the RTR-PR model approximates the original system significantly better over large parts of the frequency range. In order to evaluate the computational cost of the proposed framework, we computed the cost functional $\mathcal{F}$ and the Riemannian gradient $\mathrm{grad}\mathcal{F}(\hat{\mathbf{J}}, \hat{\mathbf{R}}, \hat{\mathbf{b}})$ for 100 randomly created reduced-order models with order $r = 20$ on $\mathcal{M}$. On an Intel Core i7-8700 (3.2 GHz, 6-Core) CPU, both computations combined took less than two seconds on average. While the performance optimization of our current implementation is ongoing, this clearly demonstrates the potential of the proposed framework for even larger systems.

VI. CONCLUDING REMARKS

We have presented a novel approach to $\mathcal{H}_2$-optimal model reduction of port-Hamiltonian systems. Compared to existing methods on Riemannian manifolds, the approach does not require pre-processing of the original model or iterative solves of coupled Lyapunov equations and proved to be applicable for large-scale SISO systems as well. With respect to the computational effort and compared to state-of-the-art algorithms, the method is particularly powerful for small reduced orders r. Future work will involve the derivation of the Riemannian gradient in the pole-residue framework for MIMO systems and a comprehensive study of different Riemannian optimization algorithms within this framework.

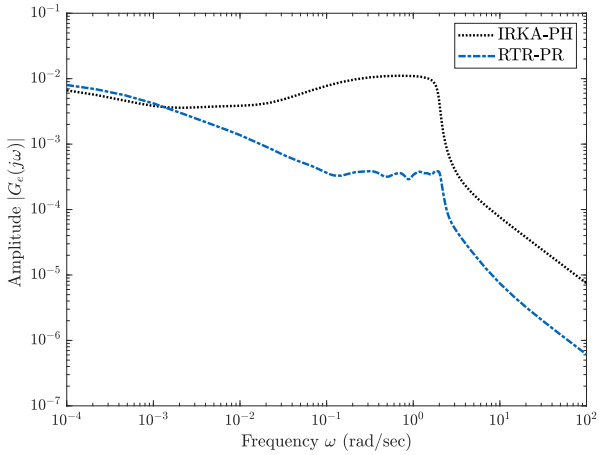

Fig. 3: Amplitude plot of error system $G_e(j\omega)$ $(r = 20, n = 10000)$

VII. ACKNOWLEDGEMENTS

We would like to thank Tatjana Stykel, Maria Cruz Varona and Paul Kotyczka for valuable discussions on the topic and for the thorough revision of the manuscript.

REFERENCES

[1] V. Duindam, A. Macchelli, S. Stramigioli, and H. Bruyninckx, *Modeling and Control of Complex Physical Systems*. Springer Berlin Heidelberg, 2009.

[2] R. Ortega, A. J. Van Der Schaft, I. Mareels, and B. Maschke, "Putting energy back in control," *IEEE Control Systems Magazine*, vol. 21, no. 2, pp. 18–33, 2001.

[3] P. Kotyczka, *Numerical Methods for Distributed Parameter Port-Hamiltonian Systems*. TUM.University Press, 2019, Habilitation.

[4] R. V. Polyuga and A. J. van der Schaft, "Effort- and flow-constraint reduction methods for structure preserving model reduction of port-Hamiltonian systems," *Systems & Control Letters*, vol. 61, no. 3, pp. 412–421, 2012.

[5] T. Wolf, B. Lohmann, R. Eid, and P. Kotyczka, "Passivity and structure preserving order reduction of linear port-Hamiltonian systems using Krylov subspaces," *European Journal of Control*, vol. 16, no. 4, pp. 401–406, 2010.

[6] S. Gugercin, R. V. Polyuga, C. Beattie, and A. van der Schaft, "Structure-preserving tangential interpolation for model reduction of port-Hamiltonian systems," *Automatica*, vol. 48, no. 9, pp. 1963–1974, 2012.

[7] D. Wilson, "Optimum solution of model-reduction problem," *Proceedings of the Institution of Electrical Engineers*, vol. 117, no. 6, pp. 1161–1165, 1970.

[8] D. Hyland and D. Bernstein, "The optimal projection equations for model reduction and the relationships among the methods of Wilson, Skelton, and Moore," *IEEE Transactions on Automatic Control*, vol. 30, no. 12, pp. 1201–1211, 1985.

[9] L. Meier and D. Luenberger, "Approximation of linear constant systems," *IEEE Transactions on Automatic Control*, vol. 12, no. 5, pp. 585–588, 1967.

[10] S. Gugercin, A. C. Antoulas, and C. Beattie, "$\mathcal{H}_2$ model reduction for large-scale linear dynamical systems," *SIAM Journal on Matrix Analysis and Applications*, vol. 30, no. 2, pp. 609–638, 2008.

[11] J. Spanos, M. Milman, and D. Mingori, "A new algorithm for L_2 optimal model reduction," *Automatica*, vol. 28, no. 5, pp. 897–909, 1992.

[12] W.-Y. Yan and J. Lam, "An approximate approach to $\mathcal{H}_2$ optimal model reduction," *IEEE Transactions on Automatic Control*, vol. 44, no. 7, pp. 1341–1358, 1999.

[13] H. Sato and K. Sato, "Riemannian trust-region methods for $\mathcal{H}_2$ optimal model reduction," in *2015 54th IEEE Conference on Decision and Control (CDC)*, IEEE, 2015.

[14] V. Simoncini, "Computational methods for linear matrix equations," *SIAM Review*, vol. 58, no. 3, pp. 377–441, 2016.

[15] K. Sato, "Riemannian optimal model reduction of linear port-Hamiltonian systems," *Automatica*, vol. 93, pp. 428–434, 2018.

[16] C. A. Beattie and S. Gugercin, "Krylov-based minimization for optimal $\mathcal{H}_2$ model reduction," in *2007 46th IEEE Conference on Decision and Control (CDC)*, IEEE, 2007.

[17] ——, "A trust region method for optimal $\mathcal{H}_2$ model reduction," in *Proceedings of the 48h IEEE Conference on Decision and Control (CDC) held jointly with 2009 28th Chinese Control Conference*, IEEE, 2009.

[18] G. Flagg, C. Beattie, and S. Gugercin, "Convergence of the iterative rational Krylov algorithm," *Systems & Control Letters*, vol. 61, no. 6, pp. 688–691, 2012.

[19] W. Krajewski, A. Lepschy, M. Redivo-Zaglia, and U. Viaro, "A program for solving the L_2 reduced-order model problem with fixed denominator degree," *Numerical Algorithms*, vol. 9, no. 2, pp. 355–377, 1995.

[20] R. V. Polyuga and A. van der Schaft, "Structure preserving model reduction of port-Hamiltonian systems by moment matching at infinity," *Automatica*, vol. 46, no. 4, pp. 665–672, 2010.

[21] J. R. Magnus and H. Neudecker, *Matrix Differential Calculus with Applications in Statistics and Econometrics (Wiley Series in Probability and Statistics: Texts and References Section)*. Wiley, 1999.

[22] P. A. Absil, R. Mahony, and R. Sepulchre, *Optimization Algorithms on Matrix Manifolds*. Princeton University Press, 2007.

[23] S. Lang, *Fundamentals of Differential Geometry*. Springer New York, 1999.

[24] R. Bhatia, *Positive Definite Matrices*. Princeton University Press, 2015.

[25] B. Jeuris, R. Vandebril, and B. Vandereycken, "A survey and comparison of contemporary algorithms for computing the matrix geometric mean," *Electronic Transactions on Numerical Analysis*, vol. 39, pp. 379–402, 2012.

[26] K. Sato and H. Sato, "Structure-preserving $\mathcal{H}_2$ optimal model reduction based on the Riemannian trust-region method," *IEEE Transactions on Automatic Control*, vol. 63, no. 2, pp. 505–512, 2018.

[27] Y.-L. Jiang and K.-L. Xu, "Model order reduction of port-Hamiltonian systems by Riemannian modified Fletcher–Reeves scheme," *IEEE Transactions on Circuits and Systems II: Express Briefs*, vol. 66, no. 11, pp. 1825–1829, 2019.

[28] N. Boumal, "Riemannian trust regions with finite-difference Hessian approximations are globally convergent," in *Lecture Notes in Computer Science*, Springer International Publishing, 2015, pp. 467–475.

[29] N. Boumal, B. Mishra, P.-A. Absil, and R. Sepulchre, "Manopt, a Matlab toolbox for optimization on manifolds," *Journal of Machine Learning Research*, vol. 15, pp. 1455–1459, 2014.

A.4 A Rosenbrock Framework for Tangential Interpolation of Port-Hamiltonian Descriptor Systems

Summary: Existing strategies for interpolatory MOR of linear, time-invariant pH-DAE models vary depending on the original model's Kronecker index and how algebraic constraints are affected by the input. In their entirety, these strategies do not cover the whole system class of pH-DAEs and some may not necessarily preserve the pH structure. In this article, we investigate whether there is an interpolatory MOR framework that allows to treat algebraic equations in a unifying way, irrespective of the original model's Kronecker index. We first show that the Rosenbrock system matrix exhibits a particular structure for pH-DAE models that can be employed for this purpose. From this, we derive a novel interpolatory MOR framework that can be used for pH-DAEs in staircase form, which often occur in modeling practice. It covers models with arbitrary Kronecker index, guarantees ROMs in pH-DAE form with minimal state-space dimension, and works with the original (typically sparse) state-space matrices. We then illustrate how existing $\mathcal{H}_2$- and $\mathcal{H}_\infty$-inspired shift selection strategies can be embedded in this framework. Our numerical examples demonstrate the application of our method in electrical circuit simulation, where pH-DAE models occur naturally.

CRediT author statement:

Tim Moser:	Conceptualization, Data Curation, Investigation, Methodology, Software, Visualization, Writing - Original Draft
Boris Lohmann:	Conceptualization, Funding Acquisition, Supervision, Writing - Review & Editing

MATHEMATICAL AND COMPUTER MODELLING OF DYNAMICAL SYSTEMS
2023, VOL. 29, NO. 01, 210–235
https://doi.org/10.1080/13873954.2023.2209798

Taylor & Francis
Taylor & Francis Group

A Rosenbrock framework for tangential interpolation of port-Hamiltonian descriptor systems

Tim Moser and Boris Lohmann

Department of Engineering Physics and Computation, TUM School of Engineering and Design, Technical University of Munich, Garching, Germany

ABSTRACT

We present a new structure-preserving model order reduction (MOR) framework for large-scale port-Hamiltonian descriptor systems (pH-DAEs). Our method exploits the structural properties of the Rosenbrock system matrix for this system class and utilizes condensed forms which often arise in applications and reveal the solution behaviour of a system. Provided that the original system has such a form, our method produces reduced-order models (ROMs) of minimal dimension, which tangentially interpolate the original model's transfer function and are guaranteed to be again in pH-DAE form. This allows the ROM to be safely coupled with other dynamical systems when modelling large system networks, which is useful, for instance, in electric circuit simulation.

ARTICLE HISTORY
Received 1 November 2022
Accepted 25 April 2023

KEYWORDS
Port-Hamiltonian systems; differential-algebraic systems; structure-preserving model reduction

1. Introduction

The port-Hamiltonian (pH) modelling paradigm provides an energy-based framework for constructing high-fidelity models of complex dynamical systems. The separation between constitutive relations and the interconnection structure enables a modular modelling approach, in which different subsystems are modelled independently and then interconnected via power flows while preserving important physical properties [1]. This flexibility is particularly advantageous when considering interactions between subsystems across different physical domains or time scales [2]. Furthermore, network laws that govern these interactions, such as Kirchhoff's laws in electrical circuits or position and velocity constraints in mechanical systems, may be incorporated via algebraic constraints, leading to pH differential-algebraic equation systems (pH-DAEs) [3]. PH-DAE systems often naturally emerge in modelling practice, e.g. when modelling electric circuits, incompressible fluid flow, multibody dynamics or pressure waves in gas networks (see [3,26] and the references therein).

If the system at hand increases in complexity, generally, the state-space dimension of its associated pH-DAE model does so too, which makes the simulation and design of

CONTACT Tim Moser tim.moser@tum.de Department of Engineering Physics and Computation, TUM School of Engineering and Design, Technical University of Munich, Boltzmannstr. 15, Garching 85748, Germany

model-based controllers computationally challenging. Model order reduction (MOR) may be applied to approximate large-scale full-order models (FOMs) with reduced-order models (ROMs) of substantially smaller dimension to decrease the computational costs. However, this comes with two major challenges. On the one hand, the impacts of the algebraic equations on the model dynamics have to be reflected in the ROM as well, but without significantly increasing the reduced state-space dimension. On the other hand, to facilitate the subsequent coupling of the ROM with other subsystems, the MOR method should be *structure-preserving*, meaning that the ROM is again a pH-DAE.

Structure-preserving MOR methods for pH-DAEs fall into three major categories: pH-preserving MOR methods, passivity-preserving MOR methods and passivity enforcement techniques. For an overview of existing approaches, the interested reader is referred to [5]. In this work, we focus on *pH-preserving, interpolatory* MOR techniques which are particularly suited for the reduction of very large-scale models due to their computational efficiency. While these methods are well-established for various system classes, including general DAE systems (see [6] for a comprehensive overview), this is still only partially the case for pH-DAEs. Tangential interpolation of pH ordinary differential equation systems (pH-ODEs) with no algebraic constraints has been addressed in [8–10,11,22] and is well understood. Extensions to the DAE case with algebraic constraints have been proposed in [12,13]. The strategies to deal with algebraic constraints vary depending on the original model's Kronecker index and how the algebraic constraints are affected by the input. However, in their entirety, these strategies do not cover the whole system class of pH-DAEs and some may not necessarily preserve the pH structure. This motivates the following research question which we address in this work: Is there a *unifying* interpolatory MOR framework that is applicable to the entire system class of linear, time-invariant pH-DAEs and guarantees a preservation of the pH structure?

A good starting point to answer this question is the staircase forms presented in [13,14]. While staircase forms are generally helpful in analysing the solution behaviour of DAEs, they are also useful for MOR since they allow the impact of algebraic constraints on the system dynamics to be analysed. In general, the transformation of a pH-DAE model to staircase form relies on a series of rank conditions which may be sensitive under perturbations; see e.g [15]. Fortunately, as demonstrated in [3,26] for various physical examples, this can be considered directly in the modelling process such that the resulting model already has (or is close to) staircase form. Since DAEs often include redundant algebraic equations which increase the computational cost for simulation, the task of MOR is to identify a minimal set of equations that describes the dynamical behaviour of the system. In 1970, Rosenbrock [16] proposed to represent dynamical systems with a polynomial matrix, which is beneficial to compute minimal representations and nowadays known as the *Rosenbrock system matrix*. Interestingly enough, this matrix has not extensively been used in the context of MOR.

In this work, we show that the Rosenbrock system matrix exhibits a particular structure for pH-DAEs which we exploit to derive a novel interpolatory MOR framework that

(i) can be used for linear, time-invariant pH-DAEs in staircase form with arbitrary Kronecker index,

(ii) guarantees ROMs in pH-DAE form with a minimal state-space dimension,

(iii) works with the original (typically sparse) state-space matrices and is therefore computationally efficient, and

(iv) enables a straightforward adaptation and integration of different interpolatory MOR strategies that have been developed for general dynamical systems.

The paper is organized as follows. In Section 2, we use the concept of the Rosenbrock system matrix to introduce the system class of pH-DAEs and its staircase forms and recapitulate the basics of tangential interpolation. In Section 3, we propose a new interpolatory MOR framework that exploits the structural properties of pH-DAEs in staircase form and show how this framework naturally generalizes to several extensions proposed for unstructured systems in Section 4. We conclude with an application of our method to two electric circuits and a discussion of the above claims in Sections 5 and 6.

2. Preliminaries

We consider linear time-invariant (LTI) systems of the form

$$\begin{aligned} E\dot{x}(t) &= Ax(t) + Bu(t), \quad x(0) = 0, \\ y(t) &= Cx(t) + Du(t), \end{aligned} \tag{1}$$

with state vector $x(t) \in \mathbb{R}^n$, inputs $u(t) \in \mathbb{R}^m$, outputs $y(t) \in \mathbb{R}^m$ for all $t \in [0, \infty)$ and constant matrices $E, A \in \mathbb{R}^{n\times n}$, $B \in \mathbb{R}^{n\times m}$, $C \in \mathbb{R}^{m\times n}$ and $D \in \mathbb{R}^{m\times m}$. Systems with a singular descriptor matrix E are referred to as DAE systems, and ODE systems otherwise. In the following, we will assume that the pencil $\lambda E - A$ is *regular*, i.e. $\det(\lambda E - A) \neq 0$ for some $\lambda \in \mathbb{C}$. We denote the ring of polynomials with coefficients in $\mathbb{R}$ by $\mathbb{R}[s]$ and the set of $n \times m$ matrices with entries in $\mathbb{R}[s]$ by $\mathbb{R}[s]^{n\times m}$.

2.1. The Rosenbrock system matrix

After a Laplace transformation of the state-space equations in (1), we obtain the following equations in matrix form:

$$\mathcal{P}(s)\begin{bmatrix} \xi(s) \\ \mu(s) \end{bmatrix} = \begin{bmatrix} 0 \\ \psi(s) \end{bmatrix}, \quad \text{where } \mathcal{P}(s) := \begin{bmatrix} sE - A & -B \\ C & D \end{bmatrix} \in \mathbb{R}[s]^{(n+m)\times(n+m)}. \tag{2}$$

where ξ, μ and ψ denote the Laplace transforms of the state, input and output vector, respectively. The polynomial matrix $\mathcal{P}$ is also called the *Rosenbrock system matrix* (in the following: system matrix) [17]. Assuming regularity, the linear mapping between inputs μ and outputs ψ that follows from (2) is given by the system's transfer function

$$H(s) := C(sE - A)^{-1}B + D. \tag{3}$$

Since all transformations of the state-space equations in (1) can be expressed by operations on $\mathcal{P}$, the system matrix proved to be particularly useful for studying the properties of these transformations [16]. In this work, we shall focus on transformations

which leave the system's transfer function H unchanged and are summarized by the notion of *strict system equivalence*.

Lemma 2.1. [16] *Let $X(s) \in \mathbb{R}[s]^{m\times n}$, $Y(s) \in \mathbb{R}[s]^{n\times m}$ and define unimodular matrices $L(s), M(s) \in \mathbb{R}[s]^{n\times n}$, i.e. their determinants are nonzero constants. Suppose that two system matrices $\mathcal{P}$ and $\widetilde{\mathcal{P}}$ are related by the transformation*

$$\widetilde{\mathcal{P}}(s) = \mathcal{T}_1(s)\mathcal{P}(s)\mathcal{T}_2(s) = \begin{bmatrix} L(s) & 0 \\ X(s) & I_m \end{bmatrix} \mathcal{P}(s) \begin{bmatrix} M(s) & Y(s) \\ 0 & I_m \end{bmatrix}. \tag{4}$$

Then we shall say that $\mathcal{P}$ and $\widetilde{\mathcal{P}}$ are related by strict system equivalence (s.s.e.). The two system matrices give rise to the same transfer function, i.e. $H(s) = \widetilde{H}(s)$ for all $s \in \mathbb{C}$.

Proof. For a proof, we refer the reader to [16, Section 3.1].

The benefits of representing a dynamical system with its system matrix are by no means restricted to system transformations; it may also be useful in the context of model reduction.

2.2. Interpolatory model reduction

The goal of MOR is to find a reduced-order model

$$\begin{aligned} E_r\dot{x}_r(t) &= A_r x_r(t) + B_r u(t), \quad x_r(0) = 0, \\ y_r(t) &= C_r x_r(t) + D_r u(t), \end{aligned} \tag{5}$$

with reduced state vector $x_r(t) \in \mathbb{R}^r$ and an associated transfer function H_r such that $r \ll n$ and $y \approx y_r$ for certain u. In projection-based MOR, these models are created by means of Petrov-Galerkin projections. Here, we define two matrices U, $V \in \mathbb{R}^{n\times r}$ with full column rank. The original state trajectory $x(t)$ is approximated on the column space of V, i.e. $x(t) \approx Vx_r(t)$ for all $t \in [0, \infty)$. The reduced system matrix is obtained by the following operation on the original system matrix $\mathcal{P}$:

$$\mathcal{P}_r(s) = \begin{bmatrix} U^\top & 0 \\ 0 & I_m \end{bmatrix} \mathcal{P} \begin{bmatrix} V & 0 \\ 0 & I_m \end{bmatrix} = \begin{bmatrix} sU^\top EV - U^\top AV & -U^\top B \\ CV & D \end{bmatrix} = \begin{bmatrix} sE_r - A_r & -B_r \\ C_r & D_r \end{bmatrix}. \tag{6}$$

The matrices U, V may be chosen for different purposes, for example, to enforce the preservation of certain system-theoretic or structural properties of the original model. In interpolatory MOR methods, they are used to enforce interpolation conditions between the original and reduced transfer function. In particular, the column space of V may be chosen such that the reduced transfer function H_r tangentially interpolates the original transfer function H at a set of interpolation points or *shifts* $\{\sigma_1, \ldots, \sigma_r\} \in \mathbb{C}$:

$$H(\sigma_i)b_i = H_r(\sigma_i)b_i, \qquad i = 1, \ldots, r, \tag{7}$$

where $b_i \in \mathbb{C}^m$ denotes the associated (right) tangential direction. For the sake of simplicity, we assume throughout this work that each shift is distinct while an extension to multiple shifts is straightforward, and we refer the interested reader to [6] for details.

In all cases, we require $\sigma_i E - A$ as well as $\sigma_i E_r - A_r$ to be nonsingular for all $i = 1, \ldots, r$, and that the sets of shifts and associated tangential directions are both closed under complex conjugation. Then, the interpolation conditions in (7) may be enforced by choosing

$$(\sigma_i E - A)^{-1} B b_i \in \mathit{range}(V), \qquad i = 1, \ldots, r, \tag{8}$$

where $\mathit{range}(V)$ denotes the associated column space of V. Similarly, U may be used to enforce additional (left) tangential interpolation conditions (see [6] for details). The approximation quality of a ROM is typically assessed by computing the $\mathcal{H}_\infty$ or $\mathcal{H}_2$ norm of the error function $H - H_r$. These are defined in the Hardy spaces $\mathcal{RH}_\infty^{m\times m}$ ($\mathcal{RH}_2^{m\times m}$) of all proper (strictly proper) real-rational $m \times m$ matrices without poles in the closed complex right half-plane (see, e. g., [18] for details).

Remark 1. Note that while the conditions in (8) hold regardless of whether E has full rank or not, as long as $\sigma_i E - A$ and $\sigma_i E_r - A_r$ are nonsingular for all $i = 1, \ldots, r$, the interpolation of DAE systems poses additional challenges. Unlike in the ODE case, where $H - H_r$ is guaranteed to be strictly proper since $\lim_{s\to\infty} H(s) - H_r(s) = D - D_r = 0$, this is not necessarily the case for DAE systems. In fact, as we will also see in Section 3, the algebraic constraints may even lead to improper transfer functions with $\lim_{s\to\infty} H(s) = \infty$. It is, therefore, crucial to analyse the impact of the algebraic constraints on H because otherwise, $H - H_r$ may grow unboundedly large for $s \to \infty$, and the error norms are no longer defined. For an overview of how to deal with this challenge for general LTI systems, the reader is referred to [6, Chapter 9].

2.3. Port-Hamiltonian descriptor systems

The system class of linear port-Hamiltonian descriptor systems with quadratic Hamiltonian was introduced in [19]. In this work, we focus on the subclass of constant-coefficient pH-DAEs, which can be characterized by a special structure of the associated system matrix.

Definition 2.2. Consider a regular LTI system of the form

$$\Sigma \; : \begin{cases} E\dot{x}(t) = (J - R)x(t) + (G - P)u(t), & x(0) = 0, \\ y(t) \;\; = (G + P)^\top x(t) + (S + N)u(t), \end{cases} \tag{9}$$

where $E, J, R \in \mathbb{R}^{n\times n}$, $G, P \in \mathbb{R}^{n\times m}$, $S, N \in \mathbb{R}^{m\times m}$. We call the system a pH-DAE system if its system matrix may be decomposed into the following sum of symmetric and skew-symmetric parts

$$\mathcal{P}(s) = s \underbrace{\begin{bmatrix} E & 0 \\ 0 & 0 \end{bmatrix}}_{=:\mathcal{E}} + \underbrace{\begin{bmatrix} -J & -G \\ G^\top & N \end{bmatrix}}_{=:\Gamma} + \underbrace{\begin{bmatrix} R & P \\ P^\top & S \end{bmatrix}}_{=:W}, \tag{10}$$

such that

(i) the *structure matrix* Γ is skew-symmetric, i.e. $\Gamma = -\Gamma^\top$,
(ii) the *dissipation matrix* W is symmetric positive semi-definite, i.e. $W = W^\top \geq 0$,

(iii) the *extended descriptor matrix* $\mathcal{E}$ is symmetric positive semi-definite, i.e. $\mathcal{E} = \mathcal{E}^\top \geq 0$.

The system has an associated quadratic Hamiltonian $\mathcal{H}(x) = \frac{1}{2}x^\top Ex$ and transfer function

$$H(s) := (G+P)^\top (sE-(J-R))^{-1}(G-P) + S + N.$$

Note that the definition proposed in [19] appears to be more general since it also allows the representation of systems governed by a quadratic Hamiltonian of the form $\mathcal{H}(x) = \frac{1}{2}x^\top Q^\top Ex$ with $Q \in \mathbb{R}^{n\times n}$ and $Q^\top E = E^\top Q \geq 0$. However, our definition does not impose any additional restrictions since it has been shown, e.g. in [3] that every pH-DAE, as defined in [19], may be reformulated to have the form in (9).

Moreover, it was shown in [13,14] that every pH-DAE may be transformed into *staircase form*. While the physical interpretation of the states is generally lost during this transformation, staircase forms are useful to study the solution behaviour of pH-DAEs [3] and, as we will show in Section 3, also simplify model reduction. We refer to [14, Algorithm 5] for details on how to perform this transformation. Before we proceed, let us highlight that it may require several subsequent full rank decompositions, which are sensitive to perturbations. Fortunately, due to the structural properties of the system matrix, the number of required decompositions is limited to three in contrast to general (unstructured) DAE systems. Moreover, if this condensed form is directly considered during modelling, fewer steps are required, as discussed in [3,26]. In some practical cases, for example, in the modelling of electric circuits, the staircase form even naturally arises or can be enforced by simple structure-preserving permutations of the system equations, as illustrated in Section 5.

Lemma 2.3. [13,14] *A regular pH-DAE system is in staircase form if it has a partitioned state vector* $x(t) = \left[x_1(t)^\top, x_2(t)^\top, x_3(t)^\top, x_4(t)^\top\right]^\top$, *where* $x_j(t) \in \mathbb{R}^{n_j}, n_j \in \mathbb{N}_0$ *for all* $j = 1,\ldots,4$ *such that*

$$E := \begin{bmatrix} E_{11} & 0 & 0 & 0 \\ 0 & E_{22} & 0 & 0 \\ 0 & 0 & 0 & 0 \\ 0 & 0 & 0 & 0 \end{bmatrix}, \quad J := \begin{bmatrix} J_{11} & J_{12} & J_{13} & J_{14} \\ J_{21} & J_{22} & J_{23} & 0 \\ J_{31} & J_{32} & J_{33} & 0 \\ J_{41} & 0 & 0 & 0 \end{bmatrix}, \tag{11}$$

$$G := \begin{bmatrix} G_1 \\ G_2 \\ G_3 \\ G_4 \end{bmatrix}, P := \begin{bmatrix} P_1 \\ P_2 \\ P_3 \\ 0 \end{bmatrix}, \quad R := \begin{bmatrix} R_{11} & R_{12} & R_{13} & 0 \\ R_{21} & R_{22} & R_{23} & 0 \\ R_{31} & R_{32} & R_{33} & 0 \\ 0 & 0 & 0 & 0 \end{bmatrix}, \tag{12}$$

where E_{11}, E_{22} *are positive definite, and the matrices* J_{41} *and* $J_{33} - R_{33}$ *are invertible (if the blocks are nonempty). The Kronecker index* ν *of the uncontrolled system satisfies*

$$\nu = \begin{cases} 0 & \text{if and only if } n_1 = n_4 = 0 \text{ and } n_3 = 0, \\ 1 & \text{if and only if } n_1 = n_4 = 0 \text{ and } n_3 > 0, \\ 2 & \text{if and only if } n_1 = n_4 > 0. \end{cases}$$

As initially stated, it is beneficial to preserve the structural properties of the original pH-DAE model during MOR. Structure-preserving MOR methods, therefore, search for a reduced pH-DAE

$$\Sigma_r : \begin{cases} E_r\dot{x}_r(t) = (J_r - R_r)x_r(t) + (G_r - P_r)u(t), \\ y_r(t) = (G_r + P_r)^\top x_r(t) + (S_r + N_r)u(t), \end{cases} \tag{13}$$

with $x_r(t) \in \mathbb{R}^r$, $r \ll n$ that fulfils the pH structural constraints, i.e. the associated system matrix may be decomposed as in Definition 2.2 such that

$$\mathcal{P}_r(s) = s\mathcal{E}_r + \Gamma_r + W_r, \tag{14}$$

with symmetric positive semi-definite $\mathcal{E}_r, W_r$ and skew-symmetric Γ_r. Note that the system matrix has also recently been used to derive a symplectic MOR method for LTI pH-ODEs without feedthrough in [20].

3. Our approach

In the following, we demonstrate how the concepts of the presented staircase form and the system matrix may be unified to derive a framework for tangential interpolation of pH-DAEs with an arbitrary Kronecker index. For this, we proceed in three steps. First, we apply a transformation under s.s.e. to the original system matrix $\mathcal{P}$ that enables us to decompose the original transfer function into proper parts and improper parts that may originate from algebraic constraints. Since all improper parts have to be preserved in the ROM exactly to keep the error $H - H_r$ bounded (see Remark 1), we propose a new method to efficiently reduce *only* the proper part in the second step. Third, we show how to reattach the original improper part to the reduced proper transfer function to construct a minimal pH-DAE representation of the ROM in staircase form.

3.1. System matrix decomposition

Let $\mathcal{P}$ denote the system matrix of a full-order pH-DAE system with transfer function H in staircase form as in Lemma 2.3. For the sake of notational simplicity, we use $A = J - R$, $B = G - P$, $C = (G + P)^\top$ and $D = S + N$ which are partitioned as in Lemma 2.3: $A_{11} \in \mathbb{R}^{n_1 \times n_1}$, for example, denotes the upper left block of $J - R$. We define the transformation matrices $\mathcal{T}_1, \mathcal{T}_2 \in \mathbb{R}^{(n+m)\times(n+m)}$ with

$$\mathcal{T}_1 := \begin{bmatrix} L & 0 \\ X & I_m \end{bmatrix} = \begin{bmatrix} I_{n_1} & 0 & -A_{13}A_{33}^{-1} & 0 & 0 \\ 0 & I_{n_2} & -A_{23}A_{33}^{-1} & -(A_{21} - A_{23}A_{33}^{-1}A_{31})A_{41}^{-1} & 0 \\ 0 & 0 & A_{33}^{-1} & 0 & 0 \\ 0 & 0 & 0 & A_{41}^{-1} & 0 \\ C_4A_{14}^{-1} & 0 & (C_3 - C_4A_{14}^{-1}A_{13})A_{33}^{-1} & 0 & I_m \end{bmatrix},$$

$$\mathcal{T}_2 := \begin{bmatrix} M & Y \\ 0 & I_m \end{bmatrix}$$
$$= \begin{bmatrix} I_{n_1} & 0 & 0 & 0 & -A_{41}^{-1}B_4 \\ 0 & I_{n_2} & 0 & 0 & 0 \\ -A_{33}^{-1}A_{31} & -A_{33}^{-1}A_{32} & I_{n_3} & 0 & -A_{33}^{-1}(B_3 - A_{31}A_{41}^{-1}B_4) \\ 0 & A_{14}^{-1}(-A_{12} + A_{13}A_{33}^{-1}A_{32}) & 0 & A_{14}^{-1} & 0 \\ 0 & 0 & 0 & 0 & I_m \end{bmatrix}.$$

It is apparent that $\mathcal{T}_1$ and $\mathcal{T}_2$ satisfy the conditions in Lemma 2.1 since the determinants of A_{33}, A_{14} and A_{41} are constant and nonzero (see Lemma 2.3 and [13,14] for a proof). Note that our definitions of L and M share similarities with the state-space transformation presented in [14, Lemma 6] for autonomous semi-dissipative Hamiltonian DAEs. We obtain a transformed s.s.e. system matrix

$$\tilde{\mathcal{P}}(s) = \mathcal{T}_1\mathcal{P}(s)\mathcal{T}_2 = \begin{bmatrix} s\tilde{E}_{11} - \tilde{A}_{11} & 0 & 0 & -I_{n_1} & -\tilde{B}_1 \\ 0 & s\boldsymbol{E_p} - \boldsymbol{A_p} & 0 & 0 & -\boldsymbol{B_p} \\ 0 & 0 & -I_{n_3} & 0 & 0 \\ -I_{n_1} & 0 & 0 & 0 & 0 \\ \tilde{C}_1 & \boldsymbol{C_p} & 0 & 0 & \boldsymbol{D_p} + s\boldsymbol{D_\infty} \end{bmatrix}, \tag{15}$$

with nonsingular $\widetilde{E}_{11}, E_\mathrm{p}$. The second and fifth block column and row entries, respectively, are highlighted since these are the only parts that contribute to the transformed transfer function $\widetilde{H}$:

$$\widetilde{H} = \widetilde{C}(s\widetilde{E} - \widetilde{A})^{-1}\widetilde{B} + D_\mathrm{p} + sD_\infty \tag{16}$$

$$= \begin{bmatrix} \widetilde{C}_1 & C_\mathrm{p} & 0 & 0 \end{bmatrix} \begin{bmatrix} 0 & 0 & 0 & -I_{n_1} \\ 0 & (sE_\mathrm{p} - A_\mathrm{p})^{-1} & 0 & 0 \\ 0 & 0 & -I_{n_3} & 0 \\ -I_{n_1} & 0 & 0 & -(s\widetilde{E}_{11} - \widetilde{A}_{11}) \end{bmatrix} \begin{bmatrix} \widetilde{B}_1 \\ B_\mathrm{p} \\ 0 \\ 0 \end{bmatrix} + D_\mathrm{p} + sD_\infty \tag{17}$$

$$= C_\mathrm{p}(sE_\mathrm{p} - A_\mathrm{p})^{-1}B_\mathrm{p} + D_\mathrm{p} + sD_\infty \tag{18}$$

Consequently, the transfer function of every pH-DAE may be represented as the sum of the transfer function of a *proper* ODE system with dimension n_2 and an additional linear, improper term. Moreover, as shown in [21, Theorem 1], the proper subsystem again satisfies the pH structural constraints in Definition 2.2. It, therefore, admits a pH-ODE representation, which can be found by using its system matrix.

Lemma 3.1. *A pH-ODE representation of the proper subsystem with transfer function* $H_\mathrm{p} = C_\mathrm{p}(sE_\mathrm{p} - A_\mathrm{p})^{-1}B_\mathrm{p} + D_\mathrm{p}$ *can be computed by simply decomposing its system matrix*

$$\mathcal{P}_\mathrm{p}(s) := \begin{bmatrix} sE_\mathrm{p} - A_\mathrm{p} & -B_\mathrm{p} \\ C_\mathrm{p} & D_\mathrm{p} \end{bmatrix},$$

into symmetric and skew-symmetric parts, respectively.

Proof. Decomposing $\mathcal{P}_\mathrm{p}$ yields

$$\mathcal{P}_\mathrm{p}(s) = s\begin{bmatrix} E_\mathrm{p} & 0 \\ 0 & 0 \end{bmatrix} + \Gamma_\mathrm{p} + W_\mathrm{p},$$

with

$$\Gamma_\mathrm{p} = \begin{bmatrix} -J_\mathrm{p} & -G_\mathrm{p} \\ G_\mathrm{p}^\top & N_\mathrm{p} \end{bmatrix} = \frac{1}{2}\begin{bmatrix} -A_\mathrm{p} + A_\mathrm{p}^\top & -B_\mathrm{p} - C_\mathrm{p}^\top \\ C_\mathrm{p} + B_\mathrm{p}^\top & D_\mathrm{p} - D_\mathrm{p}^\top \end{bmatrix},$$

$$W_\mathrm{p} = \begin{bmatrix} R_\mathrm{p} & P_\mathrm{p} \\ P_\mathrm{p}^\top & S_\mathrm{p} \end{bmatrix} = \frac{1}{2}\begin{bmatrix} -A_\mathrm{p} - A_\mathrm{p}^\top & -B_\mathrm{p} + C_\mathrm{p}^\top \\ C_\mathrm{p} - B_\mathrm{p}^\top & D_\mathrm{p} + D_\mathrm{p}^\top \end{bmatrix}.$$

The fact that the system is an ODE system follows directly from $E_\mathrm{p} = E_{22} > 0$. This also proves condition (i) in Definition 2.2. In [21, Theorem 1], it was shown that the sum $\Gamma_\mathrm{p} + W_\mathrm{p}$ may be obtained from a series of transformations of the original $\Gamma + W$. These include permutations, Schur complement constructions and congruence-like transformations, which all preserve the positive semi-definiteness of the symmetric part. Therefore, $\Gamma_\mathrm{p}, W_\mathrm{p}$ fulfil the pH structural constraints (ii) and (iii) in Definition 2.2, which completes the proof.

We highlight that the simplicity of this result is a direct consequence of the staircase form and the pH structural constraints. For general DAE systems, this system decomposition approach generally requires the computation of spectral projectors onto the left and right deflating subspaces of the pencil $\lambda E - A$ corresponding to the finite eigenvalues, which are numerically challenging to compute in the large-scale setting [4]. In some applications, such as fluid flow problems or electric circuit simulation where the matrices E and A have a special block structure, the computation of spectral projectors can be done more efficiently or even circumvented, see, e.g [4,23]. However, the proposed interpolatory MOR approaches for general (unstructured) DAE systems [4,6] vary for different Kronecker indices, and their adaptations to pH-DAE systems proposed in [12,13] do not always guarantee that the ROM is again in pH form. In the following, we show how the results in this section enable the construction of a general MOR approach that works irrespective of the original system's Kronecker index and guarantees to produce minimal ROMs in pH form.

3.2. Tangential interpolation

As discussed in Remark 1, the ROM has to match the improper part sD_∞ exactly because otherwise, $H - H_r \notin \mathcal{RH}_\infty^{m\times m}$. We will therefore set this part aside for now and focus on the reduction of the proper part. Since the proper subsystem has only dimension n_2, a natural approach would be to reduce the proper system matrix $\mathcal{P}_\mathrm{p}$ directly. According to (8), this approach requires the computation of solutions $v_i \in \mathbb{C}^{n_2}$ of

$$(\sigma_i E_\mathrm{p} - A_\mathrm{p})v_i = B_\mathrm{p} b_i, \tag{19}$$

for all $i = 1, \ldots r$. From (15), we derive

$$E_\mathrm{p} = E_{22}, \qquad A_\mathrm{p} = A_{22} - A_{23}A_{33}^{-1}A_{32}.$$

For index-1 pH-DAEs ($n_3 > 0$) with nonzero $A_{23}A_{33}^{-1}A_{32}$, the matrix A_p might be dense, and therefore, the solutions in (19) may be more expensive than for the original system with matrices E, A and B. This is illustrated by the following example.

Example 3.2. Consider a pH-DAE with Kronecker index $\nu = 1$ in staircase form. The system has dimension $n = 10^4$ with $n_2 = n_3 = \frac{n}{2}$ and one input-output pair. As shown by the sparsity patterns in Figure 1(a,b), the matrices E and A have a very simple structure with only few nonzero entries (depicted in blue). However, the matrix A_p of the proper subsystem is dense, as shown in Figure 1(d).

To demonstrate the effects on interpolatory MOR, we solved (19) for the proper subsystem and for the original system with matrices E, A and B using 100 random

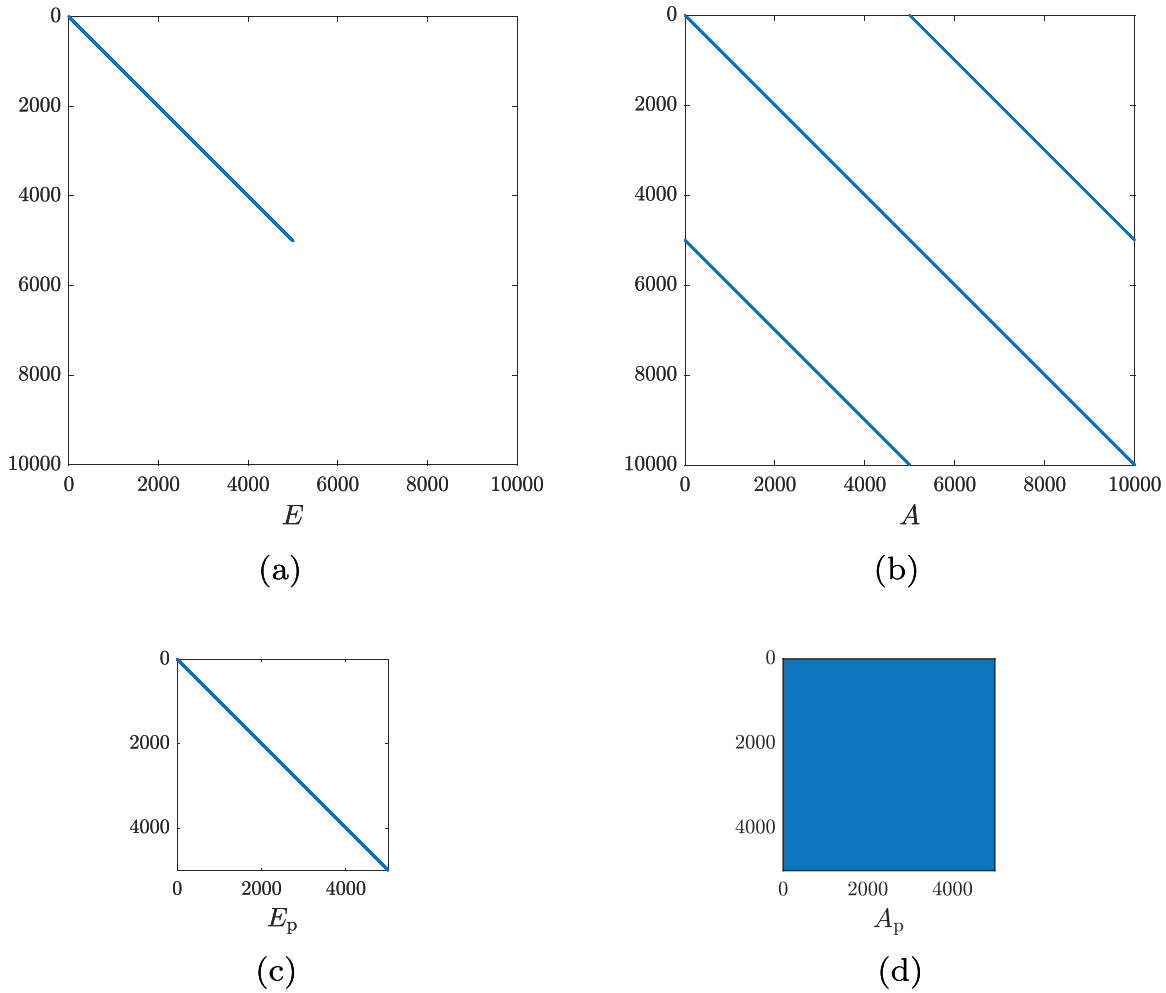

Figure 1. Sparsity patterns of exemplary full-order matrices $E, A \in \mathbb{R}^{n\times n}$ and of the matrices $E_\mathrm{p}, A_\mathrm{p} \in \mathbb{R}^{n_2\times n_2}$ of its associated proper subsystem.

complex shifts σ_i with MATLAB's mldivide command. All computations were conducted using MATLAB R2021b (version 9.11.0.1873467) on an Intel® Core™ i7–8700 CPU (3.20 GHz, 6-Core) with 32 GB RAM. The computations of (19) for the proper subsystem took 2.51 seconds on average versus only 0.013 seconds for the original model. Consequently, even though the proper subsystem is significantly smaller in size, the computation of the reduction matrix V takes more than 150 times longer.

Therefore, we propose another approach that works with the original (sparse) system matrix, irrespective of the system's Kronecker index.

Theorem 3.3. *Given a large-scale pH-DAE in staircase form with system matrix $\mathcal{P}$, as well as interpolation points $\{\sigma_1, \dots, \sigma_r\}$, and corresponding right tangential directions $\{b_1, \dots, b_r\}$, let $V \in \mathbb{R}^{n\times r}$ define a reduction matrix such that (8) holds with a decomposition $V^\top = [V_1^\top, V_2^\top, V_3^\top, V_4^\top]^\top$ with $V_j \in \mathbb{R}^{n_j\times r}$ for all $j = 1, \dots, 4$. We define the reduction matrices*

$$\mathcal{U} := \begin{bmatrix} 0 & A_{14}^{-\top} C_4^\top \\ V_2 & 0 \\ -A_{33}^{-\top} A_{23}^\top V_2 & A_{33}^{-\top} \left(C_3^\top - A_{13}^\top A_{14}^{-\top} C_4^\top\right) \\ 0 & 0 \\ 0 & I_m \end{bmatrix}, \quad \mathcal{V} := \begin{bmatrix} 0 & A_{14}^{-\top} B_4 \\ V_2 & 0 \\ 0 & 0 \\ 0 & 0 \\ 0 & I_m \end{bmatrix}, \tag{20}$$

Then, the model associated with the reduced system matrix

$$\mathcal{P}_r := \mathcal{U}^\top \mathcal{P} \mathcal{V},$$

satisfies the tangential interpolation conditions (7)*, and its proper subsystem fulfils the pH structural constraints. The reduced system matrix admits a decomposition*

$$\mathcal{P}_r = s \begin{bmatrix} E_{\mathrm{p},r} & 0 \\ 0 & D_\infty \end{bmatrix} + \begin{bmatrix} -J_{\mathrm{p},r} & -G_{\mathrm{p},r} \\ G_{\mathrm{p},r}^\top & N_{\mathrm{p},r} \end{bmatrix} + \begin{bmatrix} R_{\mathrm{p},r} & P_{\mathrm{p},r} \\ P_{\mathrm{p},r}^\top & S_{\mathrm{p},r} \end{bmatrix}.$$

Proof. Using the decomposition of V, the original system matrix $\mathcal{P}$ may initially be reduced in the following way:

$$\mathcal{P}_2(s) = \begin{bmatrix} U^\top & 0 \\ 0 & I_m \end{bmatrix} \mathcal{P} \begin{bmatrix} U & 0 \\ 0 & I_m \end{bmatrix}, \qquad U := \begin{bmatrix} I_{n_1} & 0 & 0 & 0 \\ 0 & V_2 & 0 & 0 \\ 0 & 0 & I_{n_3} & 0 \\ 0 & 0 & 0 & I_{n_4} \end{bmatrix}. \tag{21}$$

The reduced model associated with $\mathcal{P}_2$ satisfies the tangential interpolation conditions in (7) since $\operatorname{range}(V) \subseteq \operatorname{range}(U)$. Note that this approach, which was also proposed in [13] for index-1 pH-DAEs, produces ROMs that are still comparatively large: the ROM has dimension $n_1 + r + n_3 + n_4$. However, since the ROM is still a pH-DAE in staircase form, we can obtain a minimal representation by applying a transformation under s.s.e., as in Section 3.1, and extracting the proper system matrix without changing its transfer function. A combination of the reduction in (21), the transformation and extraction of

proper parts yields the reduction matrices $\mathcal{U}, \mathcal{V}$. Moreover, simple algebraic manipulations show that

$$\mathcal{P}_r = \mathcal{U}^\top \mathcal{P} \mathcal{V} = \begin{bmatrix} V_2^\top & 0 \\ 0 & I_m \end{bmatrix} \begin{bmatrix} sE_\mathrm{p} - A_\mathrm{p} & -B_\mathrm{p} \\ C_\mathrm{p} & D_\mathrm{p} + sD_\infty \end{bmatrix} \begin{bmatrix} V_2 & 0 \\ 0 & I_m \end{bmatrix},$$

and consequently, the proper part of $\mathcal{P}_r$ fulfils the pH structural constraints and may be decomposed to obtain a pH representation, which completes the proof.

To improve the numerical stability of Krylov subspace methods, the matrix V is usually orthogonalized such that $V^\top V = I_r$. This orthogonalization does not change the moment matching conditions in (8) since these only depend on the subspace that is spanned by the column vectors of V, not the basis itself. However, note that in our case, even if V is orthogonal, this is generally not the case for its submatrix V_2. To improve the numerical stability, we employ the cosine-sine decomposition, as discussed in [24]. For this, we split V into two parts: V_2 and the remaining submatrices $V_\mathrm{rem}^\mathrm{T} = [V_1^\top, V_3^\top, V_4^\top]^\top \in \mathbb{R}^{n_\mathrm{rem} \times r}$. We then compute the decomposition

$$\begin{bmatrix} V_2 \\ V_\mathrm{rem} \end{bmatrix} = \begin{bmatrix} \bar{V}_2 & 0 \\ 0 & \bar{V}_\mathrm{rem} \end{bmatrix} \begin{bmatrix} C_s \\ S_s \end{bmatrix} X_s^\top, \tag{22}$$

with orthogonal $\bar{V}_2 \in \mathbb{R}^{n_2 \times r}$, $\bar{V}_\mathrm{rem} \in \mathbb{R}^{n_\mathrm{rem} \times r}$, and $X_s \in \mathbb{R}^{r \times r}$, as well as diagonal $C_s, S_s \in \mathbb{R}^{r \times r}$ such that $C_s^\top C_s + S_s^\top S_s = I_r$. Replacing V_2 in (20) with $\bar{V}_2$ yields the final reduced system matrix $\mathcal{P}_r$.

3.3. Minimal pH-DAE representation

To find a pH-DAE representation for $\mathcal{P}_r$, we have to incorporate the improper part sD_∞ that has been separated back into the model. Two different methods have been proposed in [21] and [25] for this purpose. Since the method in [25] only leads to a minimal ROM representation if D_∞ has full rank, we proceed similarly as in [21]. We have that

$$D_\infty = -C_4 A_{14}^{-1} E_{11} A_{41}^{-1} B_4 = G_4^\top A_{41}^{-\top} E_{11} A_{41}^{-1} G_4 = D_\infty^\top \geq 0. \tag{23}$$

Consequently, there exists a rank-revealing factorization $D_\infty = L_\infty L_\infty^\top$ with $L_\infty \in \mathbb{R}^{m \times q}$. A minimal ROM representation Σ_r in staircase form can be found with

$$E_r = \begin{bmatrix} I_q & 0 & 0 \\ 0 & E_{\mathrm{p},r} & 0 \\ 0 & 0 & 0 \end{bmatrix}, \quad J_r = \begin{bmatrix} 0 & 0 & I_q \\ 0 & J_{\mathrm{p},r} & 0 \\ -I_q & 0 & 0 \end{bmatrix}, \quad R_r = \begin{bmatrix} 0 & 0 & 0 \\ 0 & R_{\mathrm{p},r} & 0 \\ 0 & 0 & 0 \end{bmatrix},$$

$$G_r = \begin{bmatrix} 0 \\ G_{\mathrm{p},r} \\ L_\infty^\top \end{bmatrix}, \quad P_r = \begin{bmatrix} 0 \\ P_{\mathrm{p},r} \\ 0 \end{bmatrix}, \quad S_r = S_{\mathrm{p},r}, \quad N_r = N_{\mathrm{p},r}.$$

We combine the obtained results of this section in Algorithm 1.

Algorithm 1: Tangential Interpolation of pH-DAEs

Input : Large-scale pH-DAE Σ in staircase form with system matrix $\mathcal{P}$; set of interpolation points $\{\sigma_1, \dots, \sigma_r\}$ and corresponding right tangential directions $\{b_1, \dots, b_r\}$ (both closed under complex conjugation).

Output: Reduced pH-DAE Σ_r with system matrix $\mathcal{P}_r$.

1 Compute $V = \left[V_1^\top, V_2^\top, V_3^\top, V_4^\top\right]^\top \in \mathbb{R}^{n\times r}$ such that (8) holds.

2 Orthogonalize V_2 via the cosine-sine decomposition in (22) such that $\operatorname{range}(V_2) = \operatorname{range}(\bar{V}_2)$ with $\bar{V}_2^\top \bar{V}_2 = I_r$.

3 Compute the reduction matrices $\mathcal{U}, \mathcal{V}$ as in Section 3.2:

$$\mathcal{U} = \begin{bmatrix} 0 & A_{14}^{-\top} C_4^\top \\ \bar{V}_2 & 0 \\ -A_{33}^{-\top} A_{23}^\top \bar{V}_2 & A_{33}^{-\top}(C_3^\top - A_{13}^\top A_{14}^{-\top} C_4^\top) \\ 0 & 0 \\ 0 & I_m \end{bmatrix}, \quad \mathcal{V} = \begin{bmatrix} 0 & A_{14}^{-\top} B_4 \\ \bar{V}_2 & 0 \\ 0 & 0 \\ 0 & 0 \\ 0 & I_m \end{bmatrix}.$$

4 Compute and decompose the reduced system matrix

$$\mathcal{P}_r = \mathcal{U}^\top \mathcal{P} \mathcal{V} = s \begin{bmatrix} E_{\mathrm{p},r} & 0 \\ 0 & D_\infty \end{bmatrix} + \begin{bmatrix} -J_{\mathrm{p},r} & -G_{\mathrm{p},r} \\ G_{\mathrm{p},r}^\top & N_{\mathrm{p},r} \end{bmatrix} + \begin{bmatrix} R_{\mathrm{p},r} & P_{\mathrm{p},r} \\ P_{\mathrm{p},r}^\top & S_{\mathrm{p},r} \end{bmatrix}.$$

5 Compute a rank-revealing factorization $D_\infty = L_\infty L_\infty^\top$ with $L_\infty \in \mathbb{R}^{m\times q}$.

6 **if** $q > 0$ **then**

7 Construct ROM Σ_r as in (13) with

$$E_r = \begin{bmatrix} I_q & 0 & 0 \\ 0 & E_{\mathrm{p},r} & 0 \\ 0 & 0 & 0 \end{bmatrix}, \quad J_r = \begin{bmatrix} 0 & 0 & I_q \\ 0 & J_{\mathrm{p},r} & 0 \\ -I_q & 0 & 0 \end{bmatrix}, \quad R_r = \begin{bmatrix} 0 & 0 & 0 \\ 0 & R_{\mathrm{p},r} & 0 \\ 0 & 0 & 0 \end{bmatrix},$$

$$G_r = \begin{bmatrix} 0 \\ G_{\mathrm{p},r} \\ L_\infty^\top \end{bmatrix}, \qquad P_r = \begin{bmatrix} 0 \\ P_{\mathrm{p},r} \\ 0 \end{bmatrix}, \qquad S_r = S_{\mathrm{p},r}, N_r = N_{\mathrm{p},r}.$$

8 **else**

9 Construct ROM Σ_r as in (13) directly from $\mathcal{P}_r$.

10 **end**

3.4. Discussion

In the following, we would like to briefly discuss the differences between the proposed Rosenbrock framework and other interpolatory MOR approaches that have been proposed for pH-DAEs. On the one hand, the approaches get more complex if the system's Kronecker index ν increases. On the other hand, as revealed in this section, if the system's transfer function has improper parts, these require special care since they have to be preserved exactly in the ROM. As shown in Lemma 2.3, the Kronecker index of LTI pH-DAEs is at most two, and improper parts may only occur if the Kronecker index is two (see (23)). Therefore, in the context of MOR, we may identify six different system

Table 1. Proposed tangential interpolation methods for pH-DAEs. The six different categories are derived from the original system's Kronecker index ν and whether its transfer function has improper parts.

Category	ν	n_2	n_3	n_4/n_1	D_∞	References
Index-0	0	$\neq 0$	0	0	0	[22, Theorem 7]
Index-1	1	$\neq 0$	$\neq 0$	0	0	[13, Theorems 1 and 2] [12, Theorem 5]
Proper Index-2	2	$\neq 0$	0	$\neq 0$	0	[13, Theorem 3]
Improper Index-2	2	$\neq 0$	0	$\neq 0$	$\neq 0$	[13, Theorem 4]
Proper Index-1–2	2	$\neq 0$	$\neq 0$	$\neq 0$	0	n/a
Improper Index-1–2	2	$\neq 0$	$\neq 0$	$\neq 0$	$\neq 0$	n/a

categories. An overview of existing methods for each category, to the best of the author's knowledge, is given in Table 1.

The tangential interpolation of pH-ODEs ($\nu = 0$), as initially proposed in [22], is well understood and leads to minimal ROM representations in pH-ODE form. For these systems, our approach is equivalent since the reduction matrices simplify to $\mathcal{U} = \mathcal{V} = \begin{bmatrix} \bar{V}_2 & 0 \\ 0 & I_m \end{bmatrix}$. For index-1 pH-DAEs, methods in [12,13] have been proposed, which rely on different semi-explicit representations of the FOM. In [13, Theorem 1], the feedthrough matrix of the ROM is modified to match the polynomial part of the FOM, which in the index-1 case, is constant. However, this method does not guarantee that the ROM fulfils the pH structural constraints. A remedy to this problem is to preserve the algebraic constraints of the FOM as proposed in [13, Theorem 2] and [12, Theorem 5]. However, this does not generally yield minimal ROMs since redundant algebraic equations cannot be removed, as discussed in [13, Remark 2]. In contrast, our method does not impose additional assumptions since it also only requires a semi-explicit FOM representation but guarantees the preservation of the pH form and yields minimal ROM representations.

For systems with $\nu = 2$ that do not have an index-1 part ($n_3 = 0$), we may distinguish between the proper and improper case. The proper index-2 case is comparable to the pH-ODE case if the system is in semi-explicit form and the method proposed in [13] yields minimal ROMs in pH form. Our method achieves the same goals, but may require one additional transformation to identify the full-rank matrix J_{41}. The improper index-2 case is treated in [13, Theorem 4]. However, this method does not guarantee that the ROM fulfils the pH structural constraints, which is generally the case for our method, again under the assumption that the system is in staircase form. To the best of the author's knowledge, methods for systems with index-1 *and* index-2 parts ($n_3 \neq 0$, $n_4 \neq 0$) have not been proposed yet. These two categories are also covered by our framework, which applies to all pH-DAEs in staircase form.

4. $\mathcal{H}_2$- and $\mathcal{H}_\infty$-inspired tangential interpolation

The question that remains is how to choose the parameters in Algorithm 1, i.e. the set of interpolation points and tangential directions. For unstructured ODE and DAE systems,

different $\mathcal{H}_2$- and $\mathcal{H}_\infty$-inspired strategies have been proposed (see, e.g. [7, 28, 29, 31, 32]) which have also partly been adapted to the pH-ODE and pH-DAE cases in [13,22].

In the following, we demonstrate how these ideas may be incorporated into the proposed Rosenbrock framework, and refer to the cited work in each section for implementation details.

4.1. Interpolatory $\mathcal{H}_2$ approximation

In $\mathcal{H}_2$-inspired interpolation methods for general DAE systems, the transfer function of the FOM is typically decomposed into the sum $H(s) = H_{\text{sp}}(s) + H_{\text{pol}}$ with a *strictly proper* part H_{sp} satisfying $\lim_{s\to\infty} H_{\text{sp}}(s) = 0$ and a polynomial part H_{pol} that potentially grows polynomially for $s \to \infty$. For the $\mathcal{H}_2$ error $\| H - H_r\|_{\mathcal{H}_2}$ to be bounded, we require $H - H_r \in \mathcal{RH}_2^{m\times m}$. Assuming a similar decomposition of H_r into $H_r(s) = H_{\text{sp,r}}(s) + H_{\text{pol,r}}(s)$, this is only the case if $H_{\text{pol,r}} = H_{\text{pol}}$. The necessary conditions for locally $\mathcal{H}_2$-optimal ROMs may then be formulated as interpolation conditions.

Lemma 4.1. [6, *Theorem 9.2.1*] *Let the transfer function $H(s) = H_{\text{sp}}(s) + H_{\text{pol}}$ be decomposed into strictly proper and polynomial parts. Let the ROM transfer function H_r have an analogous decomposition $H_r(s) = H_{\text{sp,r}}(s) + H_{\text{pol,r}}(s)$ with strictly proper part $H_{\text{sp,r}}(s) = C_{\text{sp,r}}(sE_{\text{sp,r}} - A_{\text{sp,r}})^{-1}B_{\text{sp,r}}$ such that $A_{\text{sp,r}} \in \mathbb{R}^{r\times r}$, nonsingular $E_{\text{sp,r}} \in \mathbb{R}^{r\times r}$ and $B_{\text{sp,r}}, C_{\text{sp,r}}^\top \in \mathbb{R}^{r\times m}$. If H_r minimizes the $\mathcal{H}_2$ error $\| H - H_r\|_{\mathcal{H}_2}$ over all ROMs with an r-th order strictly proper part, then $H_{\text{pol,r}} = H_{\text{pol}}$ and $H_{\text{sp,r}}$ minimizes the $\mathcal{H}_2$ error $\| H_{\text{sp}} - H_{\text{sp,r}}\|_{\mathcal{H}_2}$. Let $H_{\text{sp,r}}$ be represented by its pole-residue expansion $H_{\text{sp,r}}(s) = \sum_{i=1}^{r} \frac{l_i r_i^\top}{s-\lambda_i}$ where $r_i \in \mathbb{C}^m, l_i \in \mathbb{C}^m$ and with simple poles $\lambda_i \in \mathbb{C}$. Then, the tangential interpolation conditions*

$$H(-\lambda_i)r_i = H_r(-\lambda_i)r_i, \tag{24a}$$

$$l_i^\top H(-\lambda_i) = l_i^\top H_r(-\lambda_i), \tag{24b}$$

$$l_i^\top H'(-\lambda_i)r_i = l_i^\top H_r'(-\lambda_i)r_i, \tag{24c}$$

hold for all $i = 1, \ldots, r$.

This connection between interpolatory and $\mathcal{H}_2$-optimal model reduction is the motivation behind the well-known *iterative rational Krylov algorithm* (IRKA) [7], which utilizes a fixed-point iteration to enforce the necessary $\mathcal{H}_2$ optimality conditions for general DAE systems. Since for pH systems, the matrix U in (6) is typically chosen to enforce structure preservation, fewer degrees of freedom are available for interpolation, and it is generally only possible to fulfil a subset of (24), e.g. the conditions in (24a). Enforcing these conditions in an iterative manner using (8) leads to the IRKA-PH algorithm proposed for pH-ODE systems in [22].

Embedding the IRKA-PH algorithm into the proposed pH-DAE framework is straightforward. In each IRKA-PH iteration, we first compute the reduced system matrix

$\mathcal{P}_r$, using some initial interpolation data in the first iteration. We directly obtain the reduced strictly proper transfer function

$$H_{\mathrm{sp,r}}(s) = (G_{\mathrm{p},r} + P_{\mathrm{p},r})^\top (sE_{\mathrm{p},r} - (J_{\mathrm{p},r} - R_{\mathrm{p},r}))^{-1}(G_{\mathrm{p},r} - P_{\mathrm{p},r}).$$

Suppose that the pencil $\lambda E_{\mathrm{p},r} - (J_{\mathrm{p},r} - R_{\mathrm{p},r})$ has simple eigenvalues λ_i and let $t_i \in \mathbb{C}^{\mathrm{r}}$ denote a left eigenvector associated with λ_i, i.e.

$$t_i^\top (\lambda_i E_{\mathrm{p},r} - (J_{\mathrm{p},r} - R_{\mathrm{p},r})) = 0. \tag{25}$$

The (right) residual direction is then given by $r_i = (G_{\mathrm{p},r} - P_{\mathrm{p},r})^\top t_i$ and to enforce the interpolation conditions in (24a), we set $\sigma_i = -\lambda_i$ and $b_i = r_i$ for all $i = 1, \ldots, r$. This procedure is repeated, and upon convergence, the ROM satisfies the subset (24a) of $\mathcal{H}_2$ optimality conditions. Afterwards, we may attach the polynomial part $H_{\mathrm{pol}}(s) = D_{\mathrm{p}} + sD_\infty$ to the strictly proper ROM as described in Section 3.3. One disadvantage of this approach, which is summarized in Algorithm 2, is that a new ROM is computed in each iteration. In [27], an adaptation named *CIRKA-PH* was proposed, which has the potential to significantly accelerate IRKA-PH, especially in large-scale settings for which interpolatory methods are particularly powerful. Embedding CIRKA-PH into the pH-DAE framework works in a similar way.

Algorithm 2: IRKA-PH for pH-DAEs (based on [22])

Input : Large-scale pH-DAE Σ in staircase form; set of interpolation points $\{\sigma_1, \ldots, \sigma_r\}$ and corresponding right tangential directions $\{b_1, \ldots, b_r\}$ (both closed under complex conjugation).

Output: Reduced pH-DAE Σ_r.

1 **while** *not converged* **do**
2 | Perform steps 1-4 of Algorithm 1.
3 | Compute $t_i \in \mathbb{C}^r, \lambda_i \in \mathbb{C}$ solving (25) for all $i = 1, \ldots, r$.
4 | $\sigma_i \leftarrow -\lambda_i$ and $b_i \leftarrow (G_{\mathrm{p},r} - P_{\mathrm{p},r})^\top t_i$ for all $i = 1, \ldots, r$
5 **end**
6 Perform steps 5-10 of Algorithm 1.

4.2. Adaptive interpolation

In practice, besides the computational expense of IRKA-PH, it may sometimes be difficult to determine a suitable reduced order r in the first place. In [28,29], an *adaptive* approach was proposed that tackles this problem by iteratively adding new interpolation data in a complex region $\mathcal{S}$ where the approximation quality of the ROM is still poor. For pH-DAEs, this approach initially requires the computation of the proper system matrix $\mathcal{P}_{\mathrm{p}}$, as described in Section 3.1. The approximation quality of a ROM generated in steps 1–4 of Algorithm 1 can then be assessed at points $\mu \in \mathcal{S}$ with the following residual matrix [29]:

$$\zeta(\mu) := (A_\mathrm{p} - \mu E_\mathrm{p})\bar{V}_2(J_{\mathrm{p},r} - R_{\mathrm{p},r} - \mu E_{\mathrm{p},r})^{-1}(G_{\mathrm{p},r} - P_{\mathrm{p},r}) - B_\mathrm{p}. \tag{26}$$

In each iteration, a new interpolation point σ_{r+1} is added at the point in $\mathcal{S}$ where the norm of this residual matrix reaches its maximum, and a similar approach is taken to compute a new corresponding tangential direction b_{r+1}. Since σ_{r+1} and b_{r+1} are generally complex, their complex conjugates $\bar{\sigma}_{r+1}$ and $\bar{b}_{r+1}$ are also added to the interpolation data to keep it closed under conjugation. This way, the ROM dimension r increases in each iteration until its transfer function does not significantly change between two subsequent iterations or the predefined maximum dimension r_max is reached. For strategies on how to choose b_{r+1} and update the complex region $\mathcal{S}$, the interested reader is referred to [29]. The general approach is summarized in Algorithm 3.

Algorithm 3: TRKSM-PH for pH-DAEs (based on [28,29])

Input : Large-scale pH-DAE Σ in staircase form; set of interpolation points $\{\sigma_1, \ldots, \sigma_r\}$ and corresponding right tangential directions $\{b_1, \ldots, b_r\}$ (both closed under complex conjugation); maximum reduced order $r_\mathrm{max} > r_0$; initial complex region $\mathcal{S}$.

Output: Reduced pH-DAE Σ_r.

1 Compute and decompose $\mathcal{P}_\mathrm{p}$ as in Section 3.1.
2 **while** *not converged* ***and*** $r < r_\mathrm{max}$ **do**
3 Perform steps 1-4 of Algorithm 1.
4 Solve $\sigma_{r+1} = \arg\max_{\mu\in\mathcal{S}} \| \zeta(\mu) \|$.
5 Solve $b_{r+1} = \arg\max_{\|d\|=1} \| \zeta(\sigma_{r+1})d \|$.
6 Add $(\sigma_{r+1}, \bar{\sigma}_{r+1})$ and $(b_{r+1}, \bar{b}_{r+1})$ to the interpolation data.
7 Update the complex region $\mathcal{S}$.
8 **end**
9 Perform steps 5-10 of Algorithm 1.

4.3. Interpolatory $\mathcal{H}_\infty$ approximation

So far, we have enforced that $S_{\mathrm{p},r} = S_\mathrm{p}$ and $N_{\mathrm{p},r} = N_\mathrm{p}$ to keep the $\mathcal{H}_2$ error bounded. For $\mathcal{H}_\infty$-inspired MOR, we only require $H - H_r \in \mathcal{RH}_\infty^{m\times m}$ and thus, the reduced feedthrough matrices pose additional degrees of freedom that may be exploited in a similar manner as proposed in [30–32] for unstructured ODE systems. We may add structure-preserving perturbations to the feedthrough matrices $N_{\mathrm{p},r}$ and $S_{\mathrm{p},r}$ in the following way:

$$\widehat{N}_{\mathrm{p},r} = N_{\mathrm{p},r} + \Delta_N, \qquad \Delta_N = -\Delta_N^\top, \tag{27}$$

$$\widehat{S}_{\mathrm{p},r} = S_{\mathrm{p},r} + \Delta_S, \qquad \Delta_S = \Delta_S^\top \geq 0. \tag{28}$$

Simply adding these perturbations would only change the direct feedthrough of the ROM but not the dynamics and is therefore not expected to improve the $\mathcal{H}_\infty$ approximation quality significantly. However, as shown in [30], it is also possible to perturb the feedthrough matrix of the ROM while retaining predefined interpolation conditions with the FOM – and the same holds for pH-DAEs.

Lemma 4.2. *Assume that we have obtained a reduced system matrix* $\mathcal{P}_r = s\mathcal{E}_r + \Gamma_r + W_r$ *in steps 1–4 of Algorithm 1 using a set of interpolation points* $\{\sigma_1, \ldots, \sigma_r\}$ *and corresponding right tangential directions* $\{b_1, \ldots, b_r\}$, *both closed under complex conjugation. Let* $F \in \mathbb{R}^{n_2 \times m}$ *be a solution to*

$$F^\top \bar{V}_2 = [b_1, \ldots, b_r] T_v,$$

with $T_v \in \mathbb{C}^{r \times r}$ *such that* $\bar{V}_2 = V_2 T_v$. *If the system matrix* $\mathcal{P}_r$ *is perturbed such that*

$$\widehat{\mathcal{P}}_r = s\mathcal{E}_r + \widehat{\Gamma}_r + \widehat{W}_r,$$

with

$$\widehat{\Gamma}_r = \begin{bmatrix} -\widehat{J}_{\mathrm{p},r} & -\widehat{G}_{\mathrm{p},r} \\ \widehat{G}_{\mathrm{p},r}^{\mathrm{T}} & \widehat{N}_{\mathrm{p},r} \end{bmatrix} = \Gamma_r + \begin{bmatrix} \bar{V}_2^\top F \\ -I_m \end{bmatrix} \Delta_N \begin{bmatrix} \bar{V}_2^\top F \\ -I_m \end{bmatrix}^\top, \tag{29}$$

$$\widehat{W}_r = \begin{bmatrix} \widehat{R}_{\mathrm{p},r} & \widehat{P}_{\mathrm{p},r} \\ \widehat{P}_{\mathrm{p},r}^\top & \widehat{S}_{\mathrm{p},r} \end{bmatrix} = W_r + \begin{bmatrix} \bar{V}_2^\top F \\ -I_m \end{bmatrix} \Delta_S \begin{bmatrix} \bar{V}_2^\top F \\ -I_m \end{bmatrix}^\top, \tag{30}$$

then the perturbed ROM $\widehat{\Sigma}_r$ *with transfer function* $\widehat{H}_r$ *obtained by steps 5–10 in Algorithm 1 is a pH-DAE system, and it holds that*

$$H(\sigma_i) b_i = H_r(\sigma_i) b_i = \widehat{H}_r(\sigma_i) b_i, \tag{31}$$

for all $i = 1, \ldots, r$ *and for any* $\Delta_N = -\Delta_N^\top$ *and* $\Delta_S = \Delta_S^\top \geq 0$.

Proof. The fact that the perturbed system $\widehat{\Sigma}_r$ fulfils the pH structural constraints follows directly from the properties of Δ_N and Δ_S. The proof of (31) follows the proof of Theorem 3 in [30] for general LTI systems and is therefore omitted here.

This result enables us to optimize the new degrees of freedom Δ_N, Δ_S in an $\mathcal{H}_\infty$-inspired way. Optimizing the $\mathcal{H}_\infty$ error directly is challenging since $\mathcal{H}_\infty$ norm computations are computationally taxing, and the $\mathcal{H}_\infty$ norm depends non-smoothly on Δ_N, Δ_S (see [33] Sect 3.2.1]). Instead, the SOBMOR algorithm, proposed in [33], may be employed. Therein, the functions $vtu(\cdot)$ and $vtu(\cdot)$ are introduced, which map vectors row-wise to appropriately sized upper triangular and strictly upper triangular matrices, respectively. The function names are abbreviations for *vector-to-upper* and *vector-to-strictly-upper*, respectively. Using these functions, we may define parameter vectors $\theta_N \in \mathbb{R}^{m(m-1)/2}$ and $\theta_S \in \mathbb{R}^{m(m+1)/2}$ and design Δ_N, Δ_S in the following way:

$$\Delta_N(\theta_N) := vtsu(\theta_N)^\top - vtsu(\theta_N),$$

$$\Delta_S(\theta_S) := vtsu(\theta_S)^\top - vtsu(\theta_S).$$

Finally, a levelled least-squares approach can be taken to optimize the error $\| H - \widehat{H}_r(\cdot, \theta)\|_{\mathcal{H}_\infty}$ with $\theta := [\theta_N^\top, \theta_S^\top]^\top \in \mathbb{R}^{m^2}$, as described in [33,34], and to which we refer for implementation details. We summarize the approach in Algorithm 4.

Algorithm 4: IHA-PH for pH-DAEs (based on [32])

Input :Large-scale pH-DAE Σ in staircase form; set of interpolation points $\{\sigma_1, \ldots, \sigma_r\}$ and corresponding right tangential directions $\{b_1, \ldots, b_r\}$ (both closed under complex conjugation); initial parameter vector $\theta \in \mathbb{R}^{m^2}$.

Output: Perturbed reduced pH-DAE $\widehat{\Sigma}_r$

1 Compute the reduced system matrix $\mathcal{P}_r$ with steps 1-5 in Algorithm 2.
2 Solve $\theta^* = \arg\min_{\theta \in \mathbb{R}^{m^2}} \| H - \widehat{H}_r(\cdot, \theta)\|_{\mathcal{H}_\infty}$ using the approach in [33,34]
3 Compute $\widehat{\mathcal{P}}_r(\theta^*)$ as in Lemma 4.2.
4 Construct $\widehat{\Sigma}_r(\theta^*)$ with steps 5-10 in Algorithm 1.

4.4. Suitable representations for MOR

Since we apply Galerkin projections to preserve the pH structure, transformations of the FOM under s.s.e. will not change its transfer function, but they will have an impact on MOR, which raises the question of how to find suitable representations of the FOM that yield better approximations. This was recently examined in [35] for explicit ODE systems, and may be incorporated into our framework as follows.
Assume that we have computed the proper system matrix

$$\mathcal{P}_\mathrm{p}(s) = \begin{bmatrix} sE_\mathrm{p} - A_\mathrm{p} & -B_\mathrm{p} \\ C_\mathrm{p} & D_\mathrm{p} \end{bmatrix},$$

of the FOM as in Section 3.1. In Lemma 3.1, we obtained a pH representation of this subsystem by simply decomposing the system matrix into symmetric and skew-symmetric parts. However, there are other ways, and the family of pH representations for this system is parameterized by the *Kalman-Yakubovich-Popov (KYP) inequality*, as shown in [36]. If the proper system is *behaviourally observable*, i.e. $\operatorname{rank}[(sE_\mathrm{p} - A_\mathrm{p})^\top, C_\mathrm{p}^\top] = n_2$ for all $s \in \mathbb{C}$, which we assume in the following, the KYP inequality

$$\begin{bmatrix} -A_\mathrm{p}^\top X - X^\top A_\mathrm{p} & C_\mathrm{p}^\top - X^\top B_\mathrm{p} \\ C_\mathrm{p} - B_\mathrm{p}^\top X & D_\mathrm{p} + D_\mathrm{p}^\top \end{bmatrix} \geq 0, \quad X^\mathrm{T} E_\mathrm{p} = E_\mathrm{p}^\top X \geq 0, \tag{32}$$

has solutions $X \in \mathbb{R}^{n_2 \times n_2}$ that are bounded such that

$$0 < E_\mathrm{p}^\top X_- \leq E_\mathrm{p}^\top X \leq E_\mathrm{p}^\top X_+$$

with minimal and maximal solutions X_- and X_+, respectively (see [36,Theorem 1]). Now assume that we apply another transformation under s.s.e. on $\mathcal{P}_\mathrm{p}$ using any X satisfying (32) in the following way

$$\widetilde{\mathcal{P}}_\mathrm{p} = \begin{bmatrix} X^\top & 0 \\ 0 & I_m \end{bmatrix} \mathcal{P}_\mathrm{p} \begin{bmatrix} I_{n_2} & 0 \\ 0 & I_m \end{bmatrix},$$

then we obtain the decomposition

$$\widetilde{\mathcal{P}}_{\mathrm{p}} = \widetilde{s}E_{\mathrm{p}} + \widetilde{\Gamma}_{\mathrm{p}} + \widetilde{W}_{\mathrm{p}},$$

with matrices

$$\widetilde{E}_{\mathrm{p}} = \begin{bmatrix} X^\top E_{\mathrm{p}} & 0 \\ 0 & 0 \end{bmatrix}, \tag{33}$$

$$\widetilde{\Gamma}_{\mathrm{p}} = \begin{bmatrix} A_{\mathrm{p}}^\top X - X^\top A_{\mathrm{p}} & -(C_{\mathrm{p}}^\top + X^\top B_{\mathrm{p}}) \\ C_{\mathrm{p}} + B_{\mathrm{p}}^\top X & D_{\mathrm{p}} - D_{\mathrm{p}}^{\mathrm{T}} \end{bmatrix}, \tag{34}$$

$$\widetilde{W}_{\mathrm{p}} = \begin{bmatrix} -A_{\mathrm{p}}^\top X - X^\top A_{\mathrm{p}} & C_{\mathrm{p}}^\top - X^\top B_{\mathrm{p}} \\ C_{\mathrm{p}} - B_{\mathrm{p}}^\top X & D_{\mathrm{p}} + D_{\mathrm{p}}^\top \end{bmatrix}, \tag{35}$$

which clearly fulfils the pH structural constraints due to (32). The Hamiltonian of the system associated with $\widetilde{\mathcal{P}}_{\mathrm{p}}$ changes to

$$\widetilde{\mathcal{H}}_{\mathrm{p}}(\widetilde{x}_{\mathrm{p}}) = \frac{1}{2}\widetilde{x}_{\mathrm{p}}^\top X^\top E_{\mathrm{p}}\widetilde{x}_{\mathrm{p}}.$$

where $\widetilde{x}_{\mathrm{p}}$ denotes the new state vector of the transformed proper subsystem. As discussed in [35], choosing the minimal solution X_- for the transformation is particularly suited for MOR and may significantly improve the approximation quality. In our framework, we can include this transformation change by simply replacing $\mathcal{U}$ in step 3 of Algorithm 1 by

$$\mathcal{U}_- = \begin{bmatrix} 0 & A_{14}^{-\top} C_4^\top \\ X_- \bar{V}_2 & 0 \\ -A_{33}^{-\top} A_{23}^\top X_- \bar{V}_2 & A_{33}^{-\top}(C_3^\top - A_{13}^\top A_{14}^{-\top} C_4^\top) \\ 0 & 0 \\ 0 & I_m \end{bmatrix}.$$

Note that this does not affect the tangential interpolation conditions since we retain $\mathcal{V}$ and also does not affect the matrices $S_{\mathrm{p},r}$, $N_{\mathrm{p},r}$ or D_∞ since we keep the second block column of $\mathcal{U}$ unchanged. However, it does indeed have an effect on the strictly proper part $H_{\mathrm{sp},r}$ of the ROM's transfer function *between* the interpolation points, which is illustrated in the next section by numerical examples. Note that, especially if the matrices $E_{\mathrm{p}}, A_{\mathrm{p}}$ are very large or even dense (see Example 3.2), the solution of (32) may be computationally taxing. Therefore, efficient low-rank and/or sparse approximations of X_- are required that ideally originate from the sparse FOM matrices, which is an open research problem.

5. Numerical experiments

As initially mentioned, pH-DAE models naturally arise in different engineering fields. A prominent example are electrical RCL networks consisting of linear resistors, capacitors, inductors as well as voltage and current sources. These networks are used, for instance, for the simulation of VLSI interconnect systems or transmission lines. RCL

networks are typically modelled using modified nodal analysis (MNA), which is also used by simulation software such as SPICE. This directly yields models of the form

$$\begin{aligned} E\dot{x}(t) &= (J - R)x(t) + Gu(t), \\ y(t) &= G^\top x(t), \end{aligned}$$

which satisfy the pH structural constraints in Definition 2.2 (see, e.g [37]).

To evaluate our MOR framework, we consider two RCL ladder networks RCL-1M[1] and RCL-12S[2] whose structure is depicted in Figure 2. The number of RCL loops in the network is denoted by $\bar{n}$ and the number of state-space equations obtained by MNA is $n = 3\bar{n} + 2m$ where m denotes the number of voltage sources in the network. Both models can be transformed to pH-DAE staircase form via simple permutations of the state-space equations. For this, we use the port-Hamiltonian benchmark collection.[3] The staircase dimensions and sigma plots of RCL-1M and RCL-12S are provided in Figure 3.

RCL-1M is a multiple-input multiple-output (MIMO) version with $\bar{n} = 10000$, where the inputs are the voltages of both voltage sources and the outputs are the associated currents. For this model, the red box contains a resistor R_0 which leads to a Kronecker index $\nu = 1$ and an approximately constant input-output gain for higher frequencies (see Figure 3). In the single-input single-output (SISO) configuration used for RCL-12S, we

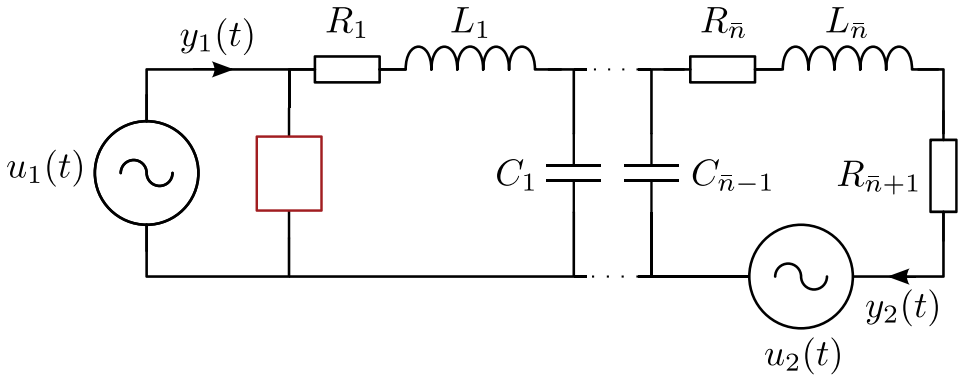

Figure 2. Structure of the RCL ladder networks modelled by RCL-1M and RCL-12S.

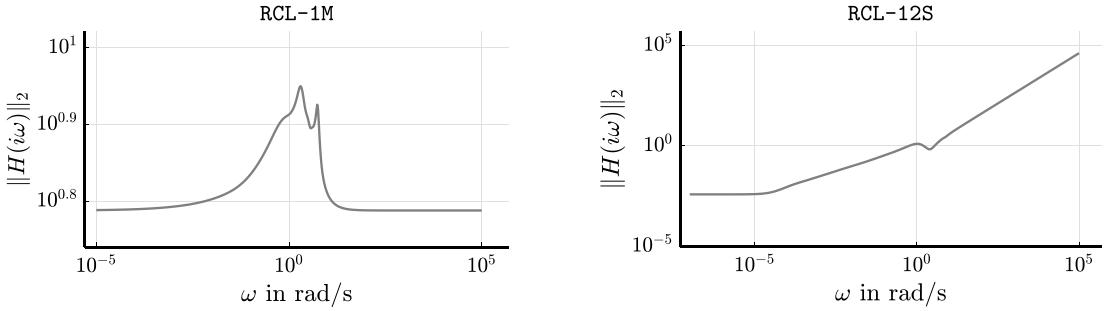

Model name	ν	n_2	n_3	n_4/n_1	D_∞	n	m
RCL-1M	1	19 999	10 005	0	0	30 004	2
RCL-12S	2	999	501	1	$\neq 0$	1 502	1

Figure 3. Model parameters and sigma plots for the RCL ladder network models RCL-1M and RCL-12S in pH-DAE staircase form.

replace the second voltage source by a wire and only consider the input-to-output behaviour from u_1 to y_1. Here, we use $\bar{n} = 500$ and the red box contains a capacitor C_0. This leads to a Kronecker index $\nu = 2$ and an improper transfer function. The value of D_∞, i.e. the slope of the transfer function in the high-frequency region is determined by its capacitance.

Let us first consider the reduction of RCL-1M. We reduce the original model to dimension $r = 40$ using the algorithms IRKA-PH, TRKSM-PH and IHA-PH. The sigma plots of the resulting ROM transfer functions and respective error systems $H - H_r$ are plotted in Figure 4. For this example, the proper matrices E_p, A_p are sparse, and therefore, the residual ζ in TRKSM-PH can be evaluated very efficiently. This makes TRKSM-PH a computationally efficient alternative to IRKA-PH since it yields a comparable performance while requiring significantly fewer solutions to large-scale linear systems of equations. The additional degrees of freedom in IHA-PH, on the other hand, enable more accurate results in small frequency regions at the expense of a constant error gain at higher frequencies, which results from the perturbation of the reduced feedthrough matrix.

For model RCL-12S, we compute ROMs of different dimensions ranging from $r = 2$ to $r = 20$. The $\mathcal{H}_2$ and $\mathcal{H}_\infty$ errors are plotted in Figure 5 for each MOR method presented in Section 4. For all methods, the errors decrease for increasing reduced orders r, which is expected since more interpolation conditions can be enforced. TRKSM-PH again yields similar $\mathcal{H}_2$ errors as IRKA-PH for larger ROM dimensions. For IHA-PH, only the $\mathcal{H}_\infty$ errors are plotted in Figure 5 since it produces unbounded $\mathcal{H}_2$ errors due to the perturbation of the feedthrough matrix. For most reduced orders, the $\mathcal{H}_\infty$ errors are only marginally smaller than those produced by IRKA-PH since the model has only one input-output pair and consequently, $\theta \in \mathbb{R}$. However, as shown for $r = 18$, even one additional parameter may improve the $\mathcal{H}_\infty$ approximation quality. Finally, we also illustrate the importance of choosing a suitable reduction matrix $\mathcal{U}$. Replacing the matrix $\mathcal{U}$ in IRKA-PH by $\mathcal{U}_-$, as described in Section 4.4, yields significantly smaller errors both in the $\mathcal{H}_2$ and $\mathcal{H}_\infty$ norm. Note that a similar basis change could, of course, also be applied to the IHA-PH and TRKSM-PH methods which is expected to yield similar improvements but is omitted here.

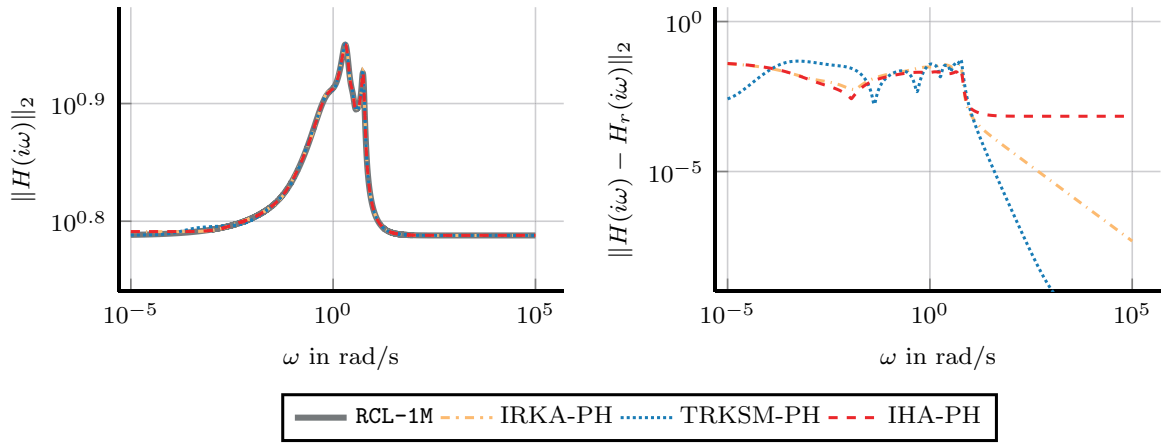

Figure 4. Reduction of the model RCL-1M to order $r = 40$ using different interpolatory MOR methods. Given are the sigma plots of the FOM and ROMs (left) and of the respective error systems (right).

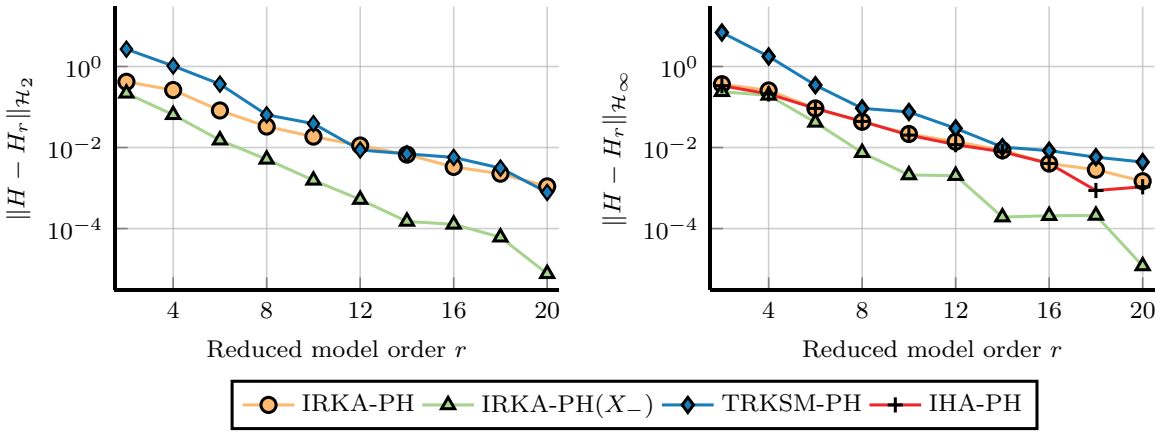

Figure 5. Reduction of the model RCL-12S to different reduced orders $r \in \{2, 4, \ldots, 20\}$. Plotted are the $\mathcal{H}_2$ errors (left) and $\mathcal{H}_\infty$ errors (right) for different interpolatory MOR methods.

When large-scale RCL networks are reduced, it is crucial that the ROM retains the passivity property of the original model to couple the ROM with other (possibly nonlinear) parts of the system. Interpolatory reduction methods that preserve the passivity or MNA structure of RCL models are given by the PRIMA [38] and SPRIM [37] algorithms, respectively. The developed MOR framework in this work extends these methods since the passivity property is inherently preserved by enforcing a pH-DAE structure of the ROM. The models RCL-1M and RCL-12S were also used for an evaluation of optimization-based MOR methods for pH-DAEs in [39] and [21], respectively, to which we refer for a comparison. Similar to these methods, all ROMs in our experiments fulfill the pH structural constraints. This is an advantage compared to passivity-preserving methods for general LTI systems (see, e.g [35,40]) which yield models of the form (5). A subsequent transformation to pH-DAE form requires the solution of a (reduced-order) KYP inequality which may lead to minor violations of the pH structural constraints caused by numerical inaccuracies (see [39, Remark 4]). We also highlight that our MOR framework directly yields ROMs with minimal state-space dimension which may require the solution of discrete-time projected Lyapunov equations for the passivity-preserving approaches proposed in [40].

6. Conclusion

Port-Hamiltonian descriptor systems are particularly suited for the energy-based modelling of multiphysical systems and naturally emerge in different applications. When large-scale pH-DAE models are reduced for simulation or controller design, it is desired to preserve their structural properties and the system dynamics which may be subject to algebraic constraints. In this work, we showed that the Rosenbrock system matrix exhibits a particular structure for pH-DAE models that can be exploited for model reduction. We have deduced a novel interpolatory MOR framework for pH-DAEs in staircase form, which, compared to other structure-preserving interpolation methods, guarantees minimal ROMs in pH-DAE form irrespective of the original system's Kronecker index. Moreover, its simple structure allows the incorporation of different

strategies for choosing suitable interpolation data which were originally proposed for unstructured DAE systems. In applications where pH-DAE models naturally arise, our approach can be considered as an alternative to stability- or passivity-preserving MOR methods since these properties directly follow from the pH structure. As a numerical example, we considered the reduction of electrical circuits which are used, for instance, in VLSI design.

Notes

1. The FOM state-space matrices of RCL-1 M are available at https://doi.org/10.5281/zenodo.6497076.
2. The FOM state-space matrices of RCL-12S are available at https://doi.org/10.5281/zenodo.6602125.
3. https://port-hamiltonian.io.

Acknowledgments

We sincerely appreciate the help of Maximilian Bonauer, Nora Reinbold and Paul Schwerdtner with the implementation of the algorithms in Section 4.

Disclosure statement

No potential conflict of interest was reported by the authors.

Funding

This research has been funded by the Deutsche Forschungsgemeinschaft (DFG, German Research Foundation) [project number 418612884].

References

[1] V. Duindam, A. Macchelli, S. Stramigioli, and H. Bruyninckx, *Modeling and Control of Complex Physical Systems*. Springer, Berlin Heidelberg, 2009.
[2] A. van der Schaft and D. Jeltsema, *Port-Hamiltonian systems theory: An introductory overview*, Found. Trends Syst. Control, 1 (2014), pp. 173–378.
[3] V. Mehrmann and B. Unger, *Control of port-Hamiltonian differential-algebraic systems and applications* (2022). arXiv Preprint arXiv:2201.06590. http://arxiv.org/abs/2201.06590.
[4] S. Gugercin, T. Stykel, and S. Wyatt, *Model reduction of descriptor systems by interpolatory projection methods*, SIAM J. Scientific Comput. 35 (2013), pp. B1010–1033.
[5] T. Moser, J. Durmann, M. Bonauer, and B. Lohmann, *MORpH – model reduction of linear port-Hamiltonian systems in MATLAB*, at-automatisierungstechnik (in press). 2023.
[6] A.C. Antoulas, C.A. Beattie, and S. Güğercin, *Interpolatory methods for model reduction*, SIAM, Philadelphia, 2020.
[7] S. Gugercin, A.C. Antoulas, and C. Beattie, $\mathcal{H}_2$ *model reduction for large-scale linear dynamical systems*, SIAM J. Matrix Analy. Appl, 300 (2008), pp. 609–638.
[8] R.V. Polyuga and A. van der Schaft, *Moment matching for linear port-Hamiltonian systems , In 2009 European control conference (ECC)*, Budapest, IEEE, 2009.

[9] R.V. Polyuga and A. van der Schaft, *Structure preserving model reduction of port-Hamiltonian systems by moment matching at infinity*, Automatica J. IFAC. 46 (2010), pp. 665–672.
[10] R.V. Polyuga and A. van der Schaft, *Structure preserving moment matching for port-Hamiltonian systems: Arnoldi and Lanczos*, IEEE Trans. Automat. Contr. 56 (2011), pp. 1458–1462.
[11] S. Gugercin, R. Polyuga, C. Beattie, and A. van der Schaft, I*nterpolation-based $\mathcal{H}_2$ model reduction for port-Hamiltonian systems. In Proceedings of the 48h IEEE conference on decision and control (CDC) held jointly with 2009 28th Chinese control conference*, Shanghai, pp. 5362–5369, 2009.
[12] S.A. Hauschild, N. Marheineke, and V. Mehrmann, *Model reduction techniques for linear constant coefficient port-Hamiltonian differential-algebraic systems*, Contrl. Cybernet. 19 (2019), pp. 125–152.
[13] C.A. Beattie, S. Gugercin, and V. Mehrmann. Structure-preserving interpolatory model reduction for port-Hamiltonian differential-algebraic systems. in C. Beattie, P. Benner, M. Embree, S. Gugercin, and S. Lefteriu, eds., *Realization and Model Reduction of Dynamical Systems: A Festschrift in Honor of the 70th Birthday of Thanos Antoulas*. Springer, Cham, 2022, pp. 235–254.
[14] F. Achleitner, A. Arnold, and V. Mehrmann, *Hypocoercivity and controllability in linear semi-dissipative Hamiltonian ordinary differential equations and differential-algebraic equations*, ZAMM. Z. Angew. Math. Mech. (2021).
[15] M.V.X.H. Byers, *A structured staircase algorithm for skew-symmetric/symmetric pencils*, ETNA. Electron Trans. Numer. Anal. [Electronic Only]. 26 (2007), pp. 1–33. http://eudml.org/doc/127545
[16] H.H. Rosenbrock, *State-Space and Multivariable Theory*, London, Thomas Nelson and Sons Ltd, 1970.
[17] H.H. Rosenbrock, *Structural properties of linear dynamical systems*, Int. J. Control. 20, 1974, pp. 191–202.
[18] K. Zhou, J.C. Doyle, and K. Glover, *Robust and Optimal Control*, Prentice-Hall, Englewood Cliffs, 1996.
[19] C. Beattie, V. Mehrmann, H. Xu, and H. Zwart, *Linear port-Hamiltonian descriptor systems*, Math. Control Signals Systems, 30, 17, 2018.
[20] M. Mamunuzzaman and H. Zwart, *Structure preserving model order reduction of port-Hamiltonian systems* (2022). arXiv Preprint arXiv:2203.07751. https://arxiv.org/abs/2203.07751 .
[21] T. Moser, P. Schwerdtner, V. Mehrmann, and M. Voigt, *Structure-preserving model order reduction for index two port-Hamiltonian descriptor systems* (2022). arXiv Preprint arXiv:2206.03942. https://arxiv.org/abs/2206.03942.
[22] S. Gugercin, R.V. Polyuga, C. Beattie, and A. van der Schaft, *Structure-preserving tangential interpolation for model reduction of port-Hamiltonian systems*, Automatica. 48 (2012), pp. 1963–1974.
[23] V. Mehrmann and T. Stykel. Balanced truncation model reduction for large-scale system in descriptor form. in P. Benner, V. Mehrmann, and D.C. Sorensen, eds., *Dimension Reduction of Large-Scale Systems, Volume 45 of Lecture Notes in Engineering and Computer Science*, pp. 83–115. Springer, Berlin/Heidelberg, 2005.
[24] H. Egger, T. Kugler, B. Liljegren-Sailer, N. Marheineke, and V. Mehrmann, *On structure preserving model reduction for damped wave propagation in transport networks*. SIAM J Sci Comput. 40 (2018), pp. A331–365.
[25] K. Cherifi, H. Gernandt, and D. Hinsen, *The difference between port-Hamiltonian, passive and positive real descriptor systems* (2022). arXiv Preprint arXiv:2204.04990. https://arxiv.org/abs/2204.04990 .
[26] C. Güdücü, J. Liesen, V. Mehrmann, and D.B. Szyld, *On non-hermitian positive (semi) definite linear algebraic systems arising from dissipative Hamiltonian DAEs* (2021). arXiv Preprint arXiv:2111.05616. https://arxiv.org/abs/2111.05616.

[27] T. Moser, J. Durmann, and B. Lohmann, *Surrogate-based $\mathcal{H}_2$ model reduction of port-Hamiltonian systems*, 2021 Eur. Control Conf. (ECC), Rotterdam, Netherlands, 2021, pp. 2058–2065.
[28] V. Druskin and V. Simoncini, *Adaptive rational Krylov subspaces for large-scale dynamical systems*, Systs Control Lett. 60, (2011), pp. 546–560.
[29] V. Druskin, V. Simoncini, and M. Zaslavsky, *Adaptive tangential interpolation in rational Krylov subspaces for MIMO dynamical systems*, SIAM J. Matrix Analy Appl. 35, 2014, pp. 476–498.
[30] C. Beattie and S. Gugercin, *Interpolatory projection methods for structure-preserving model reduction*, Syst Control Lett, 58 (2009), pp. 225–232.
[31] A. Castagnotto, C. Beattie, and S. Gugercin, *Interpolatory methods for $\mathcal{H}_\infty$ model reduction of multi-input/multi-output systems*, Model Simulat Appl. 2017, pp. 349–365.
[32] G. Flagg, C.A. Beattie, and S. Gugercin, *Interpolatory $\mathcal{H}_\infty$ model reduction*, Systs Control Lett. 62 (2013), pp. 567–574.
[33] P. Schwerdtner and M. Voigt, *Structure preserving model order reduction by parameter optimization* (2020). arXiv Preprint arXiv:2011.07567. https://arxiv.org/abs/2011.07567.
[34] P. Schwerdtner, *Port-Hamiltonian system identification from noisy frequency response data* (2021). arXiv Preprint arXiv:2106.11355. https://arxiv.org/abs/2106.11355.
[35] T. Breiten and B. Unger. *Passivity preserving model reduction via spectral factorization*. Automatica, 142 (2022), pp. 110368.
[36] C. Beattie, V. Mehrmann, and P. Van Dooren. *Robust port-Hamiltonian representations of passive systems*. Automatica, 100 (2019), pp. 182–186.
[37] R.W. Freund. The SPRIM algorithm for structure-preserving order reduction of general RCL circuits. in P. Benner, M. Hinze, and E.J.W. ter Maten, eds., *Model Reduction for Circuit Simulation, Volume 74 of Lecture Notes in Electric Engineering, Chapter 2*, pp. 25–52. Springer, Dordrecht, 2011.
[38] A. Odabasioglu, M. Celik, and L. Pileggi, *PRIMA: Passive reduced-order interconnect macromodeling algorithm*, IEEE Trans. Comput.-Aided Des. Integr. Circuits Syst. 17 (1998), pp. 645–654.
[39] P. Schwerdtner, T. Moser, V. Mehrmann, and M. Voigt, *Structure-preserving model order reduction for index one port-Hamiltonian descriptor systems* (2022). arXiv Preprint arXiv:2206.01608. https://arxiv.org/abs/2206.01608.
[40] T. Reis and T. Stykel, *Positive real and bounded real balancing for model reduction of descriptor systems*, Internat. J. Control, 83 (2010), pp. 74–88.

A.5 Optimization-Based Model Order Reduction of Port-Hamiltonian Descriptor Systems

Summary: Projection-based MOR methods for pH-DAEs typically focus on models with state-space matrices that exhibit a particular block structure, allowing the algebraic equations to be identified and treated separately. In this article, we present novel optimization-based methods which cover the entire system class of linear, time-invariant pH-DAEs in one framework and lead to high-fidelity ROMs with respect to the $\mathcal{H}_2$ or $\mathcal{H}_\infty$ norm. Our approach is based on a flexible parameterization of the ROM, and we propose different approaches to match polynomial parts of the given transfer function to keep the $\mathcal{H}_2$ and $\mathcal{H}_\infty$ errors well-defined and bounded. Optimization algorithms are derived to directly tune the parameters of the ROM such that either of the errors is minimized in a way that only samples of the original transfer function are required. These algorithms are based on the work in [142] for the $\mathcal{H}_\infty$ case and [A3] for the $\mathcal{H}_2$ case, respectively. An experimental comparison to state-of-the-art methods shows that our optimization-based approach leads to minimal ROMs which exhibit high fidelity in either of these norms and are guaranteed to fulfill the pH structural constraints. The work in this article was predominantly conducted by the first authors P. Schwerdtner and T. Moser, focusing on the $\mathcal{H}_\infty$ and $\mathcal{H}_2$ cases, respectively.

CRediT author statement:

Paul Schwerdtner:	Conceptualization, Data Curation, Methodology, Software, Visualization, Writing - Original Draft
Tim Moser:	Conceptualization, Data Curation, Methodology, Software, Visualization, Writing - Original Draft
Volker Mehrmann:	Conceptualization, Supervision, Writing - Review & Editing
Matthias Voigt:	Conceptualization, Funding Acquisition, Supervision, Writing - Review & Editing

Reference: P. Schwerdtner, T. Moser, V. Mehrmann, and M. Voigt. Optimization-based model order reduction of port-Hamiltonian descriptor systems. *Systems & Control Letters,* 182 (2023), 105655. https://doi.org/10.1016/j.sysconle.2023.105655

Systems & Control Letters 182 (2023) 105655

Contents lists available at ScienceDirect

Systems & Control Letters

journal homepage: www.elsevier.com/locate/sysconle

Optimization-based model order reduction of port-Hamiltonian descriptor systems☆

Paul Schwerdtner [a,*,1], Tim Moser [b,*,1], Volker Mehrmann [c], Matthias Voigt [d]

[a] Courant Institute of Mathematical Sciences, New York University, 251 Mercer Street, 10012 New York City, NY, United States
[b] Technical University of Munich, Chair of Automatic Control, Boltzmannstraße 15, 85748 Garching/Munich, Germany
[c] TU Berlin, Institute of Mathematics, Straße des 17. Juni 136, 10623 Berlin, Germany
[d] UniDistance Suisse, Faculty of Mathematics and Computer Science, Schinerstrasse 18, 3900 Brig, Switzerland

ARTICLE INFO

Dataset link: https://github.com/MORLab/MORpH

Keywords:
Port-Hamiltonian systems
Model order reduction
Structure-preservation
Descriptor systems

ABSTRACT

We present a new optimization-based structure-preserving model order reduction (MOR) method for port-Hamiltonian differential–algebraic equations (pH-DAEs). Our method is based on a novel parameterization that allows us to represent any linear time-invariant pH-DAE of a prescribed model order. We propose two algorithms which directly optimize the parameters of a reduced model to approximate a given large-scale model with respect to either the $\mathcal{H}_\infty$ or the $\mathcal{H}_2$ norm. This approach has several benefits. Our parameterization ensures that the reduced model is again a pH-DAE system and enables a compact representation of the algebraic part of the large-scale model, which in projection-based methods often requires a more involved treatment. The direct optimization is entirely based on transfer function evaluations of the large-scale model and is therefore independent of the structure of the system matrices. Numerical experiments are conducted to illustrate the high accuracy and small reduced model orders in comparison to other structure-preserving MOR methods.

1. Introduction

We present optimization-based structure-preserving model order reduction (MOR) algorithms for models described by port-Hamiltonian differential–algebraic equations (pH-DAEs). Differential–algebraic equations (DAEs) naturally emerge in the modeling of complex systems because they allow the inclusion of conservation laws and network laws such as mass balances in chemical processes, joints in mechanical systems, or Kirchhoff's laws in electrical circuits in the model as algebraic constraints. The use of automatic modeling systems such as `modelica`[2] or `simscape`[3] has further promoted the use of DAE-based models. In recent years, DAE modeling has increasingly addressed the physical properties of the underlying models by incorporating concepts such as passivity or a Hamiltonian structure, leading to pH-DAEs. The concept of pH-DAEs is particularly useful in the modeling of large networks that are constructed from a high number of network components such as power networks [1], gas networks [2], or district heating networks [3]. Typically, in such networks the components have widely varying dimensions and different modeling accuracies. Some models arise from a fine discretization of partial differential equations (PDEs) using finite element, finite difference, or finite volume methods, and other models are surrogate models generated purely from data, see [4] for a survey of applications.

The port-Hamiltonian paradigm is particularly suited for handling these modeling challenges because it allows for an intuitive energy-based interconnection of systems from different physical domains and of different scale or modeling accuracy, see [4–6]. A classical example of pH-DAEs are electrical circuits modeled using modified nodal analysis as described in [7–9].

When the models resulting from the modeling process of complex systems have a large state-space dimension, the direct simulation or model-based control of such large-scale systems is often infeasible. Then, typically, model order reduction is employed to determine an approximation to the given full-order model (FOM) with a smaller state-space dimension that enables efficient simulation and control. However, the need for optimized operation of large networks of complex systems has revealed the need for a more hierarchical modeling

☆ The research by P. Schwerdtner, M. Voigt, and T. Moser was supported by the German Research Foundation (DFG) within the projects 424221635 and 418612884 and that of V. Mehrmann was supported by the DFG through project B03 of SFB TRR 154.

* Corresponding authors.
E-mail addresses: paul.schwerdtner@nyu.edu (P. Schwerdtner), tim.moser@tum.de (T. Moser).

[1] Authors contributed equally.

[2] See https://modelica.org/.

[3] See https://www.mathworks.com/products/simscape.html.

https://doi.org/10.1016/j.sysconle.2023.105655
Received 2 June 2022; Received in revised form 10 October 2023; Accepted 16 October 2023
Available online 1 November 2023

approach, see, e. g., [2,10,11], which also changes MOR: Instead of computing one reduced-order model (ROM) for the whole system, separate low-order surrogate models are computed for the individual subsystems of the model hierarchy (potentially at different accuracy levels).

This paradigm shift from applying MOR to one (monolithic) system to using MOR to reduce the components of network models makes the preservation of certain structural properties of the components essential. This is because one network component may rely on the specific properties (such as passivity, see Section 2) of other components. Furthermore, the properties that result from the network structure of these components must be preserved during MOR such that the coupling of the reduced-order components can be performed in the same way as the coupling of their full-order counterparts. The preservation of the pH-DAE structure ensures the preservation of these network-relevant properties and thus enables a hierarchical low-order network based modeling approach.

However, structure-preserving MOR of pH-DAEs has still only been partially resolved. MOR methods for pH models based on ordinary differential equations (pH-ODEs), such as [12–15] have been partly extended to pH-DAEs in [16,17], but typically the algebraic equations have to be identified and treated separately to prevent destroying the constraint structure, see [17, Remark 3]. An alternative MOR approach for structure-preservation is passivity-preserving MOR (see Section 2). However, the passivity-preserving methods, such as positive-real balanced truncation (PRBT) [18], as extended to DAEs in [19], usually require further treatment to obtain a significant reduction in the equations describing the algebraic constraints. A minimal realization of the subsystem corresponding to the algebraic constraints can be determined by solving discrete-time projected Lyapunov equations [19, 20], but without preserving the pH structure. A recently proposed passivity-preserving MOR method for pH-ODEs based on spectral factorization [21] may overcome this problem but in its current form an extension to DAEs requires system transformations to identify and separately deal with the constraint equations.

In this article, we address these difficulties for linear constant-coefficient pH-DAEs, defined as follows.

Definition 1 (*[16,22]*)**.** A linear constant coefficient DAE system of the form

$$\begin{aligned} E\dot{x}(t) &= (J-R)Qx(t) + (G-P)u(t),\\ y(t) &= (G+P)^{\mathsf{T}}Qx(t) + (S-N)u(t), \end{aligned} \tag{1}$$

where $E, Q, J, R \in \mathbb{R}^{n\times n}$, $G, P \in \mathbb{R}^{n\times m}$, $S, N \in \mathbb{R}^{m\times m}$, is called a *port-Hamiltonian differential–algebraic equation (pH-DAE)*, if the following conditions are satisfied:

(i) The matrices $Q^{\mathsf{T}}JQ$ and N are skew-symmetric.
(ii) The passivity matrix

$$W_{\mathrm{P}} := \begin{bmatrix} Q^{\mathsf{T}}RQ & Q^{\mathsf{T}}P \\ P^{\mathsf{T}}Q & S \end{bmatrix}$$

and the product $Q^{\mathsf{T}}E$ are symmetric positive semi-definite (denoted as ≥ 0 in the following).

The *Hamiltonian (energy-storage) function* $\mathcal{H} : \mathbb{R}^n \to \mathbb{R}$ is then given by

$$\mathcal{H}(x) = \frac{1}{2}x^{\mathsf{T}}Q^{\mathsf{T}}Ex.$$

It has been shown in [23], see also [4], that under weak assumptions such a pH-DAE system can be reformulated or reduced to a system with $Q = I_n$. This transformation is sometimes numerically ill-conditioned but for simplicity of presentation, in the remainder of this paper we assume that $Q = I_n$. However, this is not a requirement of our algorithms. Moreover, we treat systems that satisfy the following additional assumptions: (i) the pencil $sE-(J-R)$ is *regular*, i. e., $\det(sE-(J-R))$ is not the zero polynomial; and (ii) all finite eigenvalues of $sE-(J-R)$ have a negative real part.

Structure-preserving MOR aims at computing systems of the form

$$\begin{aligned} E_r\dot{x}_r(t) &= (J_r-R_r)x_r(t) + (G_r-P_r)u(t),\\ y_r(t) &= (G_r+P_r)^{\mathsf{T}}x_r(t) + (S_r-N_r)u(t), \end{aligned}$$

where the system matrices $E_r, J_r, R_r \in \mathbb{R}^{r\times r}$, $G_r, P_r \in \mathbb{R}^{r\times m}$, $S_r, N_r \in \mathbb{R}^{m\times m}$ satisfy the structural constraints given in Definition 1 with $Q_r = I_r$, $r \ll n$, and $y_r(\cdot) \approx y(\cdot)$ for all appropriate inputs $u(\cdot)$. Moreover, we aim for regular systems and all finite eigenvalues of $sE_r-(J_r-R_r)$ having a negative real part.

The input-to-output behavior of a linear system in the frequency domain is described by its *transfer function*. This transfer function is given by

$$H(s) = (G+P)^{\mathsf{T}}(sE-(J-R))^{-1}(G-P) + (S-N),$$

which can be decomposed as

$$H(s) = H_{\mathrm{sp}}(s) + H_{\mathrm{pol}}(s),$$

where H_{sp} is a *strictly proper* rational matrix function and H_{pol} is a matrix polynomial of degree at most $\nu-1$. Here, ν denotes the Kronecker index of the uncontrolled DAE. The additional polynomial part in a FOM transfer function poses an extra challenge for MOR of DAEs because parts of it must be matched *exactly* in the ROM transfer function. Otherwise the error between FOM and ROM can become unbounded (see Section 2 for error measures). Therefore, in projection-based MOR, the algebraic part of the DAE is typically treated separately, see [16,17,20,24,25].

The Kronecker index of linear constant coefficient pH-DAEs it at most $\nu = 2$, which is shown in [26]. Therefore, H_{pol} can be decomposed as $H_{\mathrm{pol}}(s) = \mathcal{D}_0 + s\mathcal{D}_1$ (cf. Lemma 2). The coefficients $\mathcal{D}_0$ and $\mathcal{D}_1$ are the first two *Markov parameters* of H. For $\nu = 0$ and $\nu = 1$, $\mathcal{D}_1$ is zero, such that the FOM can be approximated by an ODE system with feedthrough term, but for $\nu = 2$, $\mathcal{D}_1$ may be nonzero, which results in an improper transfer function such that the FOM must be approximated with a reduced-order DAE model that is also of index $\nu = 2$.

In this article, we describe an optimization-based MOR approach for structure-preserving MOR that

(i) addresses improper, proper, and strictly proper pH-DAEs in one framework,
(ii) leads to high fidelity pH-ROMs with respect to the $\mathcal{H}_2$ norm or the $\mathcal{H}_\infty$ norm, and
(iii) preserves any polynomial part in the FOM transfer function with the minimal possible number of states.

The paper is organized as follows. In the next section, we cover objectives and state-of-the-art methods for structure-preserving MOR of pH-DAEs. For this, we first provide an analysis of the structure of pH-DAEs. In Section 3, we explain our optimization-based approach for MOR. In particular, we extend previous work [27,28] to the DAE case, which includes a parameterization of low-order pH-DAEs of all possible indices and an adapted optimization strategy. The effectiveness of the proposed methods is demonstrated by several numerical experiments in Section 4.

2. Preliminaries

In this section, we recall some error measures and algorithms that are typically used in MOR and present some preliminary results that give insight into the structure of pH-DAEs and form the basis for the construction of our MOR algorithms.

2.1. Model order reduction background

The approximation error between the FOM and the ROM is typically measured using their corresponding transfer functions H and H_r with respect to the $\mathcal{H}_\infty$ or $\mathcal{H}_2$ errors. These errors are given by

$$\|H - H_r\|_{\mathcal{H}_2} := \left(\frac{1}{2\pi}\int_{-\infty}^{\infty} \|H(\mathrm{i}\omega) - H_r(\mathrm{i}\omega)\|_{\mathrm{F}}^2 \,\mathrm{d}\omega\right)^{1/2},$$
$$\|H - H_r\|_{\mathcal{H}_\infty} := \sup_{\omega\in\mathbb{R}} \|H(\mathrm{i}\omega) - H_r(\mathrm{i}\omega)\|_2.$$

Note that for a bounded $\mathcal{H}_2$ error, both D_0 and D_1 must be matched exactly, while it suffices to match D_1 exactly for a bounded $\mathcal{H}_\infty$ error. MOR methods designed for these error measures have been proposed by many authors (for general descriptor systems), see, e. g., [20,25,29–31].

For general ODE systems, the *iterative rational Krylov algorithm* (IRKA) aims at minimizing the $\mathcal{H}_2$ error, see [32]. A structure-preserving variant that we denote by IRKA-PH, was derived in [13], which is extended to DAEs in [16,17]. Here the strictly proper part and the Markov parameters of the original transfer functions are identified to make sure that D_0 and D_1 are matched exactly in the reduced transfer function. Then the standard version of IRKA-PH can be applied. IRKA-based algorithms use tangential interpolation of the transfer function at iteratively determined interpolation points and tangential directions to construct projection spaces; see [33] for an exhaustive discussion of such interpolation methods. However, the pH-DAE adaptations of IRKA-PH in [16,17] require a separate treatment of the algebraic part in order not to destroy the pH structure and often lead to a lower accuracy compared to non-structure-preserving MOR methods. Furthermore, the method in [17] does not guarantee preservation of the pH structure when the FOM transfer function is improper and is only generally applicable to pH-DAEs where the higher-index part of the system is uncontrolled. The passivity-preserving MOR method PRBT [18,19] is based on the computation of the minimal solutions of two *algebraic Riccati equations* (or *Lur'e equations*). These minimal solutions take the role of the Gramians in classical balanced truncation (BT) model reduction, and the balancing and truncation procedure can be performed as in BT. This method admits an a priori gap metric error bound [34]. However, it generally does not preserve the pH form such that a pH realization of the resulting ROM must be computed after performing PRBT. For details on computing a pH realization from a passive descriptor system, we refer to [35].

2.2. Staircase form

In Lemma 1, we present a staircase form for pH-DAEs, which was derived for general linear pH-DAE systems without input and output in [36] and for systems with input and output in [17], see also [4]. The staircase form allows us to determine the Kronecker index of a given pH-DAE but is based on subsequent rank decisions which may be a challenging task in finite precision arithmetic. Fortunately, the staircase form often emerges naturally from the modeling process [22,37] or can be constructed using only a few permutations of the given system matrices. We use the real-valued version of this form as derived in [36].

Lemma 1 ([36]). *Consider a regular pH-DAE system as in (1) (with $Q = I_n$). Then there exists an orthogonal matrix $T \in \mathbb{R}^{n\times n}$ such that*

$$\widetilde{E} := TET^{\mathsf{T}} = \begin{bmatrix} E_{11} & E_{12} & 0 & 0 \\ E_{21} & E_{22} & 0 & 0 \\ 0 & 0 & 0 & 0 \\ 0 & 0 & 0 & 0 \end{bmatrix},$$
$$\widetilde{J} := TJT^{\mathsf{T}} = \begin{bmatrix} J_{11} & J_{12} & J_{13} & J_{14} \\ J_{21} & J_{22} & J_{23} & 0 \\ J_{31} & J_{32} & J_{33} & 0 \\ J_{41} & 0 & 0 & 0 \end{bmatrix},$$
$$\widetilde{R} := TRT^{\mathsf{T}} = \begin{bmatrix} R_{11} & R_{12} & R_{13} & 0 \\ R_{21} & R_{22} & R_{23} & 0 \\ R_{31} & R_{32} & R_{33} & 0 \\ 0 & 0 & 0 & 0 \end{bmatrix},$$
$$\widetilde{G} := TG = \begin{bmatrix} G_1 \\ G_2 \\ G_3 \\ G_4 \end{bmatrix}, \widetilde{P} := TP = \begin{bmatrix} P_1 \\ P_2 \\ P_3 \\ 0 \end{bmatrix}, \widetilde{S} := S,\ \widetilde{N} := N,$$

where $\begin{bmatrix} E_{11} & E_{12} \\ E_{21} & E_{22} \end{bmatrix}$ is positive definite and the matrices J_{41} and $J_{33} - R_{33}$ are invertible (if the blocks are nonempty).

The transformed system

$$\begin{aligned} \widetilde{E}\dot{\widetilde{x}}(t) &= (\widetilde{J} - \widetilde{R})\widetilde{x}(t) + (\widetilde{G} - \widetilde{P})u(t), \\ y(t) &= (\widetilde{G} + \widetilde{P})^{\mathsf{T}}\widetilde{x}(t) + (\widetilde{S} - \widetilde{N})u(t) \end{aligned} \tag{2}$$

is again a pH-DAE system with accordingly partitioned state vector $\widetilde{x}(t) = \left[\widetilde{x}_1(t)^{\mathsf{T}}, \widetilde{x}_2(t)^{\mathsf{T}}, \widetilde{x}_3(t)^{\mathsf{T}}, \widetilde{x}_4(t)^{\mathsf{T}}\right]^{\mathsf{T}}$, where $\widetilde{x}_i(t) \in \mathbb{R}^{n_i}, n_i \in \mathbb{N}_0$ for all $i = 1, \dots, 4$ and with $n_1 = n_4$. The Kronecker index ν of the uncontrolled system satisfies

$$\nu = \begin{cases} 0 & \text{if and only if } n_1 = n_4 = 0 \text{ and } n_3 = 0, \\ 1 & \text{if and only if } n_1 = n_4 = 0 \text{ and } n_3 > 0, \\ 2 & \text{if and only if } n_1 = n_4 > 0. \end{cases}$$

3. Our method

Our method is based on optimizing the parameters (i. e., the matrix elements) of a low-order pH-DAE such that its transfer function matches the transfer function of a given large-scale pH-DAE as well as possible. As error measures we consider both the $\mathcal{H}_2$ and the $\mathcal{H}_\infty$ norms. For this we need to

(i) determine a parameterization that encompasses all the pH-DAE types that are described in Lemma 1,
(ii) impose a matching of the polynomial part of the given transfer function to keep the errors well-defined and bounded, and
(iii) define update rules for the parameters such that the $\mathcal{H}_2$ error or the $\mathcal{H}_\infty$ error is minimized.

We set up a parameterization that allows the strictly proper part of the transfer function to be tuned independently of the polynomial part in Section 3.1. In this way, matching of the polynomial part and minimizing the errors can be addressed separately. We present several alternative methods for computing the polynomial part of a potentially large-scale pH-DAE in Section 3.2. Methods for $\mathcal{H}_\infty$ or $\mathcal{H}_2$ approximation are then given in Sections 3.3 and 3.4, respectively.

3.1. Parameterization

Before we set up the parameterization, we first recall a few properties of transfer functions of port-Hamiltonian systems. Most importantly, they are always positive real. A transfer function H is referred to as *positive real*, if

(i) H has no poles in the open right complex half-plane $\mathbb{C}^+ := \{s \in \mathbb{C} \mid \mathrm{Re}(s) > 0\}$;
(ii) $H(s) + H(s)^{\mathsf{H}} \geq 0$ for all $s \in \mathbb{C}^+$.

By [38, Theorem 2.7.2] these two conditions are equivalent to:

(i) The transfer function H has no poles in $\mathbb{C}^+$.
(ii) All poles of H on the extended imaginary axis $\mathrm{i}\mathbb{R} \cup \{-\infty, \infty\}$ are simple. Moreover, if $\mathrm{i}\omega_0 \in \mathrm{i}\mathbb{R}$ is a finite pole of H, then the residue $\lim_{s\to\mathrm{i}\omega_0}(s - \mathrm{i}\omega_0)H(s)$ is symmetric positive semi-definite. Similarly, the residue for the poles at infinity $\lim_{\omega\to\infty} \frac{H(\mathrm{i}\omega)}{\mathrm{i}\omega}$ is symmetric and positive semi-definite.
(iii) For each $\omega \in \mathbb{R}$ for which $\mathrm{i}\omega$ is not a pole of H, it holds that

$$H(\mathrm{i}\omega) + H(\mathrm{i}\omega)^{\mathsf{H}} \geq 0.$$

Lemma 2. *Let a positive real $m \times m$ transfer function H be given. We can decompose it into the sum*

$$H(s) = H_{\mathrm{sp}}(s) + \mathcal{D}_0 + \mathcal{D}_1 \cdot s,$$

where H_{sp} is strictly proper (i. e., $\lim_{s\to\infty} H_{\mathrm{sp}}(s) = 0$), $\mathcal{D}_0$, $\mathcal{D}_1 \in \mathbb{R}^{m\times m}$, and where

(a) $\mathcal{D}_1$ is symmetric positive semidefinite, and
(b) the proper part $H_{\mathrm{p}}(s) := H_{\mathrm{sp}}(s) + \mathcal{D}_0$ is positive real.

Proof. We refer to [39] for the proof of (a). To show (b), we decompose H into its proper and improper parts, and for each $\omega \in \mathbb{R}$ for which $\mathrm{i}\omega$ is not a pole of H we obtain

$$\begin{aligned} H(\mathrm{i}\omega) + H(\mathrm{i}\omega)^{\mathsf{H}} &= H_{\mathrm{p}}(\mathrm{i}\omega) + H_{\mathrm{p}}(\mathrm{i}\omega)^{\mathsf{H}} + \mathrm{i}\omega(\mathcal{D}_1 - \mathcal{D}_1^{\mathsf{T}}) \\ &= H_{\mathrm{p}}(\mathrm{i}\omega) + H_{\mathrm{p}}(\mathrm{i}\omega)^{\mathsf{H}} \geq 0, \end{aligned}$$

where we have used (a). Consequently, the proper part H_{p} is positive real. □

Remark 1. If all finite eigenvalues of the pencil $sE - (J - R)$ have negative real part as imposed by our assumptions, then its transfer function H cannot have finite poles on the imaginary axis, in particular, H_{p} has a bounded $\mathcal{H}_\infty$ norm.

Note that, in contrast to pH-DAEs with index one, the coefficient $\mathcal{D}_1$ may be non-zero for pH-DAEs with index two. Consequently, our parameterization must accommodate improper transfer functions. The previous result allows us to consider the improper part $\mathcal{D}_1 \cdot s$ separately from the proper part of the given transfer function, as the proper part H_{p} is still positive real and can thus be parameterized independently. In the following theorem, we analyze H_{p} in more detail.

Theorem 1. *The proper part H_{p} of the transfer function of any pH-DAE can be realized by an implicit ODE system of the form*

$$\begin{aligned} E_{\mathrm{p}}\dot{x}_{\mathrm{p}}(t) &= (J_{\mathrm{p}} - R_{\mathrm{p}})x_{\mathrm{p}}(t) + (G_{\mathrm{p}} - P_{\mathrm{p}})u(t), \\ y_{\mathrm{p}}(t) &= (G_{\mathrm{p}} + P_{\mathrm{p}})^{\mathsf{T}}x_{\mathrm{p}}(t) + (S_{\mathrm{p}} - N_{\mathrm{p}})u(t), \end{aligned} \tag{3}$$

with $x_{\mathrm{p}} : \mathbb{R} \to \mathbb{R}^{n_2}$ and $E_{\mathrm{p}} > 0$, where n_2 is the corresponding dimension as in Lemma 1.

Proof. The claim that the proper part of any transfer function of a pH-DAE admits a realization of the form (3) follows immediately, as any proper positive real transfer function is realizable by a passive ODE system, which can in turn be transformed into pH form [40]. In the Appendix, we show that we can build a realization with state-space dimension n_2 by deriving it directly from the staircase form in Lemma 1. □

In Theorem 2 we exploit the presented properties to derive a novel approach to parameterizing pH-DAEs of all possible Kronecker indices. Therein, the functions $\mathrm{vtu}(\cdot)$ and $\mathrm{vtsu}(\cdot)$ map vectors row-wise to appropriately sized upper triangular and strictly upper triangular matrices, respectively. The function names are abbreviations for *vector-to-upper* and *vector-to-strictly-upper*, respectively. The function $\mathrm{vtf}_m(\cdot)$ is a simple reshaping operation, which maps a vector in $\mathbb{R}^{n\cdot m}$ to a matrix in $\mathbb{R}^{n\times m}$. A detailed description of these functions can be found in [28, Definition 3.1].

Theorem 2. *Let $\theta \in \mathbb{R}^{n_\theta}$ be a parameter vector partitioned as $\theta = \left[\theta_J^{\mathsf{T}}, \theta_W^{\mathsf{T}}, \theta_G^{\mathsf{T}}, \theta_N^{\mathsf{T}}, \theta_L^{\mathsf{T}}\right]^{\mathsf{T}}$ with $\theta_J \in \mathbb{R}^{r(r-1)/2}$, $\theta_W \in \mathbb{R}^{(r+m)(r+m+1)/2}$, $\theta_G \in \mathbb{R}^{r\cdot m}$, $\theta_N \in \mathbb{R}^{m(m-1)/2}$, and $\theta_L \in \mathbb{R}^{m\cdot\ell}$ with $\ell > 0$. Furthermore, define the matrix-valued functions*

$$J_{\mathrm{p},r}(\theta) := \mathrm{vtsu}(\theta_J)^{\mathsf{T}} - \mathrm{vtsu}(\theta_J), \tag{4a}$$

$$W(\theta) := \mathrm{vtu}(\theta_W)\,\mathrm{vtu}(\theta_W)^{\mathsf{T}}, \tag{4b}$$

$$R_{\mathrm{p},r}(\theta) := \begin{bmatrix} I_r & 0 \end{bmatrix} W(\theta) \begin{bmatrix} I_r & 0 \end{bmatrix}^{\mathsf{T}}, \tag{4c}$$

$$P_{\mathrm{p},r}(\theta) := \begin{bmatrix} I_r & 0 \end{bmatrix} W(\theta) \begin{bmatrix} 0 & I_m \end{bmatrix}^{\mathsf{T}}, \tag{4d}$$

$$S_r(\theta) := \begin{bmatrix} 0 & I_m \end{bmatrix} W(\theta) \begin{bmatrix} 0 & I_m \end{bmatrix}^{\mathsf{T}}, \tag{4e}$$

$$G_{\mathrm{p},r}(\theta) := \mathrm{vtf}_m(\theta_G), \tag{4f}$$

$$L(\theta) := \mathrm{vtf}_\ell(\theta_L), \tag{4g}$$

$$N_r(\theta) := \mathrm{vtsu}(\theta_N)^{\mathsf{T}} - \mathrm{vtsu}(\theta_N). \tag{4h}$$

Then the parameter-dependent DAE

$$\Sigma_r(\theta) : \begin{cases} E_r\dot{x}_r(t) = (J_r(\theta) - R_r(\theta))x_r(t) + (G_r(\theta) - P_r(\theta))u(t), \\ y_r(t) = (G_r(\theta) + P_r(\theta))^{\mathsf{T}}x_r(t) + (S_r(\theta) - N_r(\theta))u(t), \end{cases} \tag{5}$$

with $x_r(t)$ partitioned as $x_r(t) = \left[x_1(t)^{\mathsf{T}}, x_2(t)^{\mathsf{T}}, x_3(t)^{\mathsf{T}}\right]^{\mathsf{T}}$, where $x_1(t) \in \mathbb{R}^r$, $x_2(t) \in \mathbb{R}^\ell$, $x_3(t) \in \mathbb{R}^\ell$ for each $t \in \mathbb{R}$ and

$$E_r = \begin{bmatrix} I_r & 0 & 0 \\ 0 & I_\ell & 0 \\ 0 & 0 & 0 \end{bmatrix},$$

$$J_r(\theta) = \begin{bmatrix} J_{\mathrm{p},r}(\theta) & 0 & 0 \\ 0 & 0 & -I_\ell \\ 0 & I_\ell & 0 \end{bmatrix}, \; R_r(\theta) = \begin{bmatrix} R_{\mathrm{p},r}(\theta) & 0 & 0 \\ 0 & 0 & 0 \\ 0 & 0 & 0 \end{bmatrix},$$

$$G_r(\theta) = \begin{bmatrix} G_{\mathrm{p},r}(\theta) \\ 0 \\ L(\theta)^{\mathsf{T}} \end{bmatrix}, \quad P_r(\theta) = \begin{bmatrix} P_{\mathrm{p},r}(\theta) \\ 0 \\ 0 \end{bmatrix},$$

satisfies the pH structure conditions in Definition 1 (with $Q = I_{r+2\ell}$). Its transfer function H_r is given by

$$H_r(s,\theta) = H_{\mathrm{p},r}(s,\theta) + L(\theta)L(\theta)^{\mathsf{T}} \cdot s,$$

where $H_{\mathrm{p},r}(s,\theta)$ denotes the transfer function of the pH-ODE system

$$\Sigma_{\mathrm{p},r}(\theta) : \begin{cases} \dot{x}_1(t) = (J_{\mathrm{p},r}(\theta) - R_{\mathrm{p},r}(\theta))x_1(t) + (G_{\mathrm{p},r}(\theta) - P_{\mathrm{p},r}(\theta))u(t), \\ y_{\mathrm{p},r}(t) = (G_{\mathrm{p},r}(\theta) + P_{\mathrm{p},r}(\theta))^{\mathsf{T}}x_1(t) + (S_r(\theta) - N_r(\theta))u(t). \end{cases} \tag{6}$$

Proof. For ease of notation, we omit the argument θ in the system matrices of (4). The fact that (5) is a pH-DAE system of index two follows directly from the composition of the reduced-order matrices and the parameterization in (4). Under the assumption that u is differentiable, which is necessary for the solution to be impulse-free, the system contains the subsystem (in x_1)

$$\begin{aligned} \dot{x}_1(t) &= (J_{\mathrm{p},r} - R_{\mathrm{p},r})x_1(t) + (G_{\mathrm{p},r} - P_{\mathrm{p},r})u(t), \\ y_{\mathrm{p},r}(t) &= (G_{\mathrm{p},r} + P_{\mathrm{p},r})^{\mathsf{T}}x_1(t) + (S_r - N_r)u(t) + LL^{\mathsf{T}}\dot{u}(t), \end{aligned}$$

where we have used the fact that $x_3(t) = -\dot{x}_2(t) = L^{\mathsf{T}}\dot{u}(t)$. This leads to the transfer function

$$H_r(s) = H_{\mathrm{p},r}(s) + LL^{\mathsf{T}} \cdot s,$$

with the proper part

$$H_{\mathrm{p},r}(s) = (G_{\mathrm{p},r} + P_{\mathrm{p},r})^{\mathsf{T}}(sI_r - (J_{\mathrm{p},r} - R_{\mathrm{p},r}))^{-1}(G_{\mathrm{p},r} - P_{\mathrm{p},r}) + (S_r - N_r).$$

The assertion follows from the fact that $H_{\mathrm{p},r}$ is the transfer function of the system in (6), which clearly fulfills the pH structure conditions. □

Remark 2. We highlight that this parameterization naturally carries over to pH-DAEs with a proper transfer function, i. e., with either index $\nu < 2$ or $G_4 = 0$. For these systems we have that $\ell = \mathrm{rank}(L) = 0$ and therefore it is sufficient to parameterize the system with a pH-ODE as in (6).

Remark 3. Note that for the subsystem corresponding to the proper part of the transfer function of $\Sigma_{\mathrm{p},r}(\theta)$, we assume that $E_{\mathrm{p},r}(\theta) = I_r$, which reduces the number of optimization parameters. This is not a restriction, since every pH-ODE system may be transformed into such a form using, for instance, the Cholesky factor of $E_{\mathrm{p},r}(\theta)$.

3.2. Computation of D_0 and D_1

To keep the $\mathcal{H}_\infty$ error between the FOM and ROM transfer functions bounded, the Markov parameter D_1 of the FOM transfer function must be matched exactly in the ROM. To obtain a bounded $\mathcal{H}_2$ error, both D_0 and D_1 must be matched exactly. Since our parameterization allows for the polynomial coefficients to be assigned and the remaining free parameters to be independently optimized, it remains to compute D_0 and D_1 efficiently for the FOM transfer function.

One approach is to determine D_0 and D_1 by the method outlined in [20], where these coefficients can be read off a block-Hankel matrix constructed using the solutions of two projected discrete-time Lyapunov equations. Another approach consists in transforming the FOM to the almost Kronecker canonical form derived in [36], see also Lemma 4 in the Appendix.

Alternative approaches determine D_0, D_1 by sampling the original transfer function H; hence these are independent of the specific representation of the FOM. Assume that two distinct imaginary sampling points $s_1 = \mathrm{i}\omega_1$, $s_2 = \mathrm{i}\omega_2$ with two sufficiently large values $\omega_1 \neq \omega_2$ are given. As shown in [41], we have that

$$\begin{aligned} H(\mathrm{i}\omega_1) - H(\mathrm{i}\omega_2) &= H_{\mathrm{sp}}(\mathrm{i}\omega_1) - H_{\mathrm{sp}}(\mathrm{i}\omega_2) + (\mathrm{i}\omega_1 - \mathrm{i}\omega_2)D_1 \\ &\approx (\mathrm{i}\omega_1 - \mathrm{i}\omega_2)D_1, \end{aligned}$$

which follows from $\lim_{s\to\infty} H_{\mathrm{sp}}(s) = 0$. We can then obtain an approximation for D_1 as

$$\widehat{D}_1 = \mathrm{Re}\left(\frac{H(\mathrm{i}\omega_1) - H(\mathrm{i}\omega_2)}{\mathrm{i}\omega_1 - \mathrm{i}\omega_2}\right).$$

Similarly, we have that

$$\frac{\mathrm{i}\omega_1 H(\mathrm{i}\omega_1) - \mathrm{i}\omega_2 H(\mathrm{i}\omega_2)}{\mathrm{i}\omega_1 - \mathrm{i}\omega_2} \approx D_0 + \mathrm{i}(\omega_1 + \omega_2)D_1,$$

which yields an approximation for D_0 given by

$$\widehat{D}_0 = \mathrm{Re}\left(\frac{\mathrm{i}\omega_1 H(\mathrm{i}\omega_1) - \mathrm{i}\omega_2 H(\mathrm{i}\omega_2)}{\mathrm{i}\omega_1 - \mathrm{i}\omega_2}\right).$$

The approximation quality generally depends on the choice of ω_1, ω_2, and we can adapt these sampling points in an iterative manner as in [42], until a certain tolerance is met. Another way of enhancing the accuracy is to include more than two sampling points, using the Loewner framework [41].

3.3. $\mathcal{H}_\infty$ Approximation

Since we assume that the pencil $sE - (J - R)$ is regular and its finite eigenvalues are in the open left half-plane, we can proceed as in [28] and obtain a good $\mathcal{H}_\infty$ approximation by minimizing, for decreasing values of $\gamma > 0$, the function

$$\mathcal{L}(\theta; H, \gamma, \mathcal{S}) := \frac{1}{\gamma} \sum_{s_i \in \mathcal{S}} \sum_{j=1}^{m} \left(\left[\sigma_j \left(H(s_i) - H_r(s_i, \theta) \right) - \gamma \right]_+ \right)^2 \tag{7}$$

with respect to θ, where

$$[\cdot]_+ : \mathbb{R} \to [0, \infty), \quad x \mapsto \begin{cases} x & \text{if } x \geq 0, \\ 0 & \text{if } x < 0. \end{cases}$$

Here, $\mathcal{S} \subset \mathrm{i}\mathbb{R}$ is a set of sample points at which the original and reduced transfer functions are evaluated and $\sigma_j(\cdot)$ denotes the jth singular value of its matrix argument.

Our procedure for the $\mathcal{H}_\infty$ approximation of pH-DAEs is described in Algorithm 1. It is based on repetitively minimizing $\mathcal{L}$ in conjunction with a bisection over γ. Note that $\mathcal{L}(\cdot; H, \gamma, \mathcal{S})$ attains its global minimum at zero when the error $\|H(s_i) - H_r(s_i)\|_2$ at all sample points $s_i \in \mathcal{S}$ is smaller than γ. The tolerance ε_2 that is used in line 7 of the algorithm is the maximum value of $\mathcal{L}$, which is still numerically interpreted as zero, such that γ is reduced in the subsequent bisection step. With appropriately chosen sample points (an adaptive sampling procedure is proposed in [43]), this in turn is an indication of $\|H - H_r(\cdot, \theta)\|_{\mathcal{H}_\infty} < \gamma$. Thus, finding the minimal γ (up to our bisection tolerance ε_1) such that $\mathcal{L}(\cdot; H, \gamma, \mathcal{S})$ can be minimized to zero (as in Algorithm 1) is a reasonable strategy for determining a ROM with a small $\mathcal{H}_\infty$ error. In [28], we discuss the further benefits of this general approach, also in comparison to a direct minimization of the $\mathcal{H}_\infty$ norm.

Algorithm 1: SOBMOR-$\mathcal{H}_\infty$.

Input : FOM transfer function H, initial ROM transfer function $H_r(\cdot, \theta_0)$ with parameter $\theta_0 \in \mathbb{R}^{n_\theta}$, initial sample point set $\mathcal{S} \subset \mathrm{i}\mathbb{R}$, upper bound $\gamma_{\mathrm{u}} > 0$, bisection tolerance $\varepsilon_1 > 0$, termination tolerance $\varepsilon_2 > 0$.

Output: Reduced order model as in Theorem 2 with parameter θ_{fin}.

1 Set $j := 0$ and $\gamma_{\mathrm{l}} := 0$.
2 Compute D_1 using either method in Section 3.2.
3 **while** $(\gamma_{\mathrm{u}} - \gamma_{\mathrm{l}})/(\gamma_{\mathrm{u}} + \gamma_{\mathrm{l}}) > \varepsilon_1$ **do**
4 Set $\gamma = (\gamma_{\mathrm{u}} + \gamma_{\mathrm{l}})/2$.
5 Update the sample point set $\mathcal{S}$ using [43, Alg. 3.1].
6 Solve the minimization problem

$$\begin{aligned} \alpha := \min_{\theta \in \mathbb{R}^{n_\theta}} \ & \mathcal{L}(\theta; H, \gamma, \mathcal{S}) \\ \text{s. t. } & \mathrm{vtf}_\ell(\theta_L)^{\mathsf{T}} \mathrm{vtf}_\ell(\theta_L) = D_1 \end{aligned}$$

  with minimizer $\theta_{j+1} \in \mathbb{R}^{n_\theta}$, initialized at θ_j.
7 **if** $\alpha > \varepsilon_2$ **then**
8 Set $\gamma_{\mathrm{l}} := \gamma$.
9 **else**
10 Set $\gamma_{\mathrm{u}} := \gamma$.
11 **end**
12 Set $j := j + 1$.
13 **end**
14 Set $\theta_{\mathrm{fin}} := \theta_j$.
15 Construct the ROM with θ_{fin} as in Theorem 2.

3.4. $\mathcal{H}_2$ Approximation

For $\mathcal{H}_2$-optimal model reduction, we first have to ensure that $H - H_r(\cdot, \theta)$ has a bounded $\mathcal{H}_2$ norm (see Section 3.2). Consequently, the polynomial parts of the FOM and the ROM transfer function must be equal. In addition to the condition that $L(\theta)L(\theta)^{\mathsf{T}} = D_1$, we also require that

$$N_r(\theta) = \frac{1}{2}(D_0^{\mathsf{T}} - D_0) = N_{\mathrm{p}}, \tag{8a}$$

$$S_r(\theta) = \frac{1}{2}(D_0^{\mathsf{T}} + D_0) = S_{\mathrm{p}}. \tag{8b}$$

Once D_0 and D_1 have been obtained using any of the methods in Section 3.2, we first have to fix all parameters in θ_N to enforce condition (8a). Once again we want to emphasize, that an exact matching of D_1 is required to avoid an unbounded $\mathcal{H}_\infty$ error, and matching D_0 and D_1 exactly is necessary for a bounded $\mathcal{H}_2$ error. Since we indirectly parameterize $S_r(\theta)$ via θ_W, let us analyze which parameters in θ_W have an impact on $S_r(\theta)$. For this, consider a partition of $\theta_W \in \mathbb{R}^{n_W}$ into $\theta_W =: \left[\theta_{W_1}^{\mathsf{T}}, \theta_{W_2}^{\mathsf{T}}\right]^{\mathsf{T}}$, where $\theta_{W_1} \in \mathbb{R}^{n_W - m(m+1)/2}$ and $\theta_{W_2} \in \mathbb{R}^{m(m+1)/2}$. Then we can decompose

$$\mathrm{vtu}(\theta_W) = \begin{bmatrix} \Xi_1 & \Xi_2 \\ 0 & \Xi_3 \end{bmatrix}, \tag{9}$$

where the matrices Ξ_1, Ξ_2 depend only on θ_{W_1}, and Ξ_3 depends only on θ_{W_2}. Since $S_r(\theta) = \Xi_3 \Xi_3^{\mathsf{T}}$, we can fix θ_{W_2} to enforce condition (8b) and the parameter vector which is subject to optimization reduces to $\theta := \left[\theta_J^{\mathsf{T}}, \theta_{W_1}^{\mathsf{T}}, \theta_G^{\mathsf{T}}\right]^{\mathsf{T}}$. The remaining $n_\theta - m(m + \ell)$ parameters in θ can be tuned to minimize the error $\|H - H_r(\cdot, \theta)\|_{\mathcal{H}_2}$ in the pole-residue

framework as originally proposed in [44] for unstructured LTI systems and extended to pH-ODE systems in [27].

Assume that the eigenvalues of $J_{\mathrm{p},r}(\theta) - R_{\mathrm{p},r}(\theta)$ are simple, and consider the spectral decomposition

$$(J_{\mathrm{p},r}(\theta) - R_{\mathrm{p},r}(\theta))Z(\theta) = Z(\theta)\Lambda(\theta), \tag{10}$$

where $\Lambda(\theta) = \operatorname{diag}(\lambda_1(\theta), \dots, \lambda_r(\theta))$ and $Z(\theta)$ is continuous in θ and contains the normalized right eigenvectors as columns. The transfer function $H_r(\cdot,\theta)$ may then be represented by the partial fraction expansion

$$H_r(s,\theta) = \sum_{i=1}^{r} \frac{c_i(\theta)b_i(\theta)^\mathsf{T}}{s - \lambda_i(\theta)} + S_r(\theta) - N_r(\theta) + L(\theta)L(\theta)^\mathsf{T} \cdot s,$$

where $c_i(\theta),\ b_i(\theta) \in \mathbb{C}^m$ with

$$c_i(\theta) = (G_{\mathrm{p},r}(\theta) + P_{\mathrm{p},r}(\theta))^\mathsf{T} Z(\theta) e_i,$$
$$b_i(\theta) = (G_{\mathrm{p},r}(\theta) - P_{\mathrm{p},r}(\theta))^\mathsf{T} Z(\theta)^{-\mathsf{T}} e_i,$$

and where e_i denotes the ith standard basis vector of $\mathbb{R}^r$. As shown in [44, Theorem 2.1], we may then express the $\mathcal{H}_2$ error by

$$\|H - H_r(\cdot,\theta)\|_{\mathcal{H}_2}^2 = \|H_{\mathrm{sp}}\|_{\mathcal{H}_2}^2 - 2\sum_{i=1}^{r} c_i(\theta)^\mathsf{T} H_{\mathrm{sp}}(-\lambda_i(\theta))b_i(\theta) + \sum_{j,k=1}^{r} \frac{c_j(\theta)^\mathsf{T} c_k(\theta) b_k(\theta)^\mathsf{T} b_j(\theta)}{-\lambda_j(\theta) - \lambda_k(\theta)},$$

where H_{sp} again denotes the strictly proper part of H. For an extension of the $\mathcal{H}_2$ optimization problem to higher-order poles, see [45].

Since $\|H_{\mathrm{sp}}\|_{\mathcal{H}_2}^2$ does not depend on θ, it can be neglected in the optimization. Consequently, we define the objective functional

$$\begin{aligned}\mathcal{F}(\theta; H) &:= \|H - H_r(\cdot,\theta)\|_{\mathcal{H}_2}^2 - \|H_{\mathrm{sp}}\|_{\mathcal{H}_2}^2 \\ &:= \widehat{\mathcal{F}}\Big(\big[c_1(\theta)^\mathsf{T}, \dots, c_r(\theta)^\mathsf{T}, b_1(\theta)^\mathsf{T}, \dots, b_r(\theta)^\mathsf{T}, \lambda_1(\theta)^\mathsf{T}, \dots, \lambda_r(\theta)^\mathsf{T}\big]^\mathsf{T}\Big) \\ &= \big(\widehat{\mathcal{F}} \circ q\big)(\theta),\end{aligned}$$

where

$$q(\theta) := \big[c_1(\theta)^\mathsf{T}, \dots, c_r(\theta)^\mathsf{T}, b_1(\theta)^\mathsf{T}, \dots, b_r(\theta)^\mathsf{T}, \lambda_1(\theta), \dots, \lambda_r(\theta)\big]^\mathsf{T} \in \mathbb{C}^{n_q}.$$

The eigenvalues $\lambda_i(\theta)$ and rank-one residues $c_i(\theta)b_i(\theta)^\mathsf{T}$ are functions of the parameter vector θ. If $\bar\theta \in \mathbb{R}^{n_\theta}$ is chosen such that all eigenvalues of $J_{p,r}(\bar\theta) - R_{p,r}(\bar\theta)$ are simple, then $\mathcal{F}$ is differentiable in a neighborhood of $\bar\theta$. Its derivative is obtained by applying the chain rule, i. e., with the differentiation operator D we obtain

$$\mathrm{D}\mathcal{F}(\bar\theta) = \big(\nabla\mathcal{F}(\bar\theta)\big)^\mathsf{T} = \mathrm{D}\widehat{\mathcal{F}}(q(\bar\theta)) \cdot \mathrm{D}q(\bar\theta),$$

with

$$\begin{aligned}\mathrm{D}\widehat{\mathcal{F}}(q(\bar\theta)) = \Big[&\mathrm{D}_{b_1}\widehat{\mathcal{F}}(q(\bar\theta)), \dots, \mathrm{D}_{b_r}\widehat{\mathcal{F}}(q(\bar\theta)), \mathrm{D}_{c_1}\widehat{\mathcal{F}}(q(\bar\theta)), \dots, \mathrm{D}_{c_r}\widehat{\mathcal{F}}(q(\bar\theta)), \dots \\ &\mathrm{D}_{\lambda_1}\widehat{\mathcal{F}}(q(\bar\theta)), \dots, \mathrm{D}_{\lambda_r}\widehat{\mathcal{F}}(q(\bar\theta))\Big] \in \mathbb{C}^{1\times n_q},\end{aligned}$$

and

$$\mathrm{D}q(\bar\theta) = \Big[\mathrm{D}_{\theta_1} q(\bar\theta), \dots, \mathrm{D}_{\theta_{n_\theta}} q(\bar\theta)\Big] \in \mathbb{C}^{n_q \times n_\theta}.$$

For all $i = 1, \dots, r$ it holds that

$$\mathrm{D}_{b_i}\widehat{\mathcal{F}}(q(\bar\theta)) = 2c_i(\bar\theta)^\mathsf{T}\big(H_r(-\lambda_i(\bar\theta)) - H(-\lambda_i(\bar\theta))\big),$$
$$\mathrm{D}_{c_i}\widehat{\mathcal{F}}(q(\bar\theta)) = 2b_i(\bar\theta)^\mathsf{T}\big(H_r(-\lambda_i(\bar\theta)) - H(-\lambda_i(\bar\theta))\big)^\mathsf{T},$$
$$\mathrm{D}_{\lambda_i}\widehat{\mathcal{F}}(q(\bar\theta)) = -2c_i(\bar\theta)^\mathsf{T}\big(H_r'(-\lambda_i(\bar\theta)) - H'(-\lambda_i(\bar\theta))\big)b_i(\bar\theta),$$

and we refer to [27] for the derivation of $\mathrm{D}q$.

Remark 4. The partial derivatives in $\mathrm{D}q(\bar\theta)$ may be computed efficiently with block-wise expressions. For instance, the derivative $\mathrm{D}_{\theta_G} c_i(\bar\theta) \in \mathbb{C}^{m\times r\cdot m}$ can be computed as

$$\mathrm{D}_{\theta_G} c_i(\bar\theta) = \begin{bmatrix} z_i(\bar\theta)^\mathsf{T} & 0 & \dots & 0 \\ 0 & \ddots & \ddots & \vdots \\ \vdots & \ddots & \ddots & 0 \\ 0 & \dots & 0 & z_i(\bar\theta)^\mathsf{T} \end{bmatrix} = I_m \otimes z_i(\bar\theta)^\mathsf{T},$$

where $z_i(\bar\theta) \in \mathbb{C}^r$ denotes the ith column in $Z(\bar\theta)$. This is also the case for the other parts of $\mathrm{D}q(\bar\theta)$.

Let us highlight some important advantages of the pole-residue framework compared to recently proposed methods that are formulated in the Lyapunov framework (see [46,47]), in particular for pH-DAEs. These methods require the solution of large-scale Lyapunov equations for the evaluation of $\mathcal{F}$ and its gradient. Currently no structure-preserving Lyapunov-based methods exist for pH-DAEs; see [48] for new Lyapunov-based formulations of pH-DAEs. If the strictly proper part of the transfer function can be easily decoupled from the polynomial part, the existing methods for pH-ODEs may be applied to this part. However, if the splitting into the strictly proper and polynomial part must first be computed via a factorization method (see, e.g., [36]), then the sparsity patterns of the original pH-DAE may be lost which complicates the repetitive solution of Lyapunov equations for these systems in the large-scale setting. In contrast, an optimization in the pole-residue framework only requires the solution of the reduced-order eigenvalue problem in (10) as well as r evaluations of H_{sp} at $-\lambda_i(\theta)$. Note that to evaluate H_{sp}, we do not require a state-space representation of the strictly proper part. Instead, we *indirectly* evaluate H_{sp} by

$$H_{\mathrm{sp}}(s) = H(s) - \mathcal{D}_0 - \mathcal{D}_1 \cdot s \tag{11}$$

for all $s \in \mathbb{C}$. Consequently, we may work directly with the sparse matrices of the original pH-DAE and do not require the solution of large-scale matrix equations.

Algorithm 2: PROPT-$\mathcal{H}_2$

Input : FOM transfer function H, reduced order $r \in \mathbb{N}$.
Output: Reduced-order model as in Theorem 2 with parameter θ_{fin}.

1 Compute $\mathcal{D}_0$, $\mathcal{D}_1$ (see Section 3.2).
2 Initialize θ_0 s. t. $S_r(\theta_0) - N_r(\theta_0) = \mathcal{D}_0$ and $L(\theta_0)L(\theta_0)^\mathsf{T} = \mathcal{D}_1$.
3 Solve

$$\theta_{\mathrm{fin}} = \operatorname*{arg\,min}_{\theta\in\mathbb{R}^{n_\theta}} \mathcal{F}(\theta; H) \quad \text{s. t. } S_r(\theta) - N_r(\theta) = \mathcal{D}_0,\ L(\theta)L(\theta)^\mathsf{T} = \mathcal{D}_1.$$

Construct the ROM with θ_{fin} as in Theorem 2.

We summarize our approach for $\mathcal{H}_2$ optimization called *Pole-Residual Optimization* (PROPT) in Algorithm 2. Since the $\mathcal{H}_2$ optimization problem is non-convex, the choice of the initial parameter vector θ_0 will generally impact the fidelity of the final ROM obtained by Algorithm 2. Simple initialization strategies are, for instance, choosing θ_0 randomly or using IRKA-PH (see [27,46]), which generally converges very quickly. Here, we propose another approach that may use *unstructured* ROMs for initialization which is based on the following parameterization.

Lemma 3. *Let $(\widetilde A, \widetilde B, \widetilde C, \widetilde D)$ be a reduced-order ODE system with state-space dimension r such that $\widetilde D = S_{\mathrm{p}} - N_{\mathrm{p}}$ and $\widetilde A$ has eigenvalues $\widetilde\lambda_i$ in the open left half of the complex plane for all $i = 1, \dots, r$. Let $\theta_G \in \mathbb{R}^{r\cdot m}$ and $\theta_K \in \mathbb{R}^{r\cdot p}$ be two parameter vectors and define the matrix-valued functions*

$$\widetilde G_{\mathrm{p},r}(\theta_G) := \mathrm{vtf}_m(\theta_G),$$
$$\widetilde K_{\mathrm{p},r}(\theta_K) := \mathrm{vtf}_p(\theta_K).$$

Let $\widetilde E_{\mathrm{p},r}(\theta_K) > 0$ solve the Lyapunov equation

$$\widetilde A^\mathsf{T}\widetilde E_{\mathrm{p},r}(\theta_K) + \widetilde E_{\mathrm{p},r}(\theta_K)\widetilde A + \widetilde K_{\mathrm{p},r}(\theta_K)\widetilde K_{\mathrm{p},r}(\theta_K)^\mathsf{T} = 0, \tag{12}$$

and define

$$\widetilde J_{\mathrm{p},r}(\theta_K) = \frac{1}{2}\Big(\widetilde E_{\mathrm{p},r}(\theta_K)\widetilde A - \widetilde A^\mathsf{T}\widetilde E_{\mathrm{p},r}(\theta_K)\Big),$$

$$\widetilde{R}_{\mathrm{p},r}(\theta_K) = -\frac{1}{2}\left(\widetilde{E}_{\mathrm{p},r}(\theta_K)\widetilde{A} + \widetilde{A}^{\mathsf{T}}\widetilde{E}_{\mathrm{p},r}(\theta_K)\right).$$

Then the parametric system

$$\widetilde{E}_{\mathrm{p},r}(\theta_K)\dot{x}_1(t) = \left(\widetilde{J}_{\mathrm{p},r}(\theta_K) - \widetilde{R}_{\mathrm{p},r}(\theta_K)\right)x_1(t) + \widetilde{G}_{\mathrm{p},r}(\theta_G)u(t),$$
$$y_{\mathrm{p},r}(t) = \widetilde{G}_{\mathrm{p},r}(\theta_G)^{\mathsf{T}}x_1(t) + (S_{\mathrm{p}} - N_{\mathrm{p}})u(t),$$

is an implicit pH-ODE system and the matrix pencil $s\widetilde{E}_{\mathrm{p},r}(\theta_K) - \left(\widetilde{J}_{\mathrm{p},r}(\theta_K) - \widetilde{R}_{\mathrm{p},r}(\theta_K)\right)$ *has the same eigenvalues as* $\widetilde{A}$.

Proof. The proof follows immediately from [49, Lemma 2]. □

Let $\widetilde{H}$ denote the transfer function of the (possibly unstructured) ROM $\left(\widetilde{A}, \widetilde{B}, \widetilde{C}, \widetilde{D}\right)$ with $\widetilde{H}(s) = \sum_{i=1}^{r} \frac{\widetilde{c}_i\widetilde{b}_i^{\mathsf{T}}}{s-\widetilde{\lambda}_i} + S_{\mathrm{p}} - N_{\mathrm{p}}$ and $\widetilde{c}_i, \widetilde{b}_i \in \mathbb{C}^m$. Based on the parameterization in Lemma 3, we can then compute an initial pH model by minimizing the weighted sum of squared errors between the residuals in the Frobenius norm, i. e.,

$$\mathcal{F}_0(\theta_G, \theta_K) := \sum_{i=1}^{r} \frac{1}{|\widetilde{\lambda}_i|}\left\|\widetilde{c}_i\widetilde{b}_i^{\mathsf{T}} - c_i(\theta_G)b_i(\theta_G, \theta_K)^{\mathsf{T}}\right\|_{\mathrm{F}}^2,$$

where

$$c_i(\theta_G) = \widetilde{G}_{\mathrm{p},r}(\theta_G)^{\mathsf{T}}\widetilde{Z}e_i,$$
$$b_i(\theta_G, \theta_K) = \widetilde{G}_{\mathrm{p},r}(\theta_G)^{\mathsf{T}}\widetilde{E}_{\mathrm{p},r}(\theta_K)^{-\mathsf{T}}\widetilde{Z}^{-\mathsf{T}}e_i,$$

for $i = 1, \ldots, r$ and $\widetilde{Z}$ is, again, under a generic diagonalizability assumption, obtained from the spectral decomposition

$$\widetilde{A}\widetilde{Z} = \widetilde{Z}\widetilde{\Lambda},$$

with $\widetilde{\Lambda} = \mathrm{diag}(\widetilde{\lambda}_1, \ldots, \widetilde{\lambda}_r)$.

Note that the computation of the gradient of $\mathcal{F}_0$ is very simple, since it does not involve a differentiation of the eigenvalues or eigenvectors. While the partial gradients of $c_i(\cdot)$ and $b_i(\cdot,\cdot)$ with respect to θ_G are straightforward, the partial gradients of $\widetilde{E}_{\mathrm{p},r}(\cdot)$ with respect to the lth entry in θ_K is the solution of the (reduced-order) Lyapunov equation

$$\widetilde{A}^{\mathsf{T}}\frac{\partial\widetilde{E}_{\mathrm{p},r}(\theta_K)}{\partial\theta_{K,l}} + \frac{\partial\widetilde{E}_{\mathrm{p},r}(\theta_K)}{\partial\theta_{K,l}}\widetilde{A} \,\mathrm{vtf}_p(e_l)\widetilde{K}_{\mathrm{p},r}(\theta_K)^{\mathsf{T}} + \widetilde{K}_{\mathrm{p},r}(\theta_K)\,\mathrm{vtf}_p(e_l)^{\mathsf{T}} = 0,$$

where e_l denotes the lth standard basis vector of $\mathbb{R}^{r\cdot p}$. As the number of optimization parameters is reduced to $r(p+m)$, this initialization generally converges very quickly. Note that improper parts of the original transfer function can be incorporated as in Theorem 2. In combination with Algorithm 2, this enables a *two-step* approach with a more restrictive (yet simpler) pre-optimization of only the residues and a subsequent (more complex) optimization of all system matrices.

Remark 5. The computational burden of our two different methods is influenced by different factors. Similar to IRKA-PH, in large-scale settings the computational cost of PROPT-$\mathcal{H}_2$ is dominated by r solves of sparse, large-scale linear systems per iteration to evaluate the FOM transfer function. For SOBMOR-$\mathcal{H}_\infty$, the transfer function evaluations can be cached for subsequent iterations since the sample set $\mathcal{S}$ only changes as γ is updated. Here the main computational cost is the repeated evaluation of the ROM transfer function for each iteration of the optimization in line 6 of Algorithm 1 for all sample points in $\mathcal{S}$.

4. Numerical examples

We illustrate the properties of our new methods using several numerical tests based on well-known benchmark examples. We test our methods for systems with $\nu = 1$ and $\nu = 2$ as well as strictly proper, proper, and improper transfer functions. Our numerical examples are published via Zenodo[4] and the algorithms used in this comparison are provided as part of a MATLAB toolbox.[5]

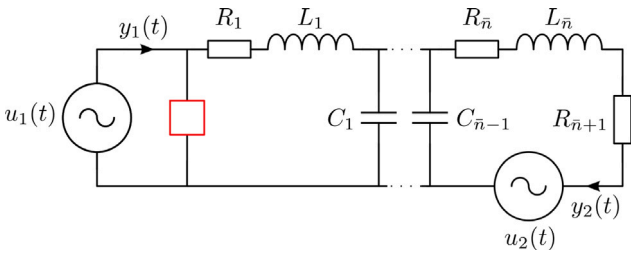

Fig. 1. RCL ladder network.

Table 1
Dimensions of benchmark systems.

Model name	n_2	n_3	$n_4 = n_1$	n	m
`Oseen-2-S`	81	0	99	279	1
`Oseen-2-L`	2401	0	2499	7399	1
`RCL-1-SISO`	999	503	0	1502	1
`RCL-1-MIMO`	19 999	10 005	0	30 004	2
`RCL-2-SISO`	999	501	1	1502	1

4.1. Benchmark models

The first type of systems that we consider model the instationary flow of incompressible fluids on the spatial domain $\Omega = (0,1)^2$ with the boundary $\partial\Omega$ and time interval $[0,T]$ as in [50]. The flow is modeled by the Oseen equation

$$\partial_t v = -(a\cdot\nabla)v + \mu\Delta v - \nabla p + f, \qquad \text{in } \Omega\times(0,T],$$
$$0 = \mathrm{div}\, v, \qquad \text{in } \Omega\times(0,T],$$

with velocity vector v, pressure p, viscosity $\mu > 0$, external forces f and a convective term with driving velocity a. As shown in [50], spatial semi-discretization of the Oseen equations by a finite difference method with associated no-slip boundary conditions and initial velocity $v_0 \in \mathbb{R}^2$, i. e.,

$$v = 0 \qquad \text{on } \partial\Omega\times(0,T],$$
$$v = v_0 \qquad \text{in } \Omega\times\{0\},$$

leads to a pH-DAE of index two. However, a transformation to the staircase form of Lemma 1 reveals that $n_3 = 0$. Additionally, we have that $G_4 = 0$, which makes the transfer function H strictly proper. We consider two models: `Oseen-2-S` with $n = 279$ and `Oseen-2-L` with $n = 7399$.

Our second type of systems are RCL circuits modeled by directed graphs as described in [51]. These relate to RCL ladder networks as shown in Fig. 1, which are part of the software package PortHamiltonianBenchmarkSystems.[6] Here, $\bar{n}$ denotes the number of loops in the system. If we choose the supplied voltages $[u_1, u_2]^{\mathsf{T}}$ as inputs and the currents $[y_1, y_2]^{\mathsf{T}}$ as outputs, we directly obtain a pH-DAE model as in (1), where the algebraic equations of the model reflect Kirchhoff's voltage law. We generate different types of systems with the setup in Fig. 1. To generate single-input single-output systems, we remove the voltage source u_2 and corresponding output y_2. To generate systems with index $\nu = 1$, we replace the red box next to the voltage source u_1 by a resistor R_0 and to obtain a system with index $\nu = 2$, we use a capacitor C_0 in its place. Our index-one RCL systems have a proper transfer function and our index-two RCL system has an improper transfer function.

The properties of our benchmark systems are described in Fig. 2 and Table 1. The maximum singular values of the transfer functions of the FOMs are shown in Fig. 2. The dimensions of our benchmark

[4] Available at: https://zenodo.org/record/7636424.
[5] Available at: https://github.com/MORLab/MORpH.
[6] https://algopaul.github.io/PortHamiltonianBenchmarkSystems.jl/RclCircuits/

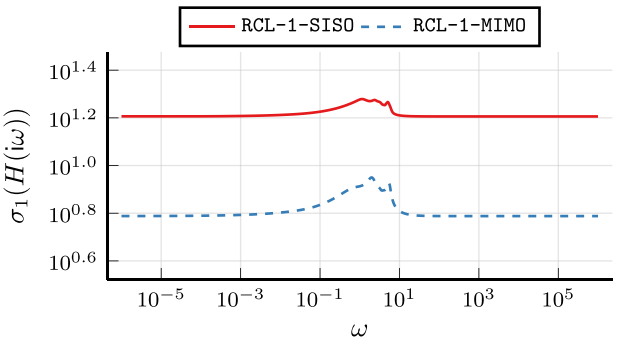

(a) Benchmark systems with $\nu = 1$

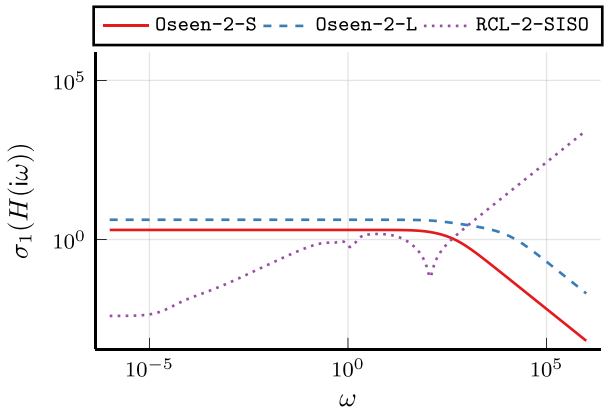

(b) Benchmark systems with $\nu = 2$

Fig. 2. Maximum singular values of considered FOM transfer functions.

systems partitioned according to the staircase form from Lemma 1 are given in Table 1. In the following, we compare the approximation errors obtained with our methods SOBMOR-$\mathcal{H}_\infty$ and PROPT-$\mathcal{H}_2$ to the DAE variants of IRKA-PH in [17] and PRBT [19].

4.2. Results

Let us first consider the results for the strictly proper `Oseen-2-S` model, shown in Figs. 3(a) and (b). It can be observed that both PROPT-$\mathcal{H}_2$ and SOBMOR-$\mathcal{H}_\infty$ lead to more accurate models in both the $\mathcal{H}_2$ and the $\mathcal{H}_\infty$ norms compared to IRKA-PH, especially when the reduced model order is increasing. Compared with PRBT, SOBMOR-$\mathcal{H}_\infty$ leads to slightly smaller $\mathcal{H}_\infty$ errors except for $r = 10$, while PROPT-$\mathcal{H}_2$ leads to slightly smaller $\mathcal{H}_2$ errors up to reduced orders of 8. Note that SOBMOR-$\mathcal{H}_\infty$ computes ROMs with an unbounded $\mathcal{H}_2$ error,[7] since it does not match D_0 and allows for an optimization of the (constant) feedthrough. Only D_1 must be matched exactly, when $\mathcal{H}_\infty$ approximations are computed.

Fig. 4 shows the results for the `Oseen-2-L` model; we show the maximum singular values of the error transfer functions, which we call *frequency response errors*, since the high FOM system dimension makes a computation of the $\mathcal{H}_\infty$ and $\mathcal{H}_2$ errors computationally prohibitively expensive. Our findings are comparable to the smaller `Oseen-2-S` model: The error transfer functions of IRKA-PH, PRBT, and PROPT-$\mathcal{H}_2$ are similar for the small reduced model order $r = 5$, while for $r = 10$, the PROPT-$\mathcal{H}_2$ and PRBT errors are clearly smaller than the error of the IRKA-PH model across a wide frequency range. SOBMOR-$\mathcal{H}_\infty$ aims at minimizing the maximum error across all frequencies and it can be observed that the frequency response errors of the SOBMOR-$\mathcal{H}_\infty$ ROMs are well below the maximum errors of the ROMs obtained with the other methods for both reduced orders. The frequency response errors are in fact nearly constant, which is a sign for a good rational $\mathcal{H}_\infty$ approximation; see [52].

We continue with the results on the RCL systems `RCL-1-SISO` and `RCL-1-MIMO` that have proper transfer functions. We report the $\mathcal{H}_\infty$ accuracy of the considered methods for `RCL-1-SISO` in Figs. 5(a). It can be seen that SOBMOR-$\mathcal{H}_\infty$ achieves the highest $\mathcal{H}_\infty$ accuracy for all reduced model orders. The second best overall accuracy is obtained by PRBT. The $\mathcal{H}_2$ methods PROPT-$\mathcal{H}_2$ and IRKA-PH have a worse $\mathcal{H}_\infty$ performance, as it is to be expected. However, we note that there is a huge difference in terms of accuracy, when comparing IRKA-PH to all the other methods for larger reduced model orders. The $\mathcal{H}_2$ errors, reported in Figs. 5(b), exhibit a less distinct behavior but PROPT-$\mathcal{H}_2$ leads to the lowest $\mathcal{H}_2$ errors for all reduced model orders. Again, it can be clearly seen that IRKA-PH has the worst accuracy for larger reduced model orders.

In Fig. 6, we report the error transfer functions between `RCL-1-MIMO` and the ROMs obtained with IRKA-PH, PRBT, and our proposed methods. Again, the exact computation of $\mathcal{H}_\infty$ or $\mathcal{H}_2$ errors is computationally prohibitive due to the vast system dimension of `RCL-1-MIMO`. The error transfer functions indicate that our methods continue to work as intended also in the MIMO case. In particular, SOBMOR-$\mathcal{H}_\infty$ leads to a flat error curve in the sigma plot, which has its highest peak value well-below the other errors and PROPT-$\mathcal{H}_2$ and PRBT have error transfer functions that are below the error of IRKA-PH over the entire imaginary axis and below the error of SOBMOR-$\mathcal{H}_\infty$ for higher frequencies.

Finally, we report the results of our experiments on `RCL-2-SISO`, which has an improper transfer function. Therefore, we only compare our methods to PRBT, since IRKA-PH is not applicable to improper systems. The results are shown in Figs. 7(a) and (b). Again, SOBMOR-$\mathcal{H}_\infty$ leads to the smallest $\mathcal{H}_\infty$ errors for all reduced model orders, while PROPT-$\mathcal{H}_2$ leads to the smallest $\mathcal{H}_2$ errors for all reduced model orders except $r = 20$.

5. Conclusion

We have presented a flexible MOR approach for $\mathcal{H}_2$ and $\mathcal{H}_\infty$ approximation of higher index pH-DAEs. Our approach is based on a novel parameterization that can provide a pH realization for any pH descriptor system with an efficient representation of the algebraic part. An adaptation of previously developed optimization-based MOR methods allows for the approximation of potentially improper transfer functions. A comparison to state-of-the-art methods shows that our optimization-based approach leads to accurate ROMs that are guaranteed to fulfill the pH structural constraints.

CRediT authorship contribution statement

Paul Schwerdtner: Conceptualization, Methodology, Software, Data curation, Writing – original draft, Visualization. **Tim Moser:** Conceptualization, Methodology, Software, Data curation, Writing – original draft, Visualization. **Volker Mehrmann:** Conceptualization, Writing – review & editing, Supervision. **Matthias Voigt:** Conceptualization, Writing – review & editing, Supervision, Funding acquisition.

Declaration of competing interest

The authors declare that they have no known competing financial interests or personal relationships that could have appeared to influence the work reported in this paper.

[7] More precisely, the error transfer function is not in the Hardy space $\mathcal{H}_2^{m\times m}$.

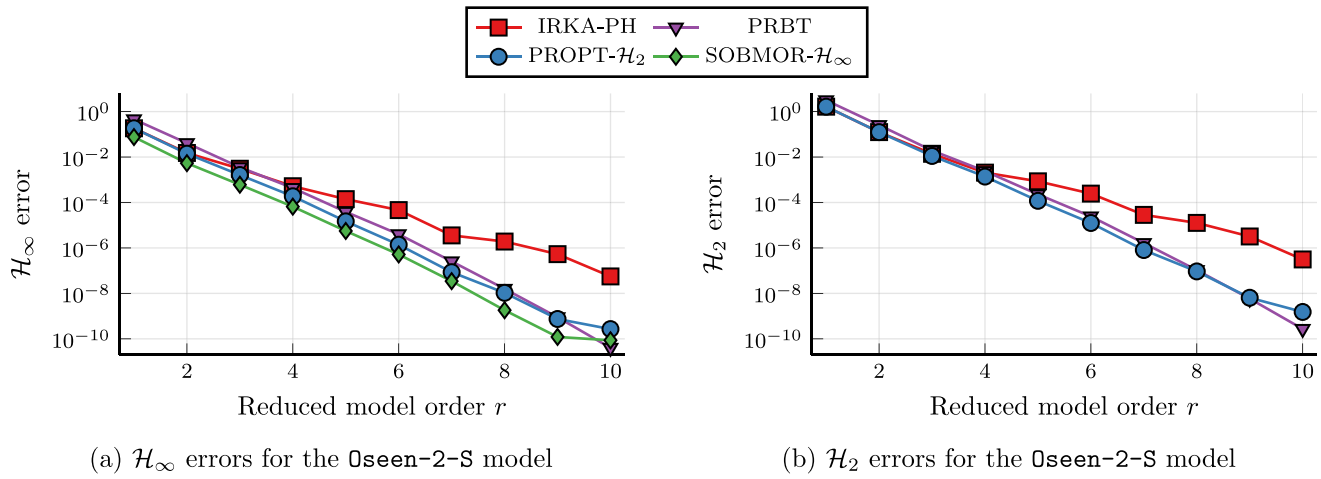

(a) $\mathcal{H}_\infty$ errors for the `Oseen-2-S` model

(b) $\mathcal{H}_2$ errors for the `Oseen-2-S` model

Fig. 3. $\mathcal{H}_\infty$ and $\mathcal{H}_2$ error comparison for the `Oseen-2-S` model.

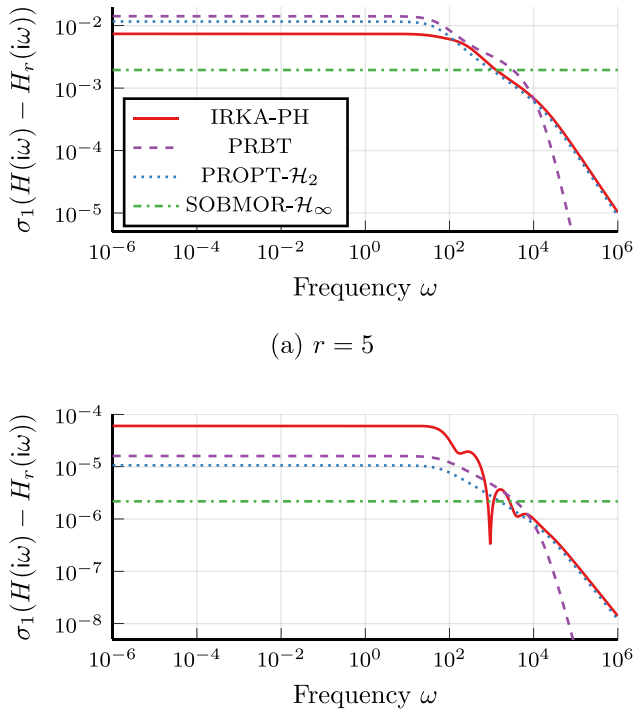

(a) $r = 5$

(b) $r = 10$

Fig. 4. Frequency response errors (measured by the maximum singular value) for the `Oseen-2-L` model.

Data availability

We provide an implementation of our algorithms in the MORpH toolbox, available at https://github.com/MORLab/MORpH .

Acknowledgment

We thank Serkan Gugercin (Virginia Tech) for providing the Matlab code to generate the Oseen models.

Appendix

The following Kronecker-like form was derived in [36], based on the staircase form.

Lemma 4. *Consider a regular pH-DAE in staircase form (2) and define* $\widetilde{A} := \widetilde{J} - \widetilde{R}$, $\widetilde{B} := \widetilde{G} - \widetilde{P}$, $\widetilde{C} := (\widetilde{G} + \widetilde{P})^\mathsf{T}$, $\widetilde{D} := \widetilde{S} - \widetilde{N}$. *Then there exist nonsingular matrices* $T_1, T_2 \in \mathbb{R}^{n\times n}$ *such that the pH-DAE may be transformed to a general linear time-invariant system of the form*

$$\begin{aligned} \check{E}\dot{\check{x}}(t) &= \check{A}\check{x}(t) + \check{B}u(t), \\ y(t) &= \check{C}\check{x}(t) + \check{D}u(t), \end{aligned} \tag{13}$$

where

$$\check{E} := T_1\widetilde{E}T_2 = \begin{bmatrix} \check{E}_{11} & 0 & 0 & 0 \\ 0 & \check{E}_{22} & 0 & 0 \\ 0 & 0 & 0 & 0 \\ 0 & 0 & 0 & 0 \end{bmatrix},$$

$$\check{A} := T_1\widetilde{A}T_2 = \begin{bmatrix} 0 & 0 & 0 & I_{n_1} \\ 0 & \check{A}_{22} & 0 & 0 \\ 0 & 0 & I_{n_3} & 0 \\ -I_{n_4} & 0 & 0 & 0 \end{bmatrix},$$

$$\check{B} := T_1\widetilde{B} = \begin{bmatrix} \check{B}_1 \\ \check{B}_2 \\ \check{B}_3 \\ \check{B}_4 \end{bmatrix}, \quad \check{C} := \widetilde{C}T_2 = \begin{bmatrix} \check{C}_1^\mathsf{T} \\ \check{C}_2^\mathsf{T} \\ \check{C}_3^\mathsf{T} \\ \check{C}_4^\mathsf{T} \end{bmatrix}^\mathsf{T}$$

and $\check{D} = \widetilde{D}$. *The matrices are partitioned in the same way as in Lemma 1 and, if present, the diagonal block matrices* $\check{E}_{11}, \check{E}_{22}$ *are symmetric positive definite.*

Proof of Theorem 1. Considering the transformed system (13) and a block diagonalization of $s\check{E} - \check{A}$ yield the transfer function

$$H(s) = \check{C}_2(s\check{E}_{22} - \check{A}_{22})^{-1}\check{B}_2 + D_0 + D_1 \cdot s,$$

where

$$\begin{aligned} D_0 &= \check{D} + \check{C}_1\check{B}_4 - \check{C}_3\check{B}_3 - \check{C}_4\check{B}_1, \\ D_1 &= \check{C}_4\check{E}_{11}\check{B}_4, \end{aligned}$$

which reveals the split into the proper and improper parts, respectively. From the definition of T_1, T_2 in [36] we have that

$$\begin{aligned} \check{E}_{11} &= \widetilde{E}_{11} - \widetilde{E}_{12}\widetilde{E}_{22}^{-1}\widetilde{E}_{21} > 0, \\ \check{B}_4 &= -\widetilde{A}_{41}^{-1}\widetilde{B}_4 = J_{14}^{-\mathsf{T}}G_4, \\ \check{C}_4 &= \widetilde{C}_4\widetilde{A}_{14}^{-1} = G_4^\mathsf{T}J_{14}^{-1} = \check{B}_4^\mathsf{T}, \end{aligned}$$

which proves that $D_1 = \check{C}_4\check{E}_{11}\check{B}_4 = D_1^\mathsf{T} \geq 0$. For $n_2 = 0$, the claim follows immediately from $H(0) + H(0)^\mathsf{H} = D_0 + D_0^\mathsf{T} \geq 0$. Now let us consider the case where $n_2 > 0$. We first assume that $n_3 > 0$. The remaining block matrices from (13) are then given by

$$\check{E}_{22} = \widetilde{E}_{22},$$

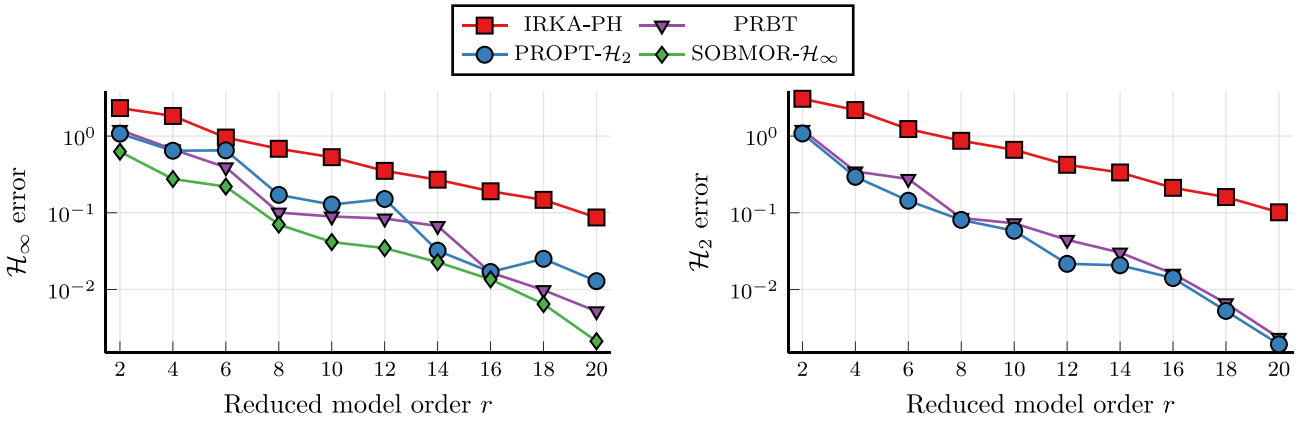

(a) $\mathcal{H}_\infty$ errors for the `RCL-1-SISO` model (b) $\mathcal{H}_2$ errors for the `RCL-1-SISO` model

Fig. 5. $\mathcal{H}_\infty$ and $\mathcal{H}_2$ error comparison for the `RCL-1-SISO` model.

$$
\begin{aligned}
\check{A}_{22} &= \widetilde{A}_{22} - \widetilde{A}_{23}\widetilde{A}_{33}^{-1}\widetilde{A}_{32},\\
\check{B}_1 &= \widetilde{B}_1 - \widetilde{A}_{13}\widetilde{A}_{33}^{-1}\widetilde{B}_3 + (-\widetilde{A}_{11} + \widetilde{A}_{13}\widetilde{A}_{33}^{-1}\widetilde{A}_{31})\widetilde{A}_{41}^{-1}\widetilde{B}_4,\\
\check{B}_2 &= \widetilde{B}_2 - \widetilde{A}_{23}\widetilde{A}_{33}^{-1}\widetilde{B}_3 + (-\widetilde{A}_{21} + \widetilde{A}_{23}\widetilde{A}_{33}^{-1}\widetilde{A}_{31})\widetilde{A}_{41}^{-1}\widetilde{B}_4,\\
\check{B}_3 &= \widetilde{A}_{33}^{-1}\widetilde{B}_3 - \widetilde{A}_{33}^{-1}\widetilde{A}_{31}\widetilde{A}_{41}^{-1}\widetilde{B}_4,\\
\check{C}_1 &= \widetilde{C}_1,\\
\check{C}_2 &= \widetilde{C}_2 - \widetilde{C}_3\widetilde{A}_{33}^{-1}\widetilde{A}_{32} + \widetilde{C}_4\widetilde{A}_{14}^{-1}(-\widetilde{A}_{12} + \widetilde{A}_{13}\widetilde{A}_{33}^{-1}\widetilde{A}_{32}),\\
\check{C}_3 &= \widetilde{C}_3,
\end{aligned}
$$

which again follows from the definition of T_1, T_2 in [36]. Define the matrices $\widetilde{\Gamma}, \widetilde{W} \in \mathbb{R}^{(n+m)\times(n+m)}$

$$
\begin{aligned}
\widetilde{\Gamma} &:= \begin{bmatrix} -\widetilde{J} & -\widetilde{G} \\ \widetilde{G}^\mathsf{T} & -\widetilde{N} \end{bmatrix} = -\widetilde{\Gamma}^\mathsf{T},\\
\widetilde{W} &:= \begin{bmatrix} \widetilde{R} & \widetilde{P} \\ \widetilde{P}^\mathsf{T} & \widetilde{S} \end{bmatrix} \quad = \widetilde{W}^\mathsf{T} \geq 0,
\end{aligned}
$$

and let the matrices be partitioned as in Lemma 1. Our proof is based on the observation that

$$
\begin{bmatrix} -\widetilde{A} & -\widetilde{B} \\ \widetilde{C} & \widetilde{D} \end{bmatrix} = \begin{bmatrix} -(\widetilde{J} - \widetilde{R}) & -(\widetilde{G} - \widetilde{P}) \\ (\widetilde{G} + \widetilde{P})^\mathsf{T} & \widetilde{S} - \widetilde{N} \end{bmatrix} = \widetilde{\Gamma} + \widetilde{W}.
$$

This is a natural generalization of a similar observation for linear dissipative Hamiltonian systems (see [37]) to port-Hamiltonian systems with power-collocated input–output pairs. We will now show that such a decomposition into skew-symmetric and symmetric positive semidefinite parts not only exists for the proper subsystem as well but may be obtained by *structure-preserving* manipulations of the sum $\widetilde{\Gamma} + \widetilde{W}$.

At first, let $P_\pi \in \mathbb{R}^{(n+m)\times(n+m)}$ define a permutation matrix which permutes the third and fifth block rows and columns in the sum $\widetilde{\Gamma} + \widetilde{W}$ such that

$$
\Psi = P_\pi^\mathsf{T}\big(\widetilde{\Gamma} + \widetilde{W}\big)P_\pi = \begin{bmatrix} \Psi_{\mathrm{uu}} & \Psi_{\mathrm{ul}} \\ \Psi_{\mathrm{lu}} & \Psi_{\mathrm{ll}} \end{bmatrix},
$$

with $\Psi_{\mathrm{ll}} = -\widetilde{J}_{33} + \widetilde{R}_{33} = -\widetilde{A}_{33}$. Since the matrix $\widetilde{A}_{33}$ is nonsingular, we may block-diagonalize Ψ with invertible matrices $X_1 = \left[\begin{smallmatrix} I_n & \Psi_{\mathrm{ul}}\Psi_{\mathrm{ll}}^{-1} \\ 0 & I_m \end{smallmatrix}\right]$, $X_2 = \left[\begin{smallmatrix} I_n & 0 \\ \Psi_{\mathrm{ll}}^{-1}\Psi_{\mathrm{lu}} & I_m \end{smallmatrix}\right] \in \mathbb{R}^{(n+m)\times(n+m)}$ such that

$$
\Xi = X_1 \Psi X_2 = \begin{bmatrix} \Psi_{\mathrm{uu}} - \Psi_{\mathrm{ul}}\Psi_{\mathrm{ll}}^{-1}\Psi_{\mathrm{lu}} & 0 \\ 0 & \Psi_{\mathrm{ll}} \end{bmatrix}.
$$

Note that Ξ still has a positive semidefinite symmetric part since the Schur complement preserves this property [37, Corollary 4.3]. Finally, it is easy to show that we may compute the proper system matrices via

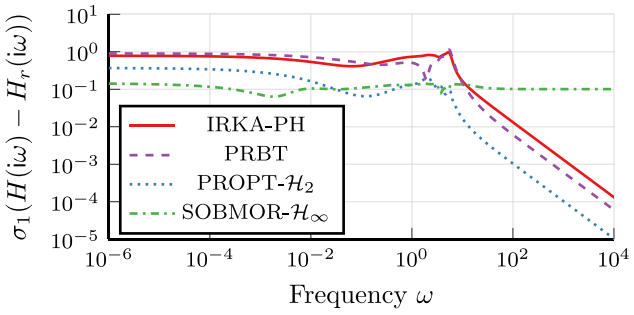

(a) $r = 10$

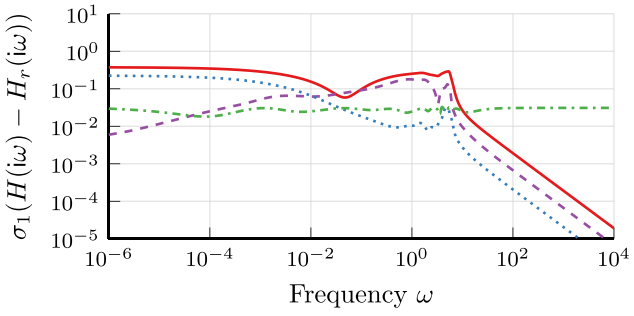

(b) $r = 20$

Fig. 6. Frequency response errors (measured by the maximum singular value) for the `RCL-1-MIMO` model.

a transformation of Ξ with the full-rank matrix $U \in \mathbb{R}^{(n+m)\times(n_2+m)}$ such that

$$
\begin{bmatrix} -\check{A}_{22} & -\check{B}_2 \\ \check{C}_2 & D_0 \end{bmatrix} = U^\mathsf{T}\Xi U, \text{ where } U = \begin{bmatrix} 0 & \check{B}_4 \\ I_m & 0 \\ 0 & I_{n_2} \\ 0 & 0 \\ 0 & 0 \end{bmatrix}.
$$

Hence, we obtain the proper system matrices by a series of permutations, block-diagonalization via Schur complements and congruence transformations of $\widetilde{\Gamma} + \widetilde{W}$. Since each of these manipulations preserves the positive semidefiniteness of the symmetric part, we obtain

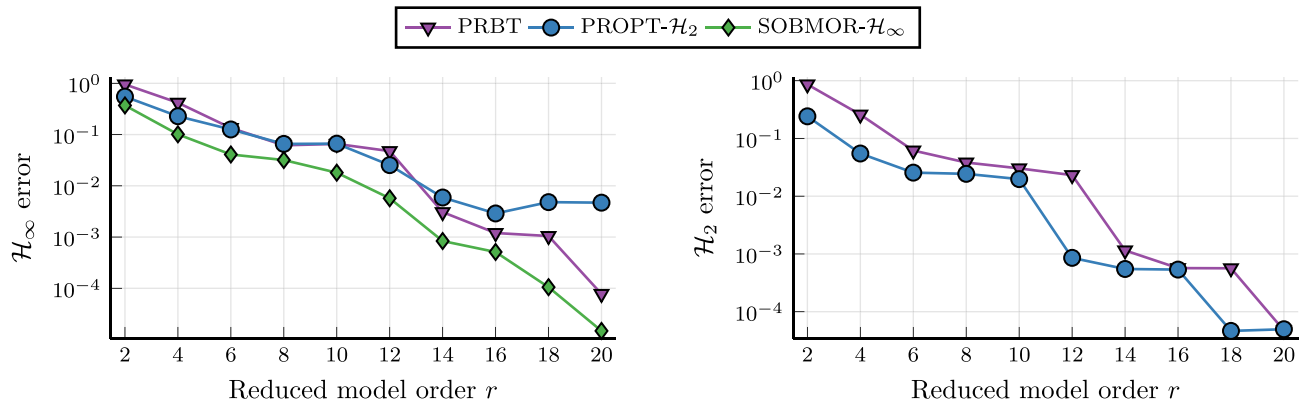

(a) $\mathcal{H}_\infty$ errors for the RCL-2-SISO model (b) $\mathcal{H}_2$ errors for the RCL-2-SISO model

Fig. 7. $\mathcal{H}_\infty$ and $\mathcal{H}_2$ error comparison for the RCL-2-SISO model. Here we denote by r the order of the dynamic parts of the ROMs.

a port-Hamiltonian representation of the proper subsystem via

$$\begin{bmatrix} -J_\mathrm{p} & -G_\mathrm{p} \\ G_\mathrm{p}^\mathsf{T} & -N_\mathrm{p} \end{bmatrix} = \frac{1}{2}\left(\begin{bmatrix} -\check{A}_{22} & -\check{B}_2 \\ \check{C}_2 & \mathcal{D}_0 \end{bmatrix} - \begin{bmatrix} -\check{A}_{22} & -\check{B}_2 \\ \check{C}_2 & \mathcal{D}_0 \end{bmatrix}^\mathsf{T}\right),$$
$$\begin{bmatrix} R_\mathrm{p} & P_\mathrm{p} \\ P_\mathrm{p}^\mathsf{T} & S_\mathrm{p} \end{bmatrix} = \frac{1}{2}\left(\begin{bmatrix} -\check{A}_{22} & -\check{B}_2 \\ \check{C}_2 & \mathcal{D}_0 \end{bmatrix} + \begin{bmatrix} -\check{A}_{22} & -\check{B}_2 \\ \check{C}_2 & \mathcal{D}_0 \end{bmatrix}^\mathsf{T}\right).$$

The fact that $E_\mathrm{p} = \check{E}_{22} > 0$ proves the claim for $n_3 > 0$. For $n_3 = 0$, similar arguments apply. Here we encounter pH-DAEs of Kronecker index two, where we have that

$$\begin{bmatrix} -\check{A}_{22} & -\check{B}_2 \\ \check{C}_2 & \mathcal{D}_0 \end{bmatrix} = U^\mathsf{T}(\widetilde{\Gamma} + \widetilde{W})U, \text{ where } U = \begin{bmatrix} 0 & \check{B}_4 \\ I_{n_2} & 0 \\ 0 & 0 \\ 0 & I_m \end{bmatrix}.$$

This concludes the proof. □

References

[1] V. Mehrmann, R. Morandin, S. Olmi, E. Schöll, Qualitative stability and synchronicity analysis of power network models in port-Hamiltonian form, Chaos 28 (10) (2018) 101102.

[2] P. Domschke, B. Hiller, J. Lang, V. Mehrmann, R. Morandin, C. Tischendorf, Gas network modeling: An overview (extended English version), 2021, URL https://perma.cc/B3SP-TZ4L.

[3] S.-A. Hauschild, N. Marheineke, V. Mehrmann, J. Mohring, A.M. Badlyan, M. Rein, M. Schmidt, Port-Hamiltonian modeling of district heating networks, in: T. Reis, S. Grundel, S. Schöps (Eds.), Progress in Differential-Algebraic Equations II, in: Differ.-Algebr. Equ. Forum, Spinger, Cham, 2020, pp. 333–355.

[4] V. Mehrmann, B. Unger, Control of port-Hamiltonian differential-algebraic systems and applications, Acta Numer. 32 (2023) 395–515.

[5] B. Jacob, H. Zwart, Linear Port-HAmiltonian Systems on Infinite-Dimensional Spaces, in: Oper. Theory Adv. Appl, vol. 223, Birkhäuser/Springer, Cham, 2012.

[6] A. van der Schaft, D. Jeltsema, Port-Hamiltonian systems theory: An introductory overview, Found. Trends Syst. Control 1 (2–3) (2014) 173–378.

[7] D. Estévez-Schwarz, C. Tischendorf, Structural analysis for electrical circuits and consequences for MNA, Int. J. Circuit Theory Appl. 28 (2000) 131–162.

[8] M. Günther, U. Feldmann, CAD-based electric-circuit modeling in industry. I. Mathematical structure and index of network equations, Surv. Math. Ind. 8 (1999) 97–129.

[9] M. Günther, U. Feldmann, CAD-based electric-circuit modeling in industry. II. Impact of circuit configurations and parameters, Surv. Math. Ind. 8 (1999) 131–157.

[10] H. Dänschel, V. Mehrmann, M. Roland, M. Schmidt, Adaptive nonlinear optimization of district heating networks based on model and discretization catalogs, SeMA J. (2023) http://dx.doi.org/10.1007/s40324-023-00332-6.

[11] V. Mehrmann, M. Schmidt, J. Stolwijk, Model and discretization error adaptivity within stationary gas transport optimization, Vietnam J. Math. 46 (4) (2018) 779–801.

[12] S. Gugercin, R.V. Polyuga, C. Beattie, A. van der Schaft, Interpolation-based $\mathcal{H}_2$ model reduction for port-Hamiltonian systems, in: Proceedings of the 48h IEEE Conference on Decision and Control (CDC) held jointly with 2009 28th Chinese Control Conference, Shanghai, China, 2009, pp. 5362–5369.

[13] S. Gugercin, R.V. Polyuga, C. Beattie, A. van der Schaft, Structure-preserving tangential interpolation for model reduction of port-Hamiltonian systems, Automatica J. IFAC 48 (9) (2012) 1963–1974.

[14] R.V. Polyuga, A.J. van der Schaft, Effort- and flow-constraint reduction methods for structure preserving model reduction of port-Hamiltonian systems, Systems Control Lett. 61 (3) (2012) 412–421.

[15] P. Borja, J.M.A. Scherpen, K. Fujimoto, Extended balancing of continuous LTI systems: A structure-preserving approach, IEEE Trans. Automat. Control 68 (1) (2023) 257–271.

[16] S.-A. Hauschild, N. Marheineke, V. Mehrmann, Model reduction techniques for linear constant coefficient port-Hamiltonian differential-algebraic systems, Control Cybern. 48 (1) (2019) 125–152.

[17] C. Beattie, S. Gugercin, V. Mehrmann, Structure-preserving interpolatory model reduction for port-Hamiltonian differential-algebraic systems, in: C. Beattie, P. Benner, M. Embree, S. Gugercin, S. Lefteriu (Eds.), Realization and Model Reduction of Dynamical Systems: A Festschrift in Honor of the 70th Birthday of Thanos Antoulas, Springer, Cham, 2022, pp. 235–254.

[18] U. Desai, D. Pal, A transformation approach to stochastic model reduction, IEEE Trans. Automat. Control 29 (12) (1984) 1097–1100.

[19] T. Reis, T. Stykel, Positive real and bounded real balancing for model reduction of descriptor systems, Internat. J. Control 83 (1) (2010) 74–88.

[20] V. Mehrmann, T. Stykel, Balanced truncation model reduction for large-scale system in descriptor form, in: P. Benner, V. Mehrmann, D.C. Sorensen (Eds.), Dimension Reduction of Large-Scale Systems, in: Lect. Notes Comput. Sci. Eng, vol. 45, Springer, Berlin/Heidelberg, 2005, pp. 83–115.

[21] T. Breiten, B. Unger, Passivity preserving model reduction via spectral factorization, Automatica J. IFAC 142 (2022) 110368.

[22] C. Beattie, V. Mehrmann, H. Xu, H. Zwart, Linear port-Hamiltonian descriptor systems, Math. Control Signals Systems 30 (4) (2018) 17–30.

[23] C. Mehl, V. Mehrmann, M. Wojtylak, Distance problems for dissipative Hamiltonian systems and related matrix polynomials, Linear Algebra Appl. 623 (2021) 335–366.

[24] P. Benner, T. Stykel, Model order reduction for differential-algebraic equations: A survey, in: A. Ilchmann, T. Reis (Eds.), Surveys in Differential-Algebraic Equations IV, in: Differ.-Algebr. Equ. Forum, Springer, Berlin/Heidelberg, 2017, pp. 107–160.

[25] S. Gugercin, T. Stykel, S. Wyatt, Model reduction of descriptor systems by interpolatory projection methods, SIAM J. Sci. Comput. 35 (5) (2013) B1010–B1033.

[26] C. Mehl, V. Mehrmann, M. Wojtylak, Linear algebra properties of dissipative Hamiltonian descriptor systems, SIAM J. Matrix Anal. Appl. 39 (3) (2018) 1489–1519.

[27] T. Moser, B. Lohmann, A new Riemannian framework for efficient $\mathcal{H}_2$-optimal model reduction of port-Hamiltonian systems, in: 2020 59th IEEE Conference on Decision and Control (CDC), Jeju Island, Republic of Korea, 2020, pp. 5043–5049.

[28] P. Schwerdtner, M. Voigt, SOBMOR: Structured optimization-based model order reduction, SIAM J. Sci. Comput. 45 (2) (2023) A502–A529.

[29] T. Stykel, Gramian-based model reduction for descriptor systems, Math. Control Signals Systems 16 (4) (2004) 297–319.

[30] P. Benner, S.W.R. Werner, Model reduction of descriptor systems with the MORLAB toolbox, IFAC-PapersOnline 51 (2) (2018) 547–552.

[31] N. Banagaaya, W. Schilders, Index-aware model order reduction for higherindex DAEs, in: S. Schöps, A. Bartel, M. Günther, E.J.W. ter Maten, P.C. Müller (Eds.), Progress in Differential-Algebraic Equations, in: Differ.-Algebr. Equ. Forum, Spinger, Berlin/Heidelberg, 2014, pp. 155–182.

[32] S. Gugercin, A.C. Antoulas, C. Beattie, $\mathcal{H}_2$ model reduction for large-scale linear dynamical systems, SIAM J. Matrix Anal. App. 30 (2) (2008) 609–638.
[33] A.C. Antoulas, C. Beattie, S. Gugercin, Interpolatory Methods for Model Reduction, SIAM, Philadelphia, 2020.
[34] C. Guiver, M.R. Opmeer, Error bounds in the gap metric for dissipative balanced approximations, Linear Algebra Appl. 439 (12) (2013) 3659–3698.
[35] K. Cherifi, H. Gernandt, D. Hinsen, The difference between port-Hamiltonian, passive and positive real descriptor systems, 2022, Preprint. arXiv:2204.04990.
[36] F. Achleitner, A. Arnold, V. Mehrmann, Hypocoercivity and controllability in linear semi-dissipative Hamiltonian ordinary differential equations and differential-algebraic equations, ZAMM J. Appl. Math. Mech. (2021) e202100171.
[37] C. Güdücü, J. Liesen, V. Mehrmann, D.B. Szyld, On non-Hermitian positive (semi)definite linear algebraic systems arising from dissipative Hamiltonian DAEs, 2021, Preprint. arXiv:2111.05616.
[38] B.D.O. Anderson, S. Vongpanitlerd, Network Analysis and Synthesis – A Modern Systems Theory Approach, Prentice-Hall, Englewood Cliffs, NJ, 1973.
[39] M.R. Wohlers, Lumped and Distributed Passive Networks: A Generalized and Advanced Viewpoint, Academic Press, New York/London, 1969.
[40] C. Beattie, V. Mehrmann, H. Xu, Port-Hamiltonian realizations of linear time invariant systems, 2022, Preprint. arXiv:2201.05355.
[41] A.C. Antoulas, I.V. Gosea, M. Heinkenschloss, Data-driven model reduction for a class of semi-explicit DAEs using the loewner framework, in: T. Reis, A. Ilchmann (Eds.), Progress in Differential-Algebraic Equations II, in: Differ.-Algebr. Equ. Forum, Springer, Cham, 2020, pp. 185–210.
[42] P. Schwerdtner, E. Mengi, M. Voigt, Certifying global optimality for the $\mathcal{L}_\infty$-norm computation of large-scale descriptor systems, IFAC-PapersOnLine 53 (2) (2020) 4279–4284.
[43] P. Schwerdtner, M. Voigt, Adaptive sampling for structure-preserving model order reduction of port-Hamiltonian systems, IFAC-PapersOnline 54 (19) (2021) 143–148.
[44] C. Beattie, S. Gugercin, A trust region method for optimal $\mathcal{H}_2$ model reduction, in: Proceedings of the 48h IEEE Conference on Decision and Control (CDC) held jointly with 2009 28th Chinese Control Conference, Shanghai, China, 2009, pp. 5370–5375.
[45] P. Van Dooren, K.A. Gallivan, P.-A. Absil, $\mathcal{H}_2$-optimal model reduction with higher-order poles, SIAM J. Matrix Anal. Appl. 31 (5) (2010) 2738–2753.
[46] K. Sato, Riemannian optimal model reduction of linear port-Hamiltonian systems, Automatica J. IFAC 93 (2018) 428–434.
[47] Y.-L. Jiang, K.-L. Xu, Model order reduction of port-Hamiltonian systems by Riemannian modified Fletcher–Reeves scheme, IEEE Trans. Circuits Syst. II Express Briefs 66 (11) (2019) 1825–1829.
[48] A. van der Schaft, V. Mehrmann, A Lagrange subspace approach to dissipation inequalities, 2022, Preprint. arXiv:2203.12527.
[49] N. Gillis, P. Sharma, On computing the distance to stability for matrices using linear dissipative Hamiltonian systems, Automatica J. IFAC 85 (2017) 113–121.
[50] S.-A. Hauschild, N. Marheineke, V. Mehrmann, Model reduction techniques for port-Hamiltonian differential-algebraic systems, PAMM. Proc. Appl. Math. Mech. 19 (1) (2019) e201900040.
[51] R.W. Freund, The SPRIM algorithm for structure-preserving order reduction of general RCL circuits, in: P. Benner, M. Hinze, E.J.W. ter Maten (Eds.), Model Reduction for Circuit Simulation, in: Lect. Notes Electr. Eng, vol. 74, Springer, Dordrecht, 2011, pp. 25–52.
[52] L.N. Trefethen, Rational Chebyshev approximation on the unit disk, Numer. Math. 37 (2) (1981) 297–320.